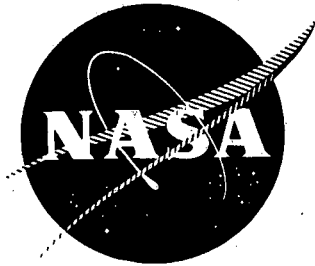


2(mix)

NJIS HC 10.75

NASA CR-120,992  
LYCOMING 105.22.21



# DESIGN STUDY OF AN AIR PUMP AND INTEGRAL LIFT ENGINE ALF-504 USING THE LYCOMING 502 CORE

by

Dale Rauch

Avco Lycoming Division  
550 South Main Street  
Stratford, Connecticut 06497

prepared for

**NATIONAL AERONAUTICS AND SPACE ADMINISTRATION**

July 1972

CONTRACT NAS 3-15696

NASA Lewis Research Center  
Cleveland, Ohio

Laurence W. Gertsma, Project Manager

(NASA-CR-120992) DESIGN STUDY OF AN AIR  
PUMP AND INTEGRAL LIFT ENGINE ALF-504  
USING THE LYCOMING 502 CORE D. Rauch  
(Avco Lycoming Div.) Jul. 1972 172 p

CSSL 131 G3/15

Unclas  
47926

N73-13471



REPRODUCED BY  
U.S. DEPARTMENT OF COMMERCE  
NATIONAL TECHNICAL INFORMATION SERVICE  
SPRINGFIELD, VA. 22161

1. Report No. NASA CR-120, 992	2. Government Accession No.	3. Recipient's Catalog No.	
4. Title and Subtitle DESIGN STUDY OF AN AIR PUMP AND INTEGRAL LIFT ENGINE ALF-504 USING THE LYCOMING 502 CORE		5. Report Date July 1972	
		6. Performing Organization Code	
7. Author(s) Dale Rauch		8. Performing Organization Report No. Lycoming Report No. 105.22.21	
		10. Work Unit No.	
9. Performing Organization Name and Address Avco Lycoming Division Stratford, Connecticut 06497		11. Contract or Grant No. NAS 3-15696	
		13. Type of Report and Period Covered Contractor Report	
12. Sponsoring Agency Name and Address National Aeronautics and Space Administration Washington, D. C. 20546		14. Sponsoring Agency Code	
15. Supplementary Notes Prepared in cooperation with Project Manager, Laurence W. Gertsma, NASA Lewis Research Center, Cleveland, Ohio			
16. Abstract  Design studies were conducted for an integral lift fan engine (ALF-504) utilizing the Lycoming 502 fan core with the final MQT power turbine. The fan is designed for a 12.5 bypass ratio and 1.25:1 pressure ratio, and provides supercharging for the core. Maximum sea level static thrust is 8370 pounds with a specific fuel consumption of 0.302 lb/hr-lb. The dry engine weight without starter is 1419 pounds including full-length duct and sound-attenuating rings. The engine envelope including duct treatment but not localized accessory protrusion is 53.25 inches in diameter and 59.2 inches long from exhaust nozzle exit to fan inlet flange.  Detailed analysis includes fan aerodynamics, fan and reduction gear mechanical design, fan dynamic analysis, engine noise analysis, engine performance, and weight analysis.			
17. Key Words (Suggested by Author(s)) High bypass ratio fan engine		18. Distribution Statement Unclassified-unlimited	
19. Security Classif. (of this report) Unclassified	20. Security Classif. (of this page) Unclassified	21. No. of Pages 171	22. Price* \$3.00

\* For sale by the National Technical Information Service, Springfield, Virginia 22151

FOREWORD

The work reported herein was conducted at Avco Lycoming Division, Stratford, Connecticut under NASA Contract No. NAS3-15696. The study was conducted under the management of the NASA Lewis Research Center with Mr. Laurence Gertsma as project manager.

Preceding page blank

PRECEDING PAGE BLANK NOT FILMED

### ABSTRACT

Design studies were conducted for an integral lift fan engine (ALF-504) utilizing the Lycoming 502 fan core with the final MQT power turbine. The fan is designed for a 12.5 bypass ratio and 1.25:1 pressure ratio, and provides supercharging for the core. Maximum sea level static thrust is 8370 pounds with a specific fuel consumption of 0.302 lb/hr-lb. The dry engine weight without starter is 1419 pounds including full-length duct and sound-attenuating rings. The engine envelope including duct treatment but not localized accessory protrusion is 53.25 inches in diameter and 59.2 inches long from exhaust nozzle exit to fan inlet flange.

Detailed analysis includes fan aerodynamics, fan and reduction gear mechanical design, fan dynamic analysis, engine noise analysis, engine performance, and weight analysis.

Preceding page blank

TABLE OF CONTENTS

	<u>Page</u>
FOREWORD	iii
ABSTRACT	v
LIST OF ILLUSTRATIONS	viii
LIST OF TABLES	xiii
SUMMARY	1
INTRODUCTION	3
PRELIMINARY STUDIES OF SUPERCHARGED AND NON-SUPERCHARGED INTEGRAL LIFT ENGINE AND AIR PUMP	4
FAN AERODYNAMIC DESIGN	7
MECHANICAL DESIGN	26
DYNAMIC ANALYSIS	42
NOISE ANALYSIS	50
ENGINE PERFORMANCE	59
POWER TURBINE ANALYSIS	90
ENGINE WEIGHT	93
SCHEDULE AND COST ESTIMATE OF INTEGRAL LIFT ENGINE	97
APPENDIXES	
I. Aerodynamic Influence of the Part-Span Shroud	102
II. Axisymmetric Flow Solution for the Fan	109
III. Dynamic Analysis Methods	160
IV. List of Symbols	167
REFERENCES	171
BIBLIOGRAPHY	171

**Preceding page blank**

## LIST OF ILLUSTRATIONS

<u>Figure</u>		<u>Page</u>
1	Rotor Polytropic Efficiency	10
2	Fan Meridional Flow Path	12
3	Fan Rotor Velocity Triangles	13
4	Fan Stator Flow Conditions	19
5	Basic Single Stage Performance Map for Fan Duct Section (Experimental Transonic Stage)	22
6	Estimated Performance Map for Duct Flow Fan A (21% Surge Margin at 100% $N/\sqrt{\theta}$ )	23
7	Estimated Performance Map for Duct Flow Fan B (14% Surge Margin at 100% $N/\sqrt{\theta}$ )	24
8	Measured Basic Single Stage Performance Map for Supercharger Fan Section (301 Fan Supercharger)	25
9	Estimated Performance Map for Fans A and B (Supercharger Section)	27
10	ALF-504 High-Bypass Fan Engine	28
11	ALF-504 Fan Engine Variable Nozzle	29
12	ALF-504 Fan Engine Installation Drawing	30
13	Fan Blade and Disc Stresses	33
14	Fan Rotor Blade Airfoil Composite, Scale Approximately 2X	34
15	Midspan Shroud	35
16	Root and Groove Stresses	37

<u>Figure</u>		<u>Page</u>
43	Fan Configuration B (SM = 14 Percent, A <sub>18</sub> = 1190 Square Inches) Estimated Performance at 5000 Feet on Standard Day	81
44	Fan Configuration B (SM = 14 Percent, A <sub>18</sub> = 1190 Square Inches) Estimated Performance at 10,000 Feet on Standard Day	82
45	Fan Configuration B (SM = 14 Percent, A <sub>18</sub> = 1190 Square Inches) Estimated Performance at 15,000 Feet on Standard Day	83
46	Fan Configuration B (SM = 14 Percent, A <sub>18</sub> = 1190 Square Inches) Estimated Performance at 20,000 Feet on Standard Day	84
47	Fan Configuration B (SM = 14 Percent, A <sub>18</sub> = 1190 Square Inches) Estimated Performance at Sea Level on Tropical Day (90° F)	85
48	Fan Configuration B (SM = 14 Percent, A <sub>18</sub> = 1190 Square Inches) Estimated Performance at 5000 Feet on Tropical Day (70° F)	86
49	Fan Configuration B (SM = 14 Percent, A <sub>18</sub> = 1190 Square Inches) Estimated Performance at 10,000 Feet on Tropical Day (51° F)	87
50	Fan Configuration B (SM = 14 Percent, A <sub>18</sub> = 1190 Square Inches) Estimated Performance at 15,000 Feet on Tropical Day (32° F)	88
51	Fan Configuration B (SM = 14 Percent, A <sub>18</sub> = 1190 Square Inches) Estimated Performance at 20,000 Feet on Tropical Day (12° F)	89
52	Estimated Fan Performance Map for Configuration A Showing Operating Lines With Two-Position Fan Exhaust Nozzle	91

<u>Figure</u>		<u>Page</u>
53	Fan Configuration A (SM = 21 Percent at 100 Percent $N/\theta$ ) Estimated Performance at Sea Level on Standard Day With Two-Position Fan Exhaust Nozzle	92
54	Modified MQT Power Turbine First Stage Velocity Triangles for 8.5 Percent Reduced Inlet Flow Function	94
55	Modified MQT Power Turbine Second Stage Velocity Triangles for 8.5 Percent Reduced Inlet Flow Function	95
56	ALF-504 Engine Program	98
57	Measured Flow Conditions Downstream of Rotor (Reference 1 - "Some Studies of Front Fans With and Without Snubbers")	103
58	Radial Surveys Downstream of ALF-502 Fan Rotor, Test -02	104
59	Analysis of Part-Span Shroud on Axial Velocity Profile Downstream of Fan Rotor	108



<u>Figure</u>		<u>Page</u>
17	Reduction Gear	38
18	Ring Gear Stresses	39
19	Reduction Gear Stress Analysis	40
20	Rotor Blade Frequency Analysis, $N = 5245$ RPM	44
21	Rotor Blade Vibration Interference Diagram	45
22	Rotor Blade Flutter Criteria	47
23	Fan-Power Turbine Torsion Analysis	48
24	Fan Rotor Deflection	49
25	Integral Lift Engine Noise at 200 Feet Radius and 110 Degrees	58
26	Engine Stations Used in Performance Evaluation	60
27	Fan Configuration A (SM = 21 Percent, $A_{18} = 1190$ Square Inches) Estimated Performance at Sea Level on Standard Day	65
28	Fan Configuration A (SM = 21 Percent, $A_{18} = 1190$ Square Inches) Estimated Performance at 5000 Feet on Standard Day	66
29	Fan Configuration A (SM = 21 Percent, $A_{18} = 1190$ Square Inches) Estimated Performance at 10,000 Feet on Standard Day	67
30	Fan Configuration A (SM = 21 Percent, $A_{18} = 1190$ Square Inches) Estimated Performance at 15,000 Feet on Standard Day	68
31	Fan Configuration A (SM = 21 Percent, $A_{18} = 1190$ Square Inches) Estimated Performance at 20,000 Feet on Standard Day	69

<u>Figure</u>		<u>Page</u>
32	Fan Configuration A (SM = 21 Percent, $A_{18} = 1190$ Square Inches) Estimated Performance at Sea Level on Tropical Day ( $90^{\circ}$ F)	70
33	Fan Configuration A (SM = 21 Percent, $A_{18} = 1190$ Square Inches) Estimated Performance at 5000 Feet on Tropical Day ( $70^{\circ}$ F)	71
34	Fan Configuration A (SM = 21 Percent, $A_{18} = 1190$ Square Inches) Estimated Performance at 10,000 Feet on Tropical Day ( $51^{\circ}$ F)	72
35	Fan Configuration A (SM = 21 Percent, $A_{18} = 1190$ Square Inches) Estimated Performance at 15,000 Feet on Tropical Day ( $32^{\circ}$ F)	73
36	Fan Configuration A (SM = 21 Percent, $A_{18} = 1190$ Square Inches) Estimated Performance at 20,000 Feet on Tropical Day ( $12^{\circ}$ F)	74
37	Estimated Fan Performance Map for Configuration A With Fixed Fan Exhaust Nozzle ( $A_{18} = 1190$ Square Inches) Showing Operating Lines	75
38	Estimated Supercharger Performance Map With Fixed Fan Exhaust Nozzle ( $A_{18} = 1190$ Square Inches) Showing Operating Lines	76
39	Gas Generator Performance Map Showing Operating Line	77
40	Estimated Fan Performance Map for Configuration B With Fixed Fan Exhaust Nozzle ( $A_{18} = 1190$ Square Inches) Showing Operating Lines	78
41	Fan Configurations A and B ( $A_{18} = 1190$ Square Inches) Estimated Performance at Sea Level on Standard Day	79
42	Fan Configuration B (SM = 14 Percent, $A_{18} = 1190$ Square Inches) Estimated Performance at Sea Level on Standard Day	80

## LIST OF TABLES

<u>Table</u>		<u>Page</u>
I	Basic Laminar-Type Profile, 10 Percent Thickness	15
II	Fan Rotor Blading Design Data, Conical Sections (Z = 32 Blades)	18
III	Fan Stator Blading Design Data, Conical Sections	18
IV	Integral Lift Engine Sideline Perceived Noise Level at 500 Feet	52
V	Integral Lift Engine Polar Perceived Noise Level at 500 Feet	52
VI	Polar Noise Field, Untreated Bypass Duct	53
VII	Sideline Noise Field, Untreated Bypass Duct	54
VIII	Attenuation of the Bypass Duct Treatment	55
IX	Polar Noise Field, Treated Bypass Duct	56
X	Sideline Noise Field, Treated Bypass Duct	57
XI	Turbofan Engine Design Cycle Data	61
XII	Turbofan Engine Design Efficiency and Loss Assumptions	62
XIII	Turbofan Engine Station Cycle Data	63

## SUMMARY

Preliminary studies and final design studies of an integral lift fan engine ALF-504 were conducted using in all cases the Lycoming 502 fan engine core and MQT power turbine. The fan full-speed design pressure ratio is 1.25:1 at sea level standard conditions as specified by NASA. Preliminary studies were conducted to determine the relative engine performance when supercharging with the fan alone and with the addition of two core inlet duct supercharging stages. The results of the preliminary studies show an increase in maximum sea level static thrust of 10 percent for the additional supercharged engine and an increase of approximately 10 percent in velocity leaving the power turbine. Considerations of the small thrust increase and added noise contribution of the hot exhaust jet\* resulted in a decision by NASA to base the final design studies on the engine without additional supercharging. Another important decision as a result of the preliminary studies resulted in an increase of fan tip speed from 985 ft/sec to 1100 ft/sec. This tip speed increase reduced the rotor blade hub overturn (turning past axial in the relative system) from 25 degrees to 10 degrees in the final design, and gives reasonable assurance of flow stability into the core compressor. The final design studies includes detail analysis of fan aerodynamics, fan and reduction gear mechanical design, fan dynamic analysis, engine noise analysis, engine performance, and weight analysis.

Aerodynamic design of the fan includes consideration of the splitter shape and location as this affects local streamline curvature and static pressure gradient. A solution is realized when the splitter stagnation streamline static pressure shows the same value for the duct and core flows. Semi-empirical analytical technique making use of test data from the Lycoming 502 fan has been included in the axisymmetric flow solution to account for the effects of part-span shroud pumping, wake profile and higher losses behind the rotor shroud.

Important design parameters of the final fan aerodynamic sea level standard design point condition for the ALF-504 fan engine are:

1. Total fan flow 421.1 lb/sec
2. Bypass ratio 12.5
3. Fan pressure ratio 1.25:1

---

\* A diffuser after the power turbine was not used in either case.

4. Fan design efficiency 88 percent polytropic
5. Fan tip speed 1100 ft/sec
6. Fan tip diameter 48.0 inches
7. Fan inlet hub-tip ratio 0.392
8. Rotor hub overturn 10 degrees
9. Rotor inlet relative tip Mach number 1.15
10. Absolute Mach number at inlet of core stator 0.74

Stress and dynamic considerations of the fan rotor blade and disc based on use of titanium material and a part-span shroud located at an 18-inch radius show the steady stresses to be low compared with the material yield stress. The tangential stress at the disc bore is 43 ksi compared with 132 ksi yield, and the hub blade centrifugal stress is 26.5 ksi. First bending frequency is free from first-, second-, and third-order excitation above 80 percent speed, and therefore should provide adequate inlet distortion margin from a mechanical standpoint. Blade flutter analysis shows adequate design margin in torsion and bending when compared with NASA criteria.

Fan noise analysis without inlet treatment based on a modified Smith and House method shows a maximum 500 feet sideline noise of 98.6 PNdB at 70 degrees from the inlet for this component.

The total 500 feet sideline maximum engine noise without any acoustical treatment is 104.5 PNdB at 100 degrees from the inlet. Use of two sound-attenuating rings in the bypass duct in addition to wall treatment of this duct reduced the 500 feet sideline engine noise at 100 degrees from the inlet to 97.0 PNdB. This 7.5 PNdB engine noise reduction requires an increase of 3.8 inches in bypass duct diameter, produces a minimum of 2.5 percent loss in sea level takeoff thrust, and adds 58 pounds in weight to the engine because of the attenuating rings alone.

Sea level maximum static thrust is 8370\* pounds with a 0.302 lb/hr per lb specific fuel consumption. Use of a two-position variable duct exhaust nozzle gives 16 percent higher net thrust at 0.4 flight Mach number sea level and 15 percent improved specific fuel consumption

---

\* Does not include added pressure loss of sound-attenuating rings in bypass duct.

The nozzle goes to the closed position (12 percent closed) when a flight Mach number of 0.4 is reached, to rematch the fan at the sea level takeoff point. Engine acceleration time from a steady-state condition of 80 percent maximum thrust to 93.2 percent (66 percent of 80 to 100 percent) is estimated to be 2.5 seconds in the sea level flight Mach number range of 0 to 0.4.

The dry engine weight without starter but including bypass duct sound-attenuating rings and wall treatment is 1419 pounds.

## INTRODUCTION

The relative simplicity and the advantages and disadvantages of VTOL and STOL aircraft have been studied and debated in this country and in Europe for more than a decade. Indeed, many system concepts have evolved and a large variety of powerplant types and aircraft systems have been built and tested. Since these aircraft have been developed largely for military application, the noise by-product was of little consequence. However with application of VTOL and STOL to commercial aircraft, noise generated during takeoff and landing has become of paramount importance, with maximum effort and considerable funding being expended both to quiet existing engines and to better understand the fundamentals of the interplay between basic aerodynamic design of fans, compressors and turbines, and noise generation.

As an effort to demonstrate the relative quiet of STOL aircraft employing internal or external wing augmentation and aircraft of the same seating capacity with VTOL capability, NASA (Lewis) has sponsored a design and study program for lift cruise fan engines with Lycoming based on the 502 fan core. These engines would provide power for a demonstrator aircraft. It is intended that the outcome of this demonstrator program would lead to the design, development, qualification, and procurement of larger commercial VTOL aircraft and more powerful engines which would be phased into commercial use in such size, range, and cruise speed as to be economically viable.

The Lycoming 502 fan engine core was chosen by NASA for the demonstrator program because of its relatively short length and low weight, the many development and flying hours of the basic core, and the currently intense fan program sponsored by the Air Force for the AX close-support aircraft.

The design studies reported herein have all been based on the 502 fan core, and demonstrate the relative ease of converting the 502 fan core to a high bypass ratio (BR = 12.5) low pressure ratio ( $P_r = 1.25:1$ ) fan for lift cruise application. The final design studies include detail analysis of fan aerodynamics, fan stress and dynamics, reduction gear design and stress analysis, fan and engine noise analysis, engine performance evaluation, and weight estimation.

## PRELIMINARY STUDIES OF SUPERCHARGED AND NONSUPERCHARGED INTEGRAL LIFT ENGINE AND AIR PUMP

### General

Prior to the final design phase of the integral lift engine, parallel studies were made to determine the relative size, weight, performance, and fan aerodynamics for the nonsupercharged engine and a design having two supercharging stages following the fan. Reduction gearing design studies for each engine were also conducted to show any significant differences involved. The results of these studies were presented to NASA in February, and the decision was made to continue the final design effort on the nonsupercharged engine. Its greater simplicity, lower development cost, and reduced hot jet velocity after the power turbine\* (which may be a major noise contributor) more than offset the 10 percent lower takeoff thrust compared with the supercharged engine.

### Engine Thermodynamic Performance

In this phase of study, only design point sea level static maximum power performance was considered. The use of two additional supercharger stages produced a higher cycle pressure ratio and increased mass flow in the core to increase the engine power. The following data summarize the performance results of the two engines studied:

---

\* In each case the MQT T55-L-11 power turbine is used without exhaust diffuser or jet nozzle.

	<u>Fan Alone</u>	<u>Fan Plus Two Supercharging Stages</u>
$W_a \text{ tot} - \text{lb/sec}$	406*	449
$W_{\text{core}} - \text{lb/sec}$	31.2	34.4
Bypass Ratio	12.02	12.02
$P_{rf}$	1.25	1.25
Total Supercharging $P_r$	1.25	1.5
Overall Pressure Ratio	9.73	10.7
$F_{\text{tot}} - \text{lb}$	8000	8800
SFC - lb/hr-lb	0.307	0.300

#### Fan Aerodynamic Design

Two fans were studied, and they reflect the requirements of the supercharged and nonsupercharged engines. These fans were based on tip speeds of 985 ft/sec, which was later increased to 1100 ft/sec with concurrence of NASA to reduce the hub "overturn" (turning past axial in the relative system) with the belief that the added noise contribution would be small and would be as much affected by the blade aerodynamic loading as the increased tip speed. A summary of the more important aerodynamic parameters follows:

	<u>Fan Alone</u>	<u>Fan Plus Two Supercharging Stages</u>
$P_{rf}$	1.25	1.25
$U_t - \text{ft/sec}$	985	985
N - RPM	4770	4550
$D_t - \text{in.}$	47.244	49.606
Hub/Tip Ratio, Inlet	0.385	0.385
$W_a \text{ tot} - \text{lb/sec}$	406.0	449.0
Rotor Tip Rel Mach No.	0.80	0.80
Rotor Hub Overturn - deg	25	25

---

\* Final design based on 421.1 lb/sec



## Reduction Gearing

Reduction gearing design studies were made for the supercharged and nonsupercharged fan designs with appropriate reduction ratios. The study included designs utilizing a rotating planet and carrier with fixed ring gear as a possibility to reduce the gear envelope and weight and to allow positioning of the gear further downstream in the inlet housing to reduce the overall engine length. The results indicated the bearing loads of the rotating carrier to be excessively high for the package required for this application, and this approach was, therefore, abandoned. Gearing having fixed planets and a rotating ring gear (the type used in the Lycoming 502 engine) was used as the basis of the final analysis. Resulting design parameters for the appropriate gearing of the nonsupercharged and supercharged fan engines are as follows:

	<u>Fan Alone</u>	<u>Fan Plus Two Supercharging Stages</u>
Reduction Ratio	3.56	3.73
Output Torque-ft/lb	9080	9520
Output Speed - RPM	4770	4550
• Number of Planets	5	4
Face Width of Sun and Planets - in.	2.85	3.12

## Air Pump

In this study major emphasis has been directed to the integral lift engine powerplant; therefore, only a cursory study has been conducted for the air pump design concept as agreed upon by NASA.

The fan design was based on a pressure ratio of 3.5:1 with the bypass ratio dependent upon the static pressure desired after the power turbine and associated exhaust nozzle configuration. The fan design could be effectively accomplished from an aerodynamic standpoint with either three or four stages.

The optimum number of stages would depend upon design trade-off studies showing the effect of relative tip speed (higher for the 3 stage design) and number of stages on fan noise, gear reduction ratio size and weight, and fan weight.

The fan supercharges the 502 core and, therefore, gives a significant temperature, pressure, and flow increase into the core of the fan engine. The study revealed that because of the temperature increase at the core inlet, the referred speed of the core compressor is 83.5 percent of design value. At this speed the core compressor requires operation with the bleed port open to prevent surge.

Two solutions to this problem are available:

1. Increase of the core rotor speed above the present 19,260 rpm value, which requires reset of the turbine nozzles and a review of the modifications required by the increased stresses.
2. Removal of one or more of the front stages of the core compressor to lower the overall pressure ratio and allow acceptable operation without requiring the bleed port to be open.

Both solutions are practical but require more extensive modifications than compatible with the minimum modification approach of this study. Accordingly, further analysis of the air pump design was not conducted.

## FAN AERODYNAMIC DESIGN

### Design Point Conditions and Data

A fan with 1.25:1 SLS (sea level static) total pressure ratio has been selected for the present study. This design pressure ratio corresponds to maximum SLS power setting of the 502 core at maximum rating turbine inlet temperature. The corresponding fan mass flow rate and bypass ratio follow from the power delivered by the supercharged engine core, the fan efficiency, and the condition of ambient static pressure level at exit of the power turbine (no turbine exit diffuser). An 88 percent polytropic fan efficiency is assumed as a realistic target value for a low hub tip ratio transonic fan stage with moderate pressure ratio and low supersonic relative tip Mach number. Initially, the fan design tip speed was set at 985 ft/sec. This speed, however, resulted in a specific work input coefficient  $\Delta h/U^2$  considerably larger than 1 at the hub section and in a positive slope of the  $\psi - \varphi$  operating characteristics for the entire supercharging section of the fan rotor blade. The tip speed was subsequently increased to 1100 ft/sec in order to minimize the risk of core flow instability.

The final fan SLS design conditions are summarized below:

Total Stage Pressure Ratio  $P/P = 1.25:1$

Total Mass Flow Rate  $W_{atot} = 421.1 \text{ lb/sec}$

Core Engine Mass Flow Rate  $W_{ae} = 31.2 \text{ lb/sec}$

Bypass Ratio  $BR = 12.5:1$

Tip Speed  $U_t = 1100 \text{ ft/sec}$

Target Total Polytropic Efficiency  $\eta_{ptot} = 0.88$

### Aerothermodynamic Design Concept

The main aerothermodynamic problem consists of designing the core supercharging fan section and matching its flow path with the existing 502 fan-core transition duct without increasing the engine length. This latter condition limits the rotor exit hub diameter and the hub work input capacity. With the tip speed increased to 1100 ft/sec, the hub  $\psi - \varphi$  characteristics still has a slight positive slope with a specific work input coefficient  $(\Delta h/U^2)_{hub} = 1.22$ .

Overtuning gradually disappears over the channel height and the flow conditions at the supercharger upper section are conventional with  $(\Delta h/U^2)_{tip} = 0.8$ . The aerodynamic conditions in the supercharger flow region are influenced by the meridional curvature of the core flow path and by the location, orientation, and thickness of the core-duct flow splitter. The meridional curvature of the core flow path raises the meridional velocity level near the inner wall. In order to minimize the core stator inlet Mach number, both the tangential and the meridional velocity components at rotor exit should be minimized in the inner wall region. Minimizing the tangential component requires an increase of the hub radius, which, however, results in an increase of the core channel curvature and the hub meridional velocity component. Similarly, the location, orientation, and thickness of the flow splitter determine the annulus area at inlet of the core stator and the average stator inlet velocity. The overall curvature of the core flow channel and the stator hub inlet velocity are also affected by these variables. The channel and splitter configurations thus markedly influence the flow conditions in the critical supercharger fan section, and their interaction must be studied in order to optimize the aerodynamic fan design. The

core flow path matches the 502 core at the upstream flange of the fan support casing. Therefore, the present design allows use of the 502 core cast inlet housing and bearing support structure.

The flow conditions are calculated with Lycoming's IBM Program R136, which solves the complete radial equilibrium equation for the axisymmetric flow field of a turbomachine with a bypass flow splitter. The splitter streamline separating the core and the fan duct flows is subject to two conditions at the splitter stagnation point, perpendicularity to the splitter nose and vanishing of the streamline curvature. Both flows domain upstream and downstream of the splitter nose are treated simultaneously in the iterative computation procedure, which usually converges within 50 iterations.

In addition to the fan design data specified above, the following assumptions are made for the calculation of the flow conditions:

The compression process through the fan rotor blading is characterized by a polytropic efficiency that varies along the blade span according to Figure 1. The stator losses are defined by a total pressure loss coefficient  $\omega = 0.05$ , which is constant over the radius except in the vicinity of the inner and outer walls, where the stator losses are increased to account for additional wall boundary layer and secondary flow effects. The rotor work input is determined in conjunction with the assumed rotor efficiency and the stator losses in such a way as to produce a constant overall fan total pressure ratio  $P/P = 1.25:1$ , except at the wall regions, where the additional stator losses are superimposed and result in a slight total pressure deficit. It will be seen in Figure 1 that the fan rotor polytropic efficiency has been decreased on the part-span-shroud streamline in order to take into account the effect of the shroud wake. The semi-empirical procedure used to simulate that effect is based on published test data (1) and in-house tests by Lycoming and is described in Appendix I. Finally global flow blockage effects of 1 percent at fan rotor exit and 2 percent at both fan duct and core stator exit stations have been assumed.

The fan hub flow conditions are critical because of the low hub rotational speed resulting from the low hub tip ratio and tip speed limitation. However, for a given tip speed and a given rotor exit hub radius, the rotor hub speed can be increased by decreasing the fan annulus area, i. e., by increasing the fan specific flow capacity. The fan inlet Mach

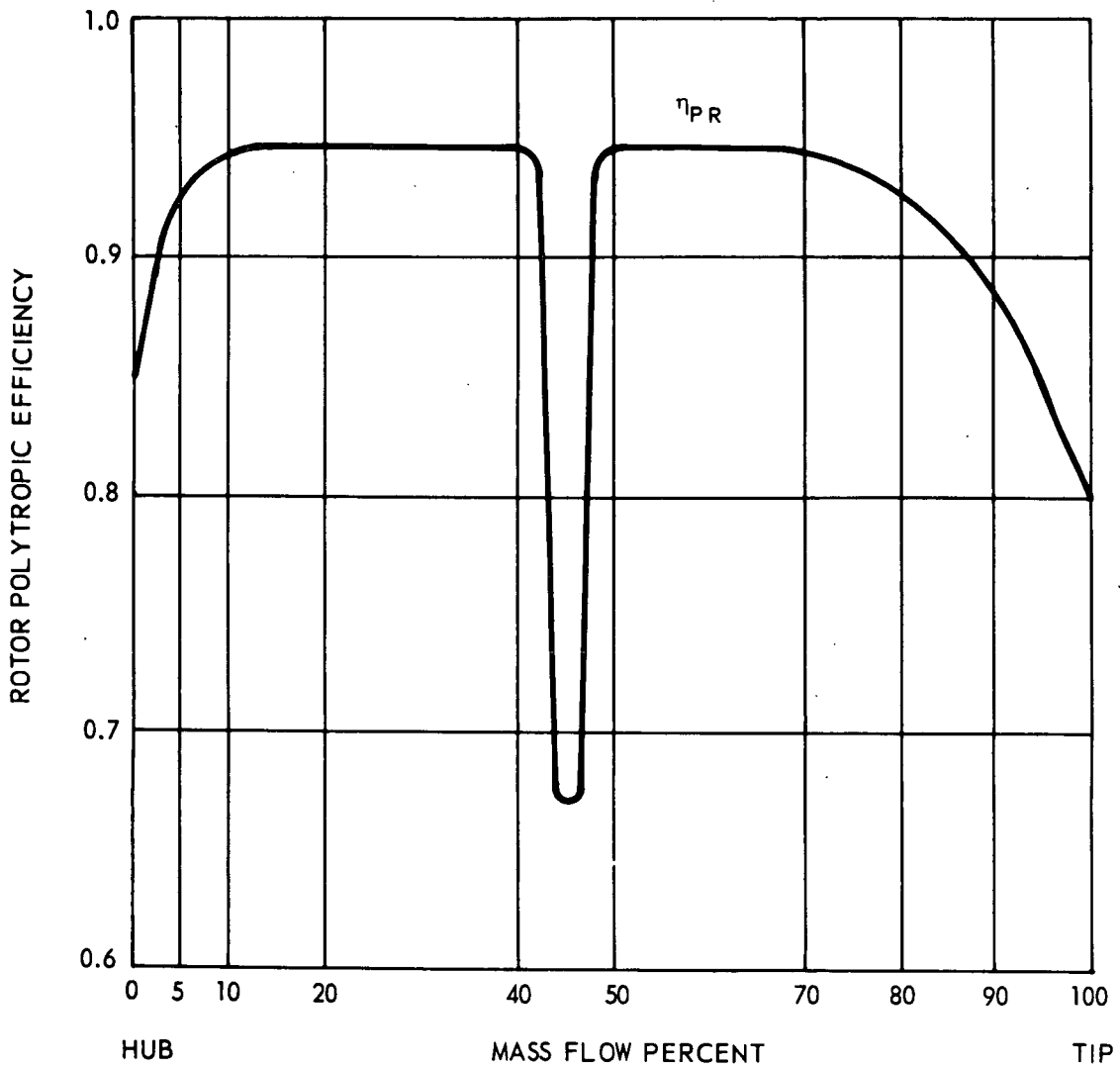


Figure 1. Rotor Polytopic Efficiency.

number consequently has been set at the highest level compatible with a favorable overspeed flow margin potential, namely 0.55 as an average value. For aerothermodynamic and noise reasons, the fan is designed without inlet guide vanes. Moreover, the core-duct flow splitter is located downstream of the rotor blading in order to allow for increased rotor-stator spacing in the duct section without increasing the length of the fan-core transition duct. In addition the fan duct stator tip is leaned in the downstream direction to further minimize wake noise. Figure 2 shows the fan meridional flow path with the stations used in the IBM program R136 calculation and the streamline pattern.

The results of the aerodynamic design optimization are illustrated by the velocity triangles shown in Figure 3. The first three triangles describe the flow conditions in the supercharger section. With the tip speed increased from 985 to 1,100 ft/sec, both the rotor flow overturning and the Mach number at entrance of the stator have been reduced to favorable levels ( $\beta_{2_{\text{hub}}} = 10.4$  degrees and  $Mv_{2_{\text{hub}}} = 0.715$ , as compared with 25 degrees and 0.75 to 0.8 with  $U_{\text{tip}} = 985$  ft/sec). As a result of the slight relative flow overturning, the highest rotor flow deceleration rate does not occur at the hub section but in the splitter region. The stator hub section, however, is subjected to the highest deceleration rate, which is somewhat above usual practice for stator design. The corresponding velocity ratio  $(V_5/V_4)_{\text{hub}} = 0.712$  is accordingly slightly lower than desirable for a shrouded design. (See "Aerodynamic Blading Design.")

The last three triangles describe the flow conditions through the upper fan section, which are typical of conventional transonic design practice.

IBM Program R136 output section given in Appendix II contains a complete set of flow data that substantiate the basic aerodynamic design concept.

### Aerodynamic Blading Design

Rotor Blading. - The main blading design problem consists of selecting a favorable compromise between the conflicting aerodynamic, weight, and acoustic design requirements. For the tip section, a profile with thin leading edge and maximum thickness located at 50 to 60 percent chord station is required. A double-circular-arc profile would be adequate.

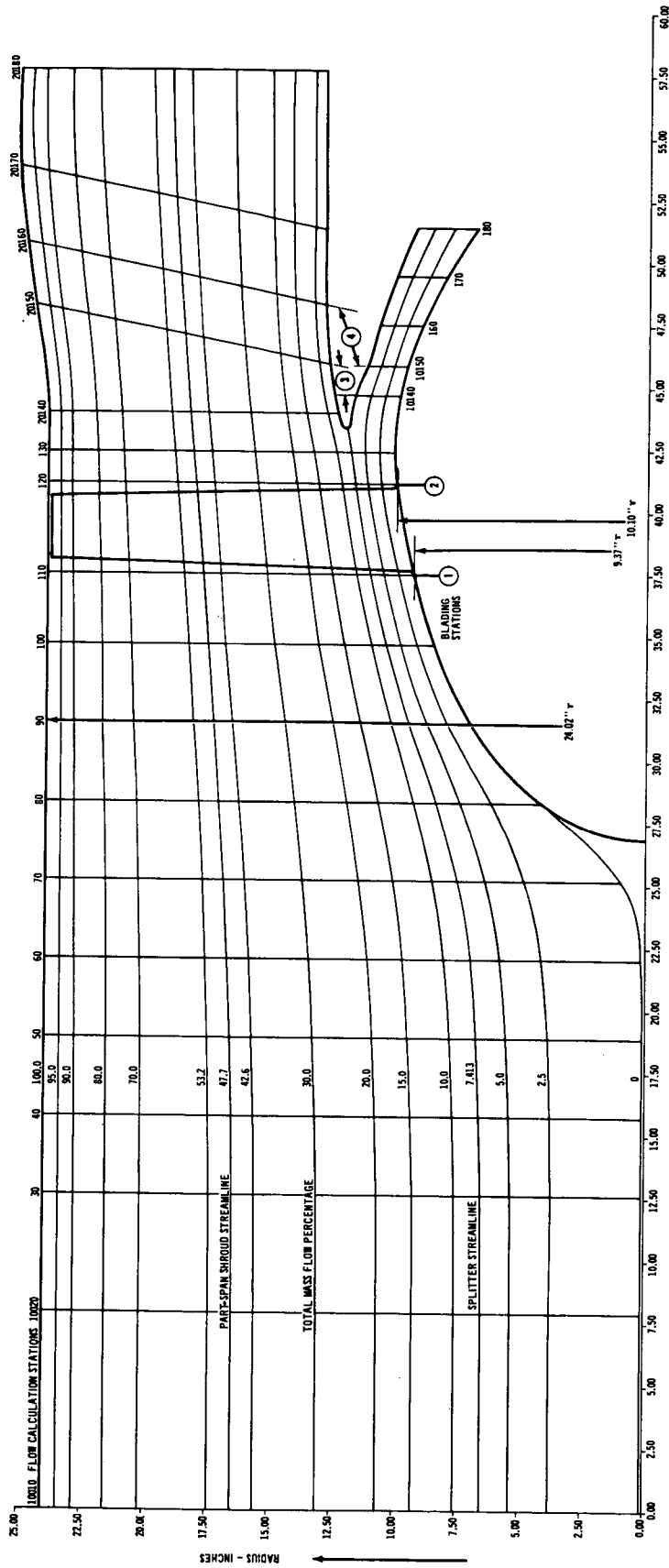


Figure 2. Fan Meridional Flow Path.

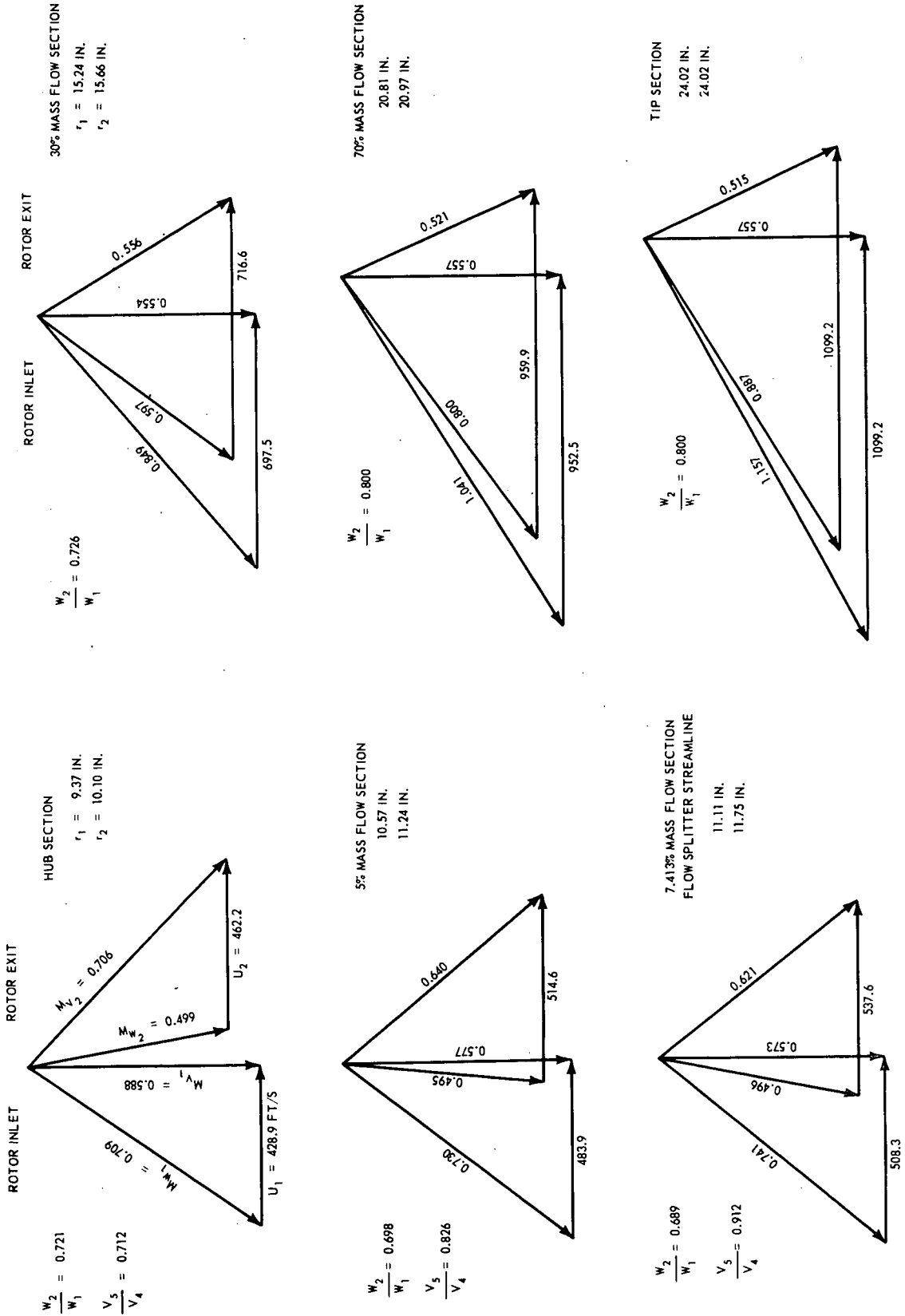


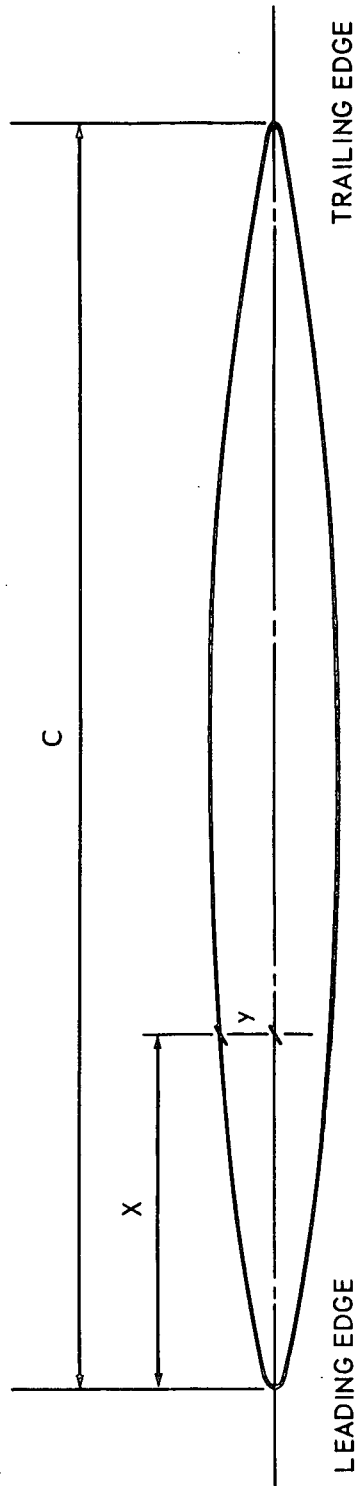
Figure 3. Fan Rotor Velocity Triangles.



A laminar type profile superimposed on a circular mean camber line, however offers better aerodynamic properties for the subsonic blade portion while retaining the favorable characteristics of the double circular type in the transonic region. Such a profile has been used extensively in classical Lycoming transonic rotors with excellent overall performance results, and it is selected here as the best design compromise for all blade sections. The basic 10 percent relative thickness distribution is shown in Table I. Any desired relative thickness value is obtained by multiplying the basic 10 percent profile ordinates by the corresponding thickness factor. For this study the number of blades has been selected so that the blade passing frequency ( $Z \times \text{RPM}/60$ ) stays below the lower limit of the critical acoustic range of 2800 to 4500 hertz. Thus  $Z = 2800 \times 60/5245 = 32$  blades. Two blade aerodynamic loading formulas are currently used to select the blading solidity, namely NACA's diffusion factor  $D$ , which is relatively insensitive to solidity, and Zweifel's aerodynamic loading factor  $\psi_a$ , which is directly proportional to relative blade spacing. Zweifel's criterion  $\psi_{a\text{opt}} = 0.9-1.1$  is often used in conventional blading design, but rotor hub sections have consistently demonstrated a higher loading capability without noticeable performance penalty. From a weight standpoint, it is of course desirable to design for minimum solidity and maximum aspect ratio compatible with good performance and mechanical integrity. On the other hand, it is imperative to insure adequate tolerance of the rotor blading to distorted inlet flow conditions, a requirement which is most efficiently fulfilled by designing for low aerodynamic loadings, i. e., high blading solidities, and low aspect ratios. For the hub section a maximum  $D$  value of 0.5 has been set as a compromise between the above conflicting requirements. The selected hub chord length  $C_{\text{hub}} = 3.38$  inches results in a solidity  $\sigma_{\text{hub}} = 1.77$ ,  $D_{\text{hub}} = 0.486$  and  $\psi_{a\text{hub}} = 1.27$ . For the tip section,  $\sigma_{\text{tip}} = 1.0$  is an adequate solidity for transonic operation with a normal shock wave in the cascade entrance region. This calls for a tip chord of 4.73 inches, thus a 40 percent blade chord elongation from hub to tip. The tip loading conditions then are  $D_{\text{tip}} = 0.298$  and  $\psi_{a\text{tip}} = 0.546$ . Based on the mean chord length of 4.05 inches, the rotor blade aspect ratio is approximately 3.5:1.

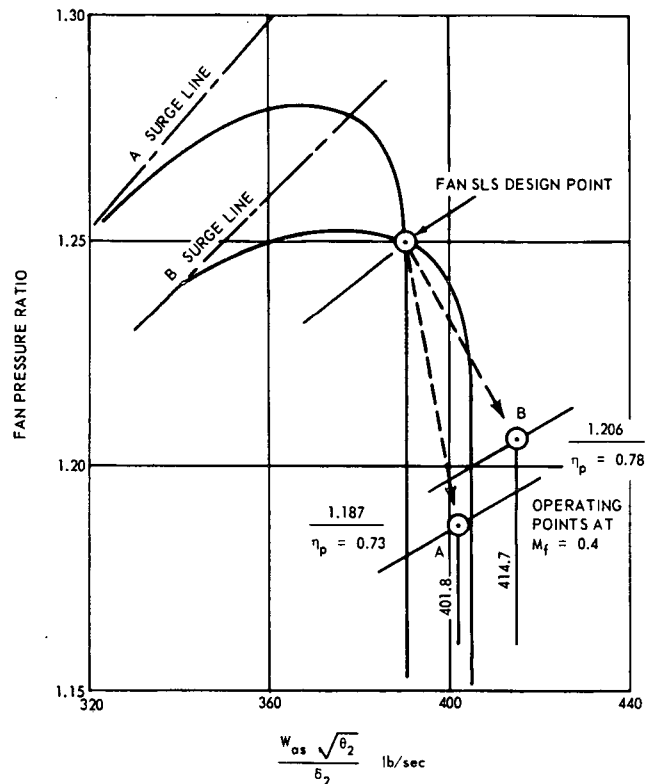
The next step consists of selecting the design point incidences. In a low pressure-ratio fan discharging through a fixed nozzle, the operating line undergoes a considerable shift between static and flight conditions. At 0.6 flight Mach, for example, the ram compression ratio is of the same order as the fan design pressure ratio, and the fan nozzle expansion

TABLE I. BASIC LAMINAR-TYPE PROFILE, 10 PERCENT THICKNESS



		Ratio (pct)									
X/C	0	1.25	2.5	5.0	7.5	10.0	15.0	20	30	40	
Y/C	0	0.887	1.165	1.650	2.055	2.400	3.000	3.505	4.275	4.778	
X/C	50	60	70	80	85	90	95	97.5	100		
Y/C	4.998	4.882	4.250	3.155	2.525	1.829	1.133	0.785	0		

ratio thus would increase from the SLS design value of 1.25:1 to 1.55:1. If the nozzle is sized for SLS conditions, its area will be too large for cruise operation, and the actual fan cruise operating pressure ratio consequently will drop to a substantially lower value than the SLS design value, which would result in lower fan efficiency and thrust performances. Both effects can be minimized by selecting positive angles of incidence at SLS conditions. This relationship is shown schematically in the following sketch (the performance data quoted on the sketch corresponds to SLS and 0.4 Mach flight conditions and are taken from the performance evaluation presented under "Engine Performance"). The



better cruise performance of fan B is obtained at the expense of operating the blading closer to the surge line at sea level static conditions. The reduced SLS surge margin, however, is critical with regard to operating conditions with inlet flow distortion, and it is advisable to select conventional design incidences for safer VTOL operating conditions.

A variable fan nozzle area will be required to achieve optimum cruise performance.

For the subsonic portion of the blading, a 0-degree incidence relative to the mean camber line constitutes an optimum compromise between efficiency and surge margin. In the transonic region, the profiles are usually designed and set so that the tangent to the suction contour at the midstation of the uncovered segment is aligned with the direction of the relative inlet velocity.

The above ground rules will be followed for final blading design. It must be emphasized that the selection of 32 blades to avoid the critical noise frequency band of 2,800 to 4,500 hertz constitutes a major design constraint, which is reflected by the comparatively large chords necessary to obtain favorable aerodynamic loading conditions. Because of its direct bearing on engine weight, this particular aspect of the noise problem should be critically examined prior to final blading design selection.

Table II presents typical design data for the presently selected 32-blade rotor. Sample conical blade sections are defined corresponding to the velocity triangles shown in Figure 3.

Core Flow Stator. - The core stator flow conditions are illustrated in Figure 4. Although the stator inlet Mach number has been kept down to a very favorable level, the flow turning angles are comparatively large, and the deceleration rate at the hub section is close to the upper limit allowable for a shrouded stator design ( $V_5/V_4 = 0.70-0.75$ ). In this case,  $\psi_{ahub} = 1.0$  must be considered as a maximum value. This consideration requires a solidity  $\sigma_{hub} = 2.2$ , which results in  $D_{hub} = 0.45$  and 105 blades with a chord length  $C_{hub} = 1.3$  inches. The blade can be conveniently manufactured from a basic strip stock profile with constant chord, coined to produce the slight twist and camber variation required. The basic profile uses NACA 65 series of 7 percent thickness distribution superimposed on a circular mean camber line. The blade is designed and set for 0-degree incidence over the entire core channel height. Table III presents blading design data for the three sections corresponding to the flow conditions shown in Figure 4.

It will be seen from Figure 4 that for a single row stator, it is necessary to increase the meridional velocity level across the blading in order to achieve favorable aerodynamic blade loading conditions. This

TABLE II. FAN ROTOR BLADING DESIGN DATA, CONICAL SECTIONS (Z = 32 blades)

Radius (in.)	Relative Flow Angles (deg) $\beta_1$ $\beta_2$	Deviation Angle $\delta$ (deg)*	Camber Angle $\theta$ (deg)	Setting Angle $\gamma$ (deg)	Incidence Angle $i$ (deg)	Chord Length C (in.)	Relative Thickness $\nu$ (pct)	Cascade Pitch S (in.)	Cascade Solidity $\sigma = C/S$	Aerodynamic Loading $\psi_a$	D
9.37/10.10	-10.4	8.3	52.7	7.65	0	3.39	8.0	1.91	1.775	1.265	0.485
10.57/11.24	6.1	7.4	39.1	18.25	0	3.49	7.25	2.14	1.630	1.172	0.479
11.11/11.75	39.3	7.1	35.2	21.70	0	3.54	7.00	2.25	1.573	1.178	0.481
15.24/15.66	49.3	4.6	17.2	40.3	0	3.92	5.25	3.04	1.288	0.868	0.408
20.81/20.97	57.6	2.0	5.2	54.0	1.0	4.44	3.75	4.10	1.082	0.591	0.394
24.02	61.3	2.0	4.0	58.2	1.1	4.73	3.0	4.73	1.0	0.546	0.298

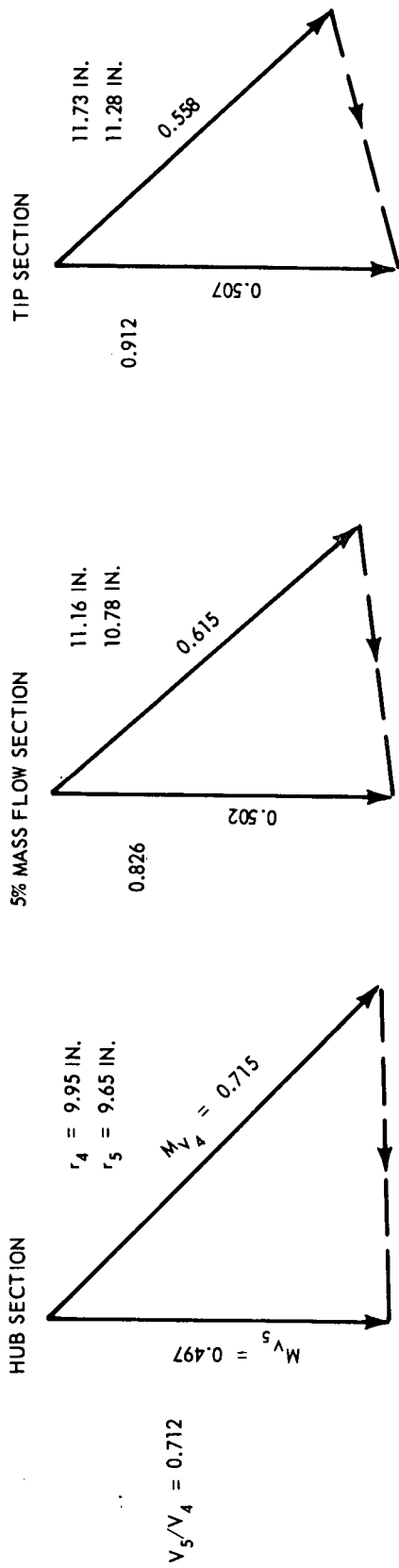
\* is calculated with Carter's empirical formula  $\delta = \frac{m\theta}{\sqrt{\sigma}}$  with  $m = 0.230 + 0.1 \frac{\beta_2(\alpha)}{50}$

TABLE III. FAN STATOR BLADING DESIGN DATA, CONICAL SECTIONS

Radius (in.)	Absolute Flow Angles (deg) $\beta_4$ $\beta_5$	Deviation Angle $\delta$ (deg)*	Camber Angle $\theta$ (deg)	Setting Angle $\gamma$ (deg)	Incidence Angle $i$ (deg)	Chord Length C (in.)	Relative Thickness $\nu$ (pct)	Cascade Pitch S (in.)	Cascade Solidity $\sigma = C/S$	Aerodynamic Loading $\psi_a$	D	Remarks
9.95/9.65	46.1	8.5	54.6	18.8	0	1.3	7.0	0.586	2.22	1.01	0.450	Core Stator Sections
11.16/10.78	42.0	8.2	50.2	16.9	0	1.3	7.0	0.656	1.97	0.845	0.344	Z = 105 blades
11.73/11.28	43.4	8.7	52.1	17.35	0	1.3	7.0	0.689	1.89	0.774	0.250	
12.78/12.95	32.3	6.0	38.3	13.15	0	2.5	7.0	1.140	2.19	0.713	0.260	Duct Stator Sections
16.25/16.41	28.5	6.0	34.5	11.25	0	2.5	7.0	1.448	1.73	0.705	0.303	Z = 71 blades
21.44/21.67	23.4	5.9	29.3	8.75	0	2.5	7.0	1.908	1.31	0.735	0.282	
24.55/24.88	25.4	7.0	32.4	9.2	0	2.5	7.0	2.185	1.14	0.924	0.333	

\* is calculated with Carter's empirical formula  $\delta = \frac{m\theta}{\sqrt{\sigma}}$  with  $m = 0.230 + 0.1 \frac{\beta_2(\alpha)}{50}$

CORE STATOR SECTIONS



DUCT STATOR SECTIONS

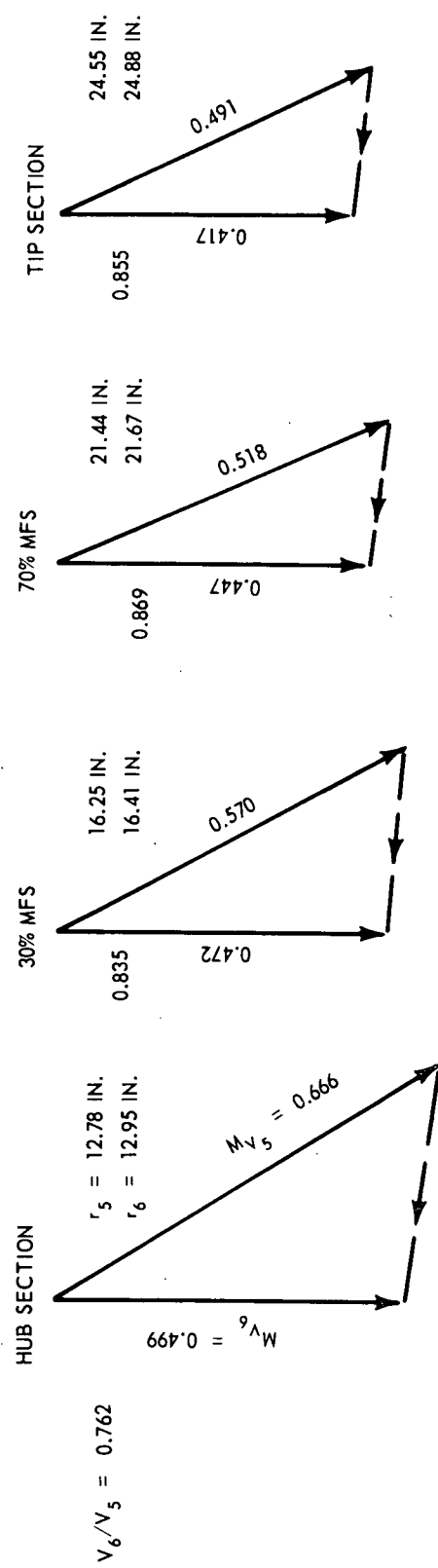


Figure 4. Fan Stator Flow Conditions.

situation generally results as part of the design in highly loaded compressor stages. A lower stator exit velocity level could be realized by using a double-row stator assembly. This alternate solution will be examined prior to final blading design selection.

Fan Duct Flow Stator. - The duct stator flow conditions are illustrated in Figure 4. They do not present any critical problem from a blading design viewpoint. Consequently, design emphasis is put on noise abatement. A stator/rotor blade number ratio of 2.25 is desirable, and this calls for 71 stator blades. The axial distance available between the trailing edge of the fan rotor and the leading edge of the fan support struts allows for an average spacing of approximately 1.5 mean rotor chords between the rotor and the stator blading.

The blades can be manufactured from a basic strip stock profile with constant chord. With the comparatively high aspect ratio of the 71-blade design, it is advisable to limit the aerodynamic loading to  $\psi_a$  values smaller than 1.0 in order to avoid or minimize the loss of surge margin generally observed in higher aspect ratio bladings. With a mean hub tip ratio of 0.52 and a constant chord design, the highest loading occurs at the tip section, where  $\psi_{a\text{tip}} = 0.95$  has been set as a maximum value. The selected 71-blade design requires a chord length of 2.5 inches resulting in a tip solidity  $\sigma_{\text{tip}} = 1.142$  and  $D_{\text{tip}} = 0.333$ . At the hub section,  $\sigma_{\text{hub}} = 2.19$ ,  $\psi_{a\text{hub}} = 0.713$  and  $D_{\text{hub}} = 0.360$ . The basic profile again uses an NACA 65 series, 7 percent thickness distribution superimposed on a circular mean camber line. The blade is designed and set for 0 degree incidence over the entire duct channel height. Table III presents blading design data for the four conical sections corresponding to the flow conditions shown in Figure 4.

#### Fan Performance Evaluation

Performance maps for both the fan duct and the supercharger sections have been established by scaling measured basic performance maps of stages with similar design conditions. The scaling is effected on the basis of prescribed ratios of the design point mass flows, pressure ratios, and efficiencies. The pressure ratios are obtained by assuming a constant effective work input factor ( $\Delta h_{\text{scaled}}/\Delta h_{\text{basic}}$ )<sub>design</sub> and a constant efficiency factor ( $\eta_{\text{scaled}}/\eta_{\text{basic}}$ )<sub>design</sub> for all corresponding off-design points.

The scaled maps predict the actual performance characteristics with an accuracy that depends upon the degree of similarity shown by the basic and the actual designs. Since existing and new designs generally exhibit only limited similarity, it is important to select the basic maps and their representative design points in such a way as to best simulate the most essential characteristics of the new design.

Fan Duct Section. - The measured basic map is shown in Figure 5. It pertains to an experimental transonic stage with the following design-point characteristics:

Total Pressure Ratio  $P_t/P_t = 1.404$

Referred Mass Flow Rate  $W_{a_{ref}} = 55.6 \text{ lb/sec}$

Tip Speed  $U_{tip} = 1188 \text{ ft/sec}$  ( $M_{u0} = \frac{U_{tip}}{a_{tot}} = 1.064$ )

Hub-Tip Ratio  $v = 0.47$

Adiabatic Efficiency  $\eta_{ad} = 0.83$

For scaling, basic design points of fans A and B (with 21 percent and 14 percent surge margin at 100 percent  $N/\sqrt{\theta}$  respectively) have been selected on the  $MU0 = 1.0$  speed line, which corresponds to 1115 ft/sec tip speed. This provision insures good aerodynamic similarity for the transonic tip region, and also reflects the requirement for a favorable overspeed flow margin necessary to optimize cruise performance. With  $(P/P)_{basic} = 1.37$ , point A is representative of the conventional blading design approach adopted for fan A (SM = 21 percent at 100 percent  $N/\sqrt{\theta}$ ). With  $(P/P)_{basic} = 1.406$ , point B represents a design that compromises surge margin in order to minimize cruise performance degradation with a constant fan nozzle area. The efficiencies have been slightly scaled to the assumed 88 percent target polytropic value for both A and B fans.

Figures 6 and 7 show the resulting estimated maps used for the engine performance evaluation.

Supercharger Section. - The basic tested map is shown in Figure 8. The map represents the supercharger section of the T53-301 fan with the following design-point characteristics:



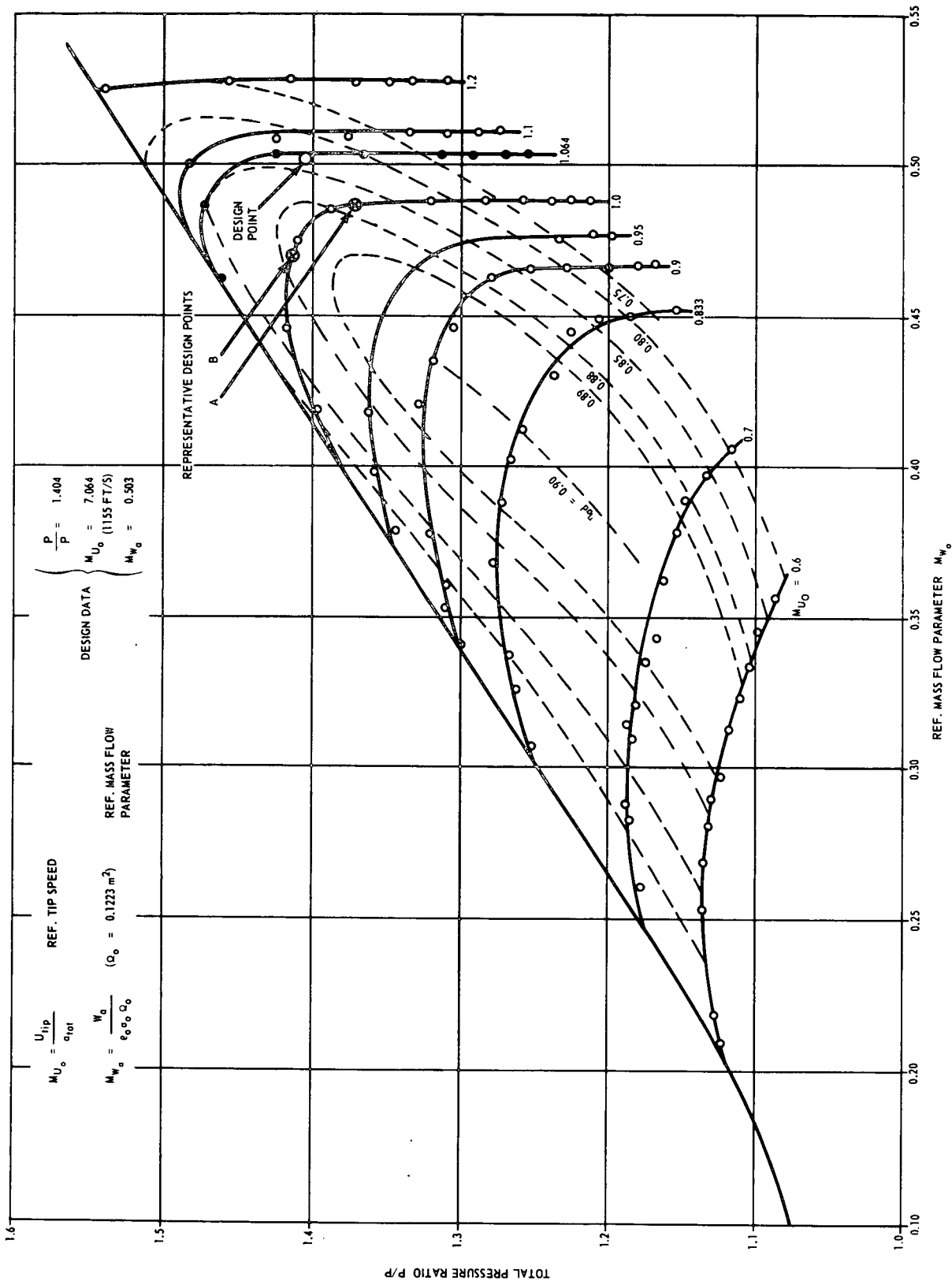


Figure 5. Basic Single Stage Performance Map for Fan Duct Section (Experimental Transonic Stage).

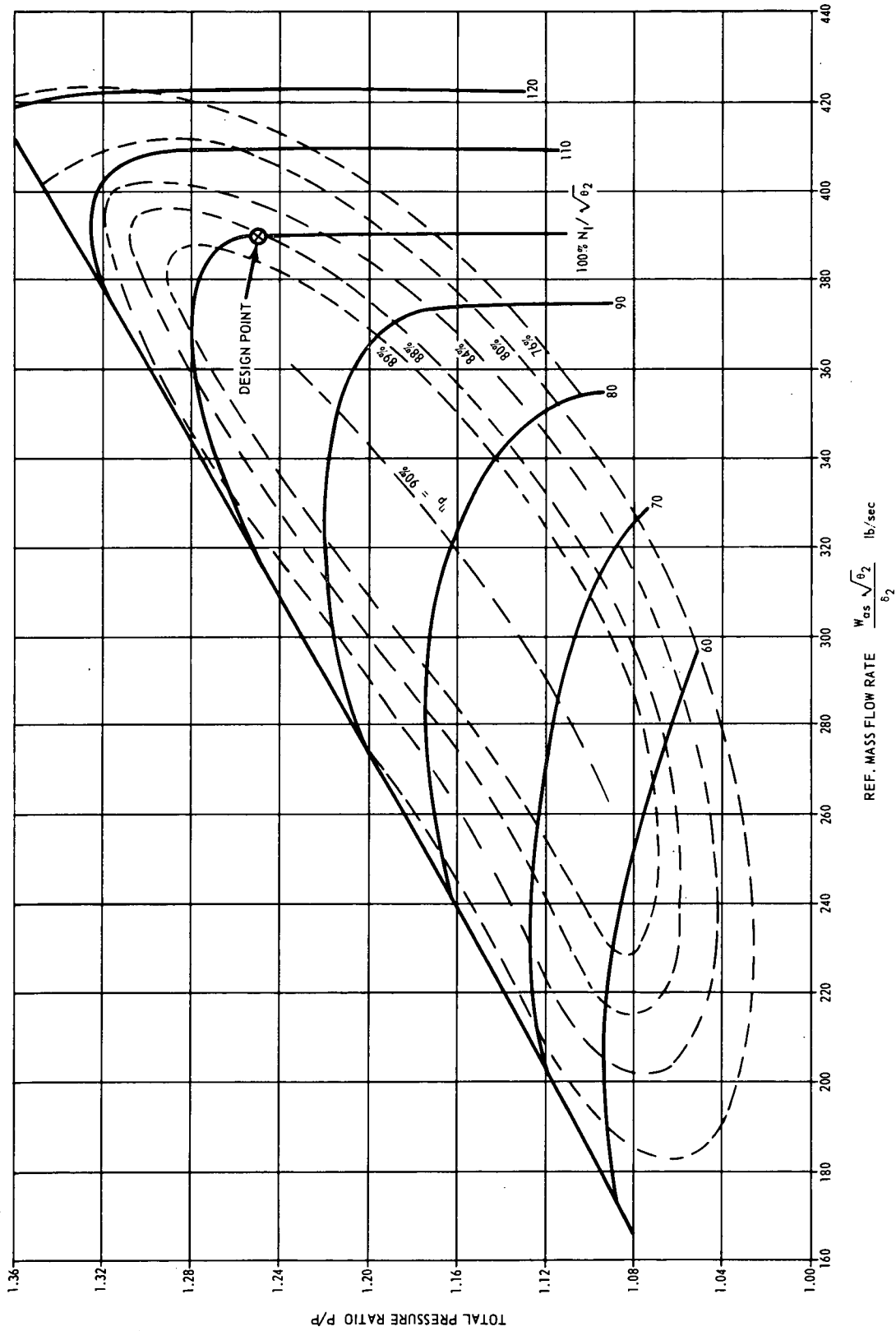


Figure 6. Estimated Performance Map for Duct Flow Fan A (21% Surge Margin at 100%  $N/\theta$ ).

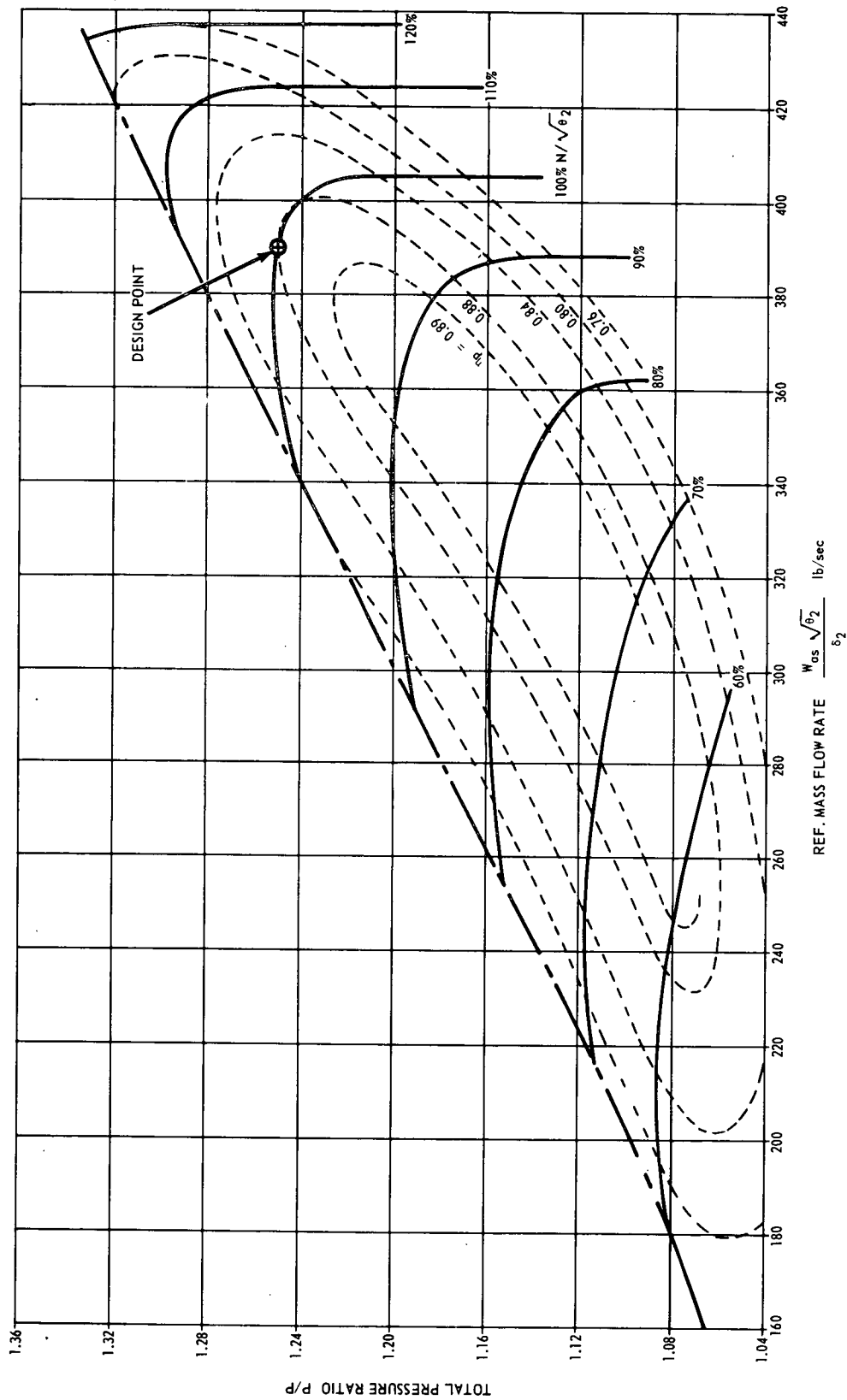


Figure 7. Estimated Performance Map for Duct Flow Fan B (14% Surge Margin at 100%  $N/\theta$ ).

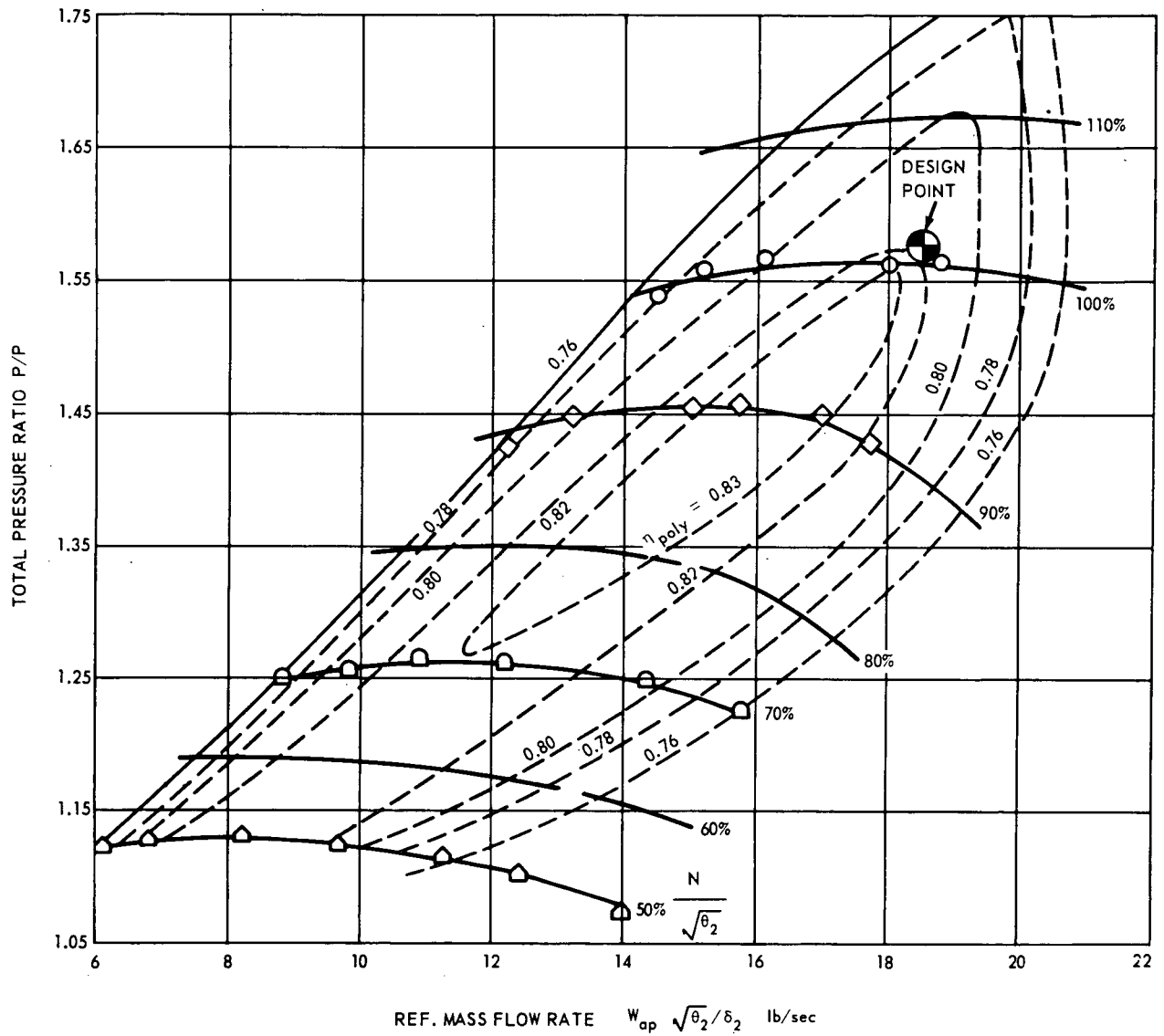


Figure 8. Measured Basic Single Stage Performance Map for Supercharger Fan Section (301 Fan Supercharger).

Total Pressure Ratio ( $P_t/P_t$ ) = 1.577

Referred Mass Flow Rate  $W_{a_{ref}} = 18.5 \text{ lb/sec}$

Mean Specific Work Input Coefficient ( $\Delta h/U^2$ ) = 0.82

Polytropic Efficiency  $\eta_p = 0.82$

Since the flow conditions are subsonic, the essential similarity parameter for scaling is the mean specific work coefficient  $\Delta h/U^2$ . The 0.82 value of the 301 supercharger section comes reasonably close to the 0.92 value of the present supercharger design. This ensures that the main characteristics of the supercharger section, namely the flat slope of the speed lines, is satisfactorily reproduced by the predicted map. The design-point polytropic efficiency has been sealed up from 82 to 86 percent to account for the favorable effects of the larger size and the lower blading Mach level of the present design.

Figure 9 shows the resulting estimated map used for the engine performance evaluation.

## MECHANICAL DESIGN

### General

The core engine LTC4B12 is completely compatible with present fan engine and is preceded by considerable work to produce the 502 fan engine. Consequently, the investigations presented in this section are restricted to the new fan component, reduction gear, housing, and exhaust nozzle.

A flow path view of the integral fan engine ALF-504 is shown in Figures 10 and 11. The core engine is identical with the 502 fan engine. The installation drawing of the engine with mounting pad locations is shown in Figure 12. The mounting pad location and engine support method are similar to those of the 502 fan engine. The new fan design is based on the following mechanical data at sea level, standard day, static conditions:

Gas Generator Speed	19,260 rpm
Power Turbine Speed	16,870 rpm
Fan Wheel Speed	5,245 rpm

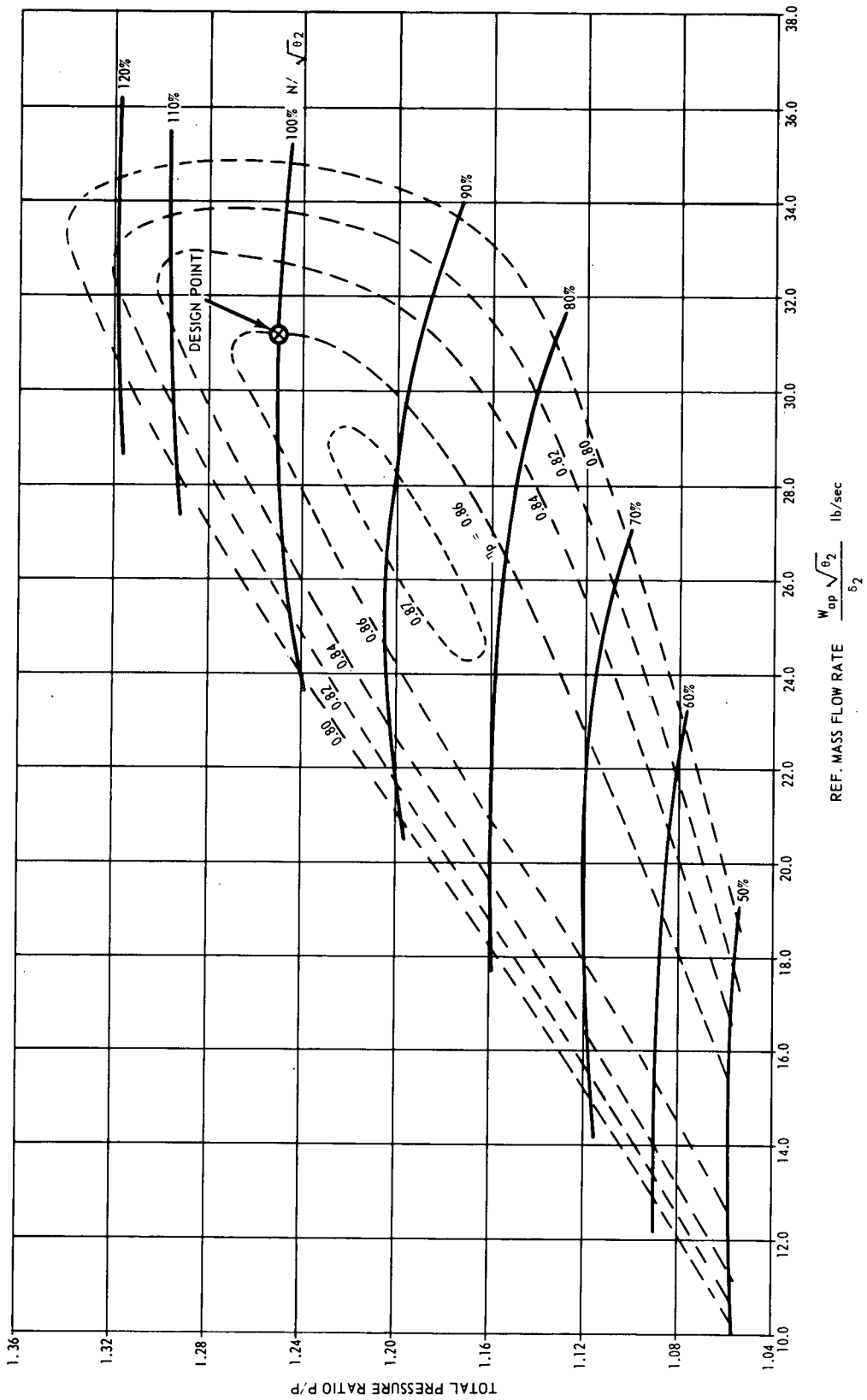


Figure 9. Estimated Performance Map for Fans A and B (Supercharger Section).

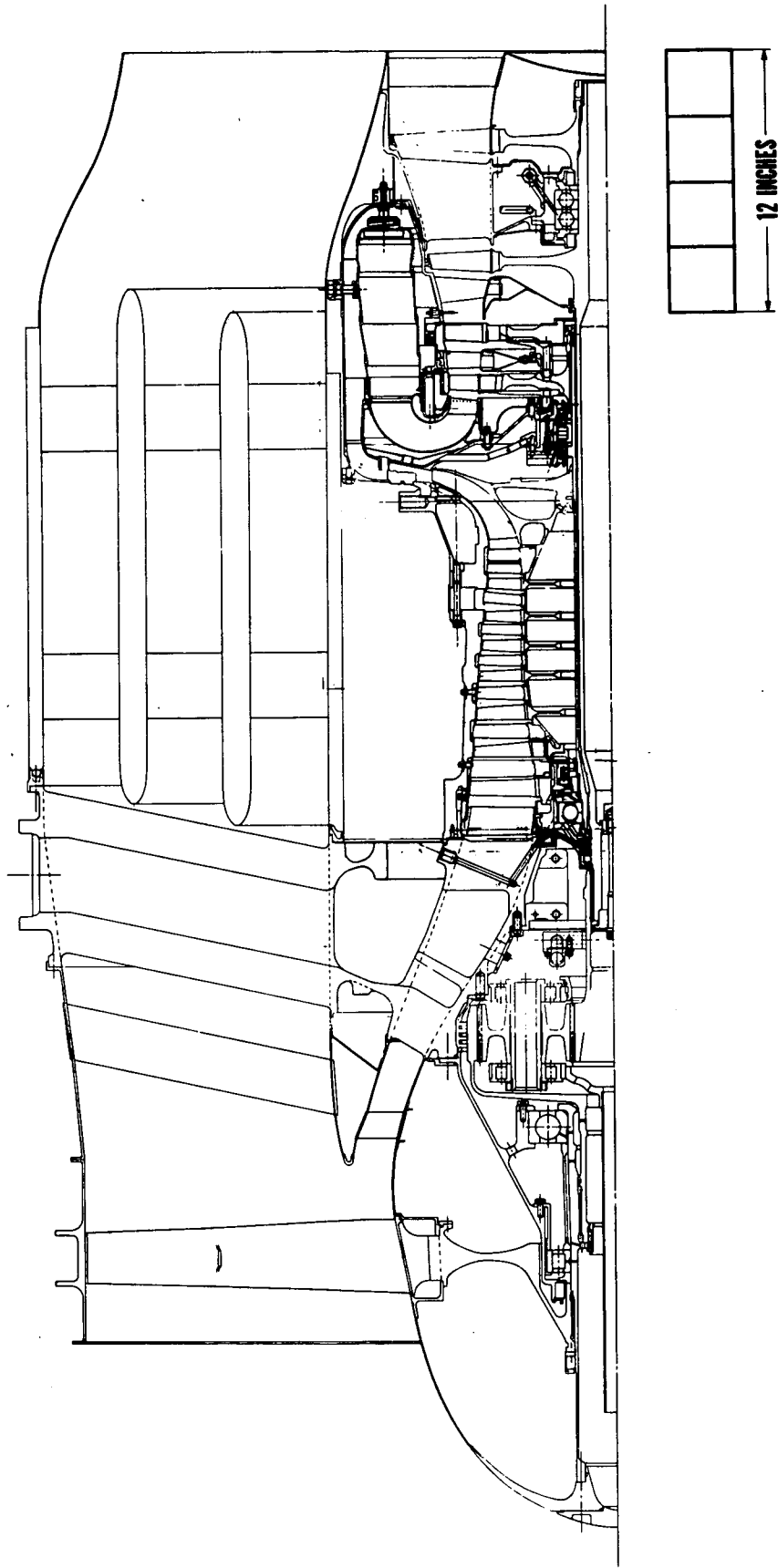


Figure 10. ALF-504 High-Bypass Fan Engine.

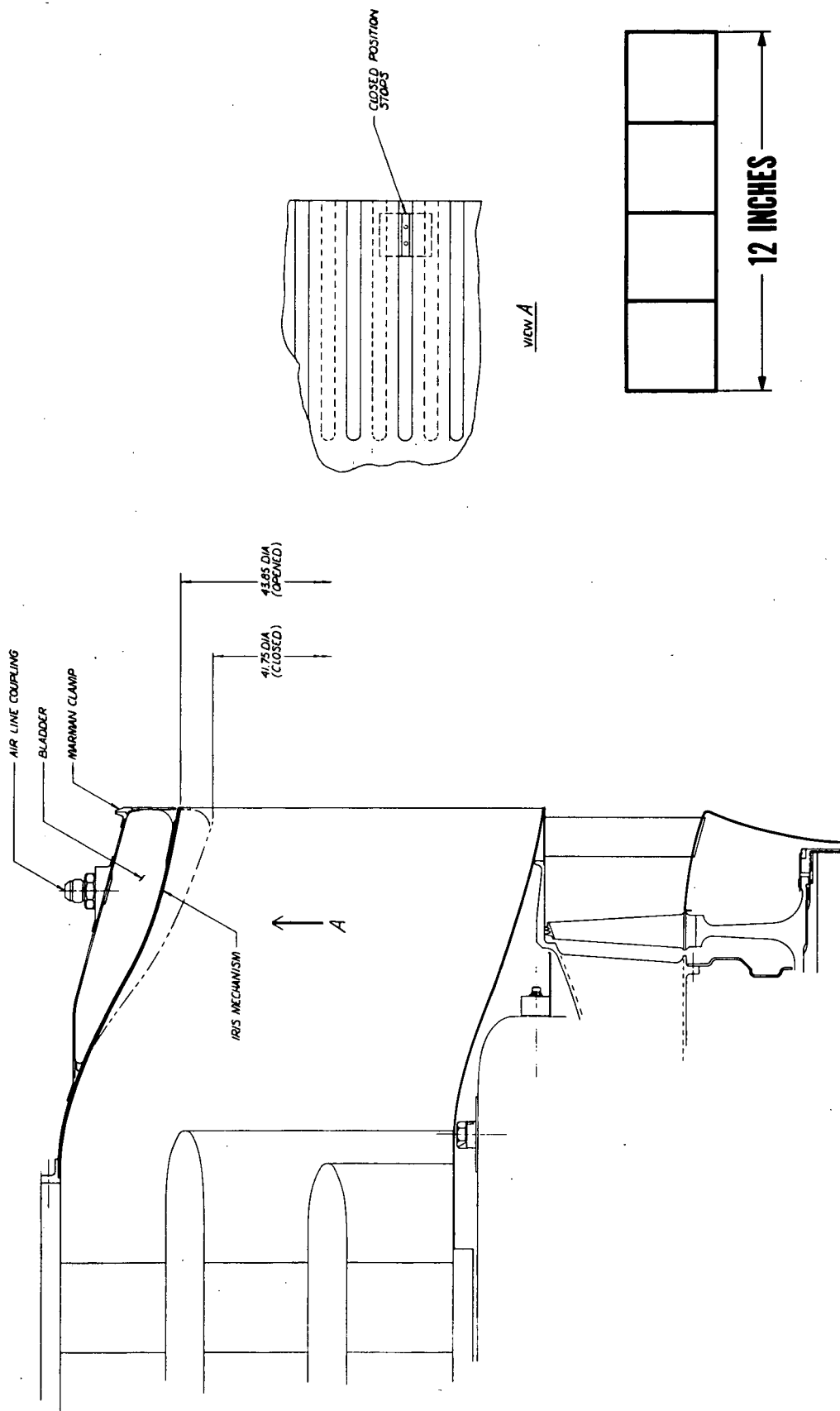


Figure 11. ALF-504 Fan Engine Variable Nozzle.



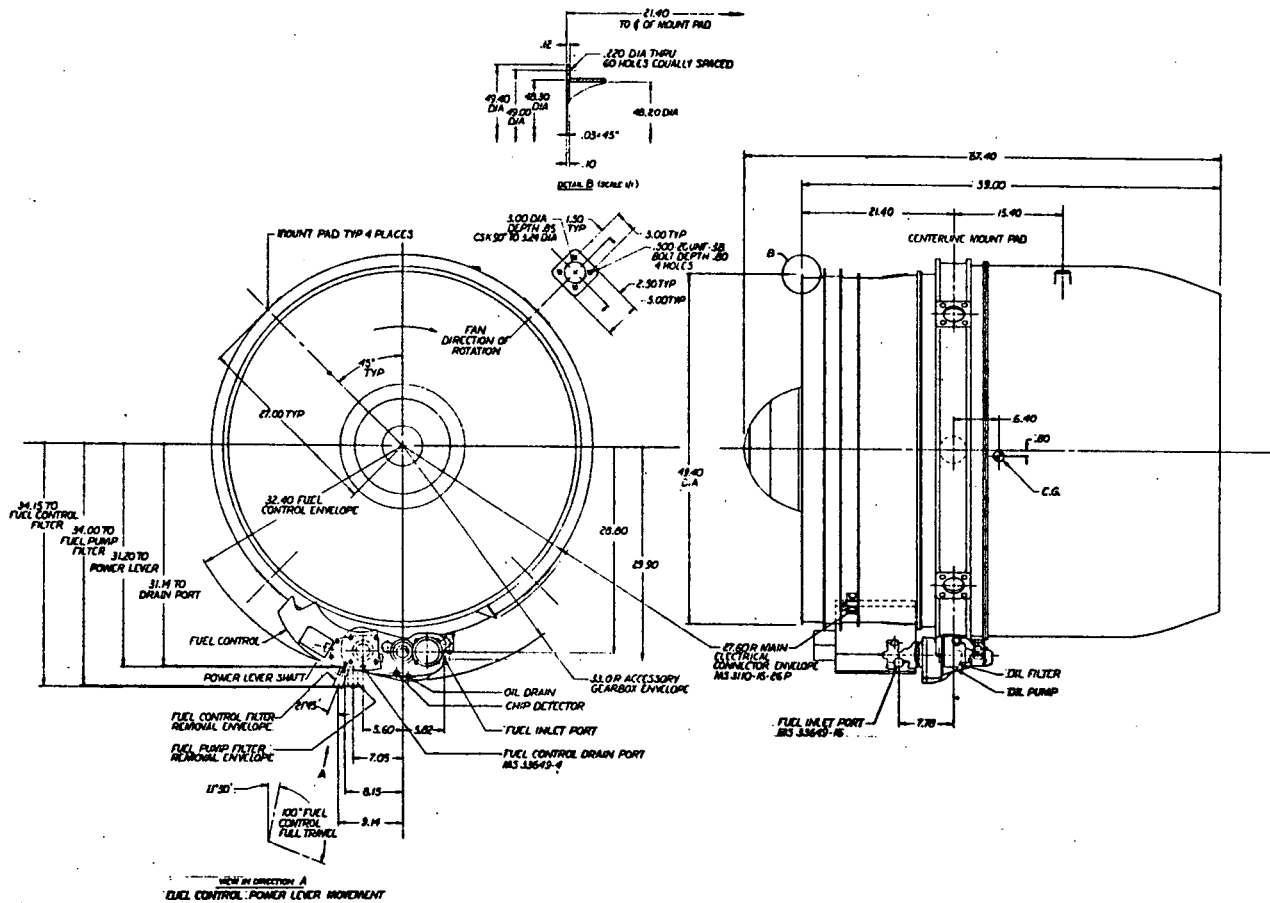


Figure 12. ALF-504 Fan Engine Installation Drawing.



Fan Wheel Limit Speed	5,600 rpm
Fan Wheel Maximum Speed	6,400 rpm (mandatory inspection required)
Power Turbine Power	6,240 hp (10 percent over SLS cycle value)

The geometry of the fan wheel is shown in Figure 13 with the material strengths and the corresponding stress and strain distributions for the blade and disc. These distributions are based on a constant temperature of 200° F and a speed of 5,245 rpm.

#### Disc

It is seen from Figure 13 that the stresses in the disc at the operational speed of 5,245 rpm are much lower than the allowable stresses and that the low-cycle-fatigue life, resulting from the disc strain distribution, is greater than  $10^5$  cycles. For the fan overspeed condition of 6,400 rpm, the low-cycle-fatigue life exceeds the design criterion of 20,000 cycles.

#### Rotor Blade

The blade stress distribution that is shown in Figure 13 is a result of the centrifugal loads developed from the fan speed of 5,245 rpm. The bending stresses in the blade due to gas loading have not been included. The anticipated bending stress is in the order of 40 ksi at the base of the blade and will exist only if the blade airfoil sections are stacked on a radial line from the hub to the tip. This blade will not be a stacked blade, but rather a leaned blade, and the centrifugal bending stresses resulting from the lean will be adjusted so that they will cancel the gas bending stresses. The ultimate result will be a blade stress distribution close to the distribution shown in Figure 13. The stacked set of airfoil sections is shown in Figure 14.

#### Midspan Shroud

The geometry of the midspan shroud is shown in Figure 15. Bending stresses due to centrifugal loads have been calculated at sections x-x and y-y for a radial shroud thickness of 0.14 inch. The values of these bending stresses are shown in Figure 15 along with the yield and ultimate strengths for the blade material, Ti-6Al-4V.

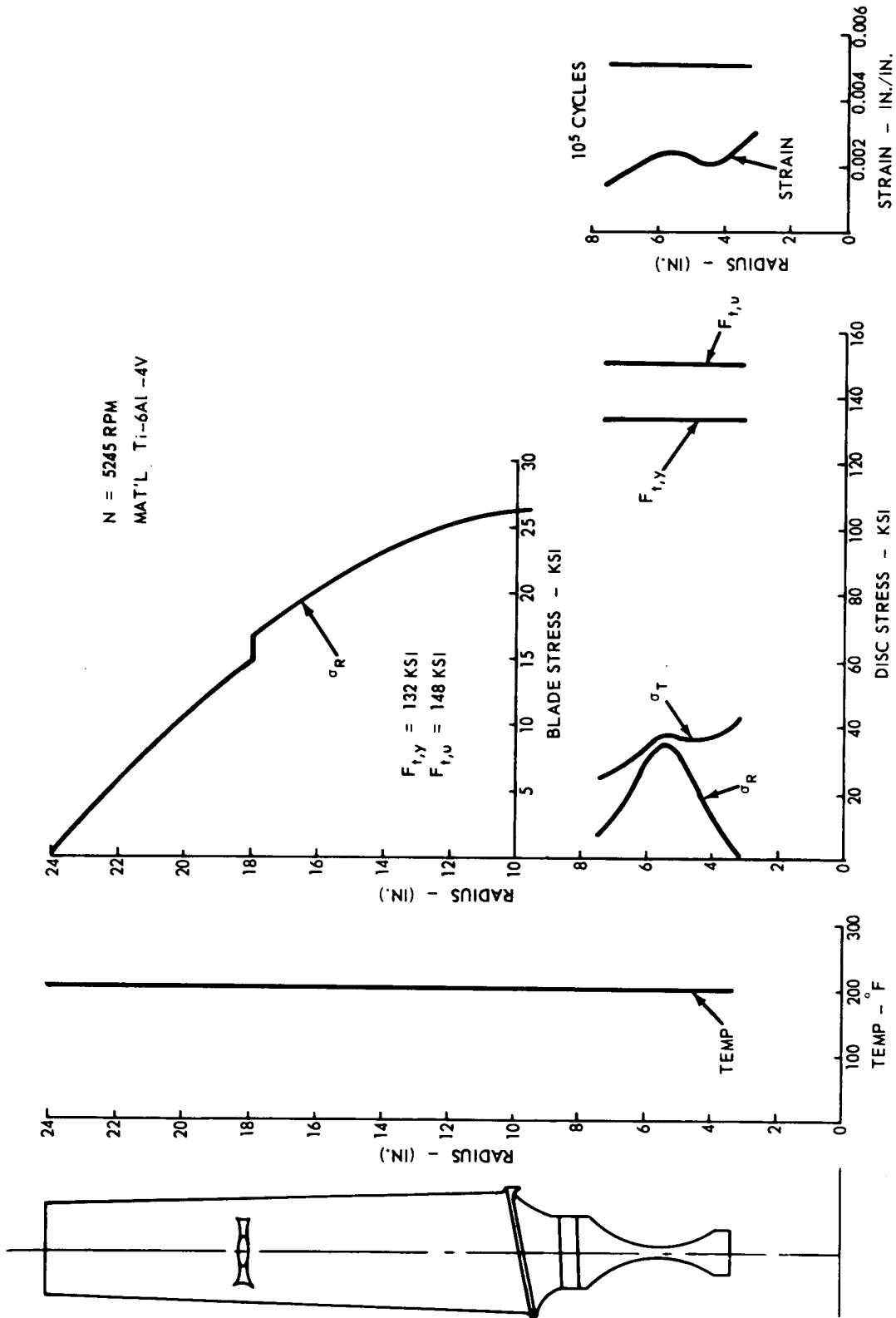


Figure 13. Fan Blade and Disc Stresses. (See Figure 16 for root stresses.).

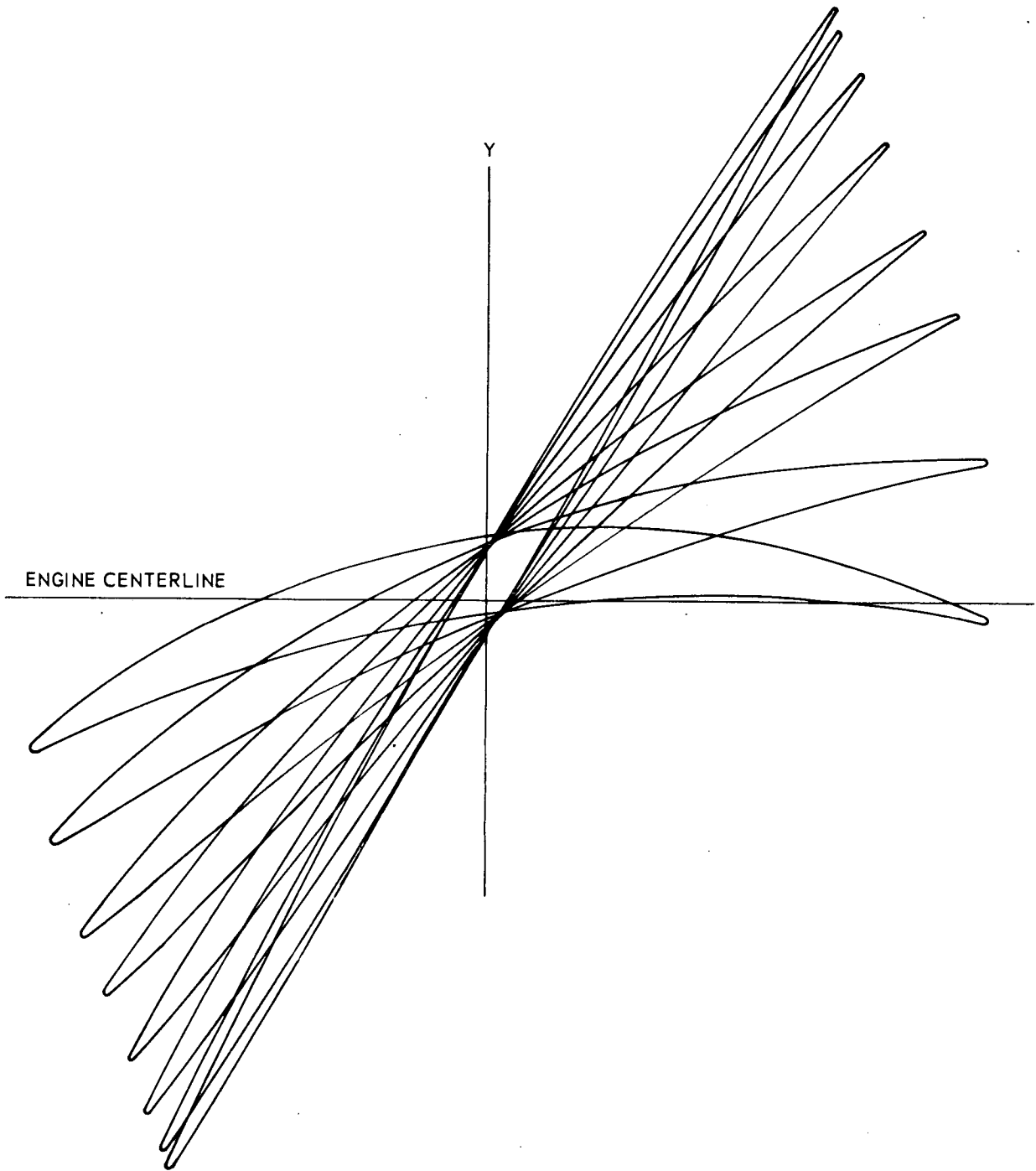


Figure 14. Fan Rotor Blade Airfoil Composite, Scale Approximately 2X.

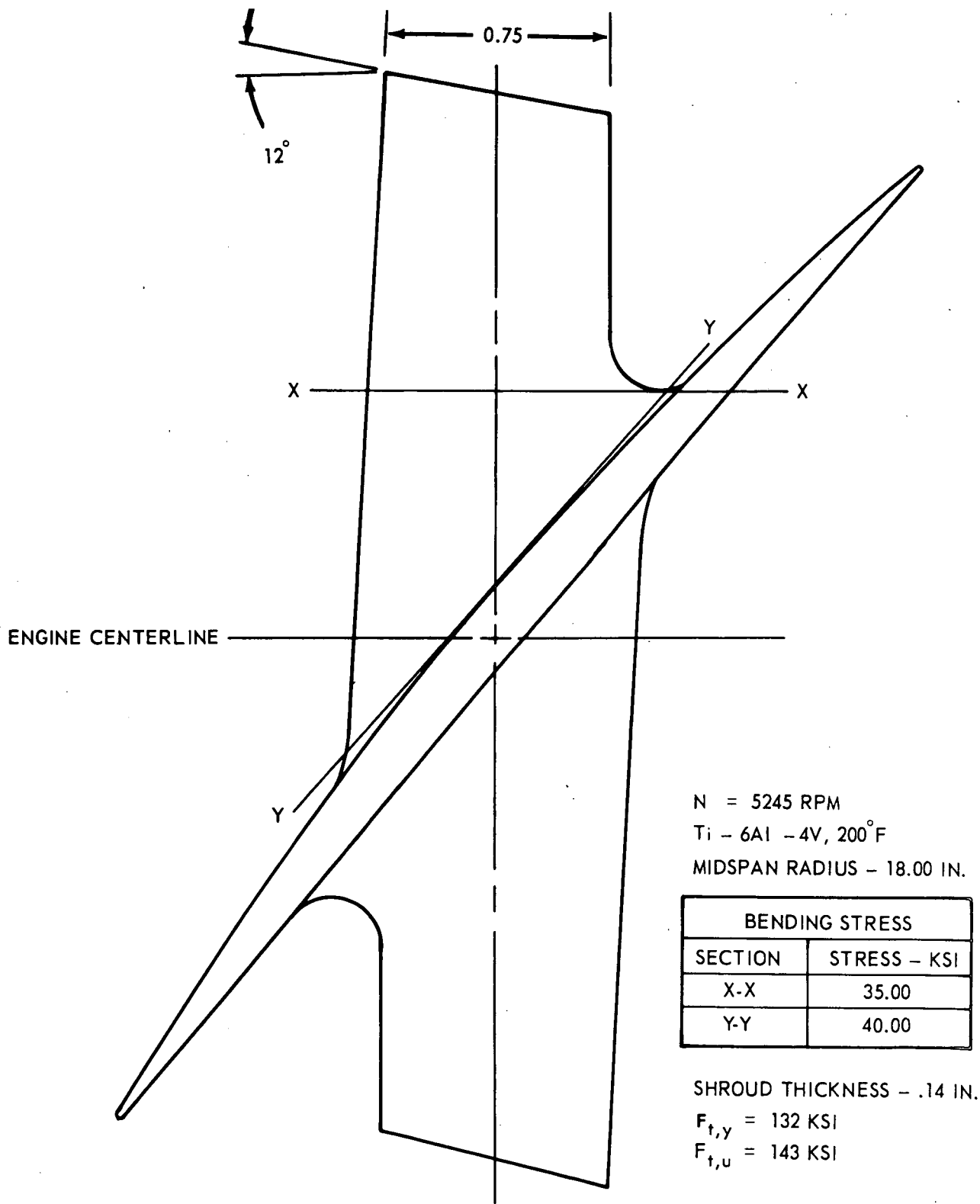


Figure 15. Midspan Shroud.

## Blade and Disc Root

The root and groove geometry shown in Figure 16 is the same as the dovetail that is used in the 502 core engine. The nominal and maximum tenon hoop stress and the nominal and maximum tenon tensile stress have been computed at the base of the root groove. The tenon tensile stress concentration factor is 3.8, and the tenon hoop concentration factor is 2.0. The stress values are tabulated in Figure 16, and the groove low-cycle-fatigue life resulting from these stresses is greater than  $10^5$  cycles.

## Gears

The new reduction gear train design (Figure 17) is similar in principle to that of the 502 engine. The reduction ratio has been increased from 2.30:1 for the 502 to 3.22:1 for the ALF-504 design. To transmit the additional torque, the gears were made larger in face width to operate within the allowable tooth bending stress required for infinite gear tooth life. The five planet gears are more critical in design than the sun gear since they operate under reversed bending loads; therefore, the maximum tooth bending stress was set at 28 ksi. The resulting planet gear face width is 2.61 inches, and the corresponding tooth compressive stress is 133 ksi with an allowable stress of 145 ksi.

The ring gear has been analyzed to determine the hoop stresses resulting from the loads applied by the five planet gears. The loads applied by each planet are the radial load  $W_r$ , the tangential load  $W_t$ , and the bending moment  $M$ . A hoop stress also exists because of the rotational speed  $W$  of 5,245 rpm. The hoop stress distributions over that segment of the ring between the planets are shown in Figure 18 for both the inside and outside surfaces. These four distributions are summed to obtain the total hoop stress distribution, and is shown in Figure 18. For the inside surface of the ring, the bending stress of  $\pm 28$  ksi at the base of the gear tooth has been added to the total hoop stress distribution, at points on each side of the ring gear tooth, meshed at each planet (see Figure 18). This is a conservative practice because both of these stresses do not occur at an exact point, but it has been done because they occur in the same plane.

Tabulated in Figure 18 are the maximum, minimum, mean, and alternating stresses for the inner and outer surfaces of the ring. Applying the alternating and the mean stresses to the modified Goodman diagram shown in Figure 19 it is seen that the ring gear stresses are well within the safe operating range.

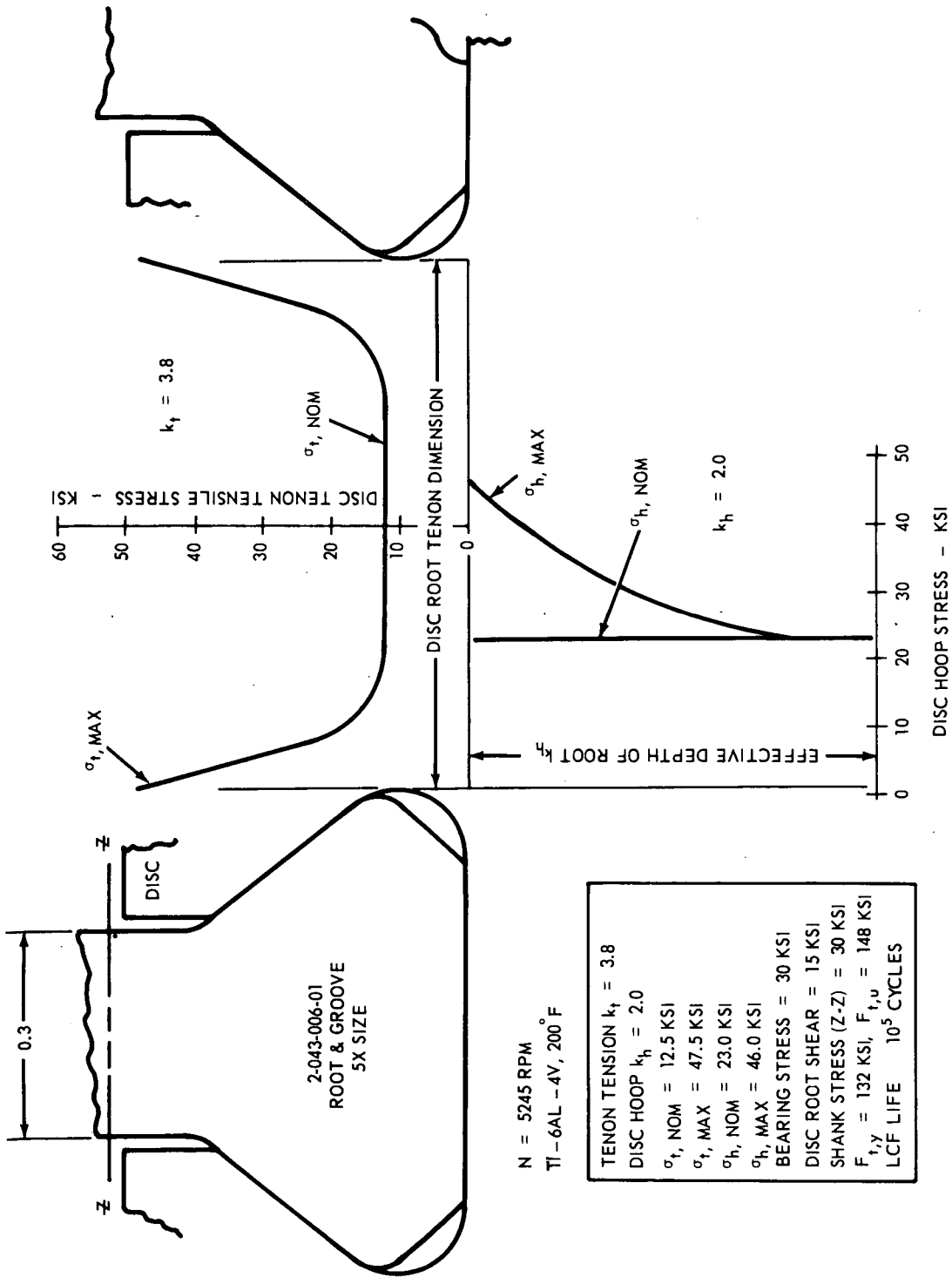


Figure 16. Root and Groove Stresses.



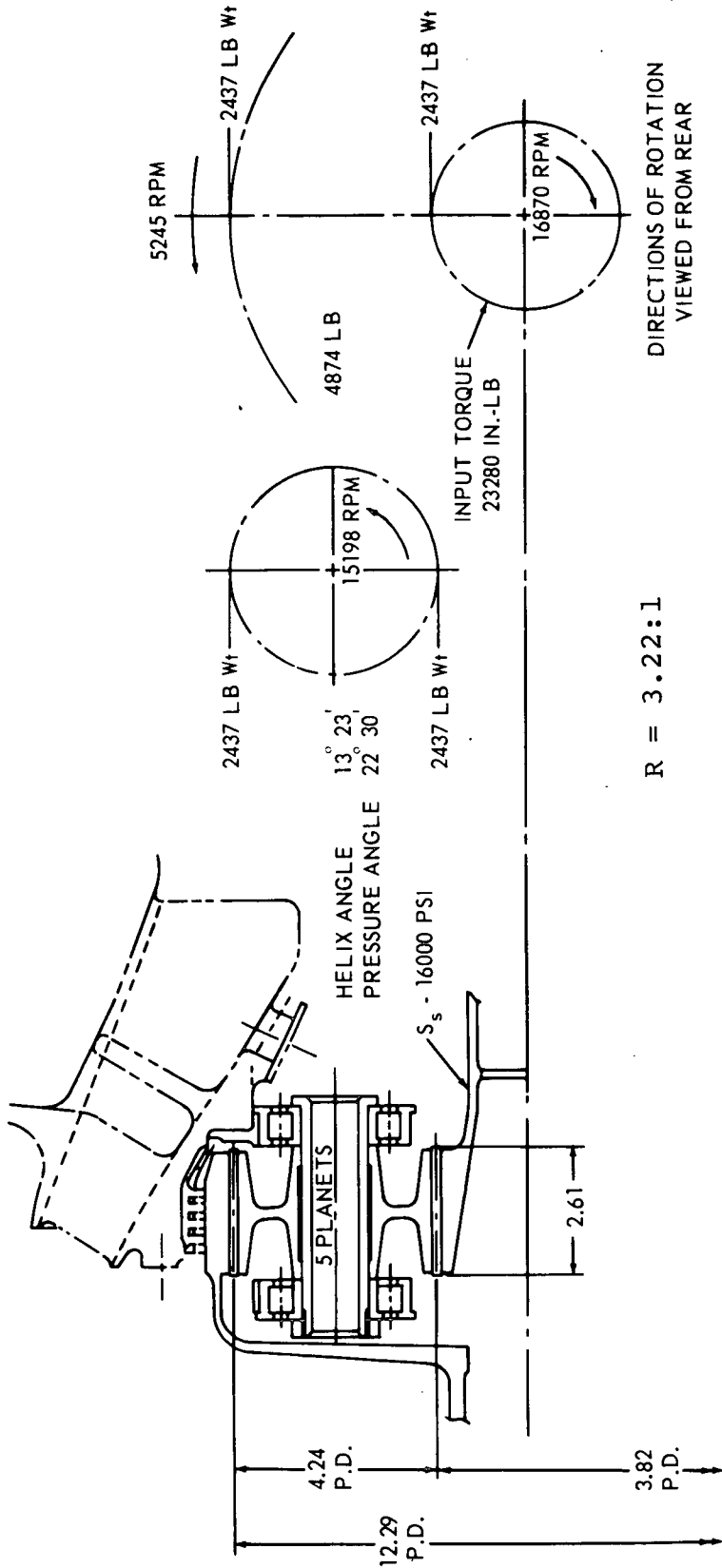


Figure 17. Reduction Gear.

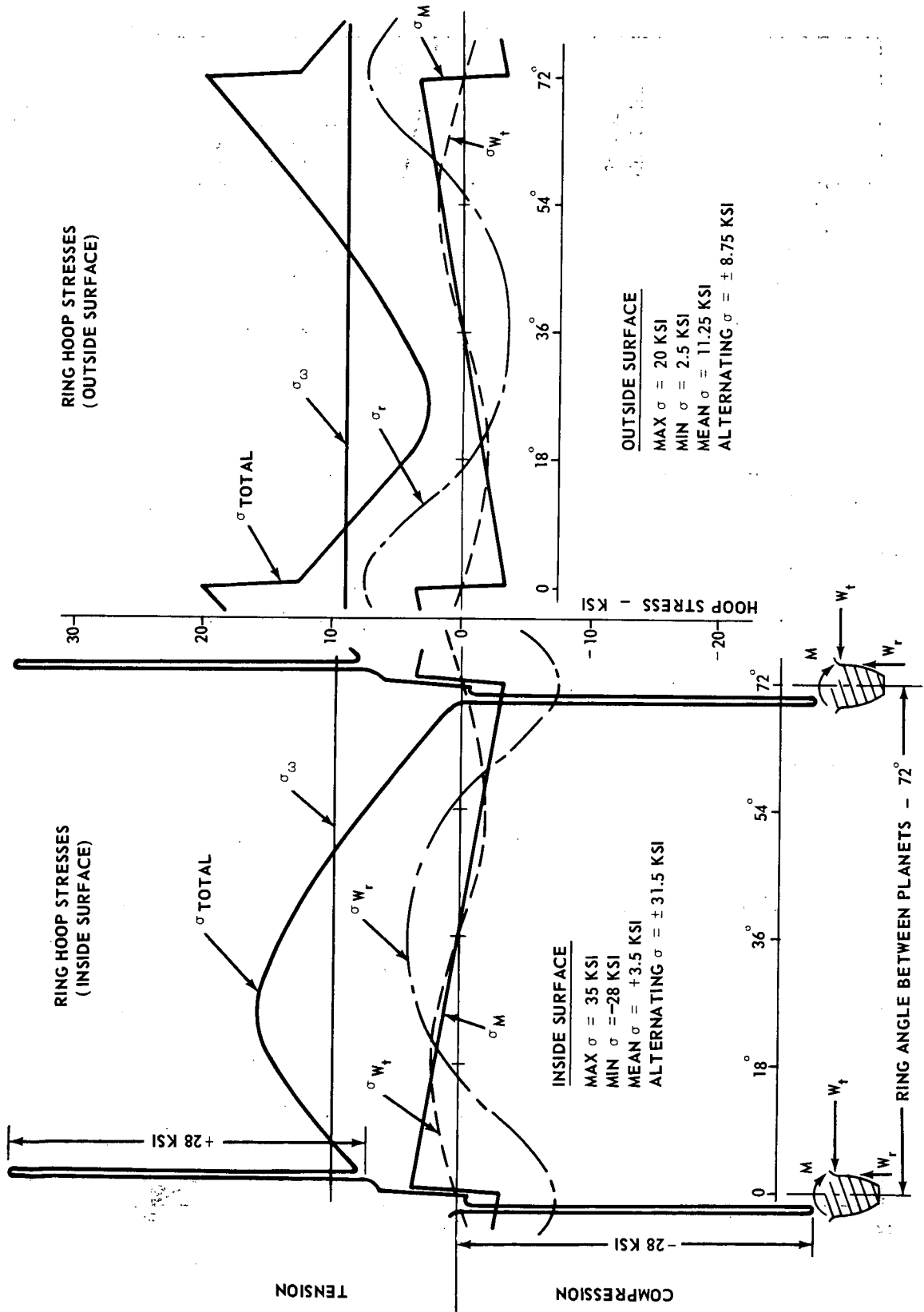


Figure 18. Ring Gear Stresses.

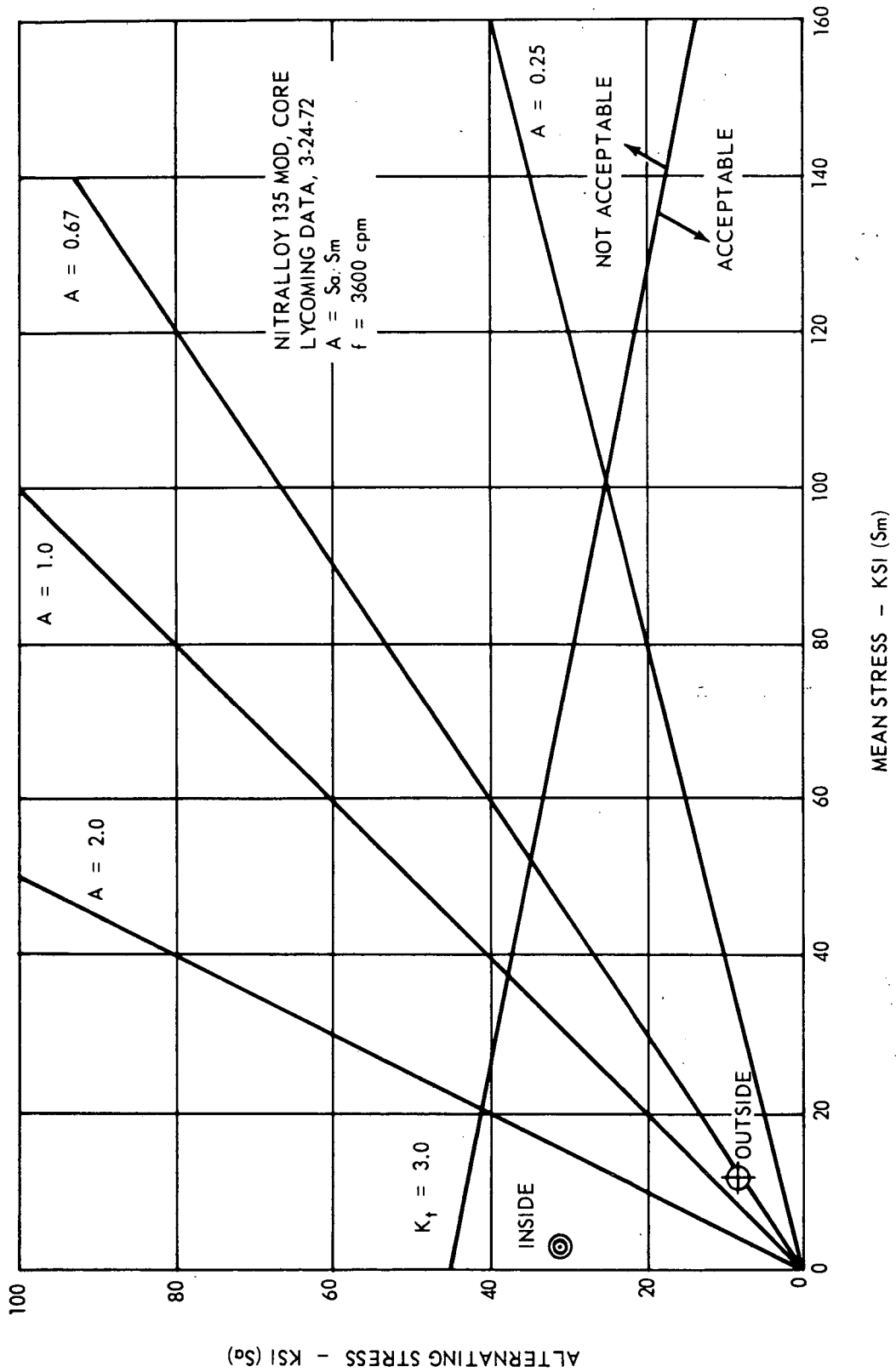


Figure 19. Reduction Gear Stress Analysis.

## Fan Housing and Support

The fan housing and front frame will be cast magnesium and includes the same design concepts as the 502 fan inlet housing. There are 12 struts, one of which contains the accessory drive and starter shaft.

Engine mounting is accomplished through three mount pads on the housing. The top two pads support the engine weight and transmit thrust through a yoke, while the third pad gives mounting stability to the system. Similarity of the housing design with that of the 502 fan engine insures an optimal mechanical design.

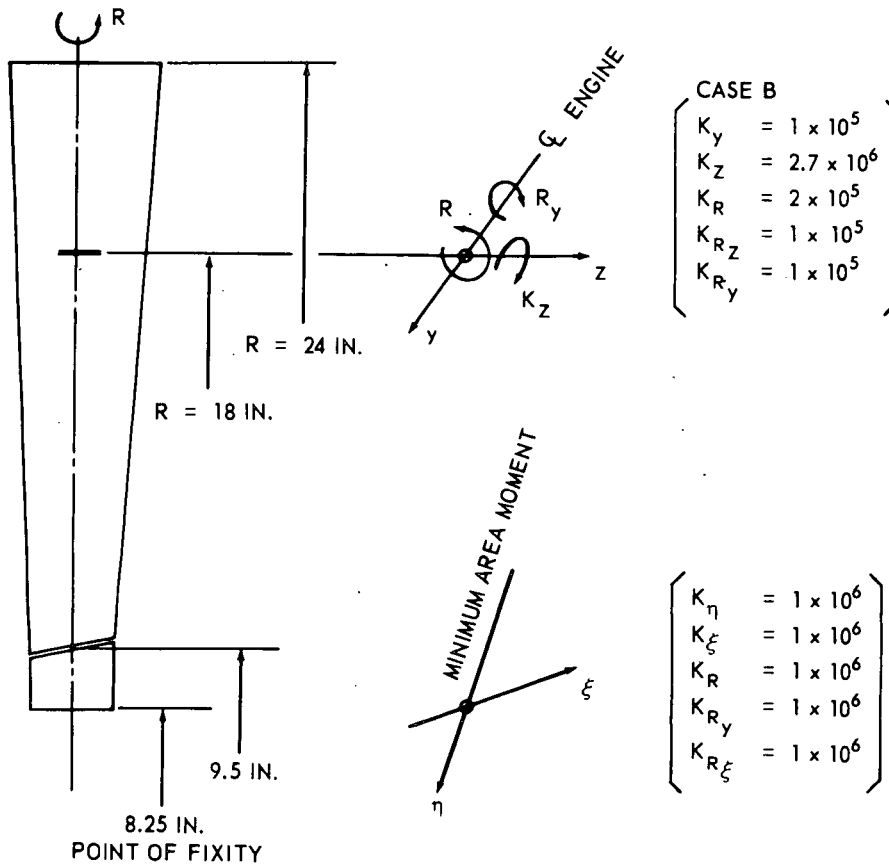
### Mechanical Design Study of Fan Duct Variable Area Nozzle

The variable area nozzle type selected is an iris construction made of two conically shaped and slotted members actuated by a contained air bladder mounted around the external circumference. The design concept and mechanical details are shown in Figure 11. The conical members are slotted to form individual fingers which permit the required deflection and necessary area reduction (from 1190 to 1045 square inches). The design of the nozzle is based on a two-position geometry, and "overshoot" is prevented by mechanical stops that are welded to the outer side of the nozzle wall. The bladder was chosen to provide the actuating mechanism because of its simplicity, the low temperature of the bypass duct, and the low force required to oppose the nozzle aerodynamic load (470 pounds radial and 250 pounds axial). Air pressure to inflate the bladder is supplied from the compressor or fan when the flight Mach number exceeds 0.4. The nozzle will automatically go to the open position (the fail-safe position) in the event of bladder failure and prevent fan surge at flight Mach number above 0.4.

## DYNAMIC ANALYSIS

### Vibration and Flutter Analysis of the Rotor Blade

**General.** - For the analysis, the fan blade is represented by a lumped mass model that is supported at the base (cantilevered), and partially restrained at a part-span shroud location. The sketch below shows the system of axes used in the analysis:



MATERIAL: TITANIUM  
 MODULUS OF ELASTICITY = 0.163 LB/IN.<sup>3</sup>  
 $E = 15 \times 10^6$  LB/IN.<sup>2</sup>  
 SHEAR MOD.  $G = 6.5 \times 10^6$  LB/IN.<sup>2</sup>

NUMBER OF BLADES  
 $Z = 32$   
 100% SPEED  
 $N = 5245$  RPM  
 WEIGHT OF BLADE  
 $W = 1.42$  LB

A transfer matrix method (Lycoming library program D105) \* is used to calculate the natural bending and torsional frequencies (uncoupled). In the analysis, the part-span shroud location was varied in order to find the optimum frequencies for a blade to be free from resonances and flutter. The trend of frequencies is shown in Figure 20. For the selected shroud location R = 18.0 inches, the frequencies are shown in the Campbell diagram in Figure 21. The shroud is 0.75 inch wide and 0.14 inch thick, and is cut at midspan (12 degrees with engine axis) to produce locking and prevent clockwise rotation looking down from tip to hub.

Results of Vibration Analysis. - In Figure 21, a band for the first two frequencies is given to indicate the influence of different spring-restraint conditions at the shroud (case A and B) because of some uncertainty in its prediction.

The first bending frequency is principally free from resonance excitation of low order (first, second, and third engine orders) above 80 percent speed. There is no fixed source of excitation in a fan inlet, but it is known from experience that inlet distortions could contain second or third order sources. The fan has to operate at speed below 80 percent and, therefore, experimental test verification is recommended to determine a tolerable stress limit in the blade.

The first torsion frequency also is free of direct intersection at 100 percent speed. No fifth or sixth order of engine excitation are apparent, and the torsion mode will be free from resonances in its range of operation.

Aeroelastic Analysis of Rotor Blades - The aeroelastic behavior of the blade is judged by the flutter coefficients represented in the form of

$$\lambda = \frac{W}{2\pi f c}$$

where W = relative inlet velocity  
f = blade frequency  
c = blade chord

---

\* Appendix III gives a more complete engineering development.

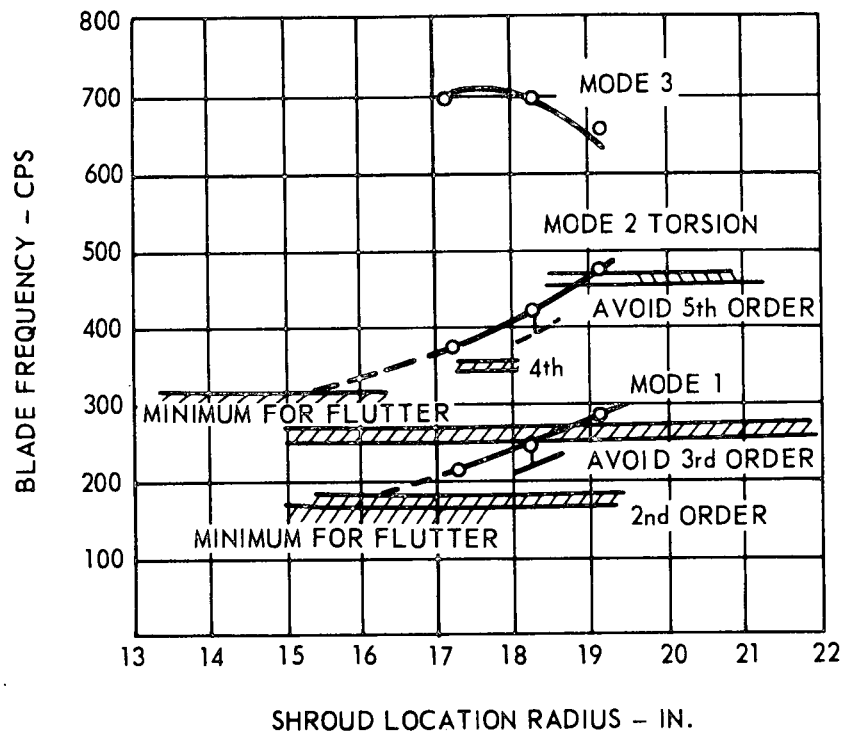


Figure 20. Rotor Blade Frequency Analysis, N = 5245 RPM.

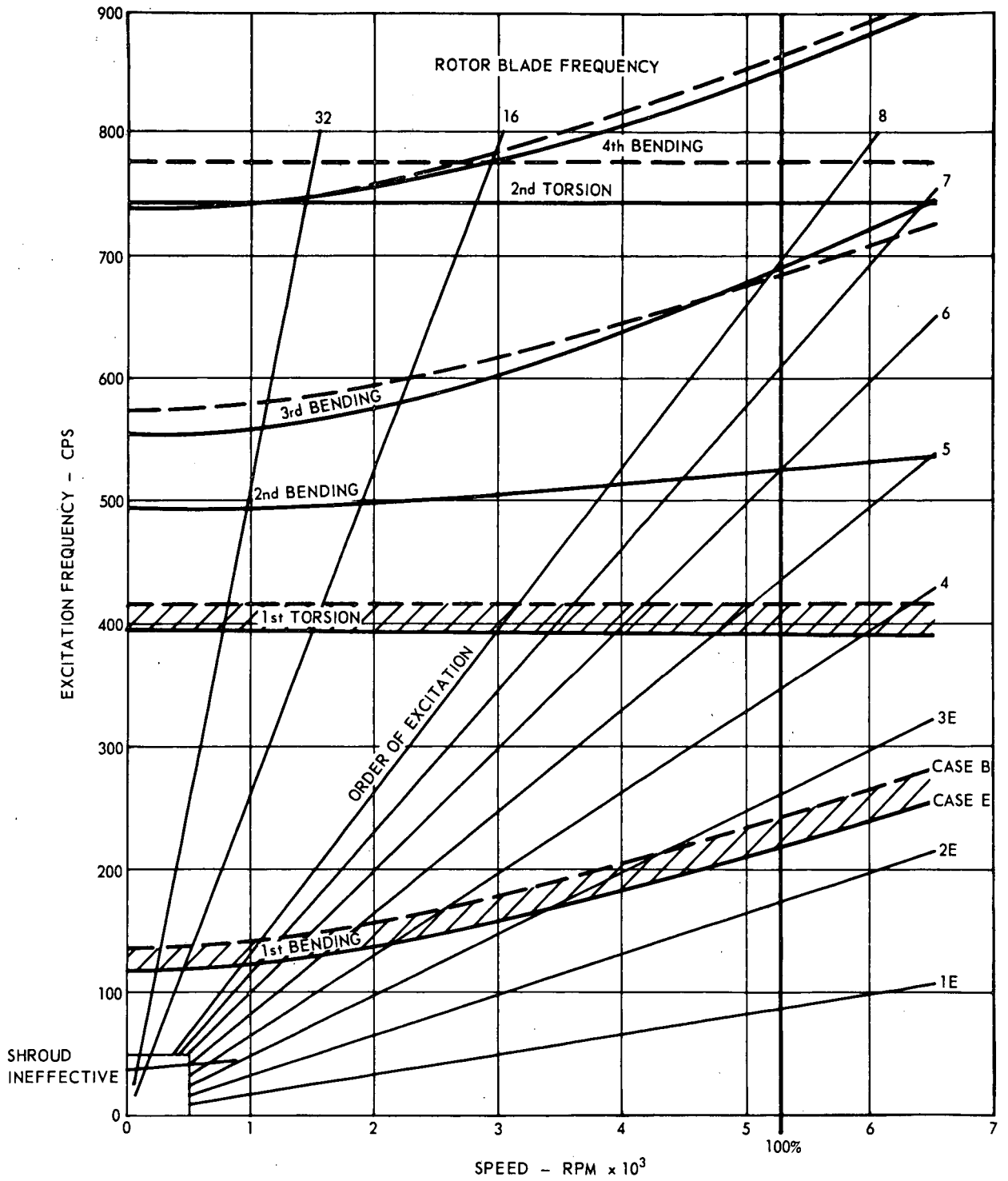


Figure 21. Rotor Blade Vibration Interference Diagram.



Speed (rpm)	%	Relative Flow Vel		Stagger Angle (deg)	Flow Angle (deg)	Frequency		Flutter Coeff.	
						Bend	Tors.	Bending	Tors.
5245	100	Tip	1234	58.6	60.7	240	418	1.93	1.1
		3/4 Span	1127 ft/sec	54	57.5	240	418	1.908	1.04

In Figure 22 the values of the flutter coefficient for the blade 3/4 span are plotted against a limit that is obtained from publications and Lycoming test data. A satisfactory safety margin exists for a shrouded blade even if some uncertainty in the data exists.

### Critical Speed Calculation

Power Train Torsion. - The power-train system from the fan to the power turbines is represented by lumped inertias that are connected by flexible elements. By a transfer matrix-type calculation (Lycoming Library program D112) \* the natural frequencies of the system are determined. There is one natural frequency of  $N_{T_1} = 6060$  cpm for the turbine shaft (36 percent speed) in the operating range where the fan rotor oscillates against the power turbines. The system and its corresponding mode shape are shown in Figure 23. The second mode occurs at  $N_{T_2} = 31,200$  cpm (185 percent design speed).

The sources of excitation originate in the reduction gearing from faulty meshing. Experience has shown that these torsional excitation forces are very small and of no threat to the system.

Fan Module Lateral Vibrations. - A lumped mass model of three levels is employed to calculate the lateral natural frequencies of the fan module and are found by the use of Lycoming program D103 \*. It is assumed that the important lateral vibrations of the fan module occur uncoupled from the core engine (Figure 24).

The fan rotor introduces inertial stiffening against the lateral motion. Only one-half of the inertia is used to account for the flexibility of the blades. The support stiffness in the core is calculated as a shell

\* See Appendix III for more complete analysis.

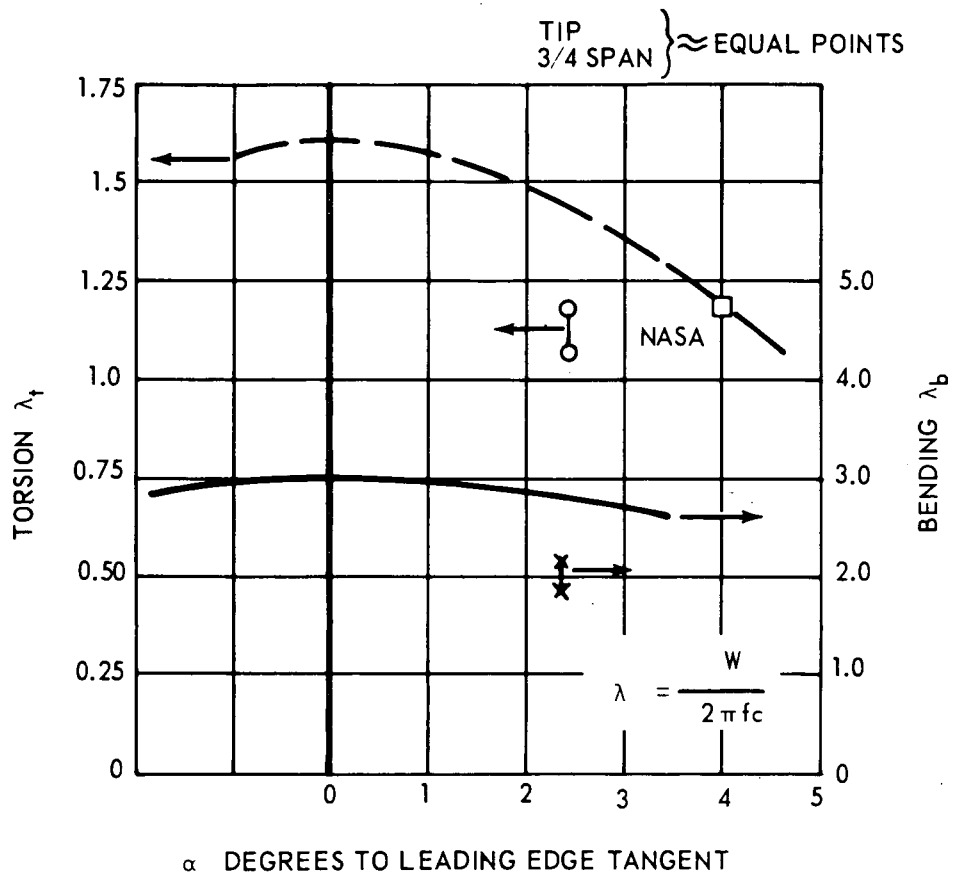


Figure 22. Rotor Blade Flutter Criteria.

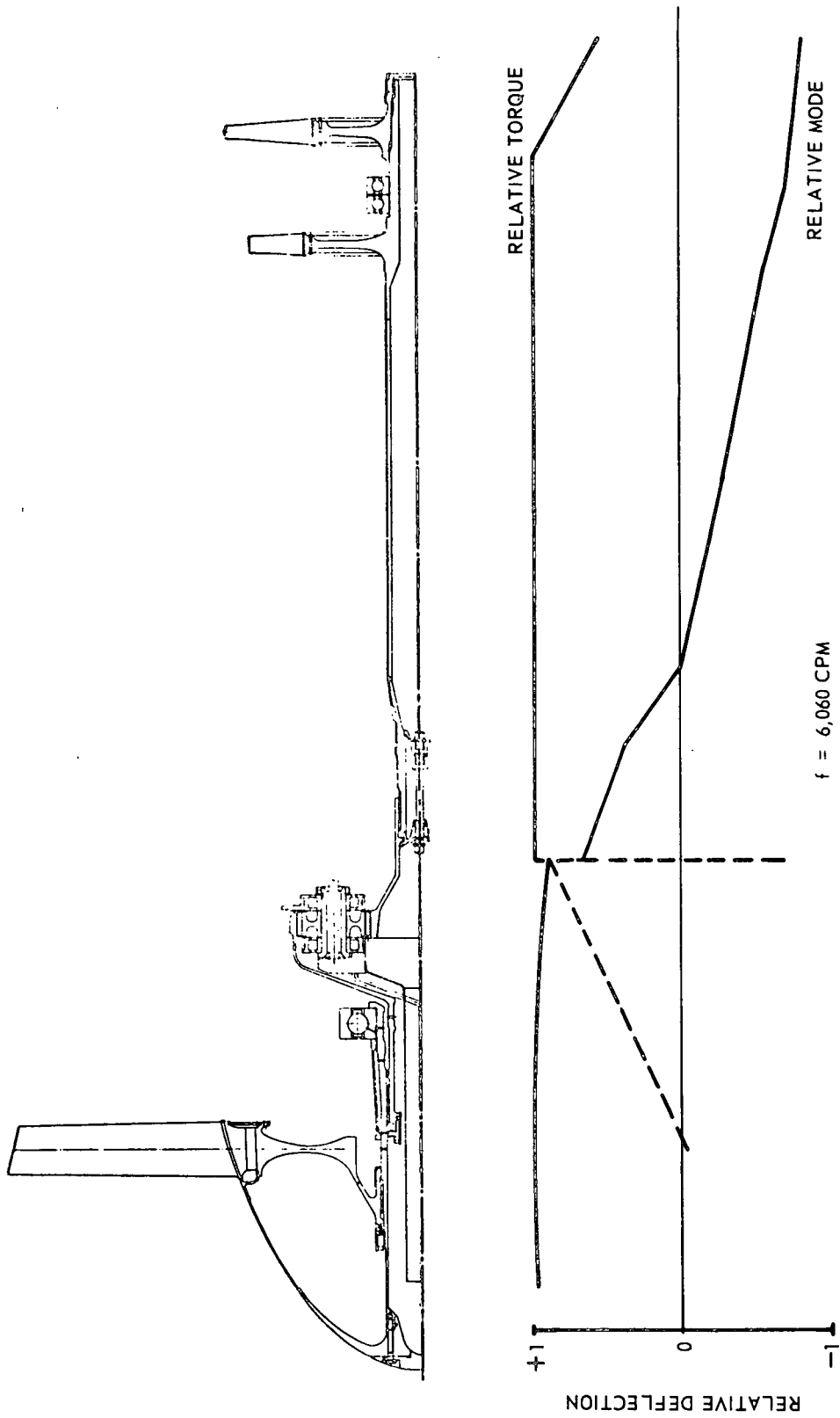


Figure 23. Fan-Power Turbine Torsion Analysis.

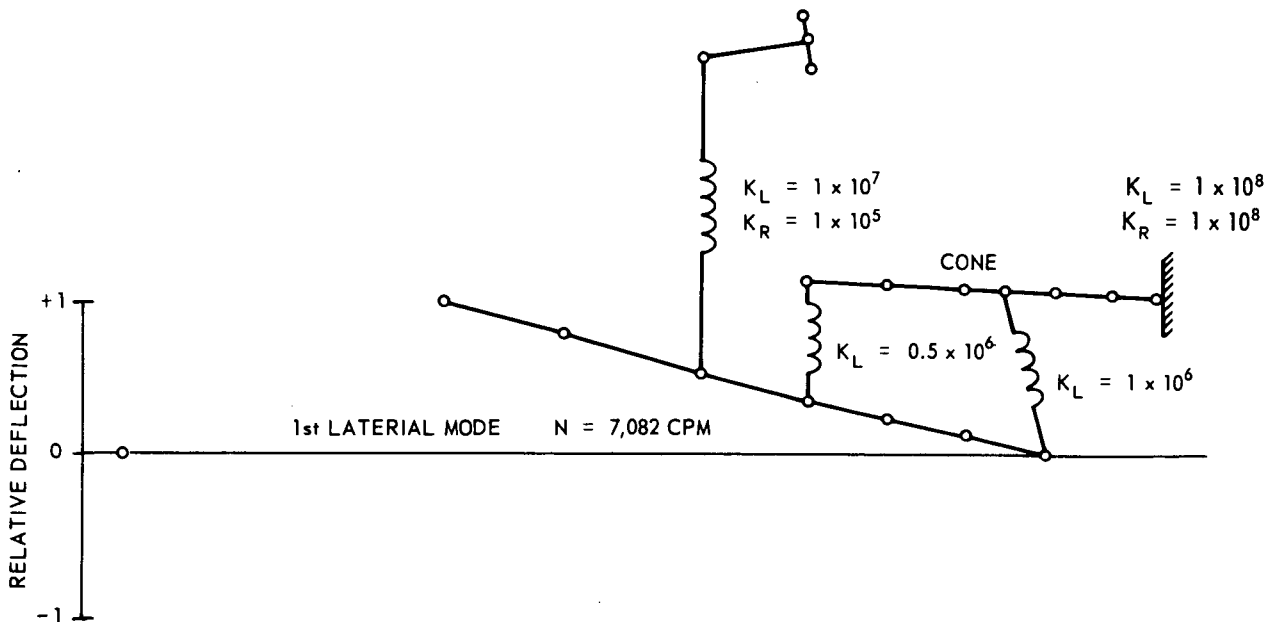
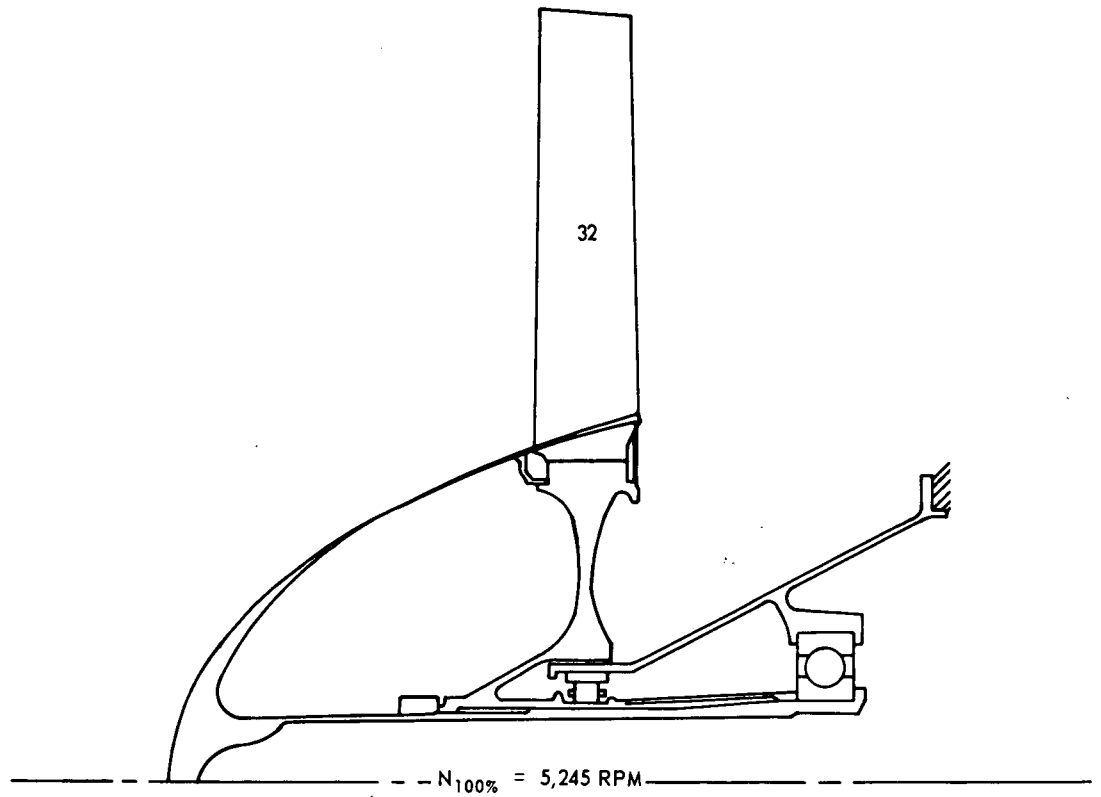


Figure 24. Fan Rotor Deflection.

structure and conservative numbers are used. For the flexibilities of the bearings, represented as lateral springs, conservative values have been taken. The calculated natural frequency, therefore, should represent a lower bound. The mode shape is shown in Figure 24 and it would occur at the first fan shaft critical  $N_1 = 7,082 \text{ rpm} = 135 \text{ percent}$  operating speed.

There should be no problem from excitation resulting from unbalances, and aerodynamic excitations from the inlet are unlikely to cause resonance problems.

## NOISE ANALYSIS

### Fan Noise

Noise generated by the fan is governed by the tip speed of the fan, the mass flow, and the spacing of the stator and rotor. The spectrum of the noise is determined by the number of fan blades and their chord length. The noise propagation is governed by the ratio of stator vanes to rotor blades, and the duct aspect ratio.

The noise was estimated by the modified "Smith and House" (2) method, which yields the pure tone and broad band noise for subsonic fans. Analysis for this fan for 500-foot sideline conditions gave a maximum perceived noise level (PNL) of 98.6 PNdB at 70 degrees from the inlet. The method, modified, by Avco Lycoming, is based on the experimental results derived from PLF 1A and 502 fan tests. The correlation with measured data is within  $\pm 2 \text{ dB}$  over the spectrum.

### Core Engine Noise

The contribution of the compressor to the total noise is based on test data for the T55-L-11A. The turbine noise was computed because this is the new design and test data are not available.

### Exhaust Noise

Exhaust noise was computed on the basis of the "Kobrinsky" (3) method. Since the exhaust velocities for the core are high, (above 800 ft/sec) no corrections for combustor noise were made.

## Total Noise Without Suppression

The noise generated by the engine was computed for a 500-foot polar and sideline (Tables IV and V). In the extrapolation of the data to 500 feet from 200 feet, only atmospheric attenuation was applied in addition to increase square law attenuation.

The maximum unsuppressed PNL is 106.1 PNdB at 130 degrees from the inlet. The maximum sideline noise is 104.5 PNdB at 100 degrees. The predicted sideline perceived level (SPL) spectrum at 200 feet is shown in Tables VI and VII.

## Bypass Duct Acoustical Treatment

Since the maximum engine noise is in the rear quadrant and the maximum contribution to the PNL is by the fan, the treatment of the bypass duct will reduce the noise levels in the rear quadrant.

The analysis of the bypass duct assumed equal spacing between the two splitter rings in the duct. The duct height is 3.5 inches and the flow Mach number is 0.514. In order to maximize the attenuation at the blade passage frequency of 2850 hertz, the backing depth of 0.5 inch was chosen. An attempt was made to optimize the impedance of the treatment with a perforated plate, but sufficient flow resistance could not be achieved for optimum design. Hence, reinforced plastic material was selected. The face material finally selected is fiber-glass cloth impregnated with a polyimid resin with flow resistance required of 3 rayls (MKS). The backing is 0.125 inch, hexcel 0.5 inch deep. The impervious layers are also of the fiber-glass construction.

The assumptions made in the calculations of the attenuation were two-fold: (1) the sound pressure is evenly distributed at the inlet to the splitter, and (2) the calculation is made for the least attenuated mode. The results of the duct treatment are shown in Table VIII.

TABLE IV. INTEGRAL LIFT ENGINE SIDELINE PERCEIVED NOISE LEVEL AT 500 FEET		
Degrees From Inlet	Treated Bypass Duct (PNL, dB)	Untreated Bypass Duct (PNL, dB)
20	85.0	85.0
30	91.5	91.4
40	94.5	94.4
50	96.8	96.8
60	97.3	97.2
70	97.7	97.8
80	96.6	97.6
90	97.1	100.6
100	95.7	102.6
110	97.0	104.5
120	95.4	104.2
130	96.1	103.1
140	93.1	99.9
150	93.1	96.3
160	86.9	89.0

TABLE V. INTEGRAL LIFT ENGINE POLAR PERCEIVED NOISE LEVEL AT 500 FEET		
Degrees From Inlet	Treated Bypass Duct (PNL, dB)	Untreated Bypass Duct (PNL, dB)
0	97.3	97.2
10	98.5	98.5
20	98.9	98.9
30	100.0	99.9
40	99.8	99.7
50	99.9	99.9
60	98.9	98.9
70	98.4	98.5
80	96.7	97.8
90	97.1	100.6
100	95.9	102.8
110	97.7	105.2
120	96.9	105.9
130	99.0	106.1
140	98.0	105.0
150	100.5	104.3
160	98.5	101.8

Reproduced from  
best available copy.

TABLE VI. POLAR NOISE FIELD, UNTREATED BYPASS DUCT

FREQ	NASA 1.25 FAN, 8375 LB. THRUST										POLAR COMBINED SOUND LEVELS										DEGREES					POLAR FIELD							
	7.0	10.0	20.0	30.0	40.0	50.0	60.0	70.0	80.0	90.0	100.0	110.0	120.0	130.0	140.0	150.0	160.0	7.0	10.0	20.0	30.0	40.0	50.0	60.0	70.0	80.0	90.0	100.0	110.0	120.0	130.0	140.0	150.0
20.0	70.3	70.3	68.2	70.2	68.1	68.6	65.3	67.5	65.9	68.4	66.9	67.9	69.0	74.4	75.8	80.7	81.0	73.1	73.0	72.4	70.2	70.7	67.6	69.8	69.4	70.9	69.7	72.8	72.2	77.4	79.0	83.1	83.0
25.0	73.1	73.0	70.7	72.4	70.2	72.7	69.7	72.0	70.6	73.3	72.1	75.3	74.7	79.0	81.2	85.1	84.7	75.6	75.2	74.4	75.9	73.3	74.2	71.3	72.3	75.1	73.9	77.2	76.6	81.6	82.6	86.5	85.9
31.5	75.6	75.2	72.9	74.4	72.0	74.7	69.7	72.0	70.6	73.3	72.1	75.3	74.7	79.0	81.2	85.1	84.7	77.4	77.0	74.4	75.9	73.3	74.2	71.3	72.3	75.1	73.9	77.2	76.6	81.6	82.6	86.5	85.9
40.0	77.4	77.0	74.4	75.9	73.3	76.2	71.3	73.7	72.3	75.1	73.9	77.2	76.6	77.9	82.6	87.3	86.6	78.0	78.4	76.8	74.2	75.2	72.5	74.9	73.5	76.4	75.3	70.6	77.9	82.6	87.3	90.6	87.3
50.0	78.4	78.0	75.4	76.8	74.2	76.7	71.3	73.7	72.3	75.1	73.9	77.2	76.6	77.9	82.6	87.3	86.6	79.7	79.9	78.4	75.8	76.7	74.2	76.6	75.3	78.2	77.2	80.3	79.7	84.1	84.8	88.6	87.3
63.0	79.9	79.4	76.8	78.1	75.5	76.7	71.3	73.7	72.3	75.1	73.9	77.2	76.6	77.9	82.6	87.3	86.6	80.0	80.5	78.4	75.8	76.7	74.2	76.6	75.3	78.2	77.2	80.3	79.7	84.1	84.8	88.6	87.3
80.0	80.7	80.2	77.6	79.0	76.3	77.7	71.3	73.7	72.3	75.1	73.9	77.2	76.6	77.9	82.6	87.3	86.6	81.0	81.6	79.4	76.8	77.7	75.2	77.6	76.3	79.2	78.2	81.3	80.7	85.1	85.8	89.5	88.5
100.0	81.0	80.5	77.9	79.2	76.6	78.1	71.3	73.7	72.3	75.1	73.9	77.2	76.6	77.9	82.6	87.3	86.6	82.0	82.7	80.3	77.7	78.7	76.8	79.2	77.9	80.9	80.0	83.1	82.4	86.8	87.1	90.4	89.1
125.0	81.4	80.9	78.4	79.7	77.1	78.7	71.3	73.7	72.3	75.1	73.9	77.2	76.6	77.9	82.6	87.3	86.6	83.0	83.7	81.1	78.5	79.8	77.8	80.3	79.0	82.0	81.2	84.3	83.5	87.4	87.6	91.2	89.7
160.0	82.2	81.7	79.1	80.6	77.9	79.5	77.7	80.2	78.9	82.0	81.2	84.3	83.4	83.9	87.2	87.1	86.9	84.0	84.7	82.1	79.5	80.8	78.9	82.0	80.7	83.7	82.9	86.0	85.1	88.9	89.2	93.0	91.5
200.0	81.6	81.2	78.7	80.1	77.7	79.7	78.1	80.5	79.3	82.4	81.7	84.6	83.9	84.3	87.6	87.5	87.4	85.0	85.7	83.1	80.5	81.8	79.9	82.9	82.2	85.1	84.3	87.4	86.4	90.4	89.9	93.7	92.2
315.0	81.6	81.2	78.7	80.1	77.7	79.7	78.1	80.5	79.3	82.4	81.7	84.6	83.9	84.3	87.6	87.5	87.4	85.0	85.7	83.1	80.5	81.8	79.9	82.9	82.2	85.1	84.3	87.4	86.4	90.4	89.9	93.7	92.2
400.0	81.2	80.9	78.5	80.1	77.7	79.0	78.6	81.1	79.8	82.9	82.3	85.3	84.5	84.9	88.2	88.1	88.0	85.6	86.3	83.7	81.1	82.4	80.5	83.5	82.8	85.7	84.9	88.0	87.0	90.9	90.4	94.7	93.2
500.0	80.2	80.0	77.2	78.5	77.4	79.6	78.4	80.7	79.5	82.7	82.2	85.1	84.4	84.8	88.1	88.0	87.9	85.5	86.2	83.6	81.0	82.3	80.4	83.4	82.7	85.6	84.8	87.9	86.9	90.8	90.4	95.1	93.6
630.0	79.8	79.3	76.2	77.7	77.1	79.9	78.9	80.9	79.8	83.0	82.9	85.6	84.4	84.8	88.1	88.0	87.9	85.5	86.2	83.6	81.0	82.3	80.4	83.4	82.7	85.6	84.8	87.9	86.9	90.8	90.4	95.1	93.6
800.0	79.4	79.7	79.7	80.1	79.1	80.5	79.5	81.0	80.0	83.2	83.7	86.4	85.2	85.6	88.9	88.8	88.7	86.4	87.1	84.5	81.9	83.2	81.3	84.3	83.6	86.5	85.8	88.9	87.9	91.8	91.4	96.1	94.6
1000.0	79.1	79.9	79.9	81.1	80.7	81.4	80.5	81.2	80.3	83.5	84.9	87.4	87.8	87.4	90.7	90.6	90.5	88.1	88.8	86.2	83.6	84.9	83.0	86.0	85.3	88.2	87.5	90.4	89.4	93.3	92.9	97.6	96.1
1250.0	79.7	81.0	81.7	82.7	82.9	82.9	82.1	82.0	81.4	84.5	86.7	89.1	89.8	89.5	92.8	92.7	92.6	90.2	90.9	88.4	85.7	87.0	85.1	88.1	87.4	90.3	89.6	93.5	93.2	98.0	97.5	102.7	101.2
1600.0	80.9	82.4	83.3	84.3	84.5	84.4	83.6	83.1	82.6	85.7	88.3	90.7	91.5	91.2	94.5	94.4	94.3	91.9	92.6	90.4	87.7	89.0	87.1	90.1	89.4	92.3	91.6	95.4	95.1	100.0	99.5	104.7	103.2
2000.0	81.4	83.2	84.4	85.3	85.5	85.3	84.5	83.7	83.2	86.4	89.3	91.6	92.6	92.1	95.4	95.3	95.2	92.8	93.5	91.3	88.6	90.0	88.1	91.1	90.4	93.3	92.6	96.4	96.1	101.0	100.5	105.7	104.2
2500.0	81.7	83.5	84.8	85.6	86.0	85.7	84.9	83.9	83.5	86.6	89.7	92.0	93.0	92.4	95.7	95.6	95.5	93.3	94.0	91.8	89.1	90.5	88.6	91.6	90.9	93.8	93.1	96.9	96.6	101.5	101.0	106.7	105.2
3150.0	82.5	84.4	85.7	86.5	86.9	86.6	85.8	84.6	83.9	87.1	90.0	92.3	93.3	92.8	96.0	95.9	95.8	93.6	94.3	92.1	89.4	90.8	88.9	91.9	91.2	94.1	93.4	97.2	96.9	101.6	101.1	106.8	105.3
4000.0	82.5	84.4	85.7	86.5	86.9	86.6	85.8	84.6	83.9	87.1	90.0	92.3	93.3	92.8	96.0	95.9	95.8	93.6	94.3	92.1	89.4	90.8	88.9	91.9	91.2	94.1	93.4	97.2	96.9	101.6	101.1	106.8	105.3
5000.0	77.1	79.9	80.2	81.1	81.5	81.2	80.3	79.3	78.8	81.7	84.6	87.4	88.7	88.4	91.7	91.6	91.5	89.3	90.0	87.8	85.1	86.5	84.6	87.6	86.9	89.8	89.1	92.9	92.6	97.6	97.1	102.8	101.3
6300.0	80.1	82.0	83.3	84.2	84.5	84.2	83.4	81.8	80.4	80.8	82.4	84.4	85.2	84.7	88.0	87.9	87.8	85.6	86.3	84.1	81.4	82.8	80.9	84.0	83.3	86.2	85.5	89.3	89.0	93.8	93.5	98.6	98.1
8000.0	72.3	74.1	75.4	76.3	76.6	76.4	75.5	74.5	73.7	75.8	78.1	80.2	81.1	80.7	84.0	83.9	83.8	81.6	82.3	80.1	77.4	78.8	76.9	80.0	79.3	82.2	81.5	85.3	85.0	90.0	89.7	94.8	94.5
10000.0	71.4	73.3	74.6	75.5	75.8	75.5	74.6	73.5	72.6	74.6	76.7	78.8	79.7	79.2	82.5	82.4	82.3	80.3	81.0	78.8	76.1	77.5	75.6	78.7	78.0	80.9	80.2	84.0	83.7	88.6	88.3	93.7	93.4
12500.0	76.8	78.7	80.1	80.9	81.3	80.9	80.1	78.4	76.7	76.0	77.6	79.7	80.6	80.1	83.4	83.3	83.2	81.3	82.0	80.1	77.4	78.8	76.9	80.0	79.3	82.2	81.5	85.3	85.0	90.0	89.7	94.8	94.5
16000.0	76.8	79.7	80.1	80.9	81.3	80.9	80.1	78.4	76.7	76.0	77.6	79.7	80.6	80.1	83.4	83.3	83.2	81.3	82.0	80.1	77.4	78.8	76.9	80.0	79.3	82.2	81.5	85.3	85.0	90.0	89.7	94.8	94.5
20000.0	67.3	69.2	70.5	71.4	71.8	71.4	70.5	69.3	69.0	71.7	74.7	76.9	78.0	77.3	80.6	80.5	80.4	78.4	79.1	77.2	74.5	75.9	74.0	77.1	76.4	79.3	78.6	82.4	82.1	87.0	86.7	91.8	91.5





TABLE VIII. ATTENUATION OF THE BYPASS DUCT TREATMENT	
Frequency (Hz)	Attenuation (dB)
500	2.0
630	2.5
800	3.0
1000	5.5
1250	9.0
1600	13.0
2000	17.0
2500	20.0
3150	19.5
4000	17.0
5000	13.0
6300	10.0
8000	8.0
10000	8.0

#### Total Noise With Treatment

When the computed attenuation for the bypass duct was applied to the bypass radiated noise, the polar and sideline noise changed in amplitude and directivity. The maximum polar PNL is at 150 degrees and is 100.5 PNdB (Table V). The maximum sideline noise is at 70 degrees and is 97.7 PNdB (Table IV). The predicted SPL spectrum at 200 feet is shown in Tables IX and X.

The treatment reduced the sideline noise at 100 degrees from 104.5 PNdB to 97.0 PNdB, a difference of 7.5 PNdB. The reduction is not as large as would be expected from the duct treatment, because the fan noise was suppressed below the jet noise up to 5 kilohertz (Figure 25). Therefore, in order to reduce the noise further, the core exhaust nozzle exit velocity must be lowered to reduce the noise on the sideline. The turbine noise is above 10 kilohertz and does not contribute significantly to the PNL, hence no acoustic treatment is required in the hot exhaust nozzle.

TABLE IX. POLAR NOISE FIELD, TREATED BYPASS DUCT

FREQ	NASA 1.25 FAN, 8375 LB THRUST										POLAR COMBINED SOUND LEVELS										POLAR FIELD													
	0.0	10.0	20.0	30.0	40.0	50.0	60.0	70.0	80.0	90.0	100.0	110.0	120.0	130.0	140.0	150.0	160.0	0.0	10.0	20.0	30.0	40.0	50.0	60.0	70.0	80.0	90.0	100.0	110.0	120.0	130.0	140.0	150.0	160.0
20.0	70.3	70.3	68.2	70.2	68.1	68.6	65.3	67.5	65.9	68.4	66.9	69.9	69.0	74.4	75.8	82.7	81.0	70.3	70.3	68.2	70.2	68.1	68.6	65.3	67.5	65.9	68.4	66.9	69.9	69.0	74.4	75.8	82.7	81.0
25.0	73.1	73.0	70.7	72.4	70.2	70.7	67.6	69.8	68.4	70.9	69.7	72.8	72.2	77.4	79.0	85.9	84.3	73.1	73.0	70.7	72.4	70.2	70.7	67.6	69.8	68.4	70.9	69.7	72.8	72.2	77.4	79.0	85.9	84.3
31.5	75.6	75.2	72.9	74.4	72.0	72.7	69.7	72.0	70.6	73.3	72.1	75.3	74.7	79.9	81.2	88.1	86.5	75.6	75.2	72.9	74.4	72.0	72.7	69.7	72.0	70.6	73.3	72.1	75.3	74.7	79.9	81.2	88.1	86.5
40.0	77.4	77.0	74.4	75.9	73.3	74.2	71.3	73.7	72.3	75.1	73.9	77.2	76.6	81.6	82.6	89.5	87.9	77.4	77.0	74.4	75.9	73.3	74.2	71.3	73.7	72.3	75.1	73.9	77.2	76.6	81.6	82.6	89.5	87.9
50.0	78.4	78.0	75.4	76.8	74.2	75.2	72.5	74.9	73.5	76.4	75.3	78.6	77.9	82.9	83.9	90.8	89.2	78.4	78.0	75.4	76.8	74.2	75.2	72.5	74.9	73.5	76.4	75.3	78.6	77.9	82.9	83.9	90.8	89.2
63.0	79.9	79.4	76.8	78.1	75.9	76.7	74.2	76.6	75.3	78.2	77.2	80.3	79.7	84.7	85.7	92.6	91.0	79.9	79.4	76.8	78.1	75.9	76.7	74.2	76.6	75.3	78.2	77.2	80.3	79.7	84.7	85.7	92.6	91.0
80.0	80.7	80.2	77.6	79.0	76.3	77.7	75.3	77.8	76.4	79.4	78.3	81.6	80.8	85.8	86.8	93.7	92.1	80.7	80.2	77.6	79.0	76.3	77.7	75.3	77.8	76.4	79.4	78.3	81.6	80.8	85.8	86.8	93.7	92.1
100.0	81.0	80.5	77.9	79.2	76.6	78.1	75.9	78.4	77.0	80.0	79.1	82.2	81.5	86.5	87.5	94.4	92.8	81.0	80.5	77.9	79.2	76.6	78.1	75.9	78.4	77.0	80.0	79.1	82.2	81.5	86.5	87.5	94.4	92.8
125.0	81.4	80.9	79.4	79.7	77.1	78.7	76.8	79.2	77.9	80.9	80.0	83.1	82.4	87.4	88.4	95.3	93.7	81.4	80.9	79.4	79.7	77.1	78.7	76.8	79.2	77.9	80.9	80.0	83.1	82.4	87.4	88.4	95.3	93.7
160.0	82.2	81.7	79.1	80.6	77.9	79.8	77.8	80.3	79.0	82.1	81.2	84.3	83.5	88.5	89.5	96.4	94.8	82.2	81.7	79.1	80.6	77.9	79.8	77.8	80.3	79.0	82.1	81.2	84.3	83.5	88.5	89.5	96.4	94.8
200.0	81.6	81.2	78.7	80.1	77.5	79.5	77.7	80.2	78.9	82.0	81.2	84.3	83.4	88.4	89.4	96.3	94.7	81.6	81.2	78.7	80.1	77.5	79.5	77.7	80.2	78.9	82.0	81.2	84.3	83.4	88.4	89.4	96.3	94.7
250.0	81.6	81.2	78.7	80.1	77.7	79.7	78.1	80.5	79.3	82.4	81.7	84.6	83.9	88.9	89.9	96.8	95.2	81.6	81.2	78.7	80.1	77.7	79.7	78.1	80.5	79.3	82.4	81.7	84.6	83.9	88.9	89.9	96.8	95.2
315.0	81.6	81.2	78.8	80.3	77.9	80.0	78.5	81.0	79.7	82.9	82.2	85.1	84.5	89.5	90.5	97.4	95.8	81.6	81.2	78.8	80.3	77.9	80.0	78.5	81.0	79.7	82.9	82.2	85.1	84.5	89.5	90.5	97.4	95.8
400.0	81.2	80.9	78.5	80.1	77.7	80.0	78.6	81.1	79.8	83.0	82.3	85.3	84.5	89.5	90.5	97.4	95.8	81.2	80.9	78.5	80.1	77.7	80.0	78.6	81.1	79.8	83.0	82.3	85.3	84.5	89.5	90.5	97.4	95.8
500.0	80.2	80.0	77.9	79.5	77.4	79.6	78.4	80.7	79.4	82.6	82.0	84.9	84.1	89.1	90.1	97.0	95.4	80.2	80.0	77.9	79.5	77.4	79.6	78.4	80.7	79.4	82.6	82.0	84.9	84.1	89.1	90.1	97.0	95.4
630.0	79.8	79.8	78.2	79.7	78.1	79.9	78.9	80.9	79.7	82.8	82.4	85.2	84.6	89.6	90.6	97.5	95.9	79.8	79.8	78.2	79.7	78.1	79.9	78.9	80.9	79.7	82.8	82.4	85.2	84.6	89.6	90.6	97.5	95.9
800.0	79.4	79.7	78.7	80.1	79.1	80.5	79.5	81.0	79.8	82.8	82.7	85.4	85.0	90.0	91.0	97.9	96.3	79.4	79.7	78.7	80.1	79.1	80.5	79.5	81.0	79.8	82.8	82.7	85.4	85.0	90.0	91.0	97.9	96.3
1000.0	79.1	79.9	79.9	81.1	80.7	81.4	80.5	81.1	79.8	82.3	82.3	84.9	84.7	89.7	90.7	97.6	96.0	79.1	79.9	79.9	81.1	80.7	81.4	80.5	81.1	79.8	82.3	82.3	84.9	84.7	89.7	90.7	97.6	96.0
1250.0	79.7	81.0	81.7	82.7	82.7	82.9	82.1	81.8	80.4	81.9	81.8	84.2	83.9	88.9	89.9	96.8	95.2	79.7	81.0	81.7	82.7	82.7	82.9	82.1	81.8	80.4	81.9	81.8	84.2	83.9	88.9	89.9	96.8	95.2
1600.0	90.8	82.4	83.3	84.3	84.5	84.4	83.6	82.9	81.2	82.0	81.3	83.5	82.9	84.3	82.6	81.0	82.6	90.8	82.4	83.3	84.3	84.5	84.4	83.6	82.9	81.2	82.0	81.3	83.5	82.9	84.3	82.6	81.0	82.6
2000.0	81.4	83.2	84.4	85.3	85.5	85.3	84.5	83.4	81.6	81.4	80.0	81.8	81.0	84.9	84.9	91.8	90.2	81.4	83.2	84.4	85.3	85.5	85.3	84.5	83.4	81.6	81.4	80.0	81.8	81.0	84.9	84.9	91.8	90.2
2500.0	81.7	83.5	84.8	85.6	86.0	85.7	84.9	83.5	81.7	80.9	79.2	80.4	79.4	84.9	84.9	91.8	90.2	81.7	83.5	84.8	85.6	86.0	85.7	84.9	83.5	81.7	80.9	79.2	80.4	79.4	84.9	84.9	91.8	90.2
3150.0	82.5	84.4	85.7	86.5	86.9	86.6	85.8	84.3	82.4	81.1	79.1	79.9	78.8	84.9	84.9	91.8	90.2	82.5	84.4	85.7	86.5	86.9	86.6	85.8	84.3	82.4	81.1	79.1	79.9	78.8	84.9	84.9	91.8	90.2
4000.0	79.5	81.3	82.7	83.5	83.9	83.6	82.8	81.4	79.6	78.8	77.2	78.4	77.6	79.2	78.4	77.6	79.2	79.5	81.3	82.7	83.5	83.9	83.6	82.8	81.4	79.6	78.8	77.2	78.4	77.6	79.2	78.4	77.6	79.2
5000.0	77.1	78.9	80.2	81.1	81.5	81.2	80.3	79.0	77.3	76.8	75.9	77.3	77.0	78.1	77.1	76.6	77.2	77.1	78.9	80.2	81.1	81.5	81.2	80.3	79.0	77.3	76.8	75.9	77.3	77.0	78.1	77.1	76.6	77.2
6300.0	80.1	82.0	83.3	84.2	84.5	84.2	83.4	81.7	79.9	78.4	77.1	77.6	77.1	78.6	77.4	76.6	77.2	80.1	82.0	83.3	84.2	84.5	84.2	83.4	81.7	79.9	78.4	77.1	77.6	77.1	78.6	77.4	76.6	77.2
8000.0	72.3	74.1	75.4	76.3	76.6	76.4	75.5	74.4	72.9	72.6	72.6	74.2	74.1	74.9	74.3	74.2	74.9	72.3	74.1	75.4	76.3	76.6	76.4	75.5	74.4	72.9	72.6	72.6	74.2	74.1	74.9	74.3	74.2	
10000.0	71.4	73.3	74.6	75.5	75.8	75.5	74.6	73.3	71.8	71.4	71.1	72.3	72.3	72.8	72.1	71.9	72.8	71.4	73.3	74.6	75.5	75.8	75.5	74.6	73.3	71.8	71.4	71.1	72.3	72.3	72.8	72.1	71.9	
12500.0	76.8	78.7	80.1	80.9	81.3	80.9	80.1	78.4	76.7	76.0	76.7	78.2	78.9	78.2	77.0	74.7	78.2	76.8	78.7	80.1	80.9	81.3	80.9	80.1	78.4	76.7	76.0	76.7	78.2	78.9	78.2	77.0	74.7	
16000.0	76.8	78.7	80.1	80.9	81.3	80.9	80.1	78.4	76.8	76.8	76.6	77.9	79.6	78.5	75.6	73.3	78.5	76.8	78.7	80.1	80.9	81.3	80.9	80.1	78.4	76.8	76.8	76.6	77.9	79.6	78.5	75.6		
20000.0	67.3	69.2	70.5	71.4	71.8	71.4	70.5	69.3	69.0	71.7	74.7	76.9	78.0	77.3	76.0	73.3	78.0	67.3	69.2	70.5	71.4	71.8	71.4	70.5	69.3	69.0	71.7	74.7	76.9	78.0	77.3	76.0		

TABLE X. SIDELINE NOISE FIELD, TREATED BYPASS DUCT

FREQ	NASA 1-25 FAN, B375 LB THRUST										SIDELINE COMBINED SOUND LEVELS										SIDELINE FIELD																																																																																																																																																																																																																																																																																																																																																																																																																																																																																										
	20.0	30.0	40.0	50.0	60.0	70.0	80.0	90.0	100.0	110.0	120.0	130.0	140.0	150.0	160.0	20.0	30.0	40.0	50.0	60.0	70.0	80.0	90.0	100.0	110.0	120.0	130.0	140.0	150.0	160.0	DEGREES	DEGREES																																																																																																																																																																																																																																																																																																																																																																																																																																																																															
20.0	58.9	64.1	64.2	66.3	64.0	67.0	65.7	68.4	66.8	69.4	67.7	72.1	72.0	74.6	71.7	25.0	61.4	66.3	66.3	68.4	66.4	69.3	68.2	70.9	69.5	72.2	70.9	75.1	75.1	77.0	73.6	31.5	63.5	68.3	68.1	70.4	68.4	71.4	70.4	73.3	71.9	74.7	73.5	77.6	77.4	79.0	75.3	40.0	65.0	69.8	69.5	71.9	70.1	73.2	72.1	75.1	73.8	76.7	75.3	79.3	78.8	80.4	76.5	50.0	66.0	70.7	70.3	72.9	71.3	74.4	73.4	76.4	75.1	78.0	76.7	80.3	79.6	81.2	77.2	63.0	67.4	72.1	71.7	74.4	72.9	75.0	75.1	78.1	77.0	79.8	78.4	81.8	81.0	82.6	78.4	80.0	68.2	72.9	72.4	75.3	74.0	77.2	76.2	79.3	78.2	81.0	79.5	82.8	81.8	83.5	79.1	100.0	68.4	73.1	72.7	75.7	74.6	77.8	76.8	80.0	78.9	81.6	80.2	83.3	82.3	83.8	79.2	125.0	68.9	73.6	73.2	76.4	75.5	78.6	77.7	80.8	79.9	82.5	81.1	84.0	82.9	84.3	79.6	160.0	69.6	74.4	74.0	77.4	76.5	79.7	78.8	82.0	81.0	83.7	82.2	85.0	83.7	85.1	80.2	200.0	69.1	73.9	73.6	77.1	76.4	79.6	78.7	82.0	80.9	83.6	82.1	84.7	83.2	84.5	79.6	250.0	69.1	73.9	73.7	77.2	76.8	79.9	79.1	82.3	81.4	84.0	82.5	84.8	83.0	84.2	79.4	315.0	69.1	74.0	73.8	77.5	77.2	80.3	79.5	82.8	81.9	84.5	82.9	85.0	82.8	84.1	79.2	400.0	69.7	73.7	73.7	77.5	77.2	80.4	79.5	82.9	82.0	84.6	83.0	84.8	82.3	83.6	78.6	500.0	68.0	73.0	73.3	77.0	76.9	79.9	79.1	82.4	81.7	84.2	82.6	84.1	81.3	82.4	77.4	630.0	68.1	73.1	73.8	77.3	77.3	80.1	79.3	82.5	82.1	84.4	83.0	84.0	81.1	81.8	76.7	800.0	68.4	73.5	74.8	77.7	77.9	80.1	79.3	82.5	82.3	84.6	83.4	83.9	80.7	81.0	75.6	1000.0	69.4	74.2	76.3	78.5	78.8	80.1	79.3	81.9	81.8	84.0	82.9	83.1	79.9	79.5	73.9	1250.0	70.9	75.6	78.1	79.9	80.2	80.7	79.7	81.4	81.2	83.1	82.1	82.1	78.9	78.3	72.4	1600.0	72.1	77.0	79.5	81.3	81.6	81.6	80.5	81.4	80.5	82.3	80.9	81.2	77.9	77.3	71.0	2000.0	72.7	77.6	80.5	82.0	82.4	82.0	80.6	80.6	79.1	80.4	78.8	79.2	75.9	75.2	68.4	2500.0	72.5	77.6	80.6	82.1	82.5	81.9	80.6	79.9	78.0	78.8	77.0	77.5	74.3	73.3	65.1	3150.0	72.7	78.0	81.1	82.6	83.1	82.4	81.0	79.9	77.7	78.0	76.1	76.3	73.2	71.8	64.1	4000.0	68.7	74.3	77.5	79.2	79.7	79.1	77.8	77.2	75.4	76.2	74.5	74.8	71.7	69.8	61.5	5000.0	65.1	71.1	74.5	76.2	76.8	76.3	75.1	74.8	73.7	74.6	73.4	73.2	70.2	67.4	53.7	6300.0	66.6	73.1	76.8	78.6	79.2	78.5	77.2	75.8	74.0	73.9	72.5	71.6	68.6	65.1	56.0	8000.0	56.7	63.9	67.8	69.9	70.6	70.4	69.5	69.7	69.2	70.2	69.2	68.5	65.4	61.8	52.1	10000.0	53.6	61.4	65.8	68.0	68.8	68.5	67.6	67.4	66.9	67.5	66.5	65.2	62.1	57.9	47.7	12500.0	56.2	64.9	69.7	72.1	73.1	72.6	71.5	71.0	71.5	72.3	71.8	69.4	65.4	59.7	47.9	16000.0	52.0	62.1	67.5	70.2	71.4	71.1	70.2	70.2	71.3	72.3	71.9	69.1	64.7	57.0	45.0	20000.0	37.8	49.4	55.5	58.6	60.0	60.3	60.7	63.7	66.5	67.9	67.5	64.5	59.7	51.3	37.8

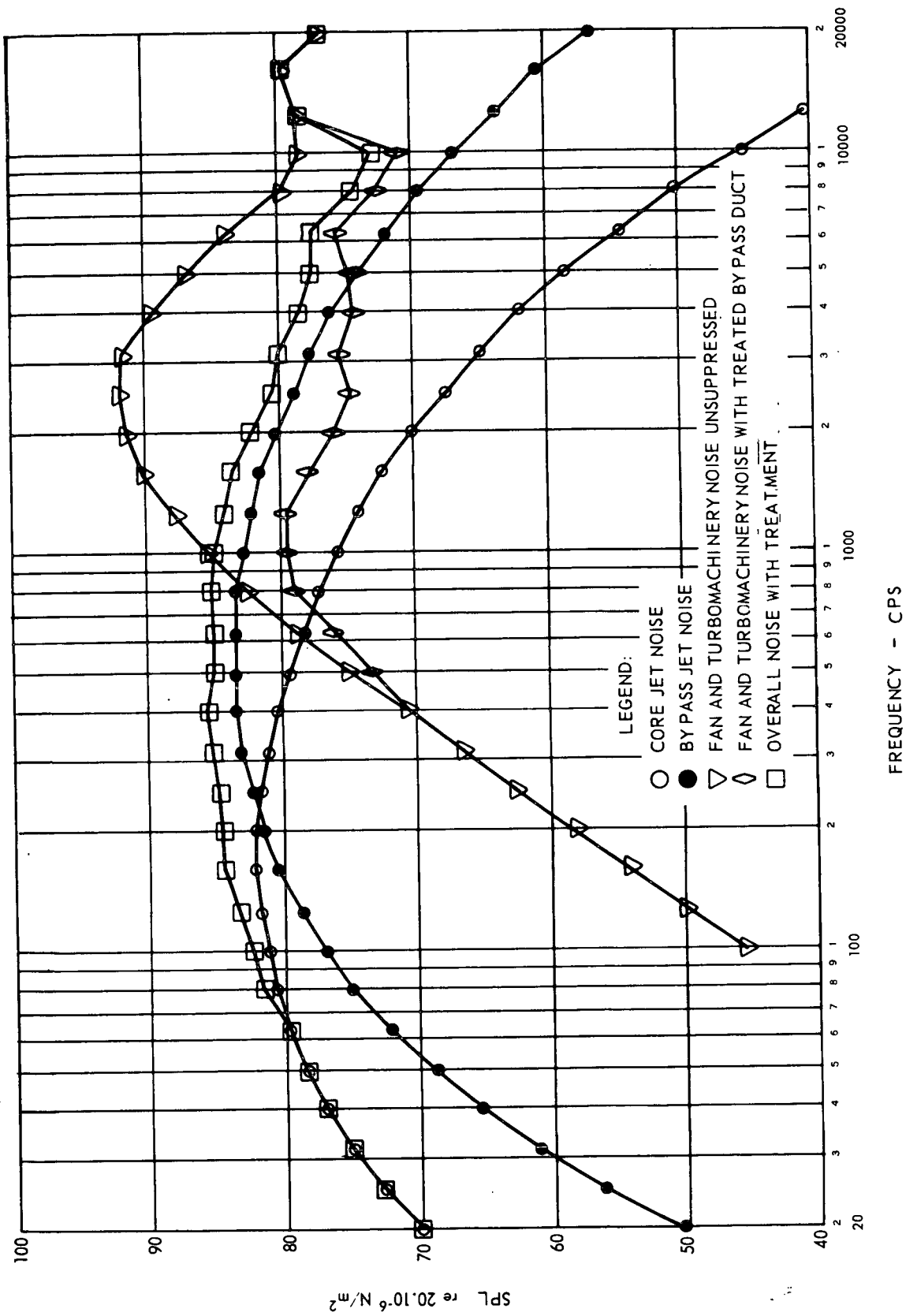


Figure 25. Integral Lift Engine Noise at 200 Feet Radius and 110 Degrees.

## ENGINE PERFORMANCE

### Design Cycle Considerations

The final turbofan engine design cycle was established at the maximum rating at sea level, static, standard conditions for the Lycoming LTC4B-12 shaft turbine engine. The B-12 engine, with minor modifications, serves as the power producer, and consequently its ratings (i. e. torque and speed limits) are applied to the fan version in addition to limits unique to the fan and reduction gearbox.

The rematch of the core engine at maximum rating when operating behind a supercharger stage is similar to the shaft engine being rammed at flight velocity. The operating point on the high compressor referred to its inlet reflects the reduction in referred turbine inlet temperature  $T_4/\theta_{2.1}$ . See the engine station diagram in Figure 26. This is manifested as a reduction in referred gas producer speed  $N_G/\sqrt{\theta_{2.1}}$ , referred compressor inlet airflow  $W_a P^{\sqrt{\theta_{2.1}}}/\delta_{2.1}$ , and compressor pressure ratio  $P_3/P_{2.1}$ . Determination of the high compressor referred inlet airflow as a function of supercharger pressure ratio and efficiency allows computation of the actual engine inlet airflow, which is also the referred inlet airflow of the engine supercharging portion of the fan.

With a prescribed fan pressure ratio selection of the design bypass ratio and, therefore, the inlet referred airflow into the bypass stream portion of the fan, is dependent on the available power turbine work resulting from the power turbine gas flow, inlet temperature, and the expansion ratio necessary to diffuse the hot nozzle exit stream to the velocity desired for minimum exhaust noise. Gas flow and power turbine inlet temperature are determined by the compressor and supercharger match, component losses, airbleeds, and the maximum turbine inlet temperature  $T_4$  of the B-12 engine. The resultant turbine power available\* to drive the fan and supercharger at their respective pressure ratios and efficiencies establish the fan total inlet airflow and bypass ratio.

### Estimated Engine Performance and Fan Matching

Estimated performance data presented herein are based on a lower heating value of 18,400 Btu/lb and are representative of typical average production engines. The standard atmospheric conditions are as given in U.S. Standard Atmosphere, 1962 (ASTIA Document 401813). Tropical atmospheric conditions are as presented in Climatic Extremes for Military Equipment, 1957 (MIL-STD-210A). Thermodynamic and performance data for the engine design point are presented in Tables XI through XIII. Part-load performance data have been generated for both the prime fan A with large design surge margin (SM = 21 percent at 100 percent

\* There is no exhaust diffuser or exhaust nozzle after the power turbine.

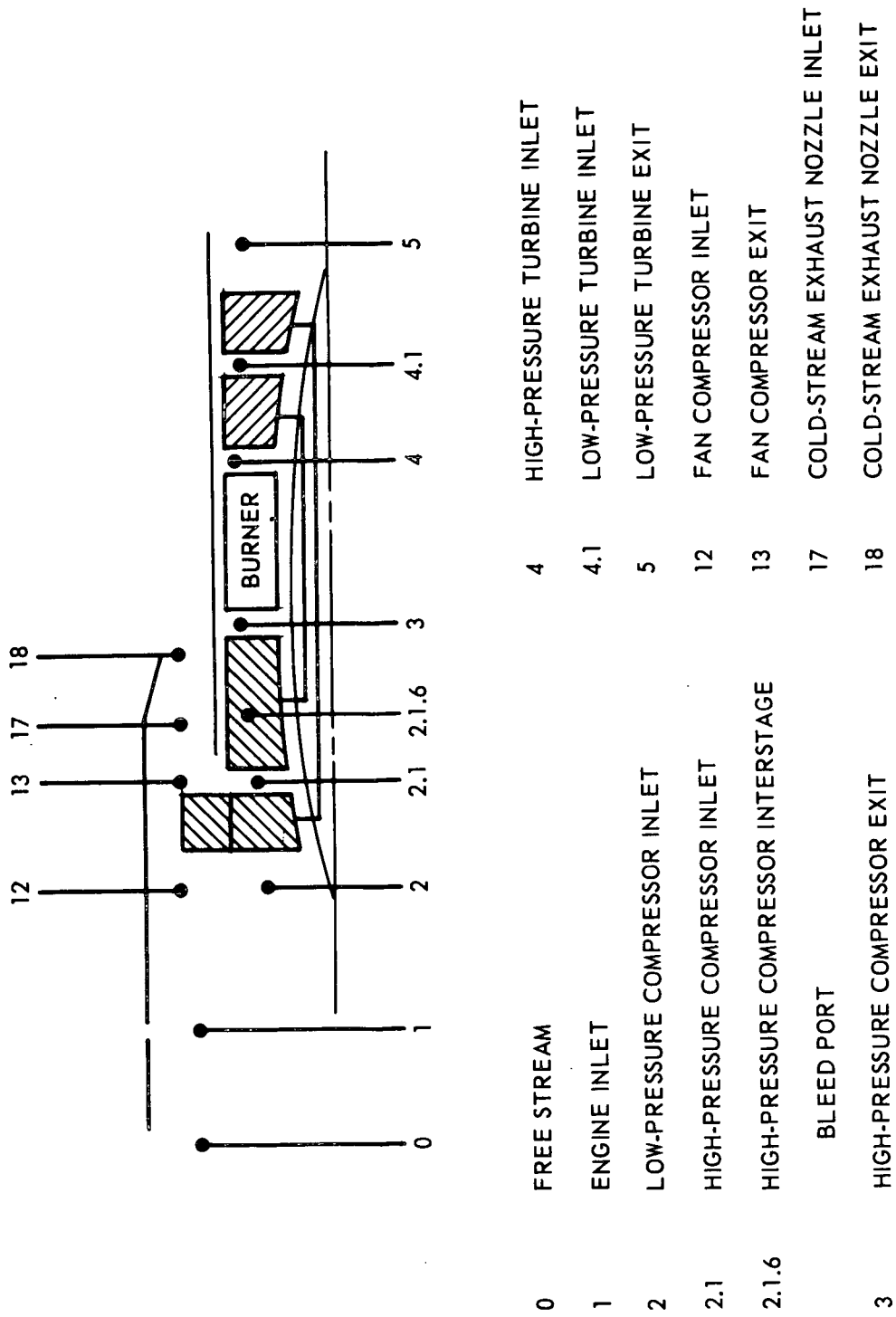


Figure 26, Engine Stations.

TABLE XI. TURBOFAN ENGINE DESIGN CYCLE DATA

Item	Symbol	Unit	
<u>Fan Engine Inlet Conditions</u>			
Altitude		ft	0
Ambient Temperature	$T_{am}$	°R	518.7
Ambient Pressure	$P_{am}$	psia	14.7
Flight Mach Number	$M_f$	-	0
Cycle Temperature *	$T_4$	°F	2067
Specific Thrust	$F_{NT} / W_{aT}$	lb <sub>f</sub> -sec/lbm	19.9
<u>Pressure Ratios</u>			
Compressor Overall	$P_3 / P_2$	-	9.8
Fan (and Supercharger)	$P_{13} / P_{12}$	-	1.25
Gas Generator Compressor	$P_3 / P_{2.1}$	-	7.84
<u>Referred Airflows</u>			
Total	$W_{aT} \sqrt{\theta_2} / \delta_2$	lb/sec	421
Gas Generator(Inlet)	$W_{aP} \sqrt{\theta_{2.1}} / \delta_{2.1}$	lb/sec	25.9
Bypass Ratio	BR	-	12.5
Fan Speed	$N_F$	rpm	5245
Power Turbine Speed	$N_{PT}$	rpm	16870
Gas Generator Spool	$N_G$	rpm	19180
Total Net Thrust	$F_{NT}$	lb	8370
Thrust Specific Fuel Consumption	TSFC	lbm/hr-lb <sub>f</sub>	.302
Engine Stream (Primary) Exhaust Velocity	$V_{JP}$	ft/sec	846
Bypass Stream (Secondary) Exhaust Velocity	$V_{JS}$	ft/sec	623
*Total temperature at first turbine rotor inlet			



TABLE XII. TURBOFAN ENGINE DESIGN EFFICIENCY AND LOSS ASSUMPTIONS

Item	Symbol	Unit		
<u>Pressure Losses in Engine</u>				
Combustor	$\Delta P/P_3$	-	.033	
Bypass Stream (Fan) Exhaust Duct	$\Delta P/P_{13}$	-	.01	
<u>Nozzle Velocity Ratios</u>				
Primary (Engine Nozzle)	$C_{VP}$	-	.99	
Secondary (Bypass Nozzle)	$C_{VS}$	-	.99	
<u>Component Efficiencies</u>				
Fan	Polytropic	$\eta_{FP}$	-	.88
	Adiabatic	$\eta_{Fa}$	-	.876
Supercharger	Polytropic	$\eta_{SCP}$	-	.86
	Adiabatic	$\eta_{Sa}$	-	.855
Gas Generator Compressor	Polytropic	$\eta_{CP}$	-	.858
	Adiabatic	$\eta_C$	-	.816
Combustor		$\eta_B$	-	.98
Gas Generator Turbine	Polytropic	$\eta_{TP}$	-	.897
	Adiabatic	$\eta_T$	-	.907
Power Turbine	Polytropic	$\eta_{TP}$	-	.871
	Adiabatic	$\eta_T$	-	.887
<u>Mechanical Rotor Efficiencies</u>				
Gas Generator		$\eta_{MG}$	-	.993
Fan		$\eta_{MF}$	-	.985
Equivalent Cooling Air Flow (Bypassing Gas Generator Turbine)		$W_c/W_{aP}$	%	3.5
Rotating Seal and Overboard Leakage		$W_L/W_{aP}$	%	0.5

TABLE XIII. TURBOFAN ENGINE STATION CYCLE DATA

Component		Total Pressure (psia)	Total Temperature (°R)	Flow Rate (lb/sec)
Engine Inlet		14.7	518.7	421
Fan	Inlet	14.7	518.7	390
	Exit	18.4	558	390
-----				
Bypass Stream (Fan) Exhaust Duct	Inlet	18.4	558	390
	Exit	18.2	558	390
-----				
Supercharger	Inlet	14.7	518.7	31.2
	Exit	18.4	559	31.2
-----				
Gas Generator Compressor	Inlet	18.4	559	31.2
	Exit	144	1096	31.2
-----				
Combustor:	Inlet	144	1096	30.0
	Exit	139.3	2527	30.7
-----				
Gas Generator Turbine	Inlet	139.3	2527	30.7
	Exit	53.5	2040	30.7
-----				
Power Turbine	Inlet	53.5	2040	31.7
	Exit	16.8	1598	31.7
-----				
Engine Stream (Gas) Exhaust Duct	Inlet	16.8	1598	31.7
	Exit	16.8	1598	31.7

$N/\sqrt{\theta_2}$ ) and fan B, which has the more moderate design surge margin (SM = 14 percent at 100 percent  $N/\sqrt{\theta_2}$ ) normally associated with fan engines configured for cruise. For each configuration, the aerodynamic fan design point has the same pressure ratio, flow, and efficiency, so Tables XI through XIII apply to both. Insofar as the effect of redesign influences only the bypass stream portion of the fan, the supercharger characteristic remains unaltered.

Fan A (Surge Margin = 21 Percent at 100 Percent  $N/\sqrt{\theta_2}$ ). - Standard and tropical day performance from sea level to 20,000 feet at various flight Mach numbers is shown, for this design, in Figures 27 through 36. Lines are presented on these curves through the loci of maximum (5 minute) ratings, military (30 minute) ratings, and continuous ratings, as well as the power turbine maximum speed where this limits engine operation.

To obtain perspective with respect to component matching, operating lines within the suitable flight envelope are superimposed on the fan, supercharger, and high-pressure compressor characteristics, and are presented as Figures 37 through 39 respectively. The design surge margins\* at 100 percent referred speed are 21 percent for the fan and 29 percent for the supercharger. The problem inherent to low-pressure-ratio fan designs shows up clearly as a rapid unloading of the fan with increased  $M_f$  (flight Mach number) with the associated severe decrease in efficiency. This is exemplified by the decay of fan efficiency at standard day maximum rating going from static to 0.4  $M_f$ , on the order of 17 percent.

Fan B (Surge Margin = 14 Percent at 100 Percent  $N/\sqrt{\theta_2}$ ). - The selection of a fan design with more moderate surge margin at the aerodynamic fan design point has the direct benefit of improved performance at the flight Mach numbers associated with cruise. The fan B characteristic is presented in Figure 40 with operating lines equivalent to those shown in Figure 37. The efficiency decay in this case traversing from the sea level, static operating line to the sea level, 0.4  $M_f$  operating line is 8 percent at maximum rating. Sea level performance for both fan designs is shown comparatively in Figure 41 to illustrate the described effect on TSFC (thrust specific fuel consumption) and thrust. It is seen that the lower surge margin fan design provides 8 1/2 percent more net thrust with 8 1/2 percent less TSFC at 0.4  $M_f$  maximum rating. Standard and tropical day performance from sea level to 20,000 feet is shown for this configuration in Figures 42 through 51.

$$* \quad SM = \left[ \left( \frac{P_{rs}}{P_{ro}} \times \frac{W_{ao}}{W_{as}} \right) - 1 \right] \times 100 \quad (\text{at constant referred speed})$$

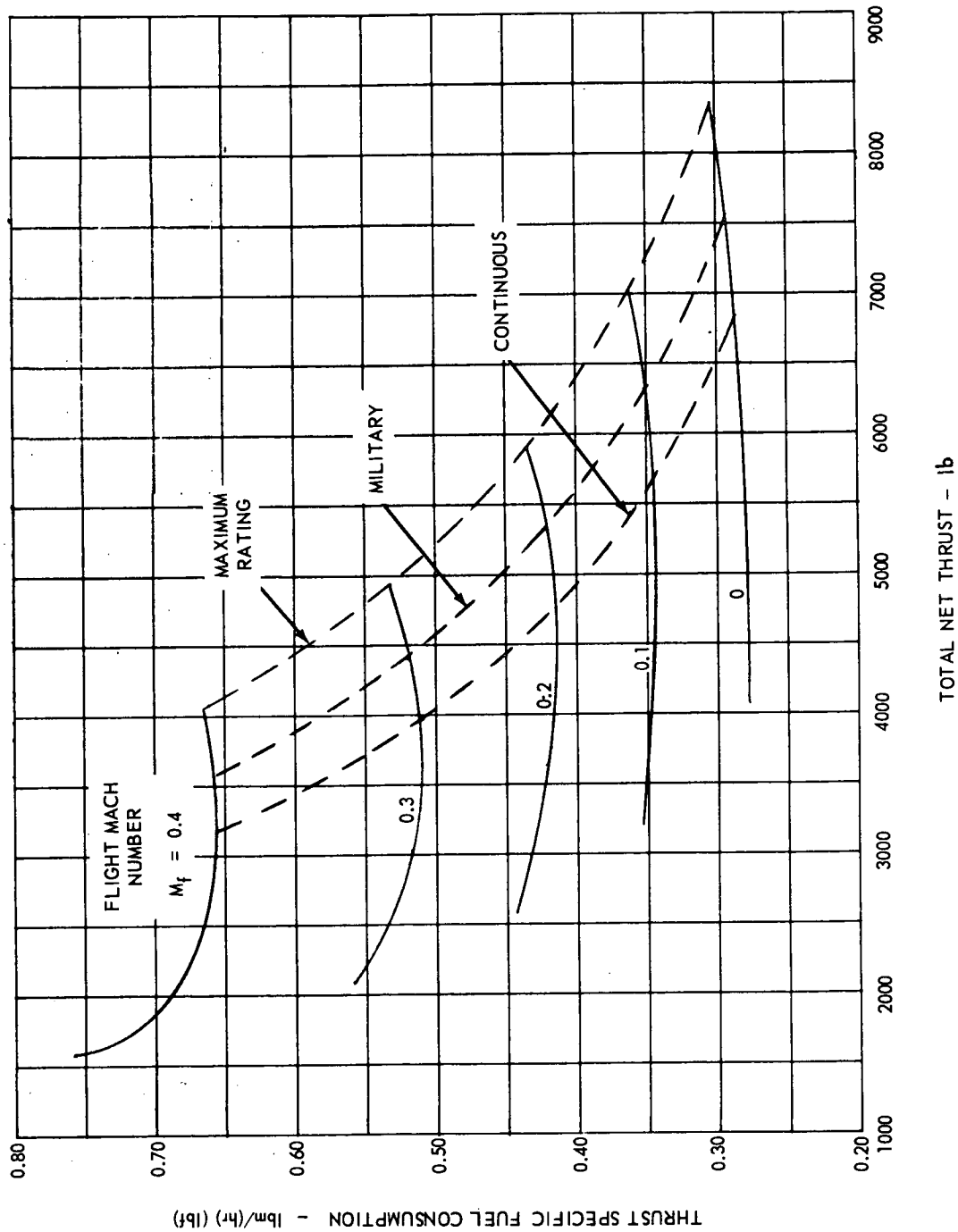


Figure 27. Fan Configuration A (SM = 21 Percent,  $A_{18} = 1190$  Square Inches)  
 Estimated Performance at Sea Level on Standard Day.

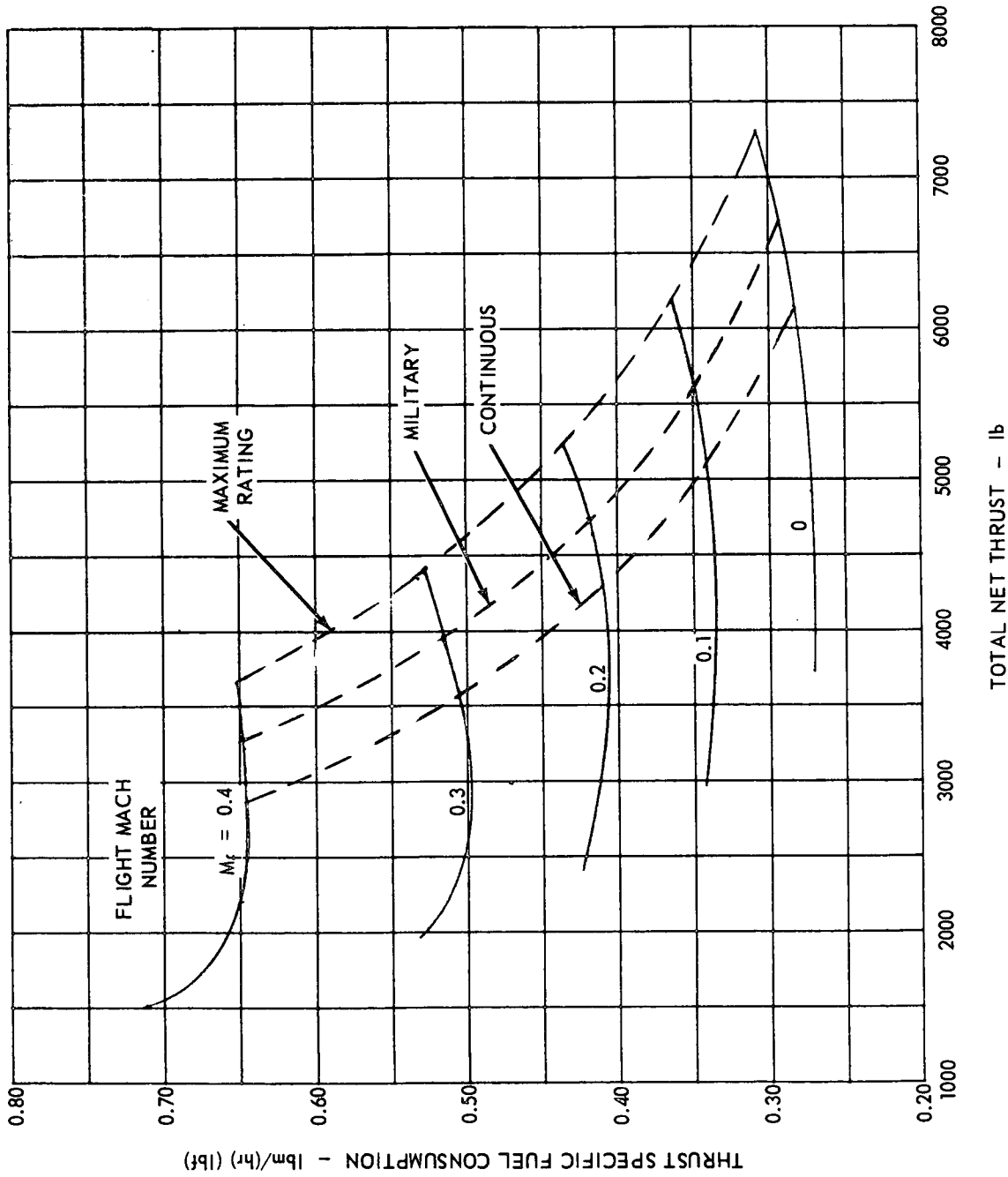


Figure 28. Fan Configuration A (SM = 21 Percent,  $A_{18} = 1190$  Square Inches)  
 Estimated Performance at 5000 Feet on Standard Day.

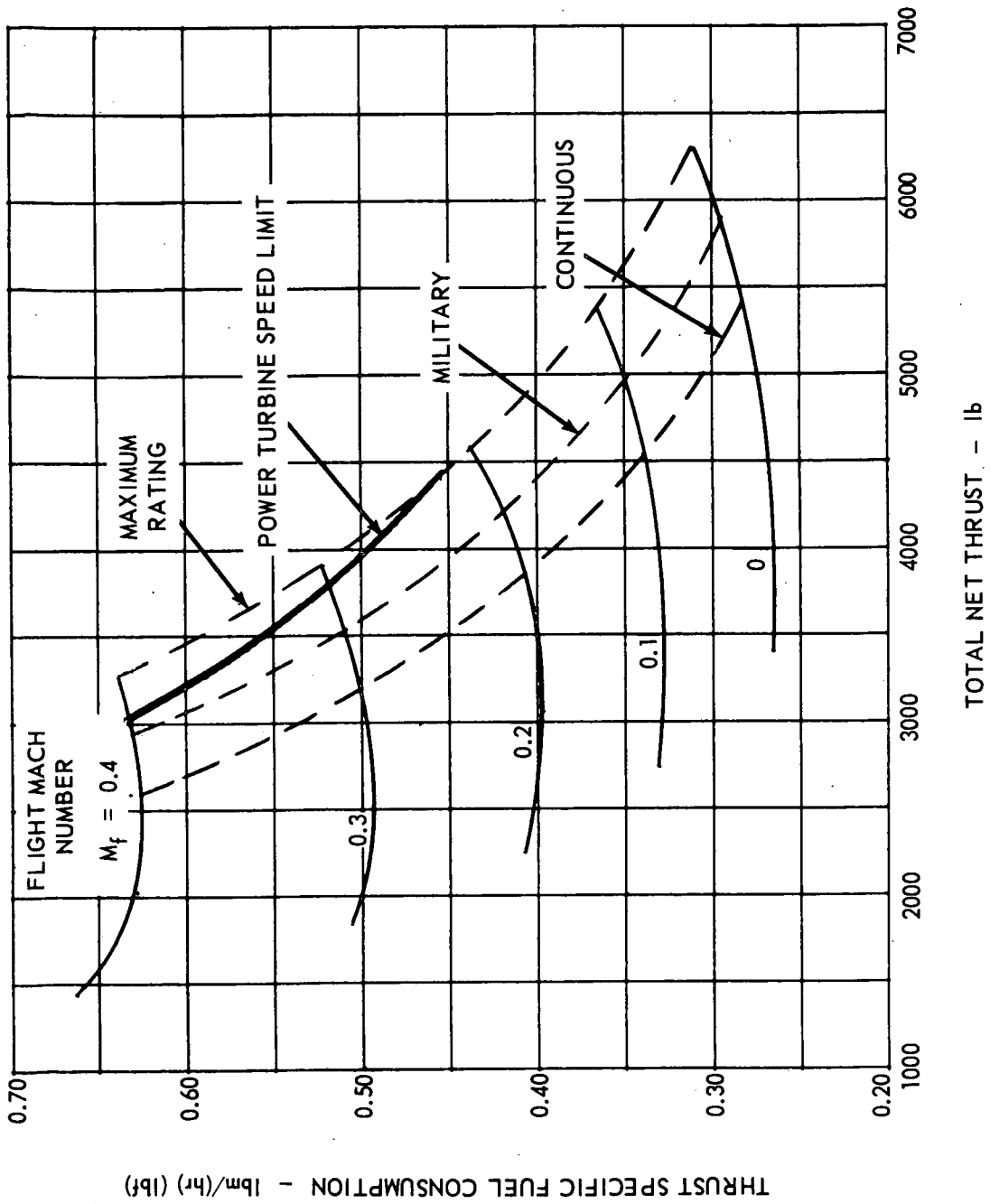


Figure 29. Fan Configuration A (SM = 21 Percent,  $A_{18} = 1190$  Square Inches)  
 Estimated Performance at 10,000 Feet on Standard Day.

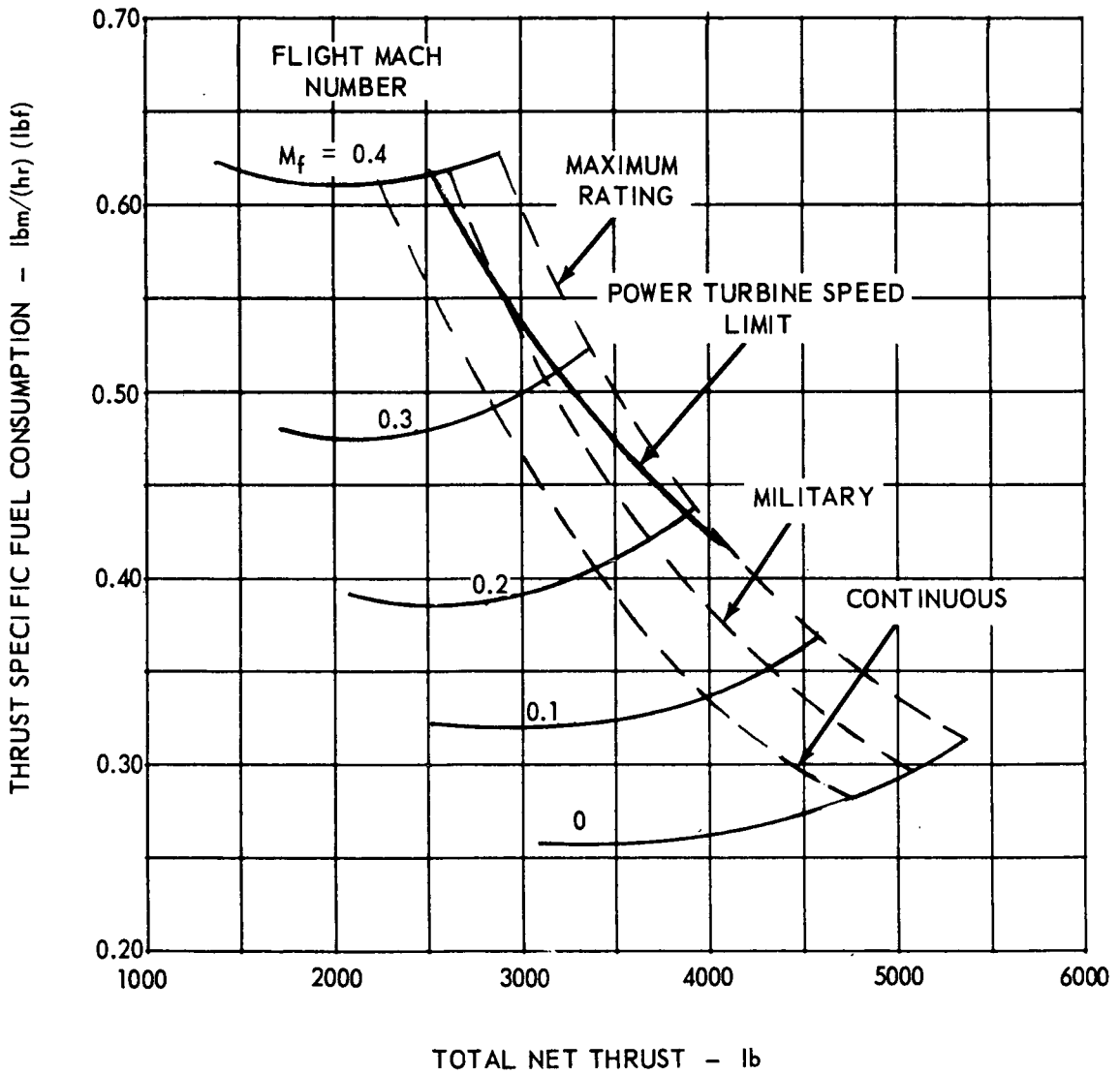


Figure 30. Fan Configuration A (SM = 21 Percent,  $A_{18} = 1190$  Square Inches) Estimated Performance at 15,000 Feet on Standard Day.

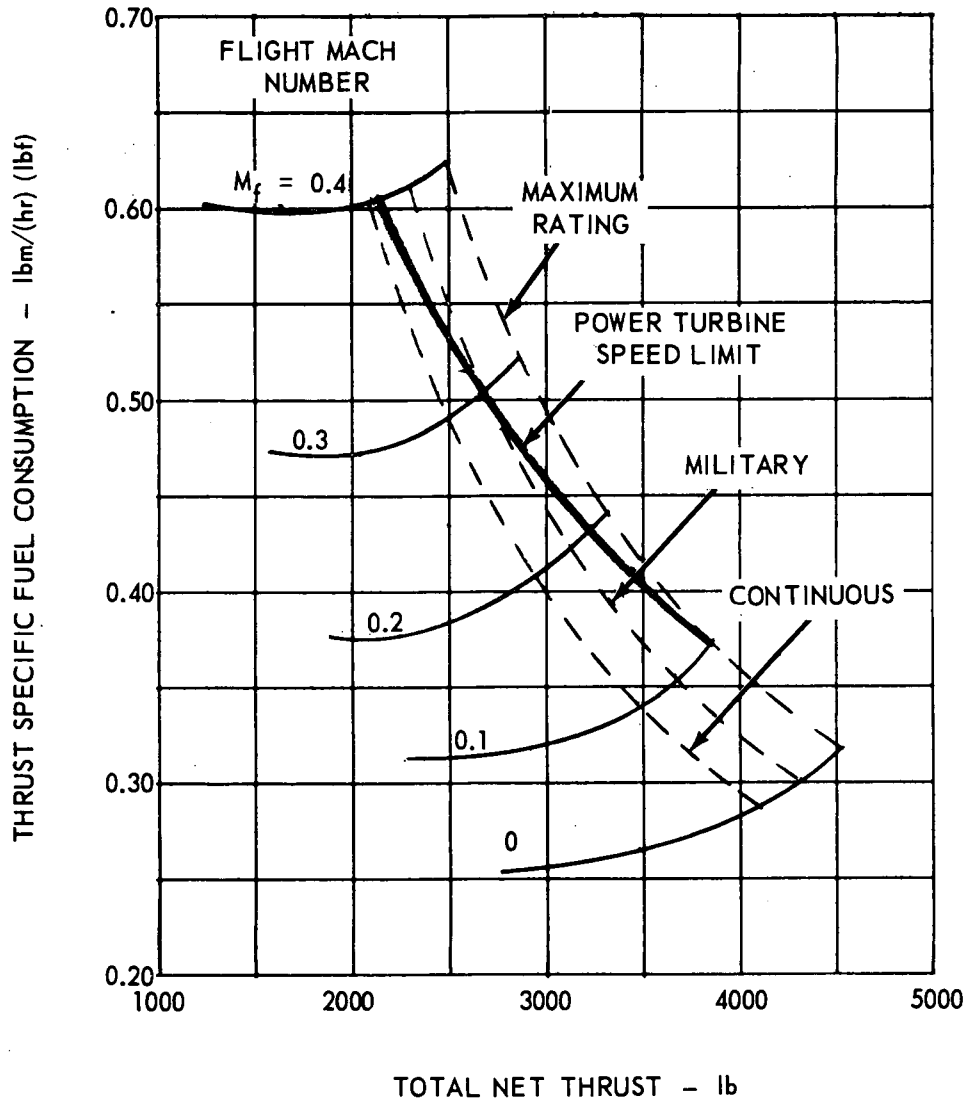


Figure 31. Fan Configuration A (SM = 21 Percent,  $A_{18} = 1190$  Square Inches) Estimated Performance at 20,000 Feet on Standard Day.



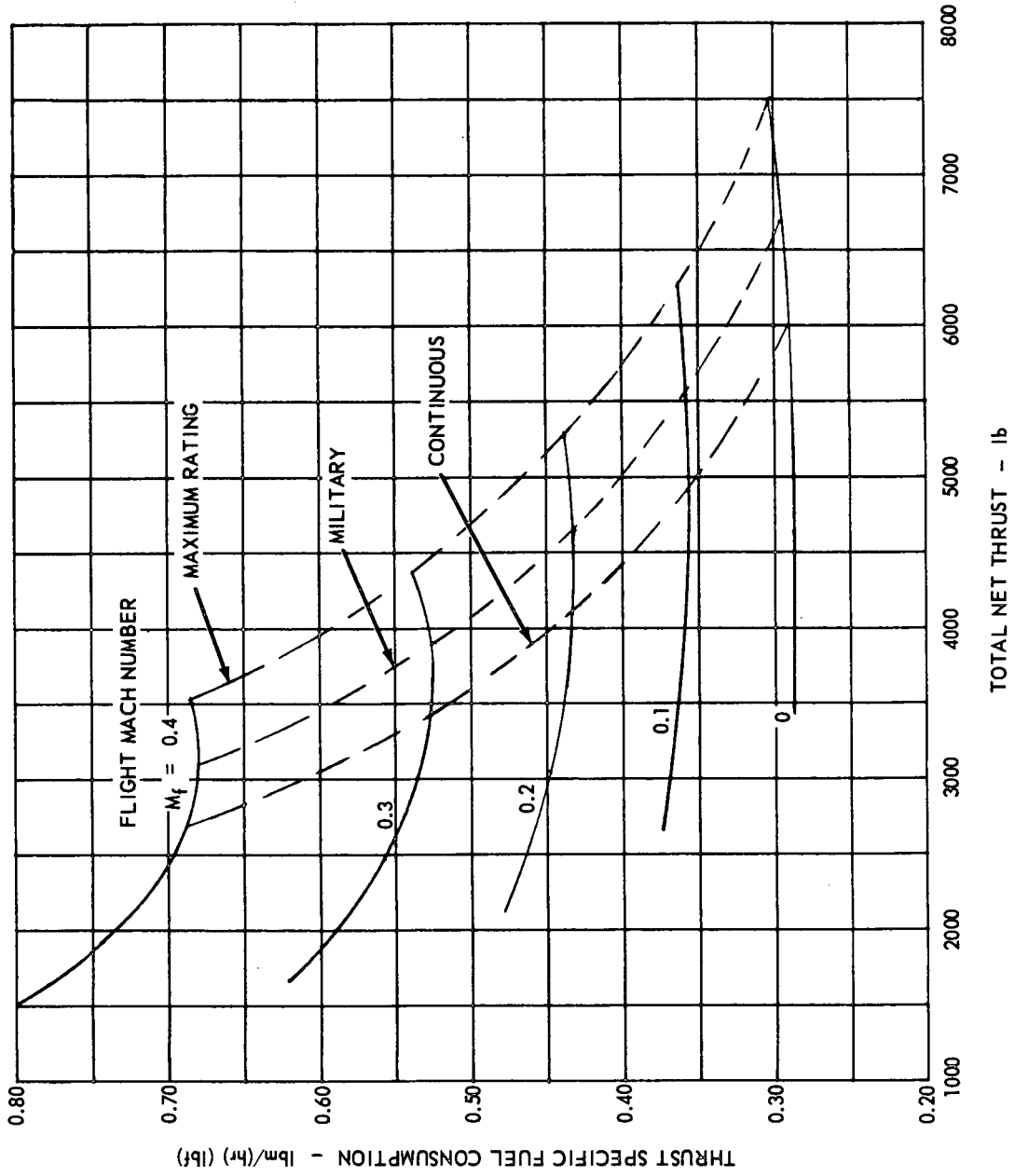


Figure 32. Fan Configuration A (SM = 21 Percent, A<sub>18</sub> = 1190 Square Inches) Estimated Performance at Sea Level on Tropical Day (90° F).

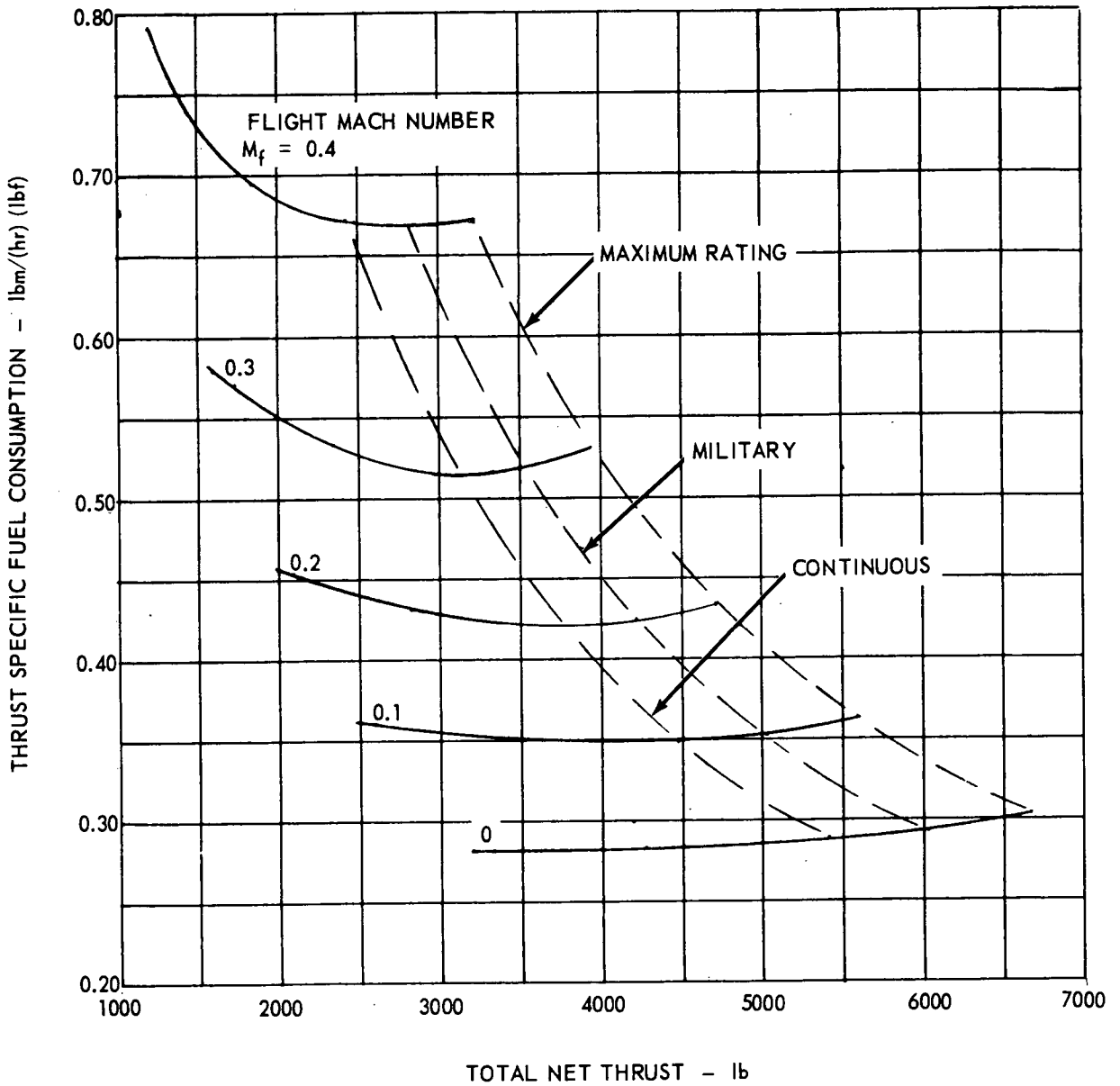


Figure 33. Fan Configuration A (SM = 21 Percent,  $A_{18} = 1190$  Square Inches) Estimated Performance at 5000 Feet on Tropical Day ( $70^{\circ}$  F).

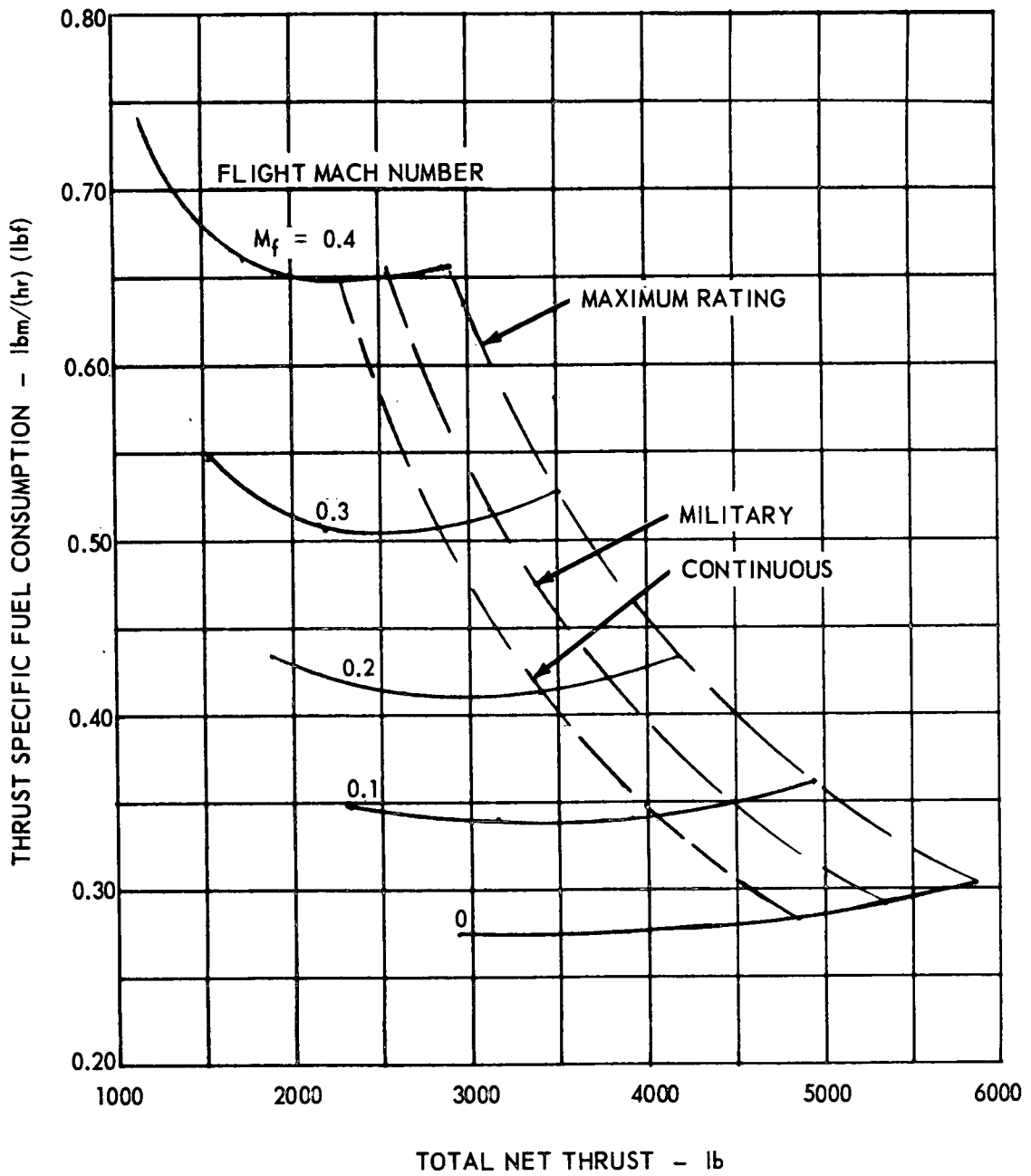


Figure 34. Fan Configuration A (SM = 21 Percent,  $A_{18} = 1190$  Square Inches) Estimated Performance at 10,000 Feet on Tropical Day ( $51^\circ$  F).

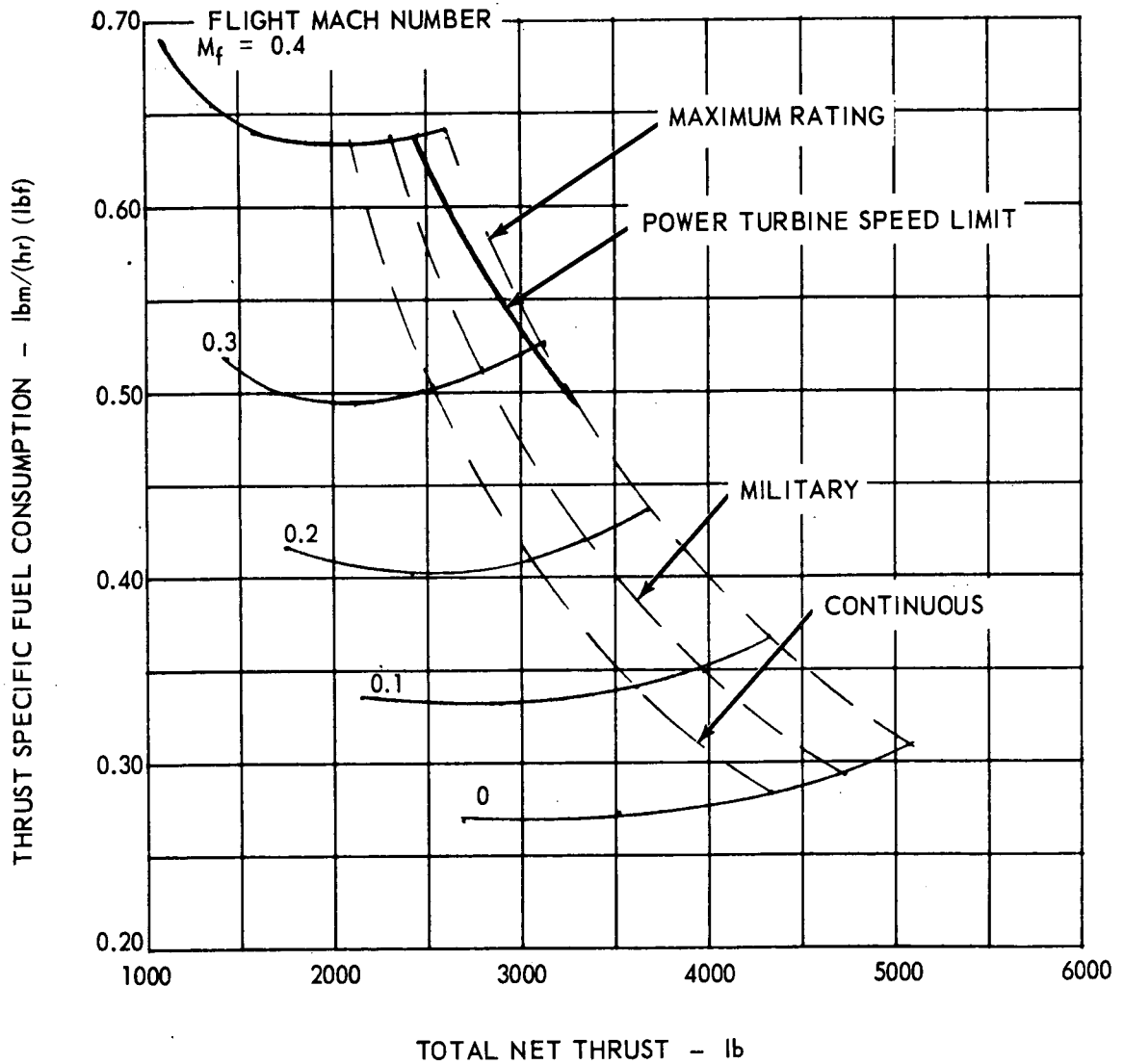


Figure 35. Fan Configuration A (SM = 21 Percent,  $A_{18} = 1190$  Square Inches) Estimated Performance at 15,000 Feet on Tropical Day ( $32^{\circ}$  F).

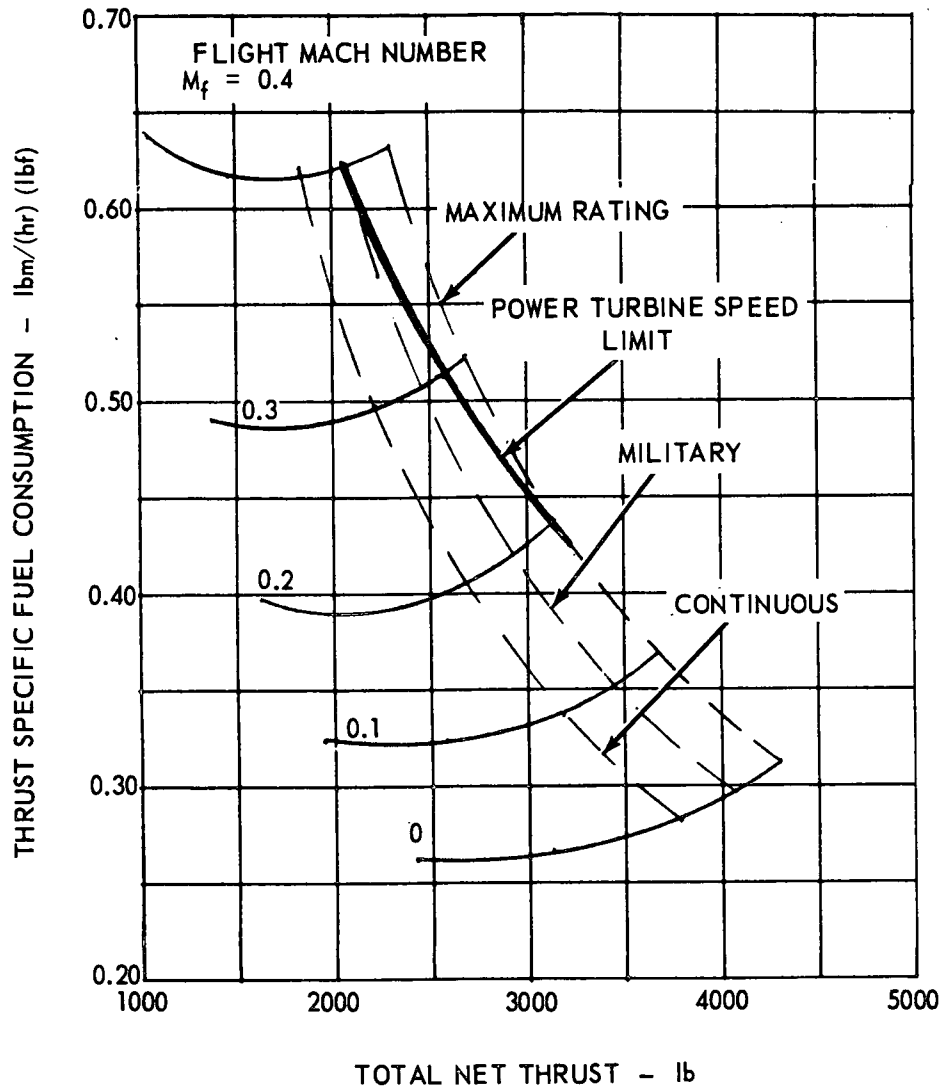


Figure 36. Fan Configuration A (SM = 21 Percent,  $A_{18} = 1190$  Square Inches) Estimated Performance at 20,000 Feet on Tropical Day ( $12^{\circ}$  F).

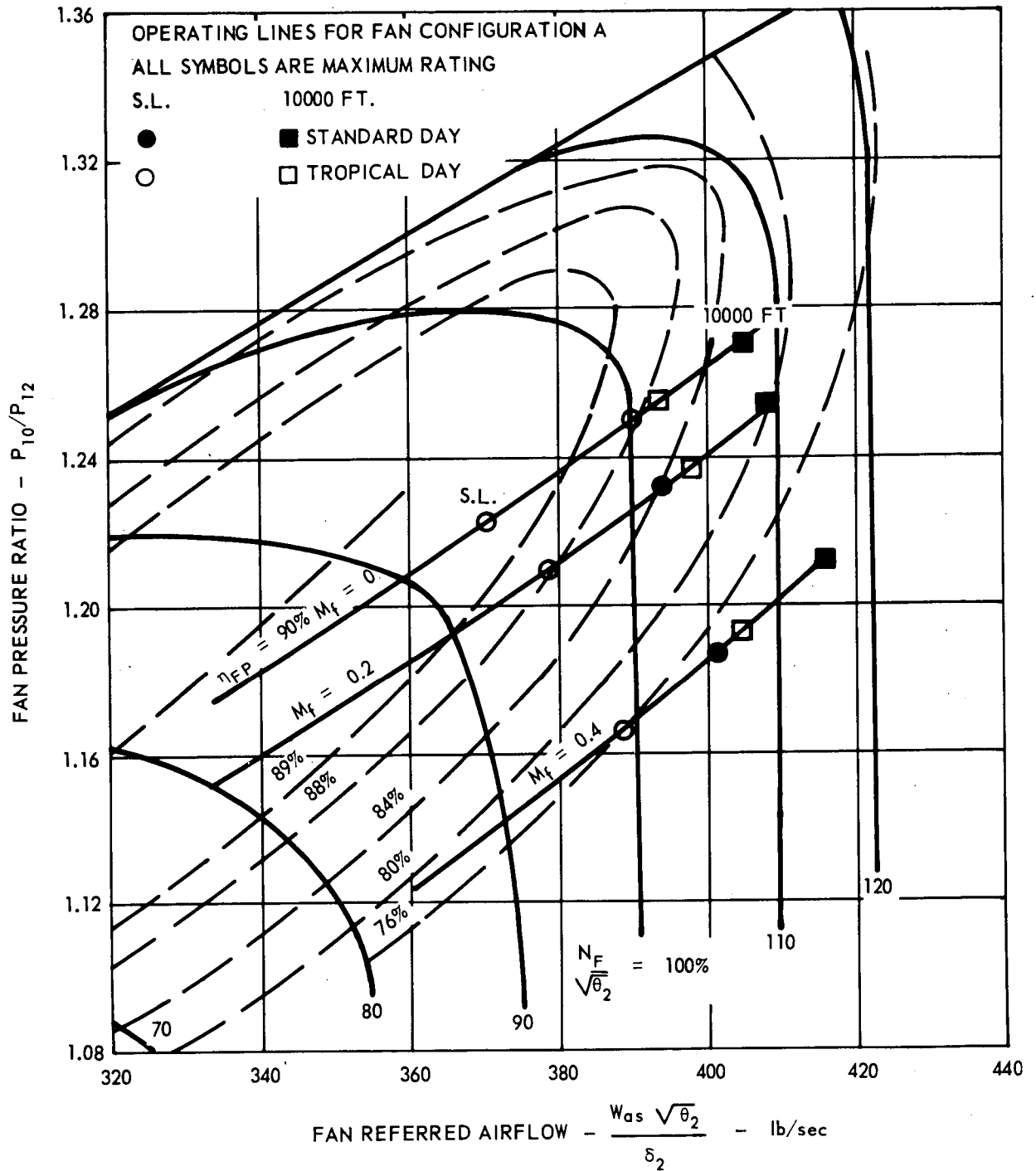


Figure 37. Estimated Fan Performance Map for Configuration A With Fixed Fan Exhaust Nozzle ( $A_{18} = 1190$  Square Inches) Showing Operating Lines.

OPERATING LINES FOR FAN CONFIGURATION A  
 ALL SYMBOLS ARE MAXIMUM RATING  
 S.L. 10000 FT.

- STANDARD DAY
- TROPICAL DAY
- STANDARD DAY
- TROPICAL DAY

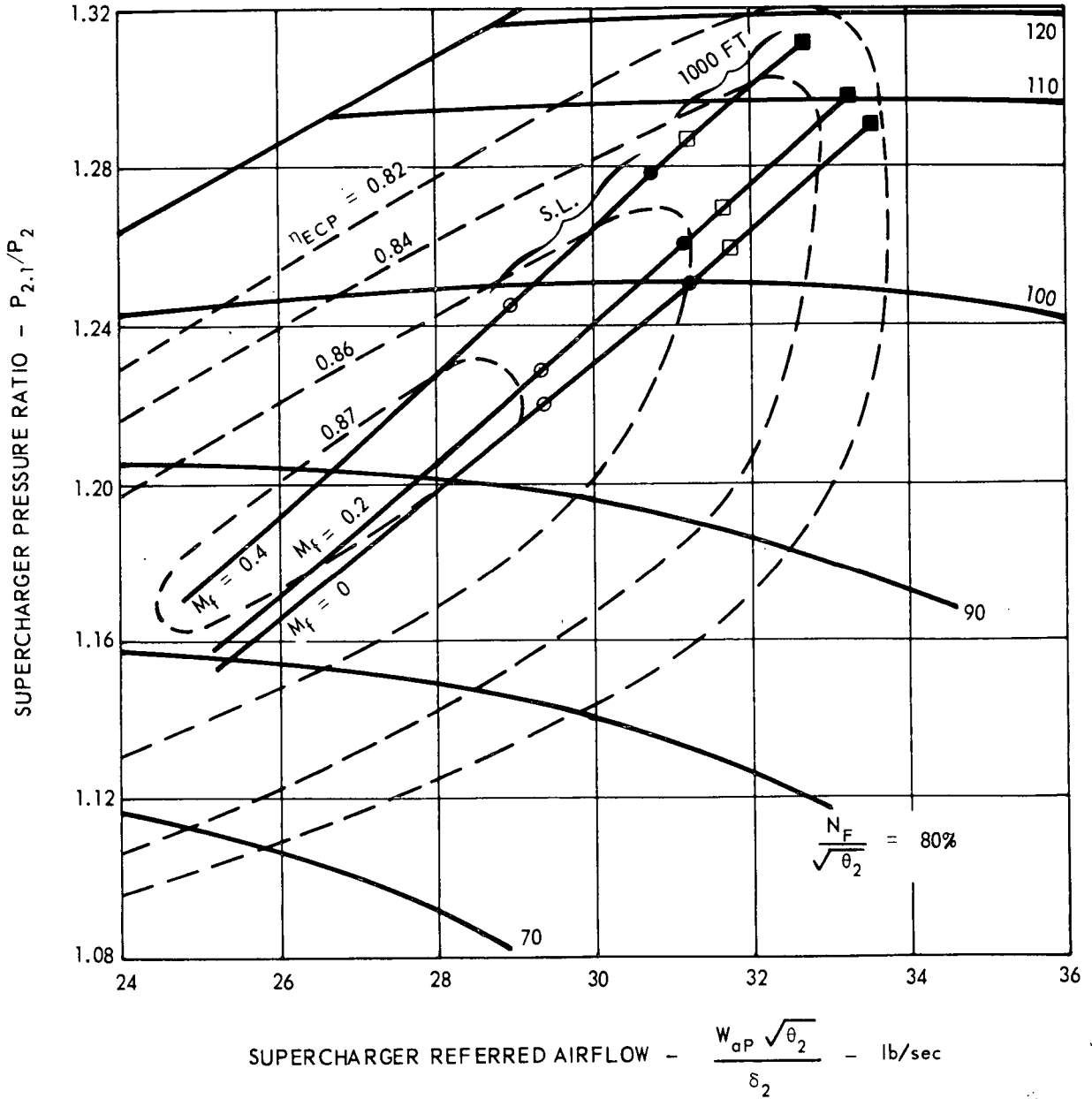


Figure 38. Estimated Supercharger Performance Map With Fixed Fan Exhaust Nozzle ( $A_{18} = 1190$  Square Inches) Showing Operating Lines.

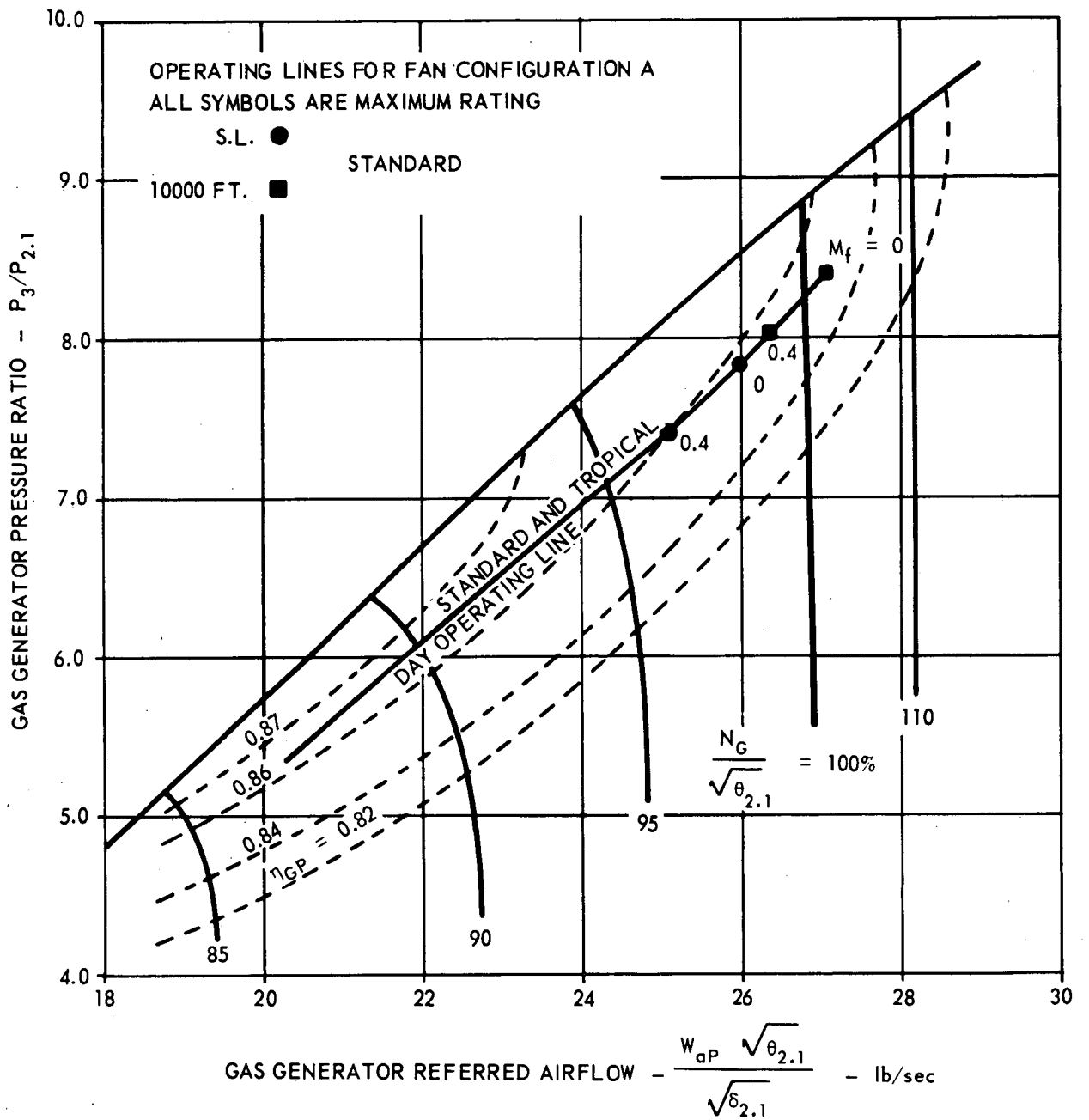


Figure 39. Gas Generator Performance Map Showing Operating Lines.



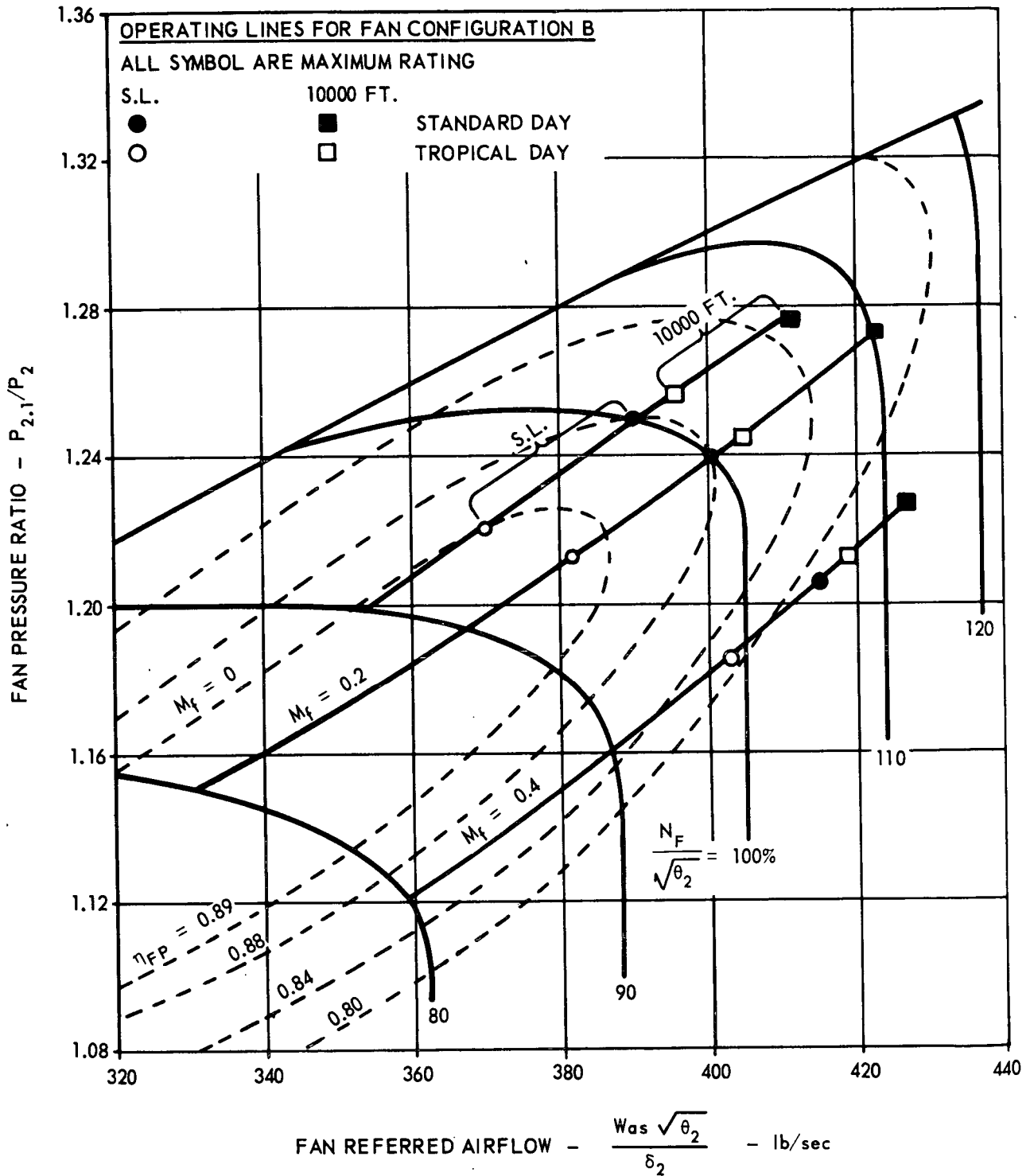


Figure 40. Estimated Fan Performance Map for Configuration B With Fixed Fan Exhaust Nozzle ( $A_{18} = 1190$  Square Inches) Showing Operating Lines.

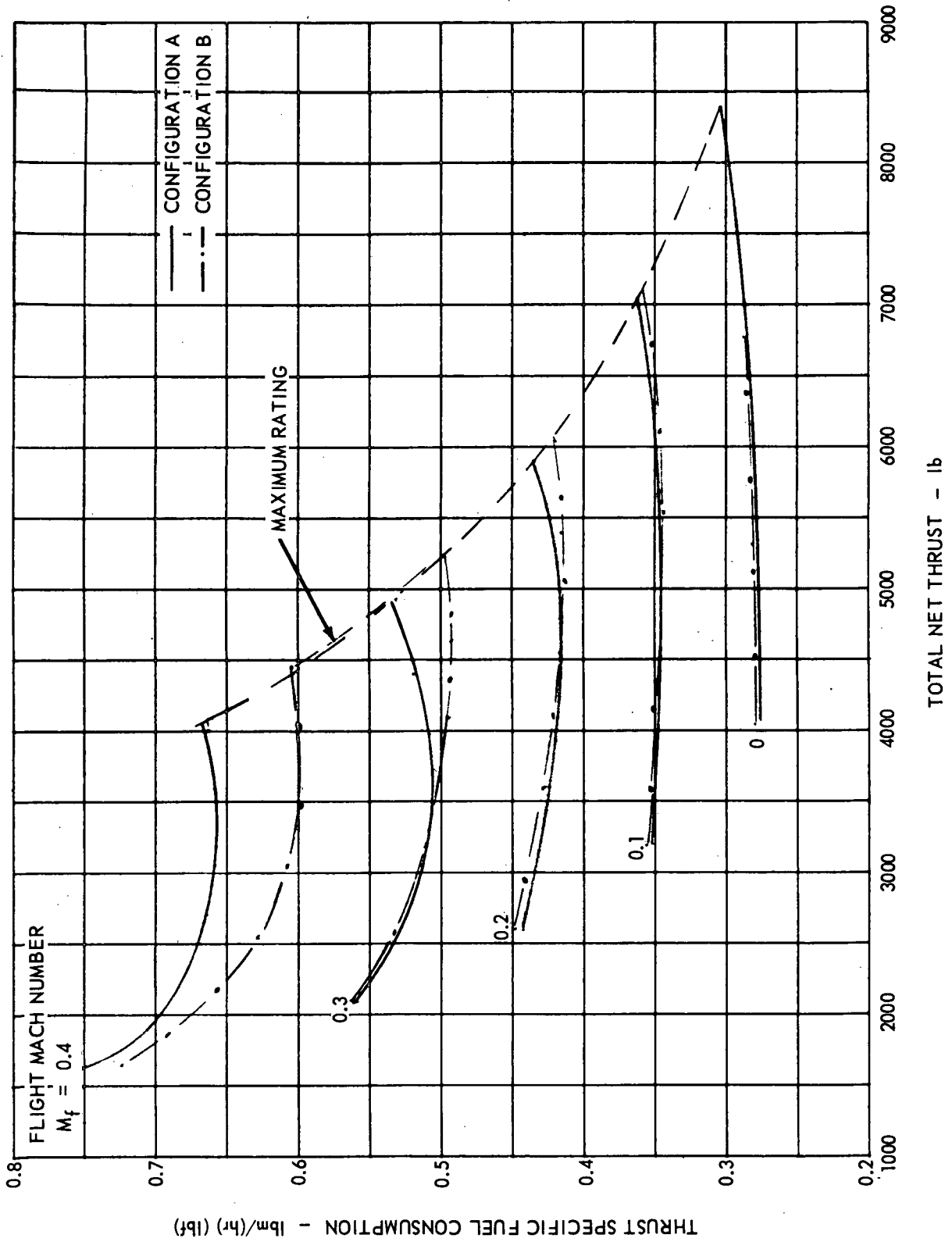


Figure 41. Fan Configurations A and B ( $A_{18} = 1190$  Square Inches) Estimated Performance at Sea Level on Standard Day.

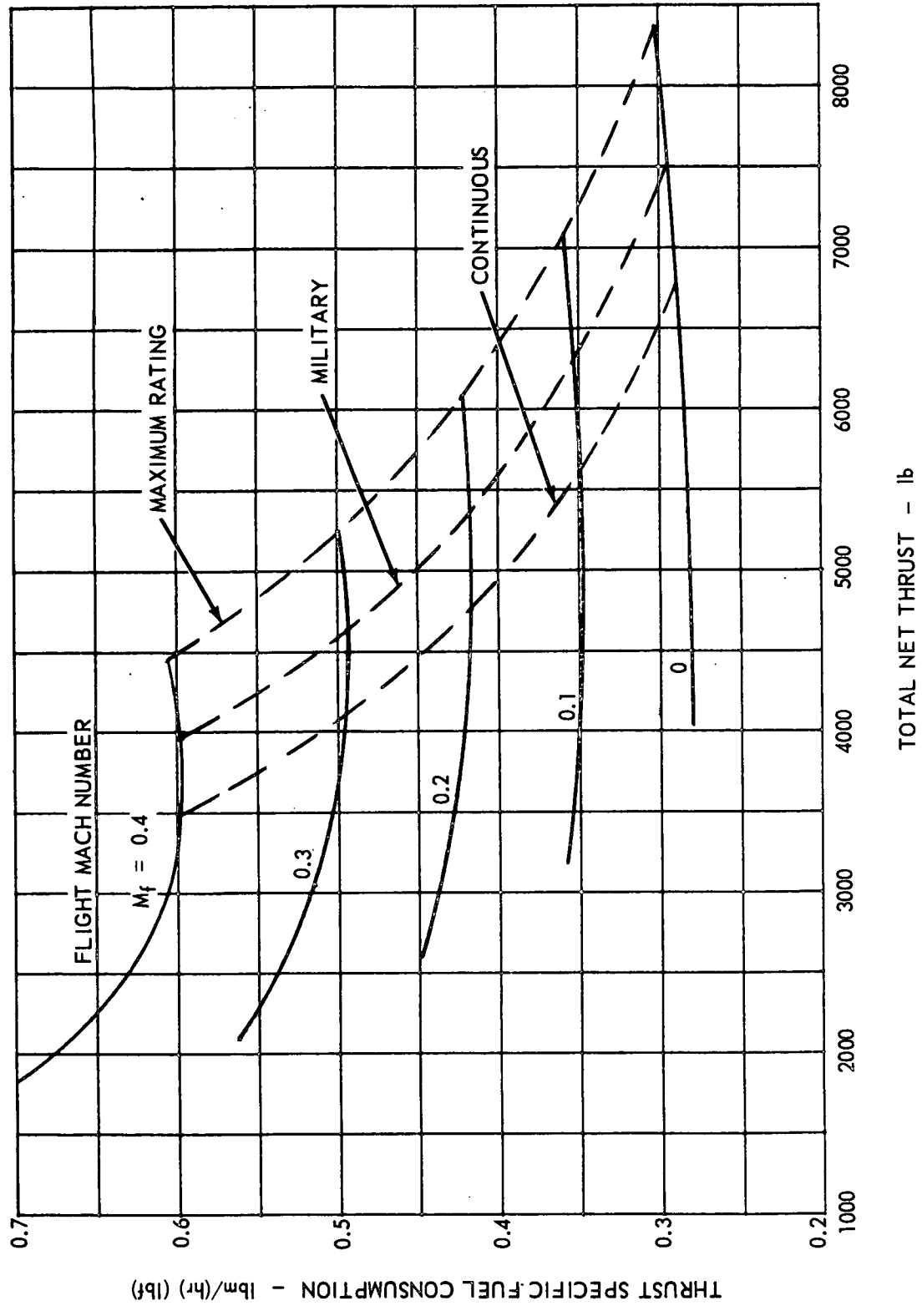
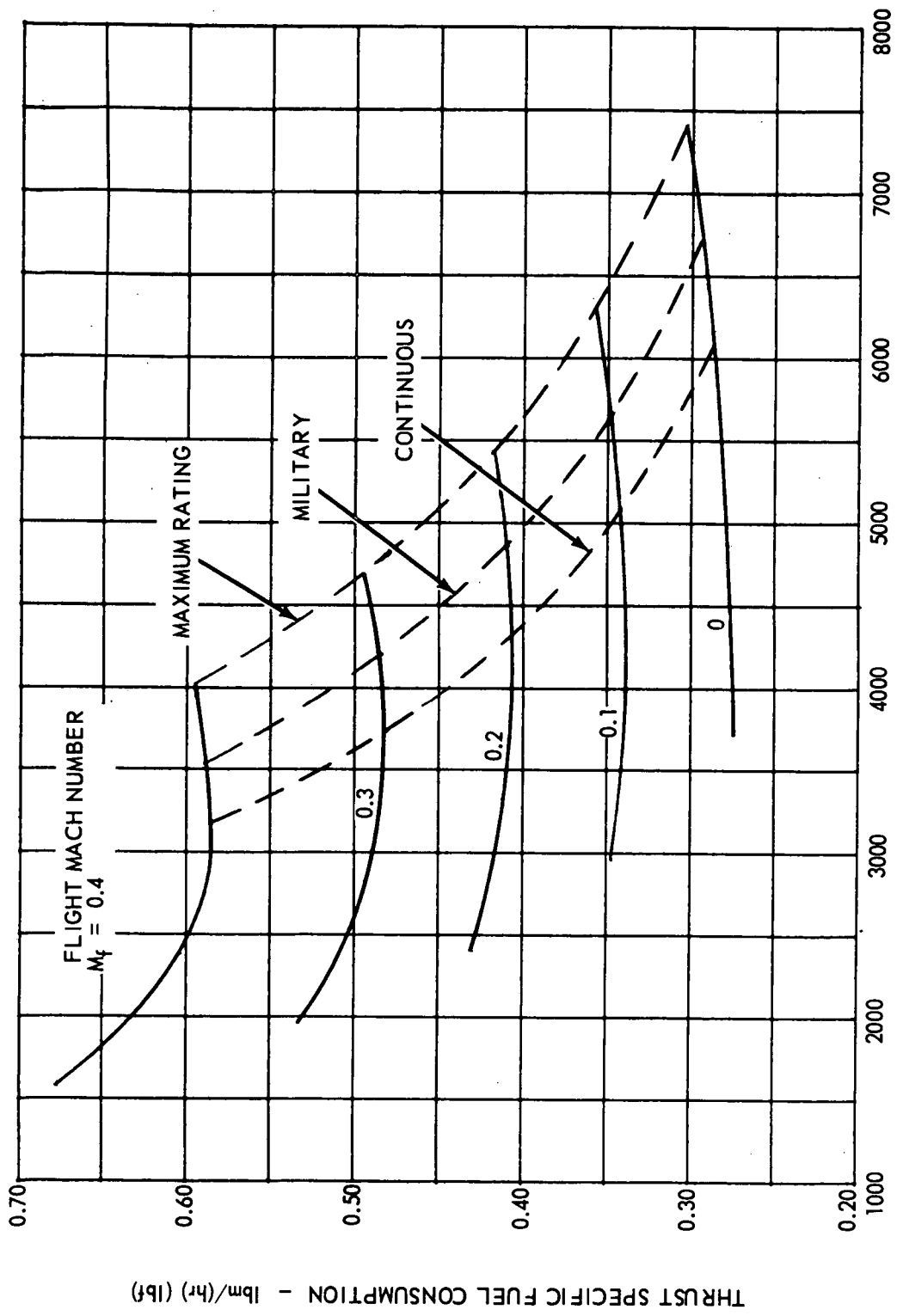


Figure 42. Fan Configuration B (SM = 14 Percent, A18 = 1190 Square Inches)  
 Estimated Performance at Sea Level on Standard Day.



TOTAL NET THRUST - lb

Figure 43. Fan Configuration B (SM = 14 Percent, A18 = 1190 Square Inches)  
 Estimated Performance at 5000 Feet on Standard Day.

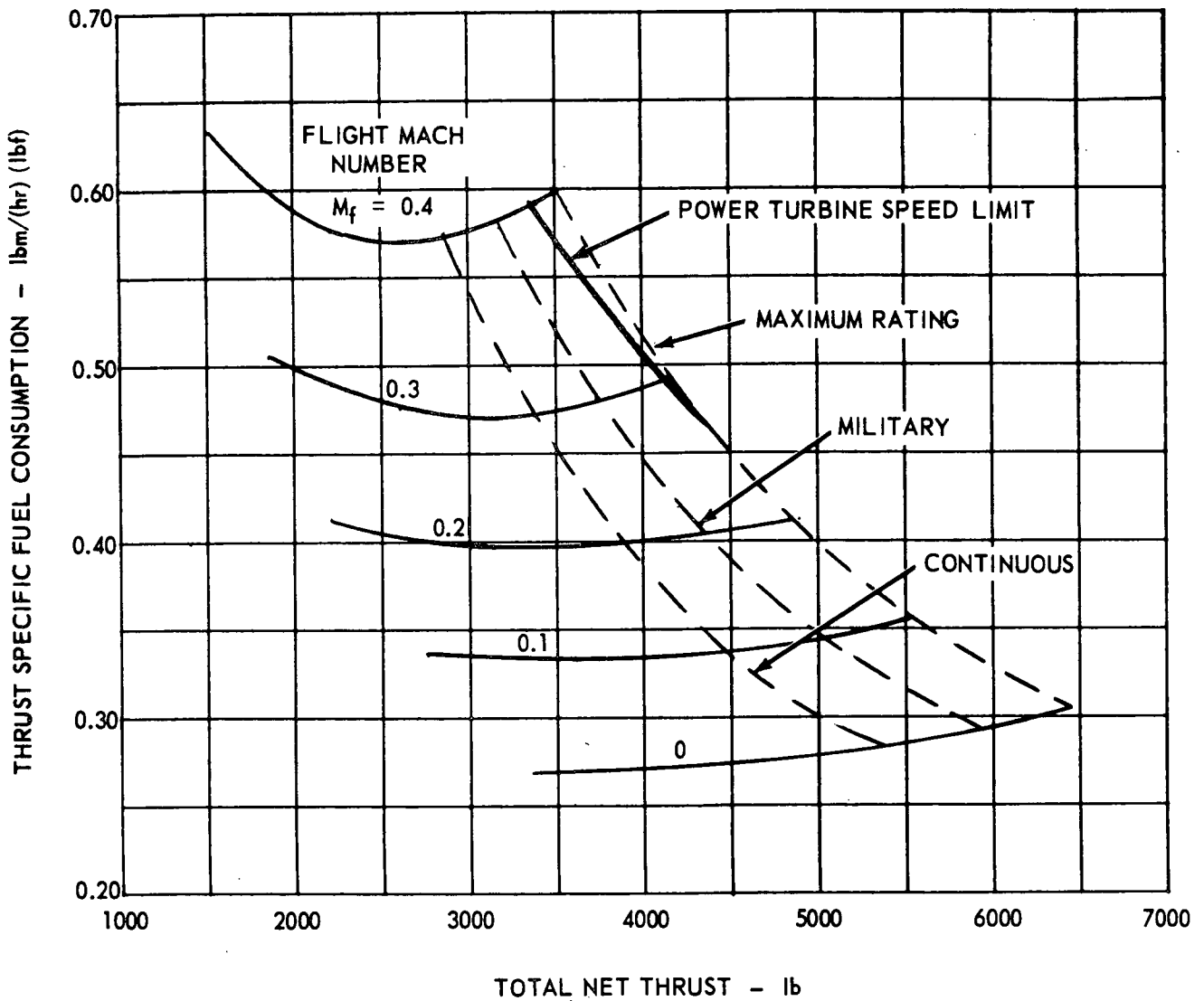


Figure 44. Fan Configuration B (SM = 14 Percent,  $A_{18} = 1190$  Square Inches) Estimated Performance at 10,000 Feet on Standard Day.

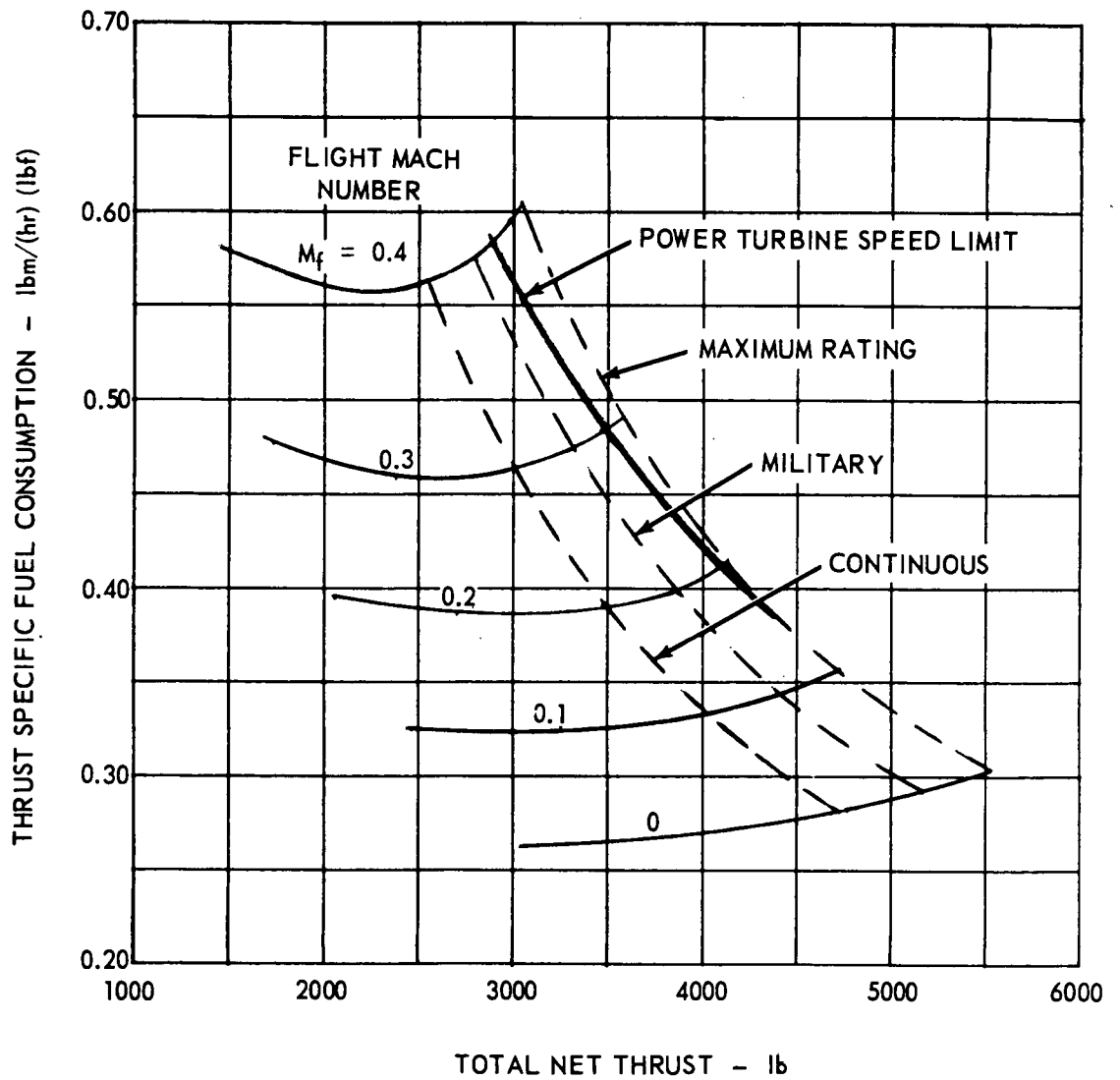


Figure 45. Fan Configuration B (SM = 14 Percent,  $A_{18} = 1190$  Square Inches) Estimated Performance at 15,000 Feet on Standard Day.

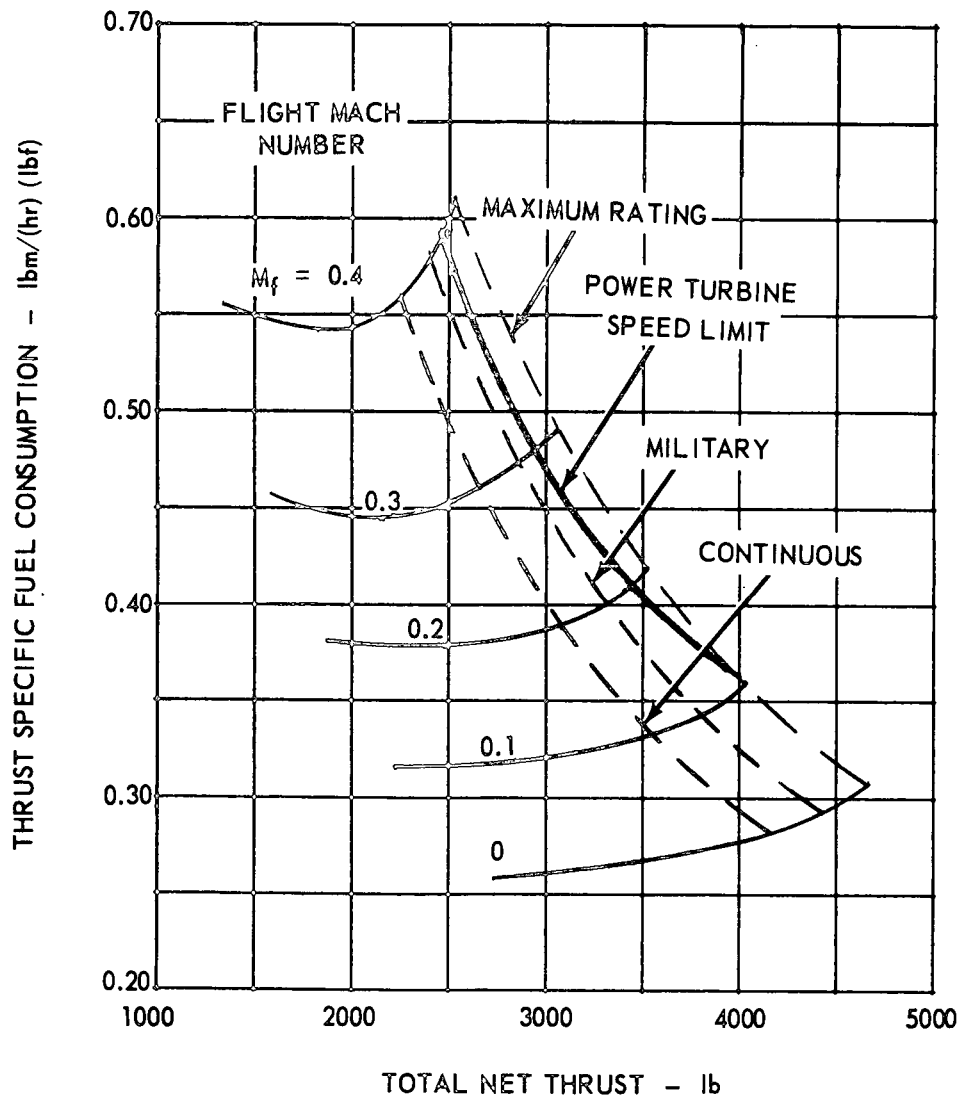


Figure 46. Fan Configuration B (SM = 14 Percent,  $A_{18} = 1190$  Square Inches) Estimated Performance at 20,000 Feet on Standard Day.

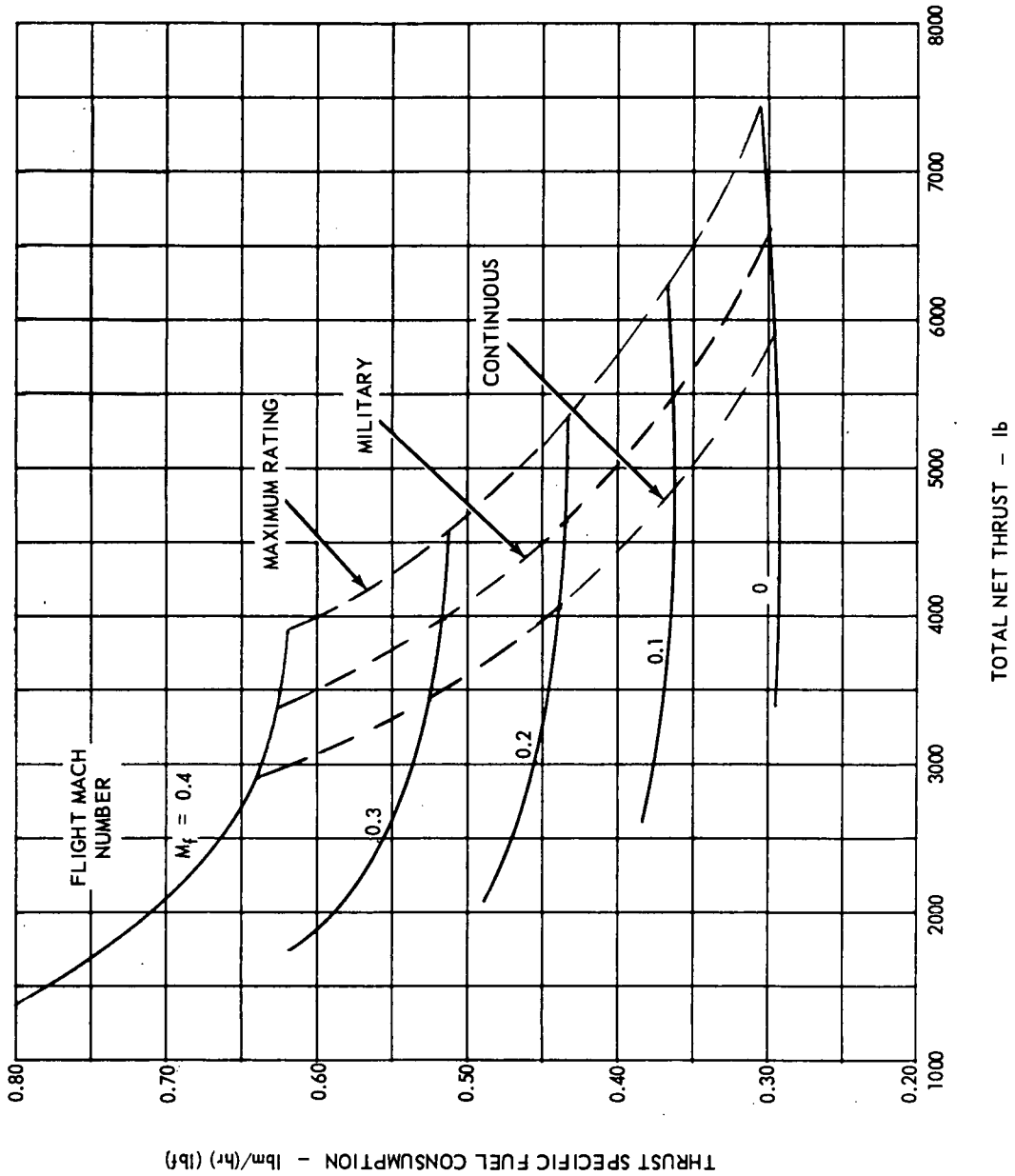


Figure 47. Fan Configuration B (SM = 14 Percent,  $A_{18} = 1190$  Square Inches) Estimated Performance at Sea Level on Tropical Day ( $90^{\circ}$  F).



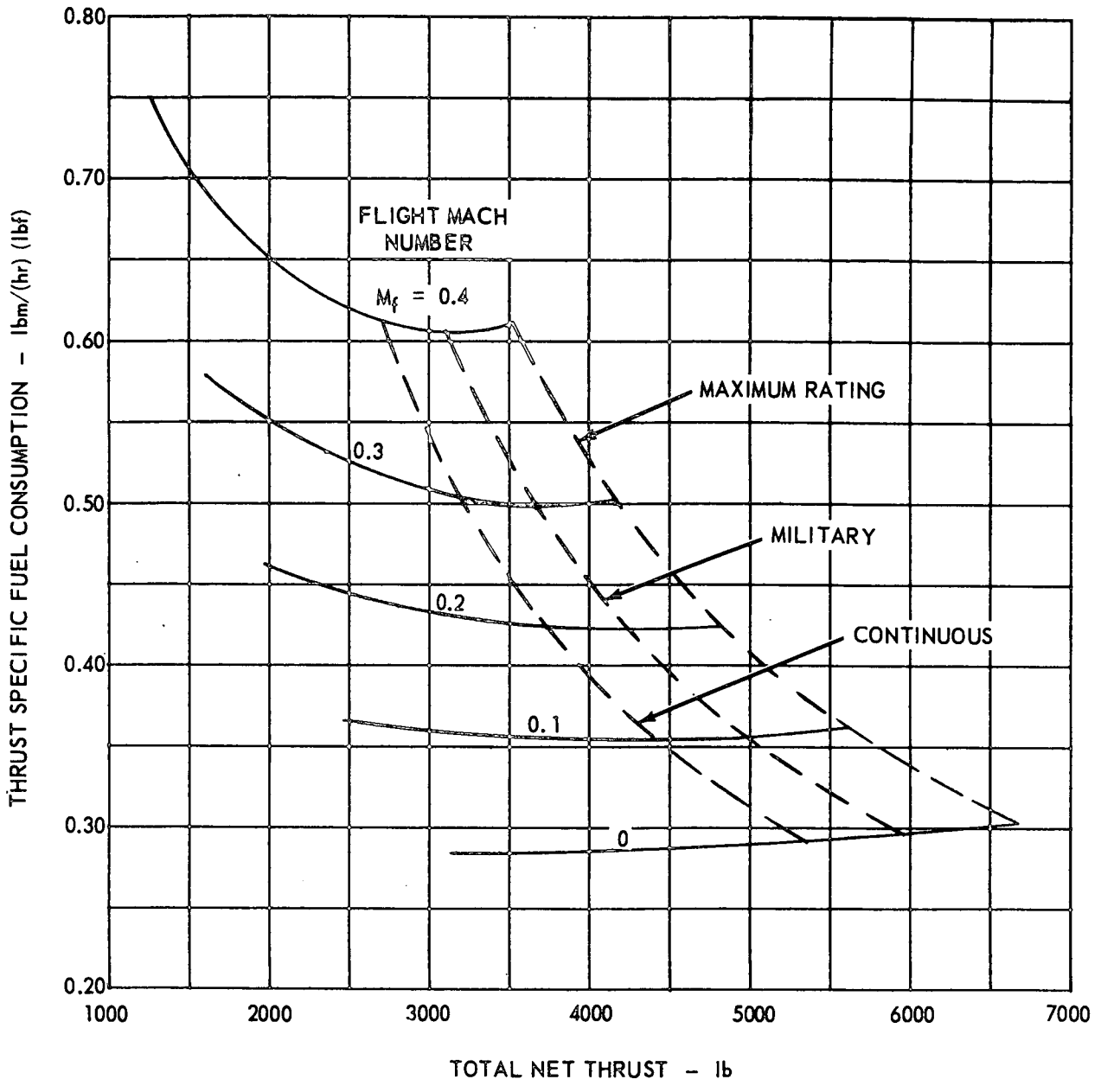


Figure 48. Fan Configuration B (SM = 14 Percent,  $A_{18} = 1190$  Square Inches) Estimated Performance at 5000 Feet on Tropical Day ( $70^\circ$  F).

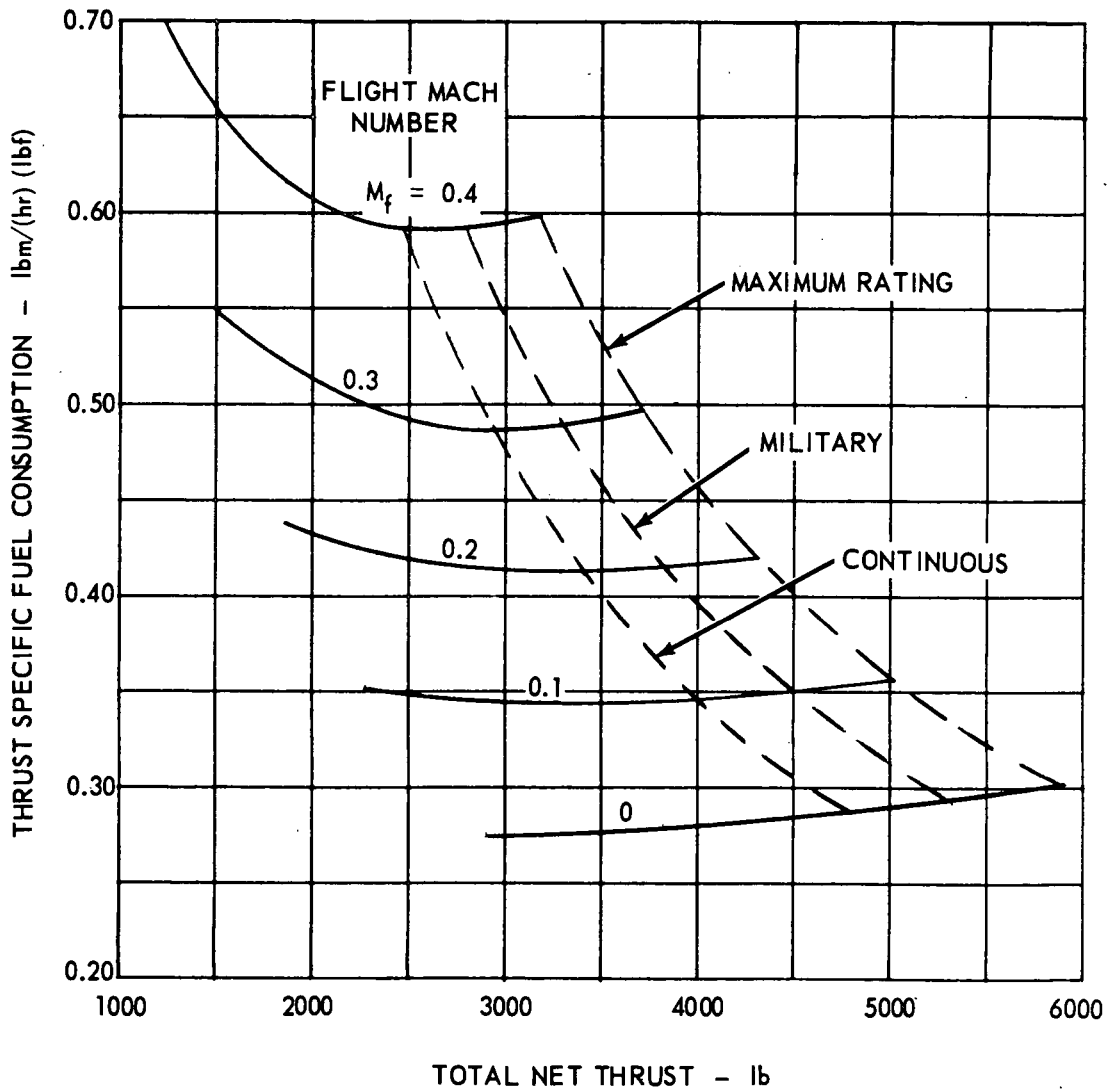


Figure 49. Fan Configuration B (SM = 14 Percent,  $A_{18} = 1190$  Square Inches) Estimated Performance at 10,000 Feet on Tropical Day ( $51^\circ$  F).

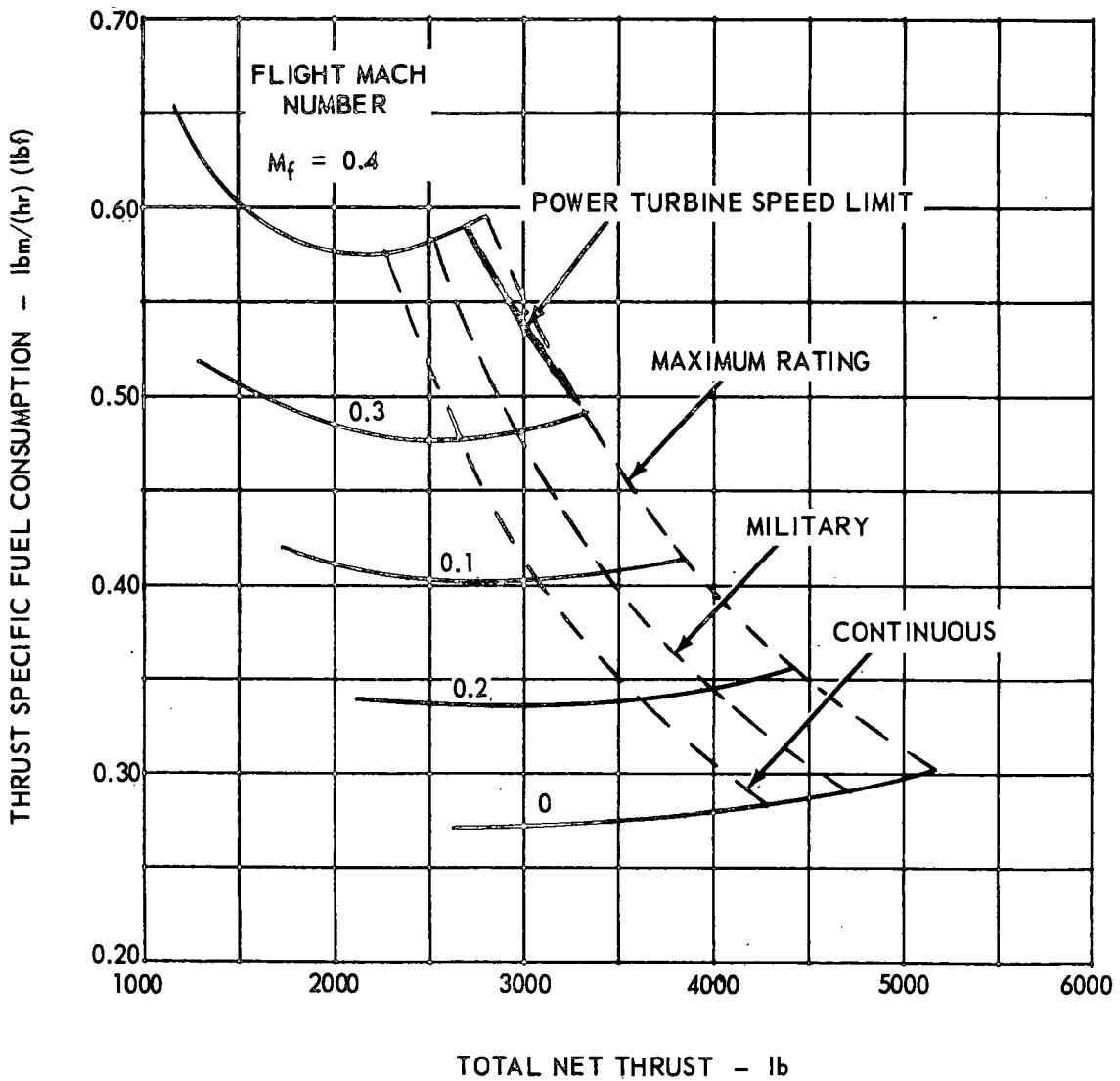


Figure 50. Fan Configuration B (SM = 14 Percent,  $A_{18} = 1190$  Square Inches) Estimated Performance at 15,000 Feet on Tropical Day ( $32^{\circ}$  F).

A

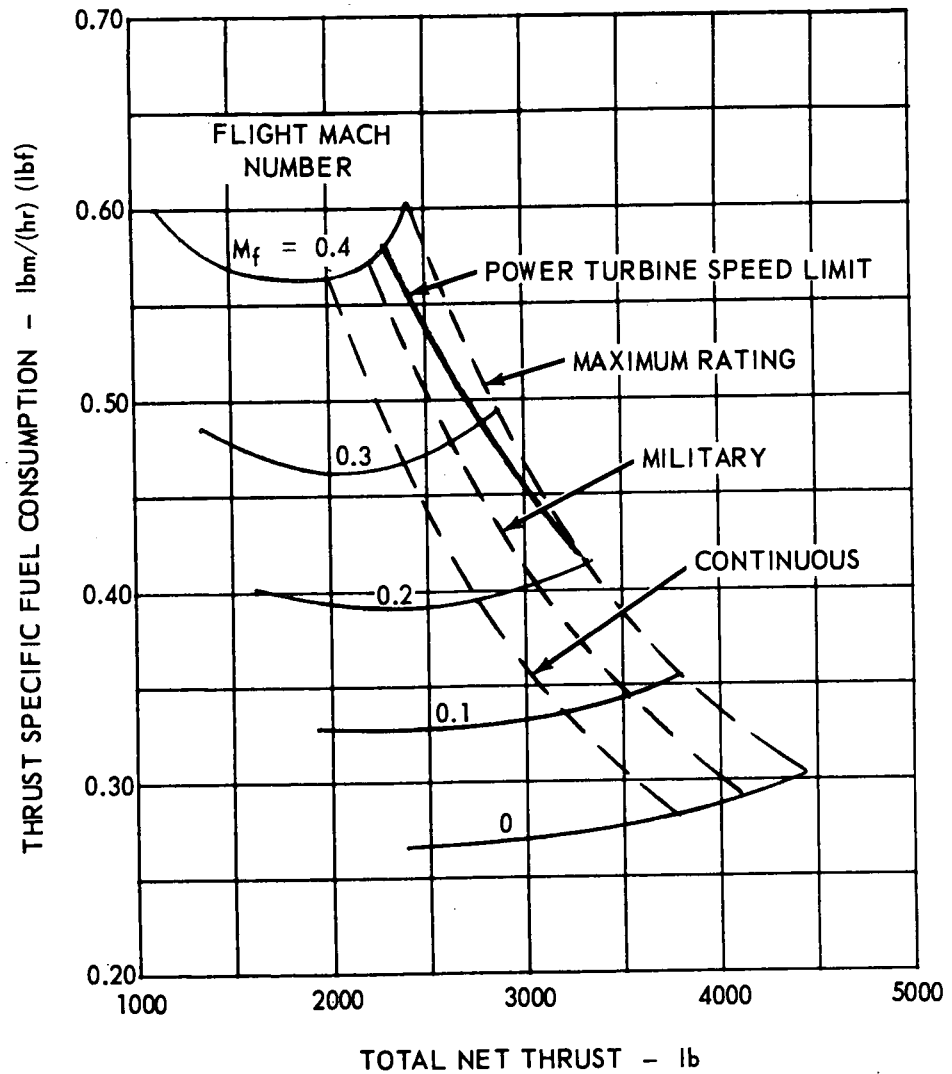


Figure 51. Fan Configuration B (SM = 14 Percent,  $A_{18} = 1190$  Square Inches) Estimated Performance at 20,000 Feet on Tropical Day ( $12^{\circ}$  F).

Estimated acceleration time for 66 percent of the interval between 80 percent maximum  $F_{NT}$  (total net thrust) and maximum  $F_{NT}$  (or, 80 percent maximum  $F_{NT}$  to 93.2 percent maximum  $F_{NT}$ ) for sea level standard conditions at Mach numbers from static to  $0.4 M_f$  is 2.5 seconds. The acceleration schedule used is the same  $W_f/\delta_{2.1} \sqrt{\theta_{2.1}}$  versus  $N_G/\sqrt{\theta_{2.1}}$  as that of the B-12 shaft engine and has full high compressor interstage bleed along the transient schedule. This insures the same high compressor referred acceleration surge margin for the fan that has been proven to be safe for the shaft engine using the same core components.

### Variable Bypass Nozzle

The degradation in fan efficiency associated with increasing flight Mach number can be neutralized with the use of an infinitely variable bypass stream exhaust nozzle. Reduction of nozzle area moves the fan operating line toward surge, thereby reversing the deleterious effect of increased Mach number with constant nozzle area. Of course, the control system associated with a nozzle that is made to vary continuously is quite complex, and the concept of a "two-position" exhaust nozzle with a more simple control requirement still affords the basic advantage of improved cruise performance.

Figure 52 is the Fan A characteristic with sea level operating lines shown at static and  $0.4 M_f$  for the base fan stream exhaust nozzle area. The result of reducing the nozzle area (12.0 percent) to relocate the  $0.4 M_f$  maximum rating match point into the static operating line, with the associated higher fan efficiency, provides a performance improvement of 16 percent  $F_{NT}$  and 15 percent TSFC. Now, free stream Mach number may be increased to  $0.7 M_f$  before returning the maximum rating point to the operating efficiency of the  $0.4 M_f$  point of the base configuration. The resultant performance improvement at cruise Mach numbers above  $0.4 M_f$  is shown in Figure 53, which presents comparative sea level standard day performance for both bypass exhaust nozzle areas.

## POWER TURBINE ANALYSIS

### General

An important aspect of the integral fan engine design includes use of the 502 MQT power turbine. This turbine has been designed with a 14 percent increased exhaust annular area, and will be phased into the 502 fan engine program much in advance of NASA time requirements. Use of the MQT power turbine reduces the exit velocity from 1,000 to 870 ft/sec for a

OPERATING LINES FOR FAN CONFIGURATION A

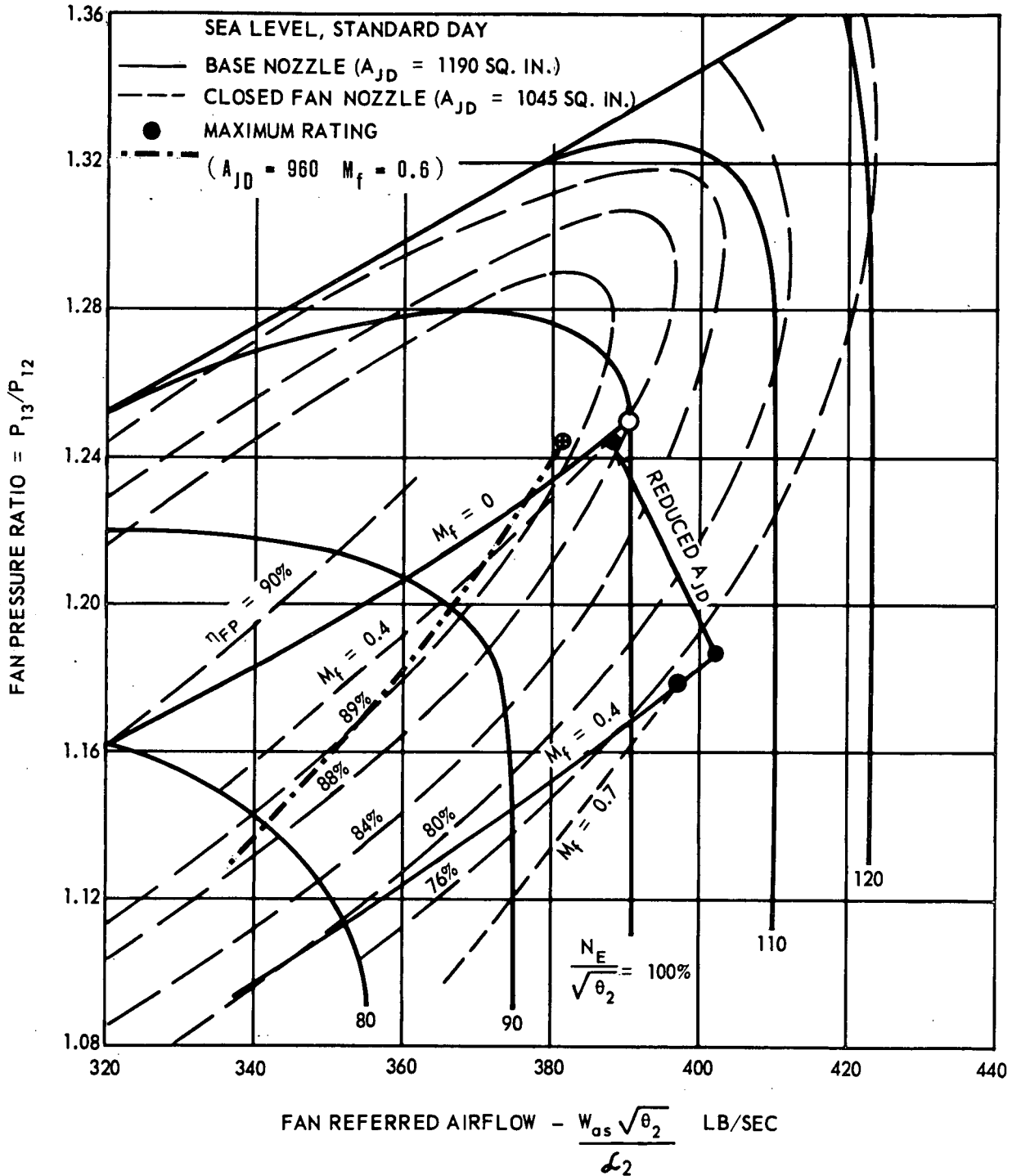


Figure 52. Estimated Fan Performance Map for Configuration A Showing Operating Lines With Two-Position Fan Exhaust Nozzle.

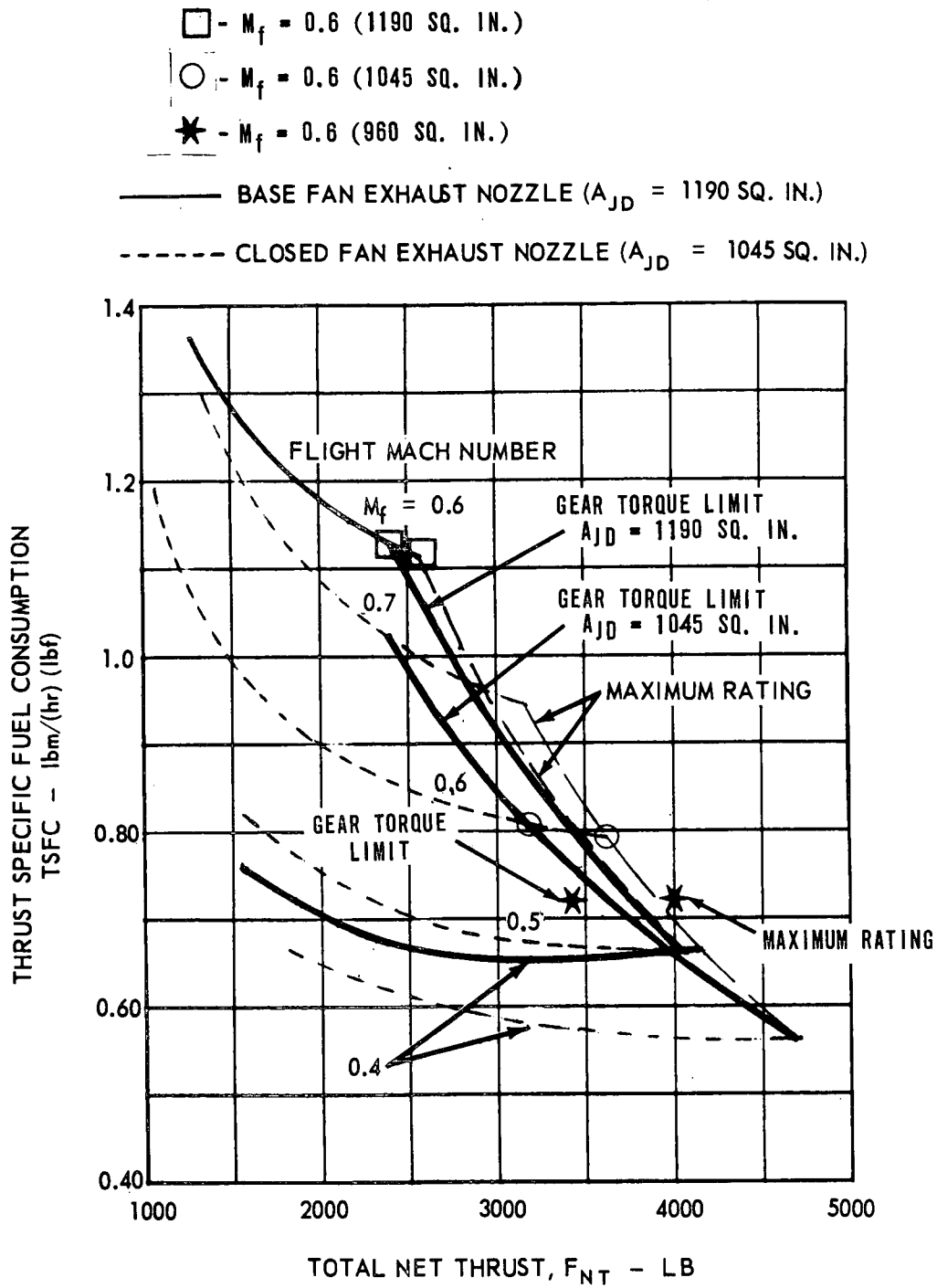


Figure 53. Fan Configuration A (SM = 21 Percent at 100 Percent  $N/\theta$ ) Estimated Performance at Sea Level on Standard Day With Two-Position Fan Exhaust Nozzle.

condition of exit static pressure equal to ambient. This reduction in hot jet exhaust velocity will have an important effect on the jet noise, since the use of a diffuser after the turbine was not acceptable because of the increase in engine length and related problems of ground clearance in the aircraft installation.

### Cycle Requirements and Turbine Aerothermodynamic Analysis

Matching studies of the 502 core engine supercharged by a 1.25:1 pressure-ratio fan show that the flow capacity  $W\sqrt{\theta_{cr}}/\delta$  of the MQT power turbine is 8.5 percent too large. As a consequence, an off-design analysis was made on the turbine blading to reduce the flow capacity to the required value of 17.03 lb/sec. Since a relatively small change in flow capacity was required to produce the proper engine matching condition at the desired compressor pressure ratio and maximum temperature, it was possible to accomplish the reduction by increasing the first stator stagger angle by 3.6 degrees to decrease the area and give the required flow capacity. The analysis accounted for change in incidence from the optimum value and Mach number change effects on each of the four cascades involved. The results showed that the loss in overall turbine efficiency resulting from the nozzle stagger angle change was 0.6 points, which assures the 0.887 value used in the cycle calculation since the MQT turbine target efficiency is 0.89 to 0.90.

Of particular interest in the analysis is the lowering of the second stage hub reaction when the flow reduction is made by the most simple change in turbine geometry involving only the first stage nozzle. The analysis indicated that a small acceleration was maintained at the second rotor hub, which should be adequate for the low camber (fluid turning 79 degrees) and low hub tip ratio (0.54) of this cascade.

Figures 54 and 55 show the hub, mean, and tip velocity triangles for the modified MQT power turbine at the sea level static design point. The thermodynamic state points are also included for additional information.

### ENGINE WEIGHT

Weight analysis for the integral life fan engine was relatively simple since the core is made up of the Lycoming T55-B12 turboshaft engine with the MQT power turbine; therefore, the weight is accurately known for these components, and only the new fan component, bypass duct including exhaust nozzle and the duct sound-attenuating rings and wall treatment had to be calculated. The weight of these new components was determined from basic aerodynamic design and mechanical design considerations already described.



$P_{t6} = 53.78 \text{ PSIA}$

$T_{t6} = 2048^\circ \text{R}$

$N = 16,870 \text{ RPM}$

$W = 31.8 \text{ lb/sec}$

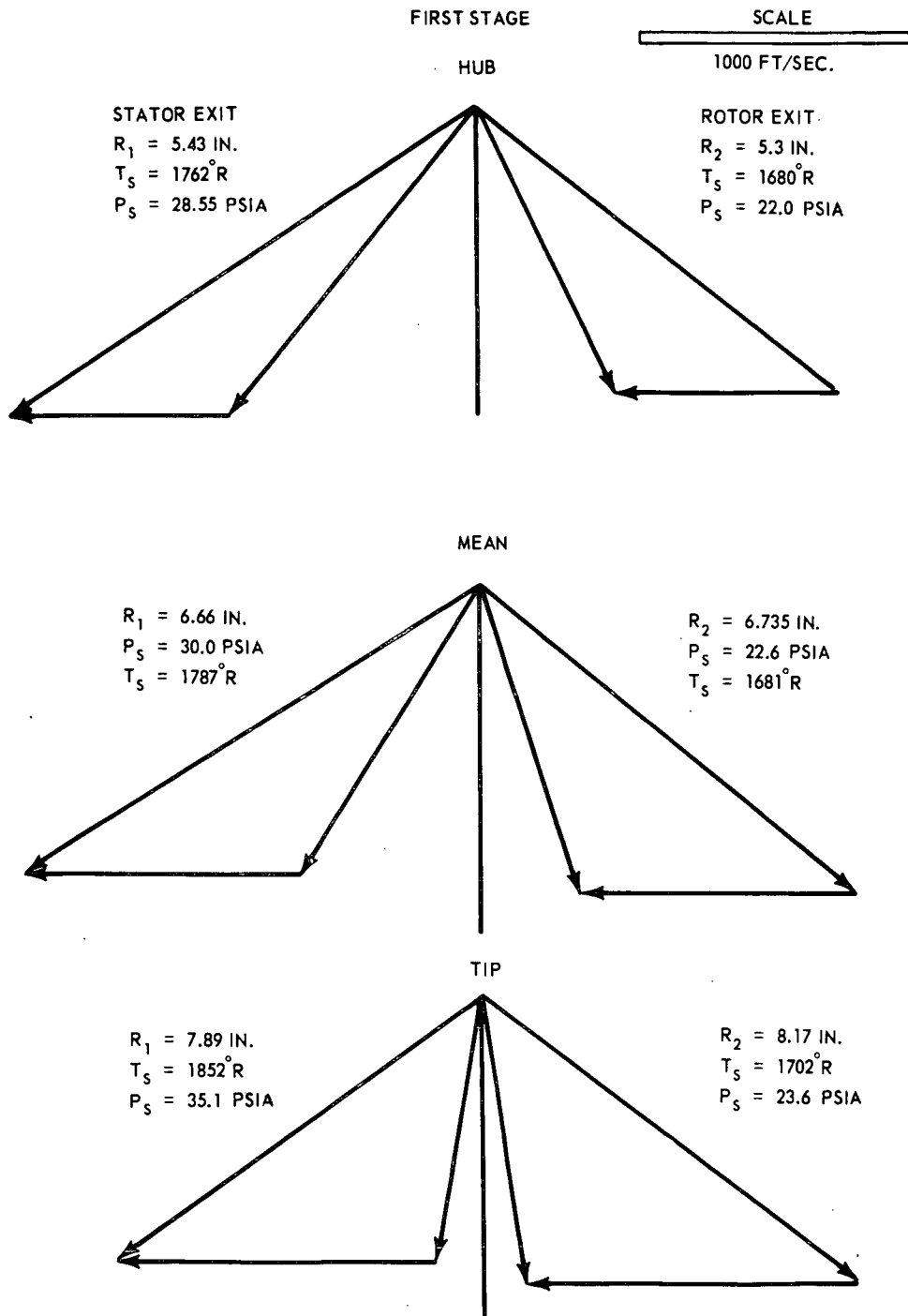


Figure 54. Modified MQT Power Turbine First Stage Velocity Triangles for 8.5 Percent Reduced Inlet Flow Function.

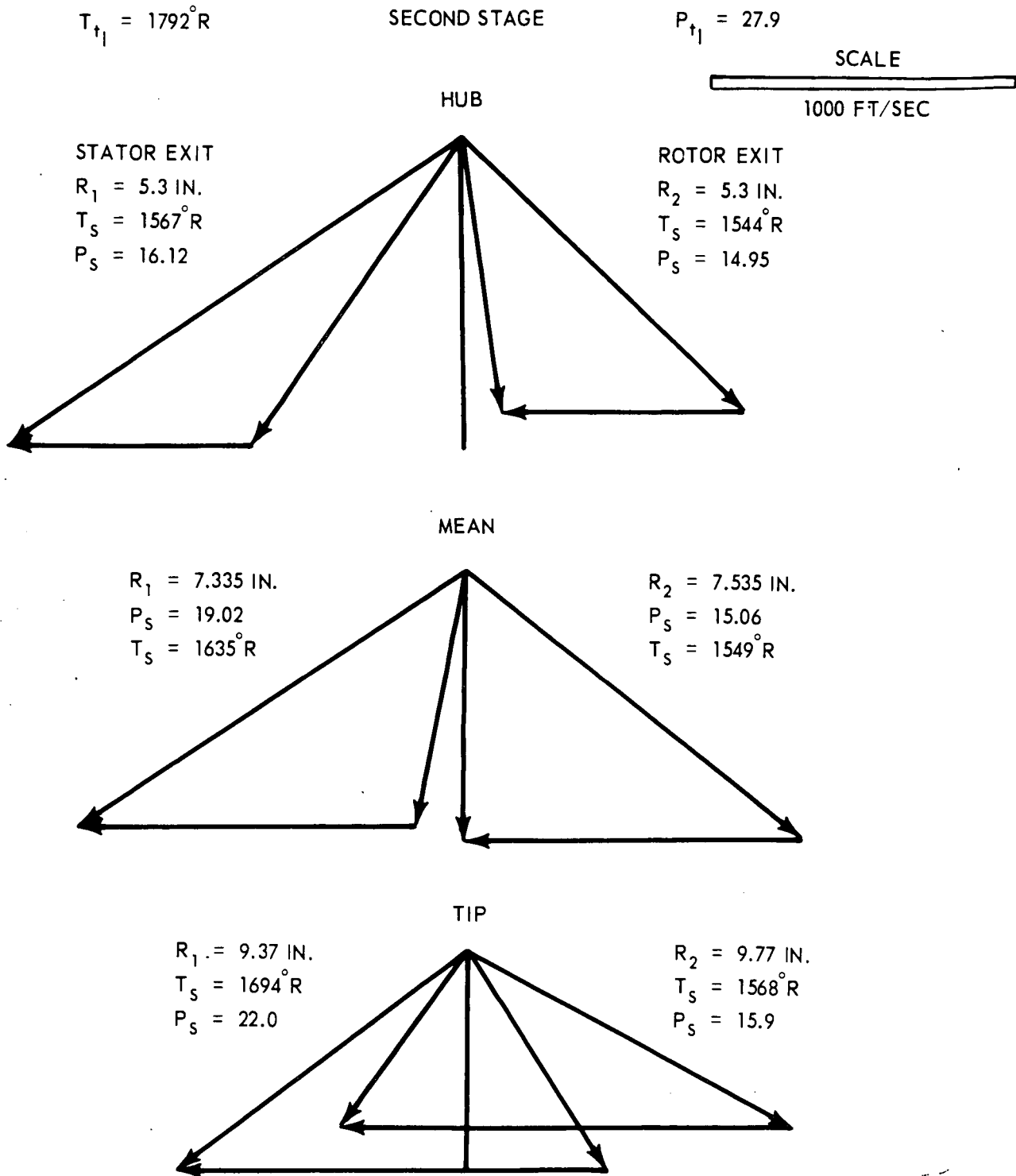


Figure 55. Modified MQT Power Turbine Second Stage Velocity Triangles for 8.5 Percent Reduced Inlet Flow Function.

The dry weight of the engine without starter is 1419 pounds, \* and is made up of the following components:

	<u>Weight (lb)</u>
Core With Accessories (excluding power turbine)	510.50
MQT Power Turbine and Drive Shaft	165.00
5-Planet Reduction Gear	172.90
Fan Rotor Plus Blades and Spinner (titanium)	153.30
Fan Shroud (titanium)	58.00
Straightening Vanes for Duct and Core (aluminum)	66.10
Support Frame (magnesium)	194.00
Bypass Duct and Nozzle (aluminum and polyimid resin)	41.00
Bypass Duct Noise-Attenuating Rings (polyimid resin)	<u>58.40</u>
Total	1,419.20

---

\* Based on fixed-area bypass duct exhaust nozzle

## SCHEDULE AND COST ESTIMATE OF INTEGRAL LIFT ENGINE

### Program Planning

An engineering program has been planned that would lead to development of the integral lift engine to a point where flightworthy engines could be provided for experimental aircraft. The overall 22-month program has been planned such that lesser objectives could be achieved in shorter periods of time.

Figure 56 shows a program schedule detailing major tasks, hardware development, and delivery schedules. This overall program schedule is segmented into three phases.

Phase I - Demonstrator Engine. - The intent of the Phase I program is to establish the credibility of the engine design by measuring static performance and establishing its noise signature. A single demonstrator engine would be procured and tested. The configuration would include downstream fan noise suppression (reference design); however, a conventional test cell bellmouth assembly would be used at the fan inlet. Suitable aerodynamic instrumentation would be installed. Preliminary testing would be limited to that necessary to establish adequate lubrication system and fuel system operation to assure satisfactory steady-state operation. Mechanical integrity instrumentation would be limited to that required for safe engine operation.

A 2- to 4-month engine test program is envisioned with 50 to 80 test hours logged in the test cell and at the free field noise site. After partial disassembly and inspection, it is anticipated that the engine could be re-assembled for continued testing and evaluation either locally or at an off-site test facility.

The demonstrator engine program would validate the design point performance of the configuration and sea level static operating line performance.

The demonstrator engine program would underwrite the detail design of the design study engine and design of required special test equipment for cell and field site operation. It would also procure soft tooling for any subsequent procurements.

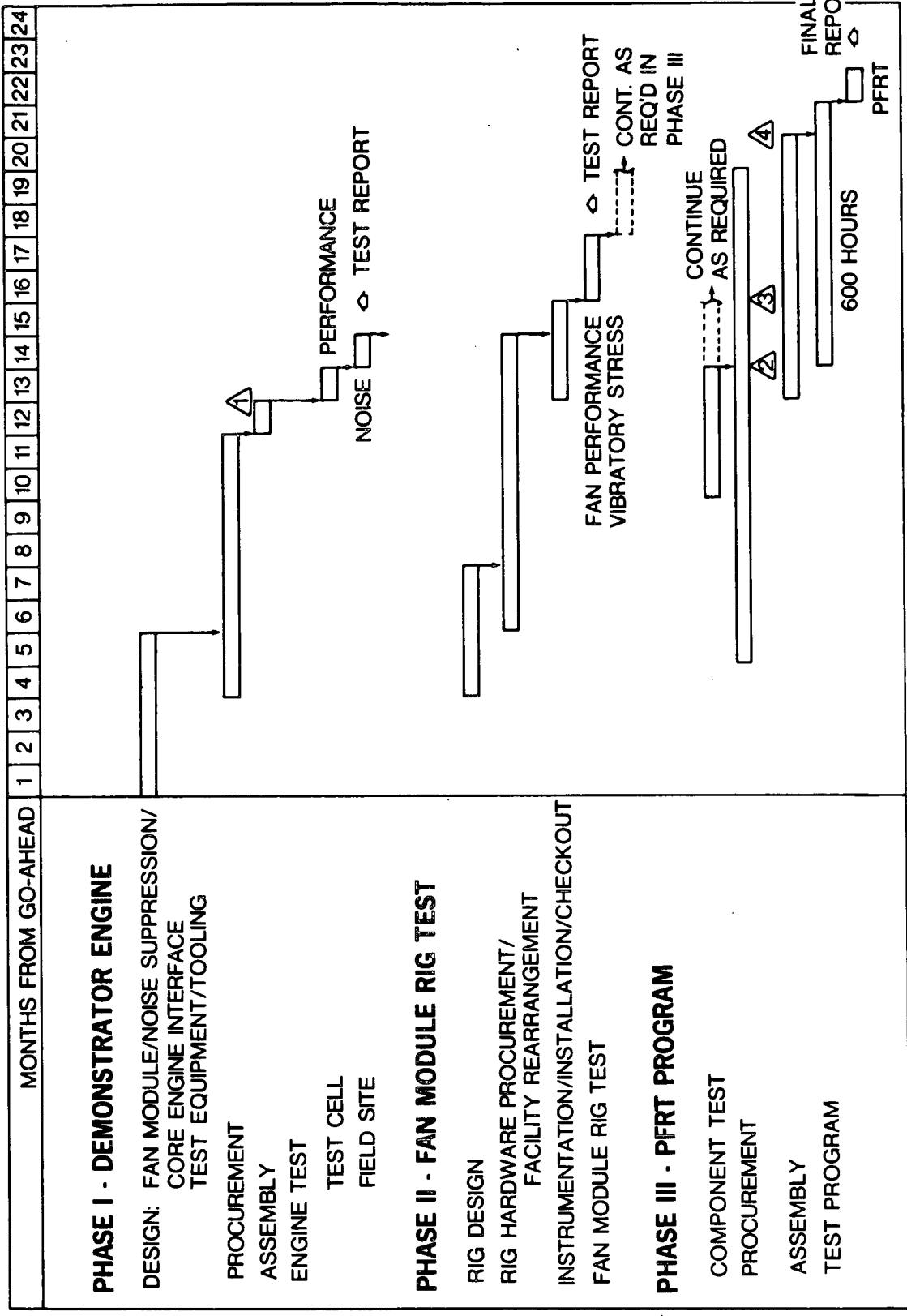


Figure 56. ALF-504 Engine Program.

Phase II - Fan Module Rig Test. - The intent of the Phase II rig test program is to enhance the demonstrator engine program by validating the predicted performance of the fan component. An overall performance map would be produced from part speed to overspeed up to, and including, the surge line for the anticipated operating range of representative aircraft applications. Available facility power may impose certain operating limitations.

Installed aerodynamic instrumentation would permit computation of overall and blade row performance parameters, including adiabatic and polytropic efficiencies and vector diagrams.

Vibratory stress instrumentation would also be installed to sense regions of rotating stall, and sufficient stall data would be gathered to define potential areas of blade vibration resonances.

In Figure 56, the fan module test rig has been planned to complement the objectives of the demonstrator engine program. It could also be considered an independent program of 16 month's duration. This latter case was the basis assumed for the Phase II budgetary cost estimate. To integrate the program with the demonstrator engine program, the rig test has been scheduled to receive the second fan module fabricated. As an independent program, rig testing could start in the fourteenth month.

Phase III - PFRT Program. - Phase I and Phase II were planned to validate in hardware the results of the engine design study by confirming predicted component and overall performance values. From this base, Phase III is a continuing development program intended to bring the configuration to limited operational status, suitable for use in experimental prototype aircraft.

Phase III will culminate in the successful completion of a PFRT (preliminary flight rating test). It is essentially an engine program with limited effort at the component level. Three additional in-house test engines would be procured with a goal of 600 engine hours to be logged before initiation of the PFRT.

Types of engine tests planned are:

Steady-State Performance

Transient Performance

Variable Attitude Operation

Determination of Surface Temperatures

Overall Vibration Survey

Oil/Fuel System Operational Evaluation and Optimization

Cyclic Endurance Testing.

The task requirements of this program are very similar to those of our ALF-502A/YF-102 engine development program where the PFRT was successfully completed in the spring of 1972. Northrop A9A aircraft are now flying powered by these Avco Lycoming high-bypass-ratio turbofans.

The ALF-502 program schedule and costing were based on this recent history.

Budgetary and Planning Cost Estimate

1. PFRT Engine Program - \$6.5M

- NOTES:
1. Total program shown on schedule, Figure 56.
  2. PFRT complete 22 months ATP.
  3. Summation of Phases I, II, and III schedules.
  4. Costs include procurement of 4 engines and 2.5 equivalent engines for component test and in-house spares.
  5. Cost assumes Government-furnished fuel and lubricants.

2. Unit Cost of Deliverable Flight Rated (PFRT) Engines - \$485K

3. Phase I - Demonstrator Engine Program - \$2.4M

- NOTES:
1. Cost based on 14 months, one engine program.
  2. Cost includes detail design of engine and special test support equipment, procurement of tooling, 1/2 equivalent engine for in-house spares, and one set engine test support equipment.

3. Cost assumes Government-furnished fuel and lubricants.
4. Phase II - Fan Rig Test Program - \$750K

NOTES: 1. Costs include fan module detail design and tooling. If Phase I and Phase II are implemented concurrently, reduce Phase II cost by \$300K.

2. Assumes a 16-month program.

#### 5. General Assumptions and Conditions

The costs shown are based on rent-free use of the Stratford facility and tooling.

For purposes of cost estimating, an assumed go-ahead date of 1 January 1973 was selected. Average labor rates were used and represent those anticipated for the CY 1973 and CY 1974 period. Material costs were estimated at current rates and increased to represent CY 1973 and CY 1974 procurements.



## APPENDIX I AERODYNAMIC INFLUENCE OF THE PART-SPAN SHROUD

The part-span shroud creates an additional channel flow blockage effect that must be taken into account in the fan design.

In Reference 1, detailed radial surveys of the various flow parameters were taken at the exit of a part-span shrouded fan rotor and compared with the corresponding data for the same rotor without shroud. It was shown that the presence of the part-span shroud substantially modifies the tangential and meridional velocity profiles at the rotor exit station over the entire channel height. This finding prompted the following investigation, which is aimed at taking into account the effect of the annulus wake of the part-span shroud on the fan rotor flow conditions.

Figure 57 reproduces the axial and tangential velocity distributions measured at rotor exit station of the fan of Reference 1. It will be seen that the part-span shroud creates a wake with lower axial velocity and a higher tangential velocity than in the surrounding flow region.

Figure 58 shows, among other data, a total temperature survey taken at exit of the 502 fan rotor, which confirms the higher work input to the wake flow by the part-span shroud. At any point in the wake, the total temperature results from the mixing of particles undergoing the normal compression process outside the shroud boundary layer and particles inside that boundary layer. Since the tangential velocity in the shroud boundary layer varies from  $U_s$  (part-span shroud rotational speed) to  $V_\theta$  (tangential flow velocity immediately outside of the boundary layer), the entire  $U_s$ ,  $V_\theta$  tangential velocity spectrum is involved in the mixing process. The situation, however, can be conveniently schematized by considering the temperature at any wake point to result from the mixing of particles with only two different tangential velocities, namely  $U_s$  and  $V_\theta$  (as imparted by the rotor blading just outside of the boundary layer). This scheme enables an equivalent mixing mass flow ratio to be defined for each temperature point in the wake downstream of the rotor. Accordingly, we write for the unit mass in the wake:

$$T_{\text{wake}} = m_1 T_{V_\theta} + m_2 T_{U_s} \quad (1)$$

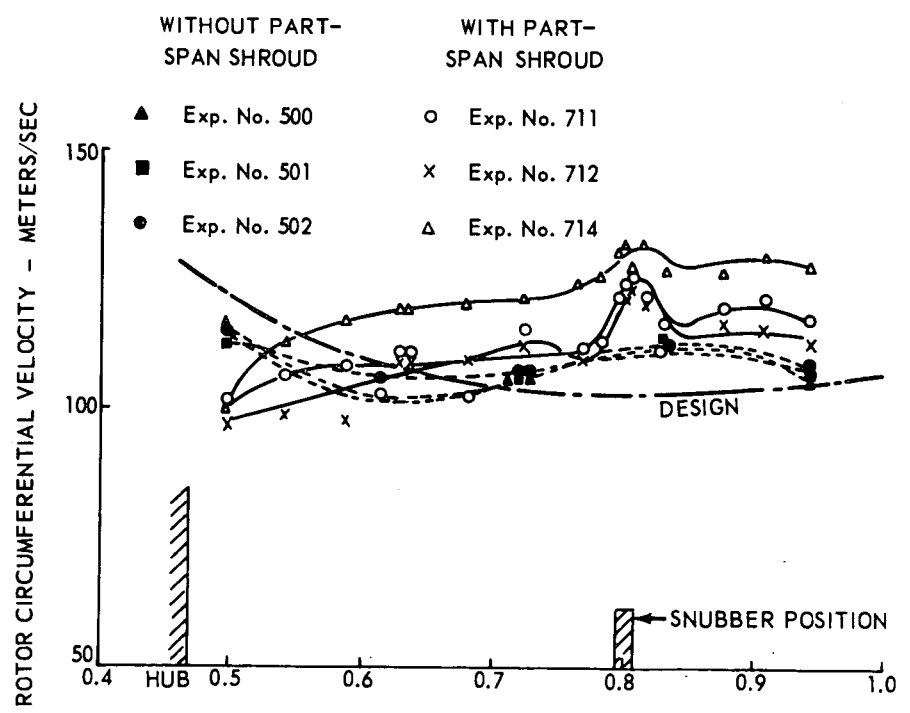
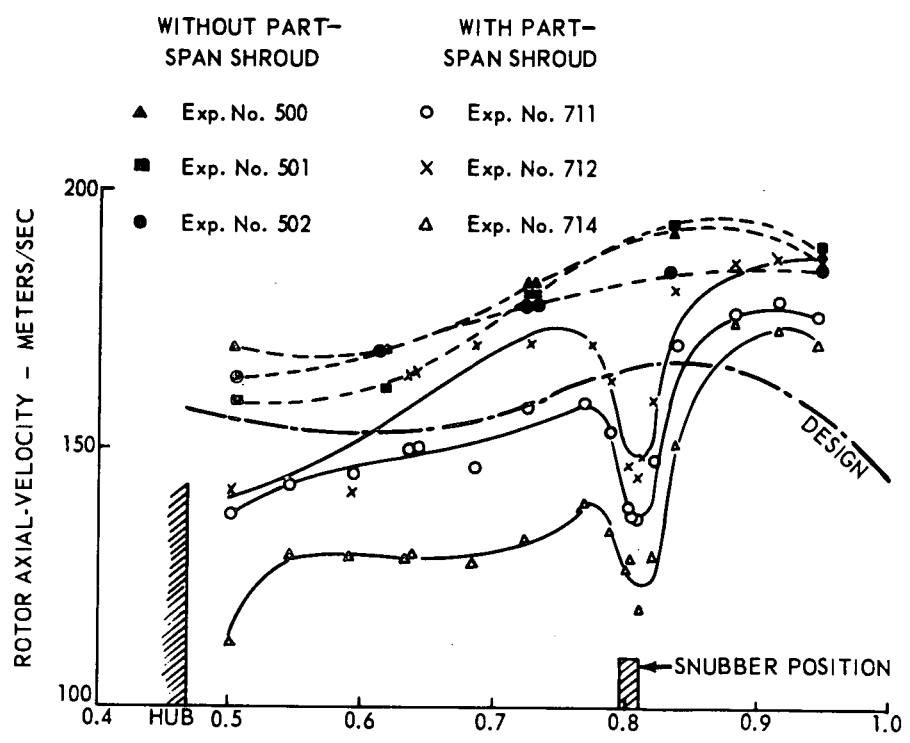


Figure 57. Measured Flow Conditions Downstream of Rotor (Reference 1, "Some Studies of Front Fans With and Without Snubbers").

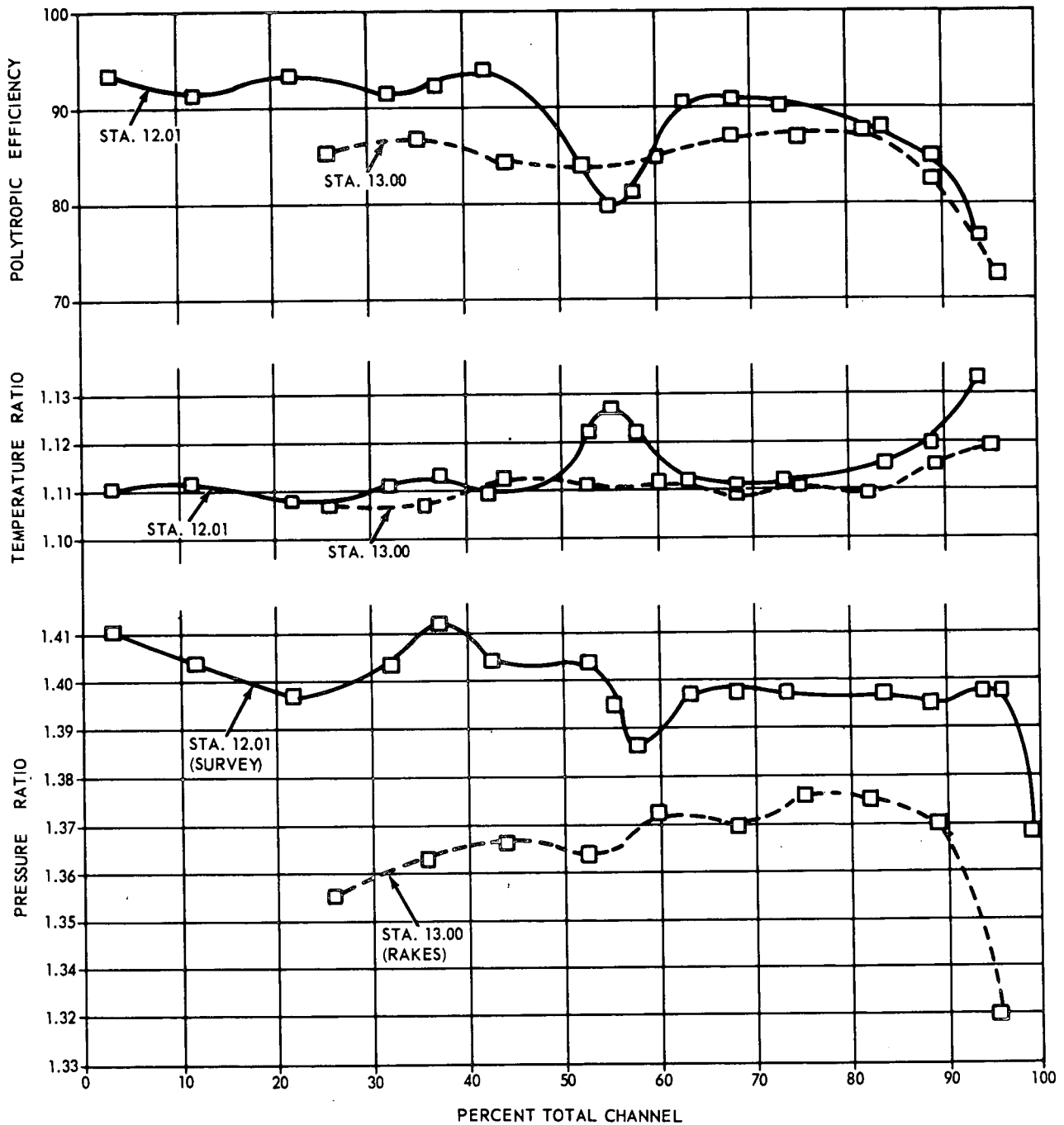


Figure 58. Radial Surveys Downstream of ALF-502 Fan Rotor, Test -02.

where  $m_1 + m_2 = 1$  and  $T_{V_\theta}$  and  $T_{U_s}$  are the total temperatures at rotor exit station resulting from the work input of the blading and of the shroud at its rotational speed  $U_s$  respectively. Hence:

$$\frac{m_2}{m_1} = \frac{T_{\text{wake}} - T_{V_\theta}}{T_{U_s} - T_{\text{wake}}} \quad (2)$$

It is now assumed that the above equivalent mixing ratio, which characterizes the local degree of mixing, is independent of the thermodynamic state of the mixing components and thus can be assumed to have essentially identical values at corresponding locations in the part-span shroud wake of different rotors.

Taking the highest wake temperature point at rotor exit of the 502 fan from the 90 percent referred design speed survey shown in Figure 58, namely:

$$T_{\text{wake}} = 1.127 T_{\text{amb}} = 584.6^\circ \text{R} \quad (3)$$

and

$$T_{V_\theta} = 1.110 T_{\text{amb}} = 575.8^\circ \text{R} \quad (4)$$

and with

$$U_s = 905 \text{ ft/sec}, \quad (5)$$

that is,  $T_{U_s} = 655.3^\circ \text{R} \quad (6)$

Equation (2) yields  $m_2/m_1 = 0.1244$ .

Applying this equivalent ratio for the present fan with the design point parameters

$$T_{V_\theta} = 556.5^\circ \text{R} \quad (7)$$

$$U_s = 824 \text{ ft/sec}, \quad (8)$$

that is,  $T_{U_s} = 631.5^\circ \text{R} \quad (9)$

Equation (1) yields  $T_{\text{wake}} = 564.8^\circ \text{R}$ .

The corresponding rotor efficiency can be calculated from the above total temperature, the resulting  $V_\theta$  component, and tentatively assumed

values of the static pressure and meridional velocity component. The meridional velocity is assumed to be in the same ratio the the unperturbed value as measured in Reference 1 and shown in Figure 57. A close value of the static pressure is available from a previous calculation without part-span shroud effect. (It can be iterated for final design purposes.) The resulting polytropic efficiency is  $\eta_{p \text{ wake}} = 0.67$  and the total wake pressure ratio  $(P/P)_{\text{wake}} = 1.221$ . The results are compared in the following table:

	Rotor Data	ALF-502 Fan Measured at 90 Pct Ref Design Speed	NASA Fan Calculated at 100 Pct Ref Design Speed
Outside of Part-Span Shroud Wake	P/P $\eta_p$	1.40 0.935	1.262 0.945
At Part Span Shroud Wake Core	P/P $\eta_p$	1.386 0.80	1.221 0.67
	$\Delta T_{\text{wake}_{\text{max}}} (^{\circ}\text{R})$	8.8	8.3

The wake core total temperature excess  $\Delta T_{\text{wake}_{\text{max}}}$  is practically the same in both cases. This is due to similar values of the difference  $U_s^2 - UV\theta$  for both rotors and follows immediately from the basic assumption of equal equivalent mixing mass ratios. The mixing losses in the present case, however, represent a substantially larger portion of the rotor work input and this is correctly reflected in both the calculated lower polytropic efficiency and the larger relative total wake pressure defect.

For the computer flow calculation procedure a 1.5-inch wake thickness has been assumed at rotor exit station 12, and the wake flow has been represented only by the two wake-limiting streamlines and the wake core streamline with the above-calculated input data. The calculated wake blockage effect is approximately 1 percent of the total annulus area.

Figure 59 compares the meridional velocity profiles at rotor exit station with and without wake effect, but with identical overall flow blockage factors. It will be seen that the part-span shroud actually influences the flow field over a large portion of the annulus and that the modification of the velocity profile is qualitatively similar to that shown in Reference 1, although both effects are less pronounced in the present case.

This preliminary investigation shows that the influence of the part-span shroud on the fan flow conditions cannot be properly accounted for by a mere additional global flow blockage factor. A proper assessment of the resulting effect on the actual blading geometry, however, would require a more detailed description of the wake and its downstream dissipation, and possibly take into account the obstruction effect of the shroud itself on the rotor inlet flow conditions.

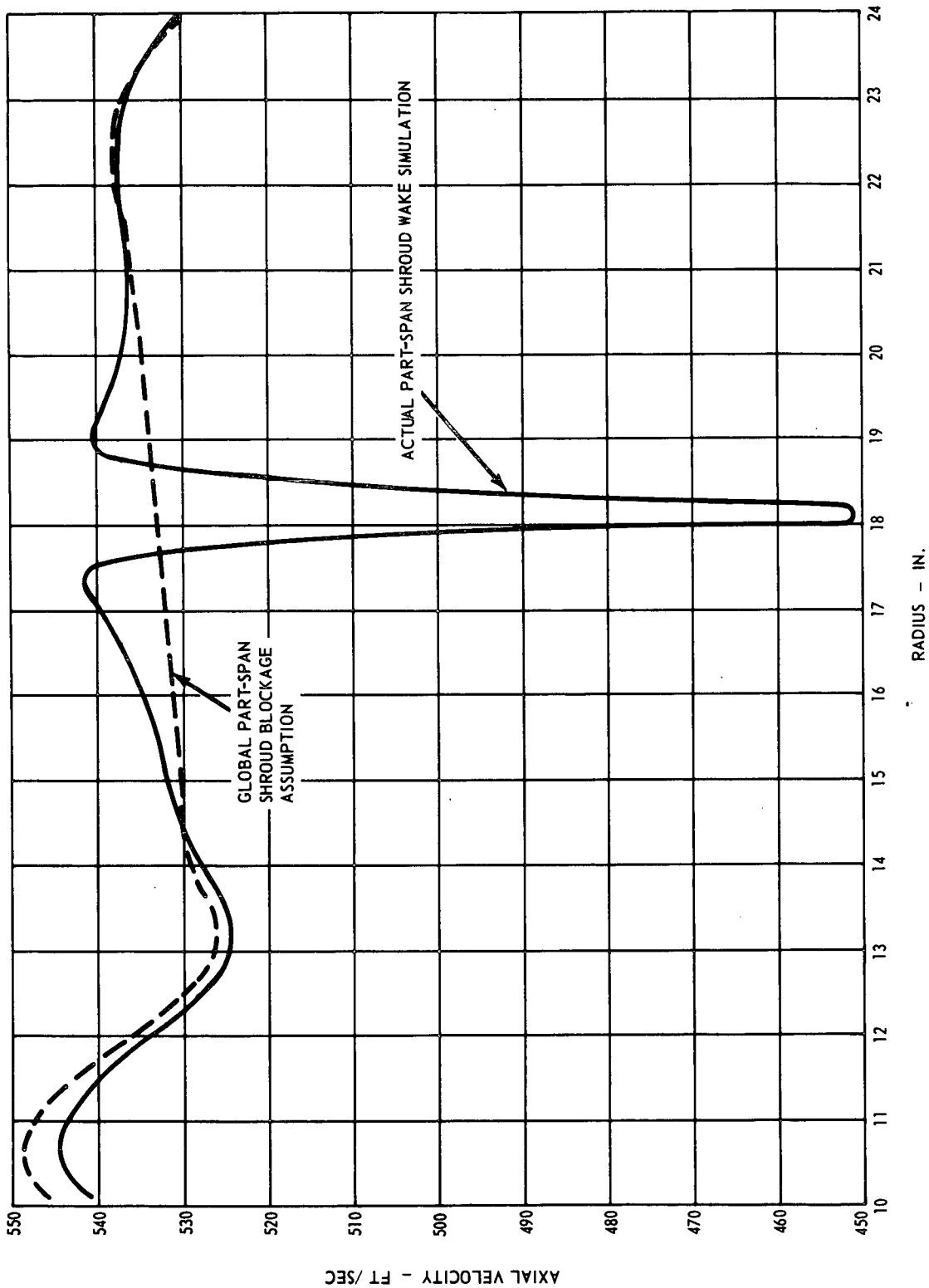


Figure 59. Analysis of Part-Span Shroud on Axial Velocity Profile Downstream of Fan Rotor.

**APPENDIX II  
FAN FLOW CONDITIONS**

Main Output

GROUP I

Group I output is repeated for each computing station in accordance with the input specification of Identifier 500. The sequence in which the stations appear in Output is:

1. Stations of the flow region upstream of splitter.
2. Stations of the lower flow region downstream, of splitter.
3. Stations of the upper flow region downstream of splitter.

A. Mass Averaged Conditions

Line 1

- Word 1:  $\bar{T}$ , average total temperature, °R.  
Word 2:  $\bar{P}$ , average total pressure, psf.  
Word 3:  $\bar{P}/P$ -upstream for compressor  
 $P$ -upstream/ $\bar{P}$  for turbine.  
Word 4:  $\eta_{\text{poly-T}}$  (upstream to n-station).  
Word 5:  $\eta_{\text{adi-T}}$  (upstream to n-station).  
Word 6:  $\bar{P}/\bar{P}_I$  for compressor.  
 $\bar{P}_I/\bar{P}$  for turbine.  
Word 7:  $\eta_{\text{poly-T}}$  (stage inlet to n-station). \*

\* NOTE:

Stage inlet definition:

1. For compressor, the n-station directly preceding the rotor exit station or the first blade station of the rotor, if blade stations are used.
2. For turbine, the n-station directly preceding the stator exit station or the first blade station of the stator, if blade stations are used.



- Word 8:  $\eta_{adi-T}$  (stage inlet to n-station).  
 Word 9:  $\overline{T}_s$ , average static temperature, °R.  
 Word 10:  $\overline{rV}_t$ , average moment of tangential momentum, in x ft/sec.  
 Word 11:  $\overline{\Delta H}$ , average total enthalpy change from upstream temperature, Btu/lb.  
 Word 12: Station Identification. \*

Line 2

- Word 1: W, computed weight flow, lb/sec.  
 Word 2: N, rotational speed, RPM.  
 Word 3:  $W\sqrt{\theta}/\delta$ , referred computed weight flow, lb/sec, where:  
 $\theta = T/518.688$   
 $\delta = P/2116.216$   
 Word 4:  $N/\sqrt{\theta}$ , referred speed, RPM.  
 Word 5:  $W_f/W_a$ , fuel-air ratio.  
 Word 6:  $\tau$ , uniform blockage factor.  
 Word 7: Number of streamlines.  
 Word 8: Axial coordinate of the hub, in.  
 Word 9:  $\cotan \epsilon$ , slope of the computing station.

\*NOTE:

Output station Identification:

n-Station = 10x input station identification plus iteration pass identification.

b-station = Output identification of corresponding trailing edge station plus number of order of the blade station from leading edge.

B. Primary Option Definition

Line 1

Rotor or Station Option 1, 2, 3, or 4.  
Rotor Blade or Station Blade.

Line 2

ISRE or NISRE, if the entropy terms in the equilibrium equation and blade force components are neglected or included respectively.

Line 3

Blank or COUNTER ROTATING

NOTE:

One or more of the following lines may appear after Line 3 depending upon the options used:

MASS AVERAGE TOTAL PRESSURE

COOLING AIR EFFECT

TEST FACTOR SIMULATION

C. Title

D. Flow conditions at Each Streamline

Six lines for stations outside blade rows or at the trailing edge.

Four lines for stations within blade rows. \*

Line 1

Word 1: r, radius, in.

Word 2:  $V_z$ , axial velocity, ft/sec.

Word 3:  $V_m$ , meridional velocity, ft/sec.

\* NOTE

The blade station output is printed in the sequence corresponding to the location of the station in the machine.

- Word 4:  $V/V_{n-1}$  or  $W/W_{n-1}$ , velocity ratio, \*
- Word 5:  $\phi_{n-1} - \phi_n$  or  $(\phi_{n-1} - \phi_n)_W$ , turning angle, deg.
- Word 6:  $T_n - T_{n-1}$ , total temperature change, °R.
- Word 7:  $\beta$  or  $\beta_W$ , projected flow angle, degree.

Word 8: 
$$C_z = \frac{P_{s_n} - P_{s_{min}} - (P_n' - P_{n-1})_R}{P_{R_{n-1}} - P_{s_{min}}}$$

where  $P_{s_{min}}$  is calculated using Zweifel solidity and  $(P_n' - P_{n-1})_R = 0$  for stator.

- Word 9: Same as Word 8 except calculated using input solidity.

### Line 2

- Word 1:  $V_\theta$  absolute tangential velocity, ft/sec.
- Word 2:  $V$  absolute velocity, ft/sec.
- Word 3:  $M$  absolute Mach number.
- Word 4:  $rV_\theta$  absolute moment of tangential momentum, in. ft/sec.
- Word 5:  $\phi$  absolute flow angle, deg.
- Word 6:  $T$  absolute total temperature, °R.
- Word 7:  $P$  absolute total pressure, psf.

### \* NOTE

The subscript n-1 refers to the station preceding the n-station, or the first blade station when blade stations are present.

- Word 8:  $\sigma_z$  Zweifel solidity (for load coefficient of 1.0).  
 Word 9: Input solidity.

Line 3

- Word 1:  $V_{\theta w}$  relative tangential velocity, ft/sec.  
 Word 2:  $V_w$  relative velocity, ft/sec.  
 Word 3:  $M_w$  relative Mach number.  
 Word 4:  $U$  blade speed, ft/sec.  
 Word 5:  $\phi_w$  relative flow angle, deg.  
 Word 6:  $T_w$  total relative temperature.  
 Word 7:  $P_w$  total relative pressure, psf.  
 Word 8:  $(V_{\max}/V_n)_R$  where  $V_{\max R}$  is estimated using Zweifel solidity.  
 Word 9: Same as Word 8 except calculated using input solidity.

Line 4

- Word 1:  $\tan \alpha = \frac{dr}{dz}$ , streamline slope.  
 Word 2:  $Q = -\frac{d^2r}{dz^2} = -\frac{d \tan \alpha}{dz}$ ,  $\text{in}^{-1}$ .  
 Word 3:  $\frac{dV}{dz}$ , ft/sec x  $\text{in}^{-1}$ .  
 Word 4: Axial coordinate, in.  
 Word 5:  $\rho_s$ , static density, lb/cu ft.  
 Word 6:  $T_s$ , static temperature,  $^{\circ}\text{R}$ .  
 Word 7:  $P_s$ , static pressure, psf.  
 Word 8:  $(M_{\max})_R$  using Zweifel solidity.  
 Word 9: Same as Word 8 except calculated using input solidity.

Line 5

Word 1: Cpr, static pressure rise coefficient.

Word 2: D, diffusion factor.

Word 3: Deq, equivalent diffusion factor.

Word 4:  $\Delta i$ , incidence angle, deg., defined as

$$\Delta i = \beta_{n-1} - \beta \quad \text{for compressor}$$

$$\Delta i = \beta - \beta_{n-1} \quad \text{for turbine.}$$

Word 5:  $\eta_b$ , blade efficiency defined as

$$\eta_b = \frac{C_p (T - T_s)}{C_p (T - T_s)_{iso}}$$

where the total temperature T is absolute for stator and relative for rotor.

Word 6: L, total pressure loss coefficient, defined as

$$L = \frac{(P_{iso} - P)_n}{(P - P_s)_{n-1}} \quad \text{for compressor}$$

and as

$$L = \frac{(P_{iso} - P)_n}{(P - P_s)_n} \quad \text{for turbine}$$

where the total pressures P,  $P_{iso}$  are absolute for stator and relative for rotor.

Word 7:  $L'$ , total pressure loss coefficient, defined as:

$$L' = \frac{(P_{iso} - P)_n}{P_{n-1}}$$

where the total pressures P,  $P_{iso}$  are absolute for stator and relative for rotor.

Word 8:  $\sigma_x$ , computed axial solidity for Zweifel load coefficient of 1.0.

Word 9:  $(P_{s_{n-1}} - P_{s_{min}}) / (P_R - P_s)_{n-1}$  calculated using input solidity.

Line 6

- Word 1:  $P/P$ -upstream for compressor,  
 $P$ -upstream/ $P$  for turbine.
- Word 2:  $\eta_{\text{poly T}}$  (upstream to n station).
- Word 3:  $\eta_{\text{adi T}}$  (upstream to n station).
- Word 4:  $P/P_I$  for compressor,  
 $P_I/P$  for turbine.
- Word 5:  $\eta_{\text{poly T}}$  (inlet of stage to n station).
- Word 6:  $\eta_{\text{adi T}}$  (inlet of stage to n station).
- Word 7:  $P_S/P_{S_{n-1}}$  for compressor,  
 $P_{S_{n-1}}/P_S$  for turbine.
- Word 8:  $\eta_{\text{poly S}}$  (n-1 station to n station).
- Word 9:  $\eta_{\text{adi S}}$  (n-1 station to n station).
- Word 10:  $P/P_{n-1}$  for compressor,  
 $P_{n-1}/P$  for turbine.
- Word 11:  $\eta_{\text{poly T}}$  (n-1 station to n station).
- Word 12:  $\eta_{\text{adi T}}$  (n-1 station to n station).
- Word 13:  $V_{n-1}$  velocity at previous station,  
absolute for stator, relative for rotor,  
ft/sec.
- Word 14: Station Identification.

NOTE:

Words 8 and 9 of Lines 1 to 5 are printed if the calculated Zweifel solidity is  $> 0.050$ .

Lines 5 and 6 are omitted in the case of a blade station.



Main Output

518.68799 2115.99634 1.00000 1.0000 1.00000 1.00000 499.47554 0.0 0.0 10010  
 421.12158 5245.70000 421.16528 5245.00000 0.0 1.00000 16.00000 0.0 0.0

\* STATOR OPT4  
 \* NISRF  
 \* MASS AVERAGE TOTAL PRESSURE DELTA-T COOLING = 0.0 TOTAL DELTA-T = 0.0

NASA FAN ENGINE SPLITTER STUMP L00P= 0  
 0.10000 481.14282 2.40571 0.0 0.0 518.68799 2115.99634  
 0.0 0.43919 0.0 0.0 518.68799 2115.99634  
 4.57712 0.43921 4.57712 0.0 0.0 518.68799 2115.99634  
 0.00020 0.00000 0.0 0.0 499.42456 1853.43774  
 -4.56792 -1.40571 0.0 0.0 0.00014 0.00000  
 1.00000 1.00000 1.00000 1.00000 1.00000 1.00000 1.00000 1.00000 1.00000 1.0010

\* 3.76977 481.12793 2.40564 0.0 0.0 518.68799 2115.99707  
 0.0 0.43918 0.0 0.0 518.68799 2115.99707  
 172.54715 511.13257 172.54715 0.0 19.72937 2151.58594  
 0.00120 -0.70000 0.0 0.0 499.42578 1853.45337  
 -4.56759 -1.40564 0.0 0.0 0.00000 0.00000  
 1.00000 1.00000 1.00000 1.00000 1.00000 1.00000 1.00000 1.00000 1.00000 1.0010

\* 5.33032 481.14526 2.40573 0.0 0.0 518.68799 2115.99683  
 0.0 0.43920 0.0 0.0 518.68799 2115.99683  
 243.97533 539.45777 243.97533 0.0 26.89824 2187.57422  
 -0.00182 -0.70000 0.0 0.0 499.42432 1853.43457  
 -4.56799 -1.40573 0.0 0.0 0.00000 0.00000  
 1.00000 1.00000 1.00000 1.00000 1.00000 1.00000 1.00000 1.00000 1.00000 1.0010

\* 6.48596 481.09790 2.40540 0.0 0.0 518.68799 2115.99292  
 0.0 0.43915 0.0 0.0 518.68799 2115.99292  
 297.05347 565.41748 297.05347 0.0 31.69316 2227.71509  
 0.00212 -0.70000 0.0 0.0 499.42822 1853.49535  
 -4.56691 -1.40549 0.0 0.0 0.00015 0.00000  
 1.00000 1.00000 1.00000 1.00000 1.00000 1.00000 1.00000 1.00000 1.00000 1.0010

\* 7.54135 481.14233 2.40572 0.0 0.0 518.68799 2115.99341  
 0.0 0.43919 0.0 0.0 518.68799 2115.99341  
 345.17749 592.15405 345.17749 0.0 35.65405 2260.98829  
 0.00232 -0.70000 0.0 0.0 499.42456 1853.43774  
 -4.56792 -1.40572 0.0 0.0 0.00014 0.00000  
 1.00000 1.00000 1.00000 1.00000 1.00000 1.00000 1.00000 1.00000 1.00000 1.0010

\* 9.23444 481.11670 2.40559 0.0 0.0 518.68799 2115.99561  
 0.0 0.43917 0.0 0.0 518.68799 2115.99561  
 422.67139 640.41064 422.67139 0.0 41.29991 2336.00879  
 0.00256 -0.70000 0.0 0.0 499.42651 1853.46289  
 -4.56739 -1.40559 0.0 0.0 0.00000 0.00000  
 1.00000 1.00000 1.00000 1.00000 1.00000 1.00000 1.00000 1.00000 1.00000 1.0010

\* 17.66709 481.02539 2.40513 0.0 0.0 518.68799 2115.99854  
 0.0 0.43908 0.0 0.0 518.68799 2115.99854  
 489.01709 695.23438 489.01709 0.0 45.41336 2412.79979  
 0.00266 -0.70000 0.0 0.0 499.43408 1853.46152  
 -4.56530 -1.40513 0.0 0.0 0.00000 0.00000  
 1.00000 1.00000 1.00000 1.00000 1.00000 1.00000 1.00000 1.00000 1.00000 1.0010



13.05729	481.08569	2.40543	0.0	0.0	519.68799	2115.99512	0.0	1.0000	1.0000	200.00000	10010
0.0	0.43914	0.0	0.0	0.0	0.0	0.0	0.0	0.0	0.0	0.0	0.0
597.64795	0.70032	597.64795	51.16711	549.39502	549.39502	2571.73535	0.0	1.0000	1.0000	200.00000	10010
0.00256	-0.07008	0.0	0.06356	499.42970	499.42970	1353.49905	0.00010	1.0000	1.0000	200.00000	10010
-4.56664	0.46561	0.0	0.99999	0.00000	0.00000	0.00000	0.00000	1.0000	1.0000	200.00000	10010
1.00000	1.00000	1.00000	1.00000	1.00000	1.00000	1.00000	1.00000	1.0000	1.0000	200.00000	10010
15.55869	481.08911	2.40545	0.0	0.0	0.0	0.0	0.0	0.0	0.0	0.0	0.0
0.0	0.43914	0.0	0.0	0.0	0.0	0.0	0.0	0.0	0.0	0.0	0.0
712.14014	0.78448	712.14014	55.95983	550.86206	550.86206	2792.48438	0.0	1.0000	1.0000	200.00000	10010
0.00226	0.03577	0.0	0.06356	499.42896	499.42896	1853.49487	0.00007	1.0000	1.0000	200.00000	10010
-4.56671	0.46561	0.0	0.99999	0.00000	0.00000	0.00000	0.00000	1.0000	1.0000	200.00000	10010
1.00000	1.00000	1.00000	1.00000	1.00000	1.00000	1.00000	1.00000	1.0000	1.0000	200.00000	10010
16.46344	481.09936	2.40545	0.0	0.0	0.0	0.0	0.0	0.0	0.0	0.0	0.0
0.0	0.43914	0.0	0.0	0.0	0.0	0.0	0.0	0.0	0.0	0.0	0.0
753.55200	0.81608	753.55200	57.44461	565.90723	565.90723	2971.19849	0.0	1.0000	1.0000	200.00000	10010
0.00209	0.07491	0.0	0.06356	499.42996	499.42996	1853.49487	0.00007	1.0000	1.0000	200.00000	10010
-4.56671	0.46561	0.0	0.99999	0.00000	0.00000	0.00000	0.00000	1.0000	1.0000	200.00000	10010
1.00000	1.00000	1.00000	1.00000	1.00000	1.00000	1.00000	1.00000	1.0000	1.0000	200.00000	10010
17.39133	481.16406	2.40592	0.0	0.0	0.0	0.0	0.0	0.0	0.0	0.0	0.0
0.0	0.43921	0.0	0.0	0.0	0.0	0.0	0.0	0.0	0.0	0.0	0.0
796.02246	0.84905	796.02246	58.84863	571.37605	571.37605	2969.63574	0.0	1.0000	1.0000	200.00000	10010
0.00193	0.12637	0.0	0.06356	499.42285	499.42285	1853.41553	0.00012	1.0000	1.0000	200.00000	10010
-4.56439	0.46554	0.0	0.99999	0.00000	0.00000	0.00000	0.00000	1.0000	1.0000	200.00000	10010
1.00000	1.00000	1.00000	1.00000	1.00000	1.00000	1.00000	1.00000	1.0000	1.0000	200.00000	10010
20.15814	481.14307	2.40571	0.0	0.0	0.0	0.0	0.0	0.0	0.0	0.0	0.0
0.0	0.43919	0.0	0.0	0.0	0.0	0.0	0.0	0.0	0.0	0.0	0.0
922.66309	0.94985	922.66309	62.45917	599.46240	599.46240	3312.43481	0.0	1.0000	1.0000	200.00000	10010
0.00117	0.21533	0.0	0.06956	499.42456	499.42456	1953.63774	0.00014	1.0000	1.0000	200.00000	10010
-4.56792	0.46556	0.0	0.99999	0.00014	0.00014	0.00000	0.00000	1.0000	1.0000	200.00000	10010
1.00000	1.00000	1.00000	1.00000	1.00000	1.00000	1.00000	1.00000	1.0000	1.0000	200.00000	10010
21.52095	481.21582	2.40608	0.0	0.0	0.0	0.0	0.0	0.0	0.0	0.0	0.0
0.0	0.43926	0.0	0.0	0.0	0.0	0.0	0.0	0.0	0.0	0.0	0.0
945.04053	1.00072	945.04053	63.96335	599.34741	599.34741	3511.34839	0.0	1.0000	1.0000	200.00000	10010
0.00076	0.19561	0.0	0.06956	499.41870	499.41870	1853.36157	0.00011	1.0000	1.0000	200.00000	10010
-4.56954	0.46549	0.0	0.99999	0.00011	0.00011	0.00000	0.00000	1.0000	1.0000	200.00000	10010
1.00000	1.00000	1.00000	1.00000	1.00000	1.00000	1.00000	1.00000	1.0000	1.0000	200.00000	10010
22.80249	481.09644	2.40548	0.0	0.0	0.0	0.0	0.0	0.0	0.0	0.0	0.0
0.0	0.43915	0.0	0.0	0.0	0.0	0.0	0.0	0.0	0.0	0.0	0.0
1043.65924	1.04904	1043.65924	65.25244	609.22681	609.22681	3719.66699	0.0	1.0000	1.0000	200.00000	10010
0.00076	0.24806	0.0	0.06956	499.42822	499.42822	1853.49535	0.00015	1.0000	1.0000	200.00000	10010
-4.56691	0.46560	0.0	0.99999	0.00015	0.00015	0.00000	0.00000	1.0000	1.0000	200.00000	10010
1.00000	1.00000	1.00000	1.00000	1.00000	1.00000	1.00000	1.00000	1.0000	1.0000	200.00000	10010

\*

\*

\*

\*

\*

\*

23.41698	481.22852	2.40614	0.0	0.0	518.68799	2115.99438	0.0	1.0000	1.0000	200.00000	10010
0.0	0.43927	0.0	0.0	0.0	65.82077	614.16528	3825.54937	0.00000	0.00000	0.00000	0.0
1071.82397	1174.99819	1071.82397	0.0	0.0	0.06956	499.41772	1853.34888	0.99999	0.00012	0.00000	0.0
0.00018	-0.00000	0.0	0.0	0.0	0.89584	1.00000	1.00000	1.00000	1.00000	200.00000	10010
-4.56990	-1.40614	0.0	0.0	0.0	0.0	0.0	0.0	0.0	0.0	0.0	0.0
1.00000	1.00000	1.00000	1.00000	1.00000	0.0	0.0	0.0	0.0	0.0	0.0	0.0
24.01569	481.22778	2.40614	0.0	0.0	518.68799	2115.99438	0.0	1.0000	1.0000	200.00000	10010
0.0	0.43927	0.0	0.0	0.0	66.35675	619.10278	3934.59448	0.00000	0.00012	0.00000	0.0
1099.22754	1199.25044	1099.22754	0.0	0.0	0.06956	499.41772	1853.34888	0.99999	0.00012	0.00000	0.0
0.00000	0.00000	0.0	0.0	0.0	0.89584	1.00000	1.00000	1.00000	1.00000	200.00000	10010
-4.56990	-1.40614	0.0	0.0	0.0	0.0	0.0	0.0	0.0	0.0	0.0	0.0
1.00000	1.00000	1.00000	1.00000	1.00000	0.0	0.0	0.0	0.0	0.0	0.0	0.0
518.68799	2115.99194	1.00000	1.0000	1.0000	1.00000	1.00000	499.41797	0.0	0.0	0.0	10020
421.17285	5245.00000	421.21729	5245.00000	0.0	0.0	1.00000	16.00000	7.87400	0.0	0.0	0.0
*STATOR OPT4											
*NISPE											
*MASS AVERAGE TOTAL PRESSURE											
* TOTAL DELTA-T = 0.0											
* LONP = 0											
0.10000	475.77734	0.98985	0.0	0.0	518.68799	2115.99316	0.0	1.0000	1.0000	0.0	10020
0.0	475.77734	0.0	0.0	0.0	518.68799	2115.99316	0.0	1.0000	1.0000	0.0	10020
4.57712	475.79932	4.57712	0.0	0.0	518.68799	2115.99316	0.0	1.0000	1.0000	0.0	10020
-0.00040	0.00015	7.87400	0.0	0.0	499.90981	1858.98755	0.00000	0.00000	0.00000	0.00000	0.0
0.02116	0.01115	0.0	0.0	0.0	0.99999	0.00000	0.00000	0.00000	0.00000	0.00000	0.0
1.00000	1.00000	1.00000	1.00000	1.00000	1.00000	1.00000	0.9997	0.9994	1.00000	481.14292	10020
3.78627	476.30566	0.98998	0.0	0.0	518.68799	2115.99121	0.0	1.0000	1.0000	0.0	10020
0.0	476.30908	0.0	0.0	0.0	523.68115	2188.17822	0.0	1.0000	1.0000	0.0	10020
173.30219	536.45693	173.30219	0.0	0.0	499.90981	1858.98755	0.00000	0.00000	0.00000	0.00000	0.0
0.00388	-0.00069	7.87400	0.0	0.0	0.99999	0.00000	0.00000	0.00000	0.00000	0.00000	0.0
0.01901	0.01002	0.0	0.0	0.0	1.00269	0.9994	1.00000	1.00000	1.00000	481.12793	10020
1.00000	1.00000	1.00000	1.00000	1.00000	0.0	0.0	0.0	0.0	0.0	0.0	0.0
5.35257	476.72998	0.99083	0.0	0.0	518.68799	2115.99170	0.0	1.0000	1.0000	0.0	10020
0.0	476.73535	0.0	0.0	0.0	523.68115	2188.17822	0.0	1.0000	1.0000	0.0	10020
244.99387	536.70244	244.99387	0.0	0.0	499.90981	1858.98755	0.00000	0.00000	0.00000	0.00000	0.0
0.00481	-0.00077	7.87400	0.0	0.0	0.99999	0.00000	0.00000	0.00000	0.00000	0.00000	0.0
0.01740	0.00917	0.0	0.0	0.0	1.00246	0.9994	1.00000	1.00000	1.00000	481.14600	10020
1.00000	1.00000	1.00000	1.00000	1.00000	0.0	0.0	0.0	0.0	0.0	0.0	0.0
6.51583	477.16921	0.99185	0.0	0.0	518.68799	2115.99486	0.0	1.0000	1.0000	0.0	10020
0.0	477.17554	0.0	0.0	0.0	523.68115	2223.57837	0.0	1.0000	1.0000	0.0	10020
209.23730	562.70947	209.23730	0.0	0.0	499.90981	1858.98755	0.00000	0.00000	0.00000	0.00000	0.0
0.00559	-0.00089	7.87400	0.0	0.0	0.99997	0.00003	0.00000	0.00000	0.00000	0.00000	0.0
0.01547	0.00815	0.0	0.0	0.0	1.00219	0.9994	1.00000	1.00000	1.00000	481.09888	10020
0.99999	1.00000	1.00000	1.00000	1.00000	0.0	0.0	0.0	0.0	0.0	0.0	0.0
7.56674	477.92764	0.99313	0.0	0.0	518.68799	2115.99633	0.0	1.0000	1.0000	0.0	10020
0.0	477.93643	0.0	0.0	0.0	523.68115	2223.57837	0.0	1.0000	1.0000	0.0	10020
346.47607	590.23145	346.47607	0.0	0.0	499.90981	1858.98755	0.00000	0.00000	0.00000	0.00000	0.0
0.00515	-0.00098	7.87400	0.0	0.0	0.99999	0.00001	0.00000	0.00000	0.00000	0.00000	0.0
0.01306	0.00687	0.0	0.0	0.0	1.00195	0.9991	1.00000	1.00000	1.00000	481.14355	10020
0.99999	1.00000	1.00000	1.00000	1.00000	0.0	0.0	0.0	0.0	0.0	0.0	0.0







```

*
20.19009 485.14502 485.15332 1.00453 0.0 0.0 0.0 0.0 0.0 0.0
0.0 485.15332 0.44300 0.0 0.0 518.68799 2115.98218 0.0
924.12549 1043.73413 0.95304 924.12549 0.0 589.68677 3316.83447 0.0
0.00592 -0.00088 0.83453 12.59800 0.06945 499.10205 1849.24073 0.0
-0.00865 -0.00453 1.11495 0.0 0.99999 0.00002 0.00000 0.0
0.99999 1.0000 1.0000 0.99876 1.0001 1.0014 1.00000 1.0000 1.0000 482.96680 10030
*
21.54160 485.53037 485.63379 1.00555 0.0 0.0 0.0 0.0 0.0 0.0
0.0 435.63379 0.44345 0.0 0.0 518.68799 2115.98633 0.0
985.98535 1099.09375 1.00363 985.98535 0.0 599.50220 3514.51660 0.0
0.00381 -0.00056 0.87528 12.59800 0.06944 499.06323 1848.73828 0.0
-0.01060 -0.00555 1.11382 0.0 0.99999 0.00001 0.00000 0.0
0.99999 1.0000 1.0000 0.99849 1.0000 1.0011 1.00000 1.0000 1.0000 482.95386 10030
*
22.81239 485.89282 485.89355 1.00561 0.0 0.0 0.0 0.0 0.0 0.0
0.0 485.89355 0.44370 0.0 0.0 518.68799 2115.98560 0.0
1044.15137 1151.67017 1.05166 1044.15137 0.0 609.30542 3720.33911 0.0
0.00182 -0.00027 0.94979 12.59800 0.06943 499.04224 1848.46509 0.0
-0.01072 -0.00561 1.11375 0.0 0.99999 0.00001 0.00000 0.0
0.99999 1.0000 1.0000 0.99847 1.0001 1.0011 1.00000 1.0000 1.0000 483.18091 10030
*
23.42178 485.95361 485.95361 1.00569 0.0 0.0 0.0 0.0 0.0 0.0
0.0 485.95361 0.44376 0.0 0.0 518.68799 2115.98389 0.0
1072.04395 1177.04199 1.07484 1072.04395 0.0 614.20459 3826.38599 0.0
0.00089 -0.00014 0.93604 12.59800 0.06943 499.03735 1848.40503 0.0
-0.01088 -0.00569 1.11366 0.0 0.99999 0.00003 0.00000 0.0
0.99999 1.0000 1.0000 0.99844 1.0001 1.0011 1.00000 1.0000 1.0000 483.20166 10030
*
24.01569 485.99854 485.99854 1.00577 0.0 0.0 0.0 0.0 0.0 0.0
0.0 485.99854 0.44380 0.0 0.0 518.68799 2115.98164 0.0
1099.22754 1201.87134 1.09751 1099.22754 0.0 619.10278 3934.57446 0.0
-0.00000 0.00000 0.95667 12.59800 0.06943 499.03369 1848.35718 0.0
-0.01103 -0.00577 1.11357 0.0 0.99999 0.00003 0.00000 0.0
0.99999 1.0000 1.0000 0.99842 1.0001 1.0011 1.00000 1.0000 1.0000 483.20898 10030
*
518.68799 2115.07949 0.99999 1.0000 1.0000 0.99999 1.0000 1.0000 499.38745 0.0 10040
421.15739 5245.00000 421.19727 5245.00000 0.0 1.00000 15.00000 0.0
* STATOR OPT4
* NISRF
* MASS AVERAGE TOTAL PRESSURE
DELTA-T COOLING = 0.0 TOTAL DELTA-T = 0.0
LOPP= 0
NASA FAN ENGINE SPLITTER STUDY
0.10000 453.07485 453.97754 0.97279 0.0 0.0 518.68799 2115.98413 0.0
0.0 453.97754 0.41352 0.0 0.0 518.68799 2115.98413 0.0
4.57712 454.00049 0.41355 4.57712 0.57765 518.68970 2116.00610 0.0
-0.00160 0.00383 -7.74313 15.74800 0.07030 501.53882 1881.03271 0.0
0.05144 0.02721 1.15133 0.0 0.99999 0.00001 0.00000 0.0
0.99999 1.0000 1.0000 0.99999 1.0000 1.0000 1.00000 1.0000 466.67773 10040

```







518.68799	2115.97607	0.99999	1.00000	1.00000	0.99999	1.00000	1.00000	499.30737	0.0	0.0	10050
421.20776	5245.70000	421.25537	5245.00000	0.0	0.0	1.00000	1.00000	16.00000	18.89699	0.0	0.0
*STATOR NPT4											
*NISRF											
*MASS AVERAGE TOTAL PRESSURE											
*NASA FAN ENGINE SPLITTER STUDY											
0.10000	420.64526	0.92458	0.0	0.0	0.0	0.0	0.0	LOPP= 0	0.0	0.0	10050
0.0	420.64526	0.0	0.0	0.0	0.0	0.0	0.0	2115.97827	0.0	0.0	10050
4.57712	420.67317	4.57712	0.0	0.0	0.0	0.0	0.0	2115.97827	0.0	0.0	10050
0.01323	-0.01452	18.99699	0.0	0.0	0.0	0.0	0.0	2115.97827	0.0	0.0	10050
0.13637	0.07342	0.0	0.0	0.0	0.0	0.0	0.0	2115.97827	0.0	0.0	10050
0.99999	1.00000	0.99999	1.00000	1.00000	1.00000	1.00000	1.00000	2115.97827	1.00000	1.00000	10050
3.95506	436.72559	0.95942	0.0	0.0	0.0	0.0	0.0	2115.96582	0.0	0.0	10050
0.0	437.10913	0.0	0.0	0.0	0.0	0.0	0.0	2115.96582	0.0	0.0	10050
181.02803	473.11255	191.02803	0.0	0.0	0.0	0.0	0.0	2155.16016	0.0	0.0	10050
0.04192	-0.10707	18.89699	0.0	0.0	0.0	0.0	0.0	1997.49561	0.0	0.0	10050
0.07828	0.04158	0.0	0.0	0.0	0.0	0.0	0.0	0.00000	0.0	0.0	10050
0.99999	1.00000	0.99999	1.00000	1.00000	1.00000	1.00000	1.00000	0.00000	1.00000	1.00000	10050
5.56229	443.10781	0.95417	0.0	0.0	0.0	0.0	0.0	2115.96265	0.0	0.0	10050
0.0	443.10781	0.0	0.0	0.0	0.0	0.0	0.0	2115.96265	0.0	0.0	10050
254.59291	511.50146	254.59291	0.0	0.0	0.0	0.0	0.0	2193.98608	0.0	0.0	10050
0.05344	-0.01321	18.89699	0.0	0.0	0.0	0.0	0.0	1891.17529	0.0	0.0	10050
0.06757	0.03583	0.0	0.0	0.0	0.0	0.0	0.0	0.00000	0.0	0.0	10050
0.99999	1.00000	0.99999	1.00000	1.00000	1.00000	1.00000	1.00000	0.00000	1.00000	1.00000	10050
6.74743	449.45557	0.97242	0.0	0.0	0.0	0.0	0.0	2115.95850	0.0	0.0	10050
0.0	450.17578	0.0	0.0	0.0	0.0	0.0	0.0	2231.48120	0.0	0.0	10050
308.93813	545.72969	0.97714	108.93813	0.0	0.0	0.0	0.0	1884.76660	0.0	0.0	10050
0.05664	-0.01307	18.89699	0.0	0.0	0.0	0.0	0.0	0.00000	0.0	0.0	10050
0.05216	0.02758	0.0	0.0	0.0	0.0	0.0	0.0	0.00000	0.0	0.0	10050
0.99999	1.00000	0.99999	1.00000	1.00000	1.00000	1.00000	1.00000	0.00000	1.00000	1.00000	10050
7.81358	455.26636	0.97924	0.0	0.0	0.0	0.0	0.0	2115.96387	0.0	0.0	10050
0.0	456.01196	0.0	0.0	0.0	0.0	0.0	0.0	2271.88989	0.0	0.0	10050
357.63696	579.52661	0.52797	357.63696	0.0	0.0	0.0	0.0	1878.99487	0.0	0.0	10050
0.05726	-0.01230	18.89699	0.0	0.0	0.0	0.0	0.0	0.00000	0.0	0.0	10050
0.03936	0.02076	0.0	0.0	0.0	0.0	0.0	0.0	0.00000	0.0	0.0	10050
0.99999	1.00000	0.99999	1.00000	1.00000	1.00000	1.00000	1.00000	0.00000	1.00000	1.00000	10050
9.51576	453.29193	0.98842	0.0	0.0	0.0	0.0	0.0	2115.96460	0.0	0.0	10050
0.0	464.69067	0.0	0.0	0.0	0.0	0.0	0.0	2350.09814	0.0	0.0	10050
435.54810	635.93844	0.58062	435.54810	0.0	0.0	0.0	0.0	1870.28564	0.0	0.0	10050
0.05530	-0.01065	18.89699	0.0	0.0	0.0	0.0	0.0	0.00000	0.0	0.0	10050
0.02200	0.01158	0.0	0.0	0.0	0.0	0.0	0.0	0.00000	0.0	0.0	10050
0.99999	1.00000	0.99999	1.00000	1.00000	1.00000	1.00000	1.00000	0.00000	1.00000	1.00000	10050
10.93848	470.52295	0.99453	0.0	0.0	0.0	0.0	0.0	2115.97437	0.0	0.0	10050
0.0	471.14844	0.0	0.0	0.0	0.0	0.0	0.0	2429.11987	0.0	0.0	10050
500.66772	687.49463	0.62706	500.66772	0.0	0.0	0.0	0.0	1863.72754	0.0	0.0	10050
0.05158	-0.01093	18.89699	0.0	0.0	0.0	0.0	0.0	0.00000	0.0	0.0	10050
0.01041	0.10547	0.0	0.0	0.0	0.0	0.0	0.0	0.00000	0.0	0.0	10050
0.99999	1.00000	0.99999	1.00000	1.00000	1.00000	1.00000	1.00000	0.00000	1.00000	1.00000	10050

TOTAL DELTA-T = 0.0

13.30674	479.57739	480.02612	1.00190	0.0	0.0	518.68799	2115.97559	10950
0.0	480.02612	0.43813	0.0	0.0	0.0	549.54053	2590.58350	
609.06592	775.49097	0.70781	609.06592	51.75710	0.06959	499.51392	1854.57788	
0.04328	-0.30675	0.53689	18.89699	0.99999	0.00000	0.00000	0.00000	
-0.00363	-0.00190	1.11787	0.0	0.99999	1.0002	1.0034	1.00000	10950
0.99999	1.0000	0.99999	1.0000	1.0000	0.99999	1.0000	1.0000	479.11353
15.76185	486.60669	486.87427	1.00678	0.0	0.0	518.68799	2115.97485	
0.0	486.97427	0.44663	0.0	0.0	0.0	561.97021	2801.77539	
721.43945	870.35693	0.79484	721.43945	55.98593	0.06940	498.96289	1847.42920	
0.03318	-0.00469	1.36991	18.89699	0.99999	0.00001	0.00000	0.00000	
-0.01294	-0.00678	1.11246	0.0	0.99999	1.0000	1.0009	1.00000	10050
0.99999	1.0000	0.99999	1.0000	1.0000	0.99815	1.0000	1.0000	493.59741
16.64650	488.57593	488.78687	1.00784	0.0	0.0	518.68799	2115.97388	
0.0	488.78687	0.44645	0.0	0.0	0.0	566.96265	2889.97266	
761.93091	905.23535	0.82682	761.93091	57.31932	0.06930	498.80762	1845.41846	
0.02940	-0.00400	1.57205	18.89699	0.99999	0.00002	0.00000	0.00000	
-0.01498	-0.00784	1.11129	0.0	0.99999	1.0000	1.0008	1.00000	10050
0.99999	1.0000	0.99999	1.0000	1.0000	0.99784	1.0000	1.0000	484.98462
17.55273	490.30396	490.46362	1.00882	0.0	0.0	518.68799	2115.97729	
0.0	490.46362	0.44804	0.0	0.0	0.0	572.35889	2987.53931	
803.41040	941.28784	0.85987	803.41040	58.59883	0.06930	498.67090	1843.65186	
0.02553	-0.00337	1.73267	18.89699	0.99999	0.00002	0.00000	0.00000	
-0.01686	-0.00882	1.11021	0.0	0.99999	1.0000	1.0007	1.00000	10050
0.99999	1.0000	0.99999	1.0000	1.0000	0.99756	1.0000	1.0000	486.17578
20.25233	493.01455	493.96533	1.01068	0.0	0.0	518.68799	2115.97144	
0.0	493.96533	0.45137	0.0	0.0	0.0	590.12476	3325.46851	
976.97437	1050.37280	0.95979	926.97437	61.04772	0.06920	498.38423	1939.93628	
0.01438	-0.00178	2.04676	18.89699	1.00000	0.00000	0.00000	0.00000	
-0.02041	-0.01068	1.10816	0.0	1.00000	0.99701	1.0000	1.00000	10050
0.99999	1.0000	0.99999	1.0000	1.0000	0.99701	1.0000	1.0000	488.74585
21.58118	494.03555	494.95581	1.01118	0.0	0.0	518.68799	2115.97900	
0.0	494.95581	0.45231	0.0	0.0	0.0	599.79907	3520.60864	
987.79712	1108.96377	1.00967	987.79712	63.38583	0.06917	498.30249	1838.88599	
0.00909	-0.00112	2.14050	18.89699	0.99999	0.00000	0.00000	0.00000	
-0.02138	-0.01118	1.10762	0.0	1.00000	0.99886	1.0000	1.00000	10050
0.99999	1.0000	0.99999	1.0000	1.0000	0.99886	1.0000	1.0000	489.48340
22.83127	495.48340	495.48779	1.01147	0.0	0.0	518.68799	2115.97852	
0.0	495.48779	0.45282	0.0	0.0	0.0	608.45532	3721.53745	
1045.01538	1156.53149	1.05693	1045.01538	64.63226	0.06916	498.25879	1838.32642	
0.00430	-0.00054	2.17054	18.89699	0.99999	0.00000	0.00000	0.00000	
-0.02191	-0.01147	1.10730	0.0	1.00000	0.99677	1.0000	1.00000	10050
0.99999	1.0000	0.99999	1.0000	1.0000	0.99677	1.0000	1.0000	489.87109











7.49459	418.44922	451.26953	1.09323	0.0	0.0	0.0	0.0	519.69799	2115.94653	0.0	10080
0.0	451.26953	0.41097	0.0	0.0	0.0	0.0	0.0	519.69799	2115.94653	0.0	10080
343.03662	566.14957	0.51627	143.03662	0.0	37.24960	528.47681	2259.11011	501.74268	1893.67894	0.00000	10080
0.40376	-0.03522	20.31541	28.34599	0.0	0.07037	0.99999	0.00000	0.00000	0.00000	0.00000	10080
-0.18717	-0.03323	1.02448	0.0	0.99999	0.99999	1.00000	1.00000	1.00000	1.00000	1.00000	10080
0.99997	1.00000	0.99997	1.00000	1.00000	0.99997	1.00000	1.00000	1.00000	1.00000	1.00000	10080
8.44508	445.11084	468.92603	1.08203	0.0	0.0	0.0	0.0	0.0	0.0	0.0	10080
0.0	468.92603	0.42763	0.0	0.0	0.0	0.0	0.0	0.0	0.0	0.0	10080
385.54175	607.70557	0.55419	386.54175	0.0	39.49919	531.11694	2298.87402	500.39063	1865.96826	0.00000	10080
0.33147	-0.02520	16.87584	28.34599	0.0	0.06990	0.99999	0.00000	0.00000	0.00000	0.00000	10080
-0.16323	-0.04203	1.03509	0.0	0.99999	0.99999	1.00000	1.00000	1.00000	1.00000	1.00000	10080
0.99997	1.00000	0.99997	1.00000	1.00000	0.99997	1.00000	1.00000	1.00000	1.00000	1.00000	10080
9.32226	453.52524	481.38647	1.07246	0.0	0.0	0.0	0.0	0.0	0.0	0.0	10080
0.0	481.38647	0.43942	0.0	0.0	0.0	0.0	0.0	0.0	0.0	0.0	10080
425.69116	643.77148	0.58720	426.69116	0.0	41.55312	533.83752	2349.31519	499.40503	1953.14282	0.00000	10080
0.27944	-0.01916	14.43035	28.34599	0.0	0.06955	0.99999	0.00000	0.00000	0.00000	0.00000	10080
-0.14315	-0.07246	1.04433	0.0	0.99999	0.99999	1.00000	1.00000	1.00000	1.00000	1.00000	10080
0.99998	1.00000	0.99998	1.00000	1.00000	0.99998	1.00000	1.00000	1.00000	1.00000	1.00000	10080
10.76099	495.31614	496.40137	1.05992	0.0	0.0	0.0	0.0	0.0	0.0	0.0	10080
0.0	496.40137	0.45369	0.0	0.0	0.0	0.0	0.0	0.0	0.0	0.0	10080
402.54370	609.29517	0.63912	402.54370	0.0	44.77649	538.86694	2419.53198	498.18335	1837.32275	0.00000	10080
0.21495	-0.01272	11.69295	28.34599	0.0	0.06913	0.99999	0.00000	0.00000	0.00000	0.00000	10080
-0.11709	-0.04982	1.05679	0.0	0.99999	0.99999	1.00000	1.00000	1.00000	1.00000	1.00000	10080
0.99998	1.00000	0.99998	1.00000	1.00000	0.99998	1.00000	1.00000	1.00000	1.00000	1.00000	10080
11.00247	498.05396	505.52979	1.05159	0.0	0.0	0.0	0.0	0.0	0.0	0.0	10080
0.0	505.52979	0.46238	0.0	0.0	0.0	0.0	0.0	0.0	0.0	0.0	10080
548.91016	746.73218	0.68254	548.91016	0.0	47.35883	543.74854	2496.16553	497.42212	1927.52661	0.00000	10080
0.17391	-0.10943	9.96200	28.34599	0.0	0.06987	0.99999	0.00000	0.00000	0.00000	0.00000	10080
-0.10057	-0.05160	1.06495	0.0	0.99999	0.99999	1.00000	1.00000	1.00000	1.00000	1.00000	10080
0.99999	1.00000	0.99999	1.00000	1.00000	0.99999	1.00000	1.00000	1.00000	1.00000	1.00000	10080
14.09190	512.55127	516.37500	1.04243	0.0	0.0	0.0	0.0	0.0	0.0	0.0	10080
0.0	516.37500	0.47274	0.0	0.0	0.0	0.0	0.0	0.0	0.0	0.0	10080
645.00366	826.24023	0.75642	645.00366	0.0	51.32001	553.28760	2652.98755	496.49975	1915.69507	0.00000	10080
-0.12738	-0.03594	8.20345	28.34599	0.0	0.06955	0.99999	0.00000	0.00000	0.00000	0.00000	10080
-0.08198	-0.04224	1.07442	0.0	0.99999	0.99999	1.00000	1.00000	1.00000	1.00000	1.00000	10080
0.99999	1.00000	0.99999	1.00000	1.00000	0.99999	1.00000	1.00000	1.00000	1.00000	1.00000	10080
16.31728	521.22969	523.74316	1.03639	0.0	0.0	0.0	0.0	0.0	0.0	0.0	10080
0.0	523.74316	0.47979	0.0	0.0	0.0	0.0	0.0	0.0	0.0	0.0	10080
746.86182	912.20044	0.83565	746.86182	0.0	54.95759	565.07275	2856.34799	495.54914	1807.54614	0.00000	10080
0.09343	-0.00389	7.02922	28.34599	0.0	0.06933	0.99999	0.00000	0.00000	0.00000	0.00000	10080
-0.07081	-0.03680	1.08024	0.0	0.99999	0.99999	1.00000	1.00000	1.00000	1.00000	1.00000	10080
0.99999	1.00000	0.99999	1.00000	1.00000	0.99999	1.00000	1.00000	1.00000	1.00000	1.00000	10080
17.12963	524.34912	525.65492	1.03540	0.0	0.0	0.0	0.0	0.0	0.0	0.0	10080
0.0	525.65492	0.48166	0.0	0.0	0.0	0.0	0.0	0.0	0.0	0.0	10080
783.69854	943.23262	0.96487	783.69854	0.0	56.15491	567.79785	2949.93457	495.69141	1805.37256	0.00000	10080
-0.07162	-0.00324	7.01830	28.34599	0.0	0.06927	0.99999	0.00000	0.00000	0.00000	0.00000	10080
-0.06820	-0.03549	1.09161	0.0	0.99999	0.99999	1.00000	1.00000	1.00000	1.00000	1.00000	10080
0.99999	1.00000	0.99999	1.00000	1.00000	0.99999	1.00000	1.00000	1.00000	1.00000	1.00000	10080





519.68799	2115.05801	0.00098	1.00000	1.00000	0.00000	0.00000	1.00000	1.00000	493.51416	0.0	10090
421.18348	5245.00000	421.23975	5245.00000	0.0	0.0	0.0	1.00000	1.00000	16.00000	31.49599	0.0
* STATOP OPT4											
* NISSP											
* MASS AVERAGE TOTAL PRESSURE											
* TOTAL DELTA-T = 0.0											
* LUMP = 0											
* NASA FAN ENGINE SPLITTER STIMY											
7.03000	496.40352	586.43579	1.02881	0.0	0.0	0.0	0.0	0.0	2115.94775	0.0	10090
0.0	596.43579	0.54039	0.0	0.0	0.0	0.0	519.68799	2115.94775	0.0	0.0	10090
321.77173	648.91235	0.61639	321.77173	0.0	0.0	0.0	527.30103	2241.57104	0.0	0.0	10090
0.67262	0.16929	64.47115	31.49599	0.0	0.0	0.0	400.06909	1734.70972	0.0	0.0	10090
-1.54040	-0.42881	0.68762	0.0	0.0	0.0	0.0	0.00000	0.00000	0.0	0.0	10090
0.99999	1.00000	0.99999	1.00000	1.00000	0.0	0.0	1.00000	1.00000	1.00000	1.00000	10090
7.08771	503.59897	562.09790	1.34012	0.0	0.0	0.0	0.0	0.0	0.0	0.0	10090
0.0	562.09790	0.51674	0.0	0.0	0.0	0.0	519.68799	2115.94775	0.0	0.0	10090
365.60742	670.53906	0.61639	365.60742	0.0	0.0	0.0	33.04132	2279.08667	0.0	0.0	10090
0.49533	0.30117	40.67439	31.49599	0.0	0.0	0.0	492.39575	1763.59385	0.0	0.0	10090
-0.74621	-0.34032	0.83562	0.0	0.0	0.0	0.0	1.00000	0.00000	0.0	0.0	10090
0.99999	1.00000	0.99999	1.00000	1.00000	0.0	0.0	1.00000	1.00000	1.00000	1.00000	10090
9.81489	512.49561	550.99639	1.27099	0.0	0.0	0.0	0.0	0.0	0.0	0.0	10090
0.0	550.99639	0.50600	0.0	0.0	0.0	0.0	519.68799	2115.94116	0.0	0.0	10090
403.46892	632.92114	0.62716	403.46892	0.0	0.0	0.0	36.21461	2315.77344	0.0	0.0	10090
0.39482	0.36088	29.63440	31.49599	0.0	0.0	0.0	493.42432	1776.61890	0.0	0.0	10090
-0.46092	-0.22099	0.81729	0.0	0.0	0.0	0.0	1.00000	0.00000	0.0	0.0	10090
0.99997	1.00000	0.99997	1.00000	1.00000	0.0	0.0	1.00000	1.00000	1.00000	1.00000	10090
9.53307	519.25391	546.37012	1.16515	0.0	0.0	0.0	0.0	0.0	0.0	0.0	10090
0.0	546.37012	0.50154	0.0	0.0	0.0	0.0	519.68799	2115.94214	0.0	0.0	10090
436.34009	699.22114	0.64195	436.34009	0.0	0.0	0.0	33.61142	2350.95703	0.0	0.0	10090
0.33394	0.22377	23.48830	31.49599	0.0	0.0	0.0	493.84668	1781.94336	0.0	0.0	10090
-0.33612	-0.16515	0.86125	0.0	0.0	0.0	0.0	1.00000	-0.00000	0.0	0.0	10090
0.99997	1.00000	0.99997	1.00000	1.00000	0.0	0.0	1.00000	1.00000	1.00000	1.00000	10090
10.24184	523.07910	544.21582	1.13052	0.0	0.0	0.0	0.0	0.0	0.0	0.0	10090
0.0	544.21582	0.49947	0.0	0.0	0.0	0.0	519.68799	2115.95020	0.0	0.0	10090
468.78174	719.28076	0.65922	468.78174	0.0	0.0	0.0	536.06720	2398.80290	0.0	0.0	10090
0.29714	0.21426	19.26358	31.49599	0.0	0.0	0.0	494.04224	1794.42090	0.0	0.0	10090
-0.26148	-0.13052	0.89070	0.0	0.0	0.0	0.0	1.00000	-0.00000	0.0	0.0	10090
0.99993	1.00000	0.99999	1.00000	1.00000	0.0	0.0	1.00000	1.00000	1.00000	1.00000	10090
11.47019	529.76611	543.10693	1.09402	0.0	0.0	0.0	0.0	0.0	0.0	0.0	10090
0.0	543.10693	0.49440	0.0	0.0	0.0	0.0	519.68799	2115.94459	0.0	0.0	10090
525.00364	755.37744	0.65319	525.00364	0.0	0.0	0.0	44.02296	2461.98584	0.0	0.0	10090
0.22593	0.10570	13.84368	31.49599	0.0	0.0	0.0	494.14253	1795.48972	0.0	0.0	10090
-0.18631	-0.10400	1.02368	0.0	0.0	0.0	0.0	1.00000	0.00000	0.0	0.0	10090
0.99997	1.00000	0.99997	1.00000	1.00000	0.0	0.0	1.00000	1.00000	1.00000	1.00000	10090
12.56759	534.15497	543.65879	1.07542	0.0	0.0	0.0	0.0	0.0	0.0	0.0	10090
0.0	543.65879	0.49893	0.0	0.0	0.0	0.0	519.68799	2115.95410	0.0	0.0	10090
575.23399	791.59121	0.72637	575.23399	0.0	0.0	0.0	46.61544	2575.95410	0.0	0.0	10090
0.19334	0.10216	11.30636	31.49599	0.0	0.0	0.0	474.09277	1785.06592	0.0	0.0	10090
-0.14719	-0.17542	1.06415	0.0	0.0	0.0	0.0	1.00000	0.00000	0.0	0.0	10090
0.99999	1.00000	0.99999	1.00000	1.00000	0.0	0.0	1.00000	1.00000	1.00000	1.00000	10090















10.69295	544.74219	549.05200	0.70649	37.06828	40.65308	-1.04842	0.38297	10120
499.39944	742.19727	0.66816	5340.04297	42.24954	559.34106	2680.62012	0.38297	10120
-0.06899	549.14258	0.49436	489.42944	-1.04919	538.61304	2348.43872	1.41546	1.41546
0.12604	0.05011	-36.65102	41.10199	0.07254	513.52856	1987.23218	0.71946	0.71946
0.38297	0.52570	2.04923	0.0	0.96091	0.09541	0.02787	2.11539	0.0
1.26683	0.8949	1.26687	0.8950	1.18118	0.8572	0.09537	0.8950	0.8914
11.24340	542.12329	547.79297	0.69777	31.68158	39.02856	6.17609	0.42084	0.42084
455.95972	712.72461	0.64042	5176.53516	39.77255	557.71655	2676.60132	1.09949	1.09949
58.66455	550.92529	0.49503	514.62427	6.11265	540.71704	2401.50635	1.43314	1.43314
0.14500	0.02655	-45.23656	41.10199	0.07386	515.67046	2031.24438	0.73045	0.73045
0.42084	0.50987	2.01635	0.0	0.90926	0.06426	0.01919	1.91553	0.0
1.26493	0.9229	1.26498	0.9250	1.20309	0.9065	0.9941	0.9250	0.9225
11.74520	537.17651	542.49634	0.68971	29.13351	38.66807	11.31338	0.44233	0.44233
430.16995	692.34937	0.62102	5052.94766	38.44124	557.15601	2676.60132	1.90232	1.90232
107.46999	553.03882	0.49606	537.63794	11.20527	542.73120	2441.58252	1.44989	1.44989
0.14109	0.02657	-43.33667	41.10199	0.07479	517.29126	2063.73486	0.74154	0.74154
0.44233	0.59606	2.00114	0.0	0.91743	0.05123	0.01567	1.78099	0.0
1.26493	0.9377	1.26498	0.9380	1.271892	0.9272	0.9252	0.9180	0.9159
12.25445	529.31201	535.50000	0.68171	25.23695	38.65059	15.76324	0.45638	0.45638
411.90420	575.53149	0.60483	5050.55078	37.56059	557.13967	2679.01514	1.83026	1.83026
149.55469	555.19170	0.49740	561.35389	15.40401	544.89917	2478.42285	1.46691	1.46691
0.14473	0.01342	-48.87311	41.10199	0.07554	519.18774	2092.66945	0.75399	0.75399
0.45638	0.57721	1.99348	0.0	0.92289	0.04668	0.01466	1.67192	0.0
1.26663	0.9419	1.26612	0.9420	1.23301	0.9352	0.9332	0.9420	0.9400
13.20675	524.33984	531.35889	0.68583	20.52789	39.17785	23.20595	0.45309	0.45309
379.66943	653.06299	0.58348	5014.00781	35.45475	556.86084	2676.60132	1.62735	1.62735
274.79688	576.25386	0.51548	604.66631	22.93129	549.07837	2547.80933	1.45808	1.45808
0.15417	-0.01202	-9.35627	41.10199	0.07441	521.39331	2125.54834	0.77720	0.77720
0.43309	0.54475	1.93078	0.0	0.93162	0.04196	0.01381	1.41262	0.0
1.26493	0.9449	1.26498	0.9450	1.24665	0.9416	0.9397	0.9450	0.9431
14.07916	528.43286	534.36597	0.70103	17.27281	38.03760	28.72006	0.43209	0.43209
354.87109	641.46729	0.57251	4096.28516	33.58803	556.72559	2674.45972	1.42745	1.42745
289.54932	607.77100	0.54244	644.42041	28.45129	553.22656	2616.02197	1.42647	1.42647
0.15027	-0.00955	-2.49829	41.10199	0.07683	522.50659	2141.59131	0.80053	0.80053
0.43209	0.50746	1.85095	0.0	0.93803	0.03996	0.01376	1.18057	0.0
1.26392	0.9449	1.26396	0.9450	1.25115	0.9426	0.9403	0.9450	0.9431
15.65703	533.36108	537.09766	0.72743	12.61113	37.76709	36.85414	0.39667	0.39667
316.84937	623.59229	0.55571	4060.91797	30.53757	556.45504	2470.17407	1.13222	1.13222
399.79199	669.55762	0.59667	718.64136	36.66237	561.39551	2754.16895	1.37470	1.37470
0.11958	-0.00311	-0.40697	41.10199	0.07743	524.11694	2165.00757	0.84951	0.84951
0.39467	0.44701	1.73055	0.0	0.94856	-0.03626	0.01364	0.85628	0.0
1.26190	0.9449	1.26193	0.9450	1.26056	0.9449	0.9429	0.9450	0.9432
17.61205	541.41064	543.53369	0.75871	9.49788	37.76758	43.60340	0.34898	0.34898
284.97334	613.64555	0.54635	4961.09766	27.66376	556.45557	2670.17407	0.89879	0.89879
512.04761	746.74072	0.66480	796.09795	42.29147	571.49954	2931.91567	1.31803	1.31803
0.08865	-0.01107	-3.34676	41.10199	0.07781	525.13721	2179.79443	0.90790	0.90790
0.34998	0.38724	1.61812	0.0	0.95814	0.03285	0.01359	0.61232	0.0
1.26190	0.9449	1.26193	0.9450	1.25436	0.9454	0.9436	0.9450	0.9432

18.13322	450.77241	452.62134	0.66534	6.35230	46.09933	47.72610	0.32917	0.32917	10120
333.91357	562.46265	0.49453	6054.92969	36.41740	564.77832	2583.90991	1.25311	1.00000	
496.06641	671.52661	0.59042	879.97998	47.62199	575.96021	2767.69824	1.50299	1.50299	
0.08560	-0.00112	-12.68855	41.10199	0.07610	538.47559	2186.30273	0.93990	0.93990	
0.32917	0.50146	1.86323	0.0	0.71541	0.72130	0.09479	0.80988	0.0	
1.22113	0.6699	1.22116	0.6700	1.26670	0.7061	1.22116	0.6700	0.6605	1009.29736
18.88324	536.46729	541.28516	0.77959	6.95094	37.76758	48.11586	0.31515	0.31515	
262.72754	601.67700	0.53504	4961.14453	25.89087	556.45557	2670.17407	0.74592	1.00000	
601.58154	809.25269	0.71963	864.31098	48.02002	590.79272	3102.38037	1.28272	1.28272	
0.08217	0.30908	-2.89775	41.10199	0.07826	526.35132	2197.49365	0.95762	0.95762	
0.31515	0.34801	1.55127	0.0	0.96496	0.37058	0.01361	0.47612	0.0	
1.26190	0.9449	1.26193	0.9450	1.27519	0.9472	1.26193	0.9450	0.9432	1038.04443
20.97162	536.12622	536.77710	0.79892	4.22090	37.75635	53.45738	0.28388	0.28388	
236.48897	536.56348	0.52087	4959.55469	23.77693	556.44434	2668.03003	0.59303	1.00000	
723.40796	900.80444	0.79992	959.89697	53.42413	595.28174	3379.85767	1.25169	1.25169	
0.04930	-0.00297	0.28185	41.10199	0.07875	527.83374	2217.61816	1.04100	1.04100	
0.28338	0.30636	1.48793	0.0	0.96918	0.02874	0.01427	0.34159	0.0	
1.26088	0.9419	1.26091	0.9420	1.29395	0.9475	1.26091	0.9420	0.9401	1127.52734
22.02863	537.44287	537.70068	0.80816	3.59791	38.43237	55.40126	0.26423	0.26423	
229.17210	536.50122	0.51861	5048.34375	23.09406	557.12036	2668.03003	0.54259	1.00000	
779.10522	946.63989	0.83993	1008.27734	55.38841	603.19141	3524.99638	1.23737	1.23737	
0.03099	-0.00313	1.14084	41.10199	0.07874	528.71118	2271.08594	1.08150	1.08150	
0.26423	0.29388	1.46214	0.0	0.96393	0.03540	0.01843	0.29882	0.0	
1.26088	0.9259	1.26092	0.9260	1.29615	0.9333	1.26092	0.9260	0.9235	1171.34839
22.03816	536.41528	536.46777	0.81091	3.20918	40.27905	56.96245	0.24675	0.24675	
229.66136	583.55981	0.51683	5290.97266	23.17572	559.96704	2668.03003	0.52151	1.00000	
824.82373	983.03677	0.87143	1054.48511	56.95988	611.10620	3647.44531	1.23318	1.23318	
0.01402	-0.00247	0.50972	41.10199	0.07855	530.65039	2273.80981	1.12031	1.12031	
0.24675	0.28381	1.45205	0.0	0.94657	0.05473	0.02973	0.27614	0.0	
1.26088	0.8849	1.26091	0.8850	1.27764	0.8964	1.26091	0.8850	0.8812	1213.36938
23.52960	536.00562	534.01980	0.80756	3.14282	42.26172	57.58711	0.23843	0.23843	
235.93694	583.91689	0.51611	5551.50000	23.83650	560.94971	2668.03003	0.53009	1.00000	
841.04199	996.25684	0.88073	1076.97900	57.58646	615.08716	3685.49683	1.23831	1.23831	
0.00708	-0.00223	-2.00129	41.10199	0.07830	532.60913	2224.91357	1.13902	1.13902	
0.23343	0.28811	1.45756	0.0	0.92775	0.05252	0.04168	0.27592	0.0	
1.26088	0.8449	1.26092	0.8450	1.29791	0.8598	1.26092	0.8450	0.8398	1233.67017
24.01569	529.60400	529.60645	0.80187	3.00342	44.73682	58.21069	0.23096	0.23096	
244.70512	583.43674	0.51454	5876.75781	24.79933	563.42480	2668.03003	0.54677	1.00000	
854.52222	1005.31130	0.88666	1099.23754	58.21057	619.10669	3712.99487	1.24709	1.24709	
0.00313	-0.00305	-7.91960	41.10199	0.07802	535.12849	2227.31734	1.15753	1.15753	
0.23096	0.29572	1.46814	0.0	0.90540	0.09981	0.05632	0.27977	0.0	
1.26088	0.7999	1.26092	0.8000	1.29909	0.8187	1.26092	0.8000	0.7933	1253.73682



57.73853 2667.73766 1.26040 0.9102 7.2072 1.26043 0.9103 0.9073 525.94165 5129.57422 9.37764 10130  
420.97779 5245.76000 346.38454 5058.05078 0.0 0.99000 16.00000 42.36200 0.0

\*STATOR NPT4  
\*NISRF  
\*MASS AVERAGE TOTAL PRESSURE  
\* TOTAL DELTA-T = 0.0

NASA FAN ENGINE SPLITTER STUDY  
LPOP= 0

10.17710 508.17212 508.18923 0.96453 -1.72966 0.0 47.64964  
557.48926 754.35376 0.67842 567.62109 47.64971 561.97915 2684.89941

-91.67090 516.37014 0.46441 465.81936 -10.222549 536.73706 2287.24370  
0.00901 3.09665 -9.47795 42.36200 0.07147 514.55542 1972.82861

0.06215 0.33547 1.16119 3.0 1.07000 0.00001 0.00000  
1.26986 0.8499 3.8447 1.26989 0.84950 0.84448 1.00000 1.0000 1.0000 782.09326 10130

10.79681 503.23457 504.11865 0.95153 -2.16469 0.0 44.66370  
494.58913 776.72437 0.63312 523.06875 44.65325 559.34106 2680.61304

-0.40503 504.11865 0.45173 494.18311 -0.04603 519.00244 2354.39525  
0.02704 0.17073 0.07144 42.36200 0.07408 517.86353 2046.58325

0.08560 3.04947 1.17705 0.0 1.00000 0.00001 0.00000  
1.26683 0.9949 3.4913 1.26697 0.9950 0.9914 1.00000 1.0000 1.0000 742.19727 10130

11.38050 484.93765 485.53667 0.92927 -3.08113 0.0 42.89473  
450.45605 662.31006 0.59193 512.64106 42.85369 557.71555 2476.58936

70.44360 430.51916 0.43841 520.89966 8.25513 541.25830 2409.93359  
0.05364 0.11846 0.11846 42.36200 0.07595 521.23755 2111.93018

0.12503 3.07074 1.20526 3.0 0.99999 0.00002 0.00000  
1.26493 0.9249 0.9223 1.26497 0.9250 0.9224 1.00000 1.0000 1.0000 712.72461 10130

11.92361 672.91997 478.66699 0.92336 -3.10540 0.0 41.86154  
423.75439 639.28857 0.57021 505.67857 41.51792 557.15601 2676.59375

122.00391 433.77070 0.44059 545.75830 14.29924 543.46362 2453.13794  
0.15637 0.16886 0.16886 42.36200 0.07692 523.16943 2147.01807

0.13599 0.07665 1.21297 0.0 0.99999 0.00001 0.00000  
1.26493 0.9376 0.9357 1.26497 0.9380 0.9350 1.00000 1.0000 1.0000 692.34937 10130

12.47558 430.52881 502.05615 0.95470 -1.31937 0.0 39.53191  
404.81960 644.93286 0.57558 505.73476 38.87094 557.13867 2679.00562

166.20410 529.99181 0.47198 571.92271 18.31586 545.81030 2492.96240  
0.21807 -0.12637 15.64130 42.36200 0.07677 522.54907 2140.27515

0.08157 3.04531 1.17315 3.0 0.99999 0.00002 0.00000  
1.26497 0.9417 0.9399 1.26497 0.9420 0.9400 1.00000 1.0000 1.0000 675.53149 10130

13.62499 529.62665 538.67310 1.00360 0.91296 0.0 35.19959  
373.46680 555.4788 0.58579 501.74639 34.73370 556.86084 2676.59131

241.00659 590.12939 0.52719 618.47339 24.10411 559.29394 2464.33377  
0.19562 -0.02207 18.06119 42.36200 0.07632 521.13085 2121.80371

-0.06480 -0.00368 1.11520 0.0 0.99999 0.00002 0.00000  
1.26493 0.9449 0.9439 1.26497 0.9450 0.9431 1.00000 1.0000 1.0000 653.06209 10130

14.27316 539.37085 545.99534 1.01106 0.92493 0.0 32.98172  
350.02710 649.56379 0.57924 495.09219 32.66309 556.72552 2674.65581

303.27319 624.56909 0.55784 658.30020 29.04993 554.18629 2631.95630  
0.15722 -0.00255 14.76846 42.36200 0.07655 521.74534 2130.68579

-0.02747 -0.01104 1.10777 0.0 0.99999 0.00001 0.00000  
1.26392 0.9449 0.9439 1.26396 0.9450 0.9431 1.00000 1.0000 1.0000 641.66729 10130

15.80673	543.30984	547.66650	1.01222	0.72348	0.0	29.98911	
313.93057	631.21167	0.56292	4963.63231	29.81490	556.45508	2670.16577	
400.66234	683.33140	0.60994	723.49341	36.79703	562.21451	2768.34447	
0.11033	0.00183	10.37222	42.86200	0.07713	523.32179	2153.52734	
-0.02273	-0.01220	1.10649	0.0	0.99990	0.00000	0.00000	
1.26189	0.9443	1.26192	0.9450	0.9431	1.0000	1.0000	1.0000
17.52908	545.21436	547.65039	1.00452	0.33399	0.0	27.43410	
283.02417	616.66045	0.54897	4960.84719	27.32977	556.45557	2470.16748	
510.25757	754.69481	0.67206	802.28174	43.87559	572.20874	2944.60547	
0.09464	0.00145	4.97698	42.86200	0.07770	524.85327	2175.66968	
-0.00941	-0.00451	1.11497	0.0	0.99990	0.00001	0.00000	
1.26189	0.9449	1.26192	0.9450	0.9431	1.0000	1.0000	1.0000
18.24022	453.69287	455.45571	1.00185	0.33449	0.0	36.19975	
331.94367	553.50098	0.49549	6054.66737	36.09091	564.77832	2583.00161	
502.93677	573.64005	0.59656	934.87744	47.84247	576.64282	2779.20654	
0.08570	0.00980	7.60478	42.86200	0.07607	539.37842	2184.92065	
-0.00349	-0.01183	1.11795	0.0	0.99999	0.00002	0.00000	
1.22112	0.6699	1.22115	0.6700	0.6605	1.0000	1.0000	1.0000
18.98996	543.95569	545.45801	1.00526	0.23879	0.0	25.66870	
261.36426	604.34351	0.53802	4960.94141	25.60208	556.45557	2470.16592	
607.41748	816.38257	0.72619	968.78174	48.07528	581.44238	3114.56226	
0.07580	-0.00060	5.35257	42.86200	0.07814	526.03345	2192.84937	
-0.00983	-0.00525	1.11415	0.0	0.99990	0.00001	0.00000	
1.26189	0.9449	1.26193	0.9450	0.9432	1.0000	1.0000	1.0000
21.03578	547.65801	548.26001	1.01745	0.50943	0.0	23.29897	
235.76105	596.93176	0.53047	4959.61406	23.26851	556.46434	2668.02588	
727.07251	910.61694	0.80940	962.83374	52.88131	595.75464	3389.28442	
0.05416	-0.00488	10.98478	42.86200	0.07838	526.82593	2202.82544	
-0.03284	-0.01745	1.10079	0.0	0.99999	0.00001	0.00000	
1.26089	0.9419	1.26091	0.9420	0.9401	1.0000	1.0000	1.0000
22.07104	552.35060	551.26399	1.07119	0.54376	0.0	22.54915	
228.72787	576.93179	0.53016	5049.26172	22.53430	557.12036	2668.02954	
781.49097	956.35767	0.84952	1013.31990	54.80081	603.51929	3531.71362	
0.03928	-0.00851	13.65485	42.86200	0.07920	527.49951	2203.31079	
-0.03777	-0.02109	1.09636	0.0	0.99990	0.00000	0.00000	
1.26089	0.9259	1.26091	0.9260	0.9235	1.0000	1.0000	1.0000
23.05824	551.655796	551.75391	1.07400	0.59457	0.0	22.58467	
229.46001	597.55519	0.52992	5290.94141	22.58115	559.96704	2668.02319	
825.94409	993.28540	0.88085	1055.40630	56.25594	611.26855	3650.80225	
0.01867	-0.00496	19.11850	42.86200	0.07804	529.27441	2203.68002	
-0.04531	-0.02400	1.09375	0.0	0.99999	0.00000	0.00000	
1.26089	0.8849	1.26091	0.8850	0.8811	1.0000	1.0000	1.0000



558.87305	2637.87085	1.24663	0.8434	0.8384	1.24666	0.8435	0.8395	532.18994	0.0	9.65023	10150
30.73781	5245.00000	25.59863	5052.91406	0.0	0.0	0.98000	4.00000	4.00000	45.82700	0.0	10150
*STATOR											
*NISRF											
*MASS AVERAGE TOTAL PRESSURE											
9.65000	540.07031	564.10864	0.71304	0.0	46.11729	0.0	0.0	0.0	0.39101	Blading Station 5	
0.0	564.10864	0.49739	0.0	0.0	0.0	561.87915	2620.45361	0.0	2.27437	0.39101	
441.60238	716.45703	0.63171	441.69238	0.0	38.06064	578.09302	2895.19995	1.40244	1.40244	0.71488	
-0.30166	0.07655	-0.00825	45.82700	0.0	0.07747	535.42065	2213.03149	0.71488	0.71488	0.0	
0.39101	0.45285	2.00469	0.0	0.0	0.87732	0.08316	0.07400	2.19316	0.0	791.12671	10150
1.23840	0.7559	1.23843	0.7633	0.7560	1.15861	0.8584	0.8554	0.97600	0.0	0.0	
*STATOR											
*NISRF											
*MASS AVERAGE TOTAL PRESSURE											
10.22986	539.40039	564.36157	0.76291	0.0	43.09094	0.0	0.0	0.0	0.34961	0.34961	
0.0	554.36157	0.49880	0.0	0.0	0.0	559.34106	2645.75513	1.95854	1.95854	1.00000	
468.23340	733.11201	0.64812	468.23340	0.0	39.68143	577.56274	2960.35889	1.31077	1.31077	0.66583	
-0.31427	0.01313	7.83427	45.82700	0.0	0.07852	532.85742	2232.29468	0.66583	0.66583	0.0	
0.34961	0.58420	1.87342	0.0	0.0	0.93022	0.05056	0.01300	1.89744	0.0	739.74927	10150
1.25036	0.8454	1.25040	0.8455	0.8405	1.12102	0.8972	0.9955	0.98700	0.0	0.0	
*STATOR											
*NISRF											
*MASS AVERAGE TOTAL PRESSURE											
10.77542	538.25024	567.25879	0.82676	0.0	42.04968	0.0	0.0	0.0	0.25577	0.25577	
0.0	567.25879	0.50225	0.0	0.0	0.0	557.71655	2647.14502	1.70099	1.70099	1.00000	
493.20410	751.69652	0.66554	493.20410	0.0	41.00537	577.93384	2998.99658	1.20954	1.20954	0.61474	
-0.33271	-0.05371	24.90669	45.82700	0.0	0.07867	530.95947	2228.32568	0.61474	0.61474	0.0	
0.25577	0.51393	1.72799	0.0	0.0	0.94112	0.04883	0.01100	1.65035	0.0	686.12183	10150
1.25101	0.8813	1.25106	0.8815	0.8776	1.07427	0.9663	0.8649	0.98900	0.0	0.0	
*STATOR											
*NISRF											
*MASS AVERAGE TOTAL PRESSURE											
11.28000	536.18208	571.71875	0.91227	0.0	43.41928	0.0	0.0	0.0	0.06490	0.06490	
0.0	571.71875	0.50667	0.0	0.0	0.0	557.15601	2620.37646	1.49623	1.49623	1.00000	
516.29956	770.34253	0.68269	516.29956	0.0	42.08411	579.31079	3004.11040	1.09616	1.09616	0.55831	
-0.36604	-0.15186	52.63927	45.82700	0.0	0.07778	529.97607	2199.25342	0.55831	0.55831	0.0	
0.36640	0.43811	1.56805	0.0	0.0	0.99463	0.11011	0.02100	1.44884	0.0	626.69590	10150
1.23836	0.8532	1.23840	0.8533	0.8488	1.01529	0.4170	0.4157	0.97900	0.0	0.0	
*STATOR											
*NISRF											
*MASS AVERAGE TOTAL PRESSURE											
558.87183	2637.87572	1.24667	0.8436	0.8386	1.24670	0.8437	0.8387	532.05396	0.0	9.64994	10160
30.73798	5245.00000	25.59860	5052.91797	0.0	0.0	0.98000	4.00000	4.00000	47.48000	0.0	10160
*STATOR											
*NISRF											
*MASS AVERAGE TOTAL PRESSURE											
9.05510	537.23315	581.26342	1.03941	0.0	0.0	0.0	0.0	0.0	0.0	Blading Station 5	
0.0	581.26343	0.51329	0.0	0.0	0.0	561.87915	2620.44995	0.0	0.0	0.0	
414.46289	713.89526	0.63041	414.46289	0.0	36.49030	575.15576	2861.32373	1.40244	1.40244	0.71488	
-0.41308	0.05825	-10.02024	47.48000	0.0	0.07688	533.78662	2189.45655	0.71488	0.71488	0.0	
0.05784	-0.03941	1.08695	0.0	0.0	1.00000	0.00001	0.00000	0.00000	0.0	791.12671	10160
1.23840	0.7632	1.23843	0.7633	0.7560	0.98935	1.0000	1.0001	1.00000	1.0000	564.10864	10160
*STATOR											
*NISRF											
*MASS AVERAGE TOTAL PRESSURE											
9.67374	543.47095	579.46167	1.02676	0.0	0.0	0.0	0.0	0.0	0.0	Blading Station 5	
0.0	579.46167	0.51293	0.0	0.0	0.0	559.34106	2645.74731	1.95854	1.95854	1.00000	
442.77881	723.26011	0.64541	442.77881	0.0	37.39419	575.63574	2925.87842	1.31077	1.31077	0.66583	
-0.36991	0.05619	-6.10872	47.48000	0.0	0.07807	531.42090	2217.78857	0.66583	0.66583	0.0	
0.05081	-0.02576	1.09081	0.0	0.0	0.99997	0.00002	0.00000	0.00000	0.0	739.74927	10160
1.25035	0.8453	1.25039	0.8455	0.8405	0.99039	1.0000	1.0002	1.00000	1.0000	564.10864	10160



558.84229	2638.08813	1.24673	0.8644	0.8394	1.24677	0.8445	0.8395	537.32690	0.0	9.64285	10180
30.74243	5245.00000	25.59766	5053.05469	0.0	0.0	0.98000	51.41699	4.00000	0.0	0.0	
* STATOR OPT4											
* NJSRE											
**MASS AVERAGE TOTAL PRESSURE											
		DELTA-T COOLING =		DELTA-T =		TOTAL DELTA-T =					
		0.0		0.0		0.0					
NASA FAN ENGINE SPLITTER STUDY											
LOOP= 0											
6.90000	400.88892	476.71582	0.85381	0.0	0.0	0.0	0.0	0.0	0.0	0.0	
0.0	476.71582	0.41740	0.0	0.0	0.0	561.87915	2620.42993	0.0	0.0	0.0	
315.82153	571.84009	0.50069	315.82153	0.08024	0.0	570.16943	2758.45166	0.00000	0.00000	0.00000	
-0.64348	-0.70000	-47.41689	51.41699	0.99999	0.0	542.98511	2324.48486	0.00000	0.00000	0.00000	
0.25940	0.14619	1.31177	0.0	1.04668	1.00000	0.00003	0.00000	1.00000	1.00000	1.00000	10180
1.23839	0.7632	0.7559	1.23842	0.7633	0.7560	1.00000	1.00000	1.00000	1.00000	558.34106	
7.85717	454.62427	511.85864	0.91131	0.0	0.0	0.0	0.0	0.0	0.0	0.0	
0.0	511.85864	0.45042	0.0	0.0	0.0	559.34106	2645.72388	0.00000	0.00000	0.00000	
359.63257	625.56763	0.55048	359.63257	0.08024	0.0	570.09106	2828.24902	0.00000	0.00000	0.00000	
-0.51734	-0.70000	-28.74065	51.41699	0.99997	0.0	537.55688	2301.99341	0.00000	0.00000	0.00000	
0.16110	0.08869	1.22900	0.0	1.02952	1.00000	0.00004	0.00001	1.00000	1.00000	1.00000	10180
1.25034	0.8453	0.8403	1.25039	0.8454	0.8404	1.00000	0.99999	1.00000	1.00000	561.67334	
8.64444	475.59398	520.47070	0.93702	0.0	0.0	0.0	0.0	0.0	0.0	0.0	
0.0	520.47070	0.45901	0.0	0.0	0.0	557.71655	2647.10791	0.00000	0.00000	0.00000	
395.66650	653.79028	0.57658	395.66650	0.08024	0.0	570.72900	2869.94849	0.00000	0.00000	0.00000	
-0.44460	-0.70000	-20.98418	51.41699	0.99999	0.0	535.19214	2291.13867	0.00000	0.00000	0.00000	
0.11573	0.06298	1.19528	0.0	1.02076	1.00000	0.00003	0.00000	1.00000	1.00000	1.00000	10180
1.25109	0.8813	0.8774	1.25104	0.8814	0.8776	1.00000	0.99999	1.00000	1.00000	555.45454	
9.33060	472.15186	507.40967	0.94904	0.0	0.0	0.0	0.0	0.0	0.0	0.0	
0.0	507.40967	0.44726	0.0	0.0	0.0	557.15601	2620.36060	0.00000	0.00000	0.00000	
427.07300	663.21631	0.58459	427.07300	0.07992	0.0	572.31592	2879.85889	0.00000	0.00000	0.00000	
-0.39361	-0.70000	-19.41212	51.41699	0.99999	0.0	535.74805	2284.27710	0.00000	0.00000	0.00000	
0.09449	0.05096	1.18014	0.0	1.01559	1.00000	0.00000	0.00000	1.00000	1.00000	1.00000	10180
1.23336	0.8531	0.8486	1.23840	0.8533	0.8487	1.00000	0.99999	1.00000	1.00000	534.65454	



*STATION	557.65283	390.33081	2666.02490	1.25994	0.9107	0.9077	1.25397	0.9108	0.9079	524.69141	5118.16016	9.35709	20140
Opt4	Opt4	5245.00000	321.26025	5058.44141	0.0	0.0	0.0	0.99000	13.00000	43.93660	0.0	0.0	
* NISRE	TOTAL PRESSURE												
* MASS AVERAGE	TOTAL DELTA-T = 0.0												
* DELTA-T	COOLING = 0.0												
NASA FAN ENGINE SPLITTER STUDY													
LOOP= 0													
12.43000	600.70244	617.18115	1.15600	8.14795	0.0	0.0	34.11691						
406.49072	735.01782	0.66645	5052.67578	33.56987	557.15601	2676.58521							
167.44556	638.70142	0.57554	568.93628	14.74612	545.61206	2487.27174							
0.24100	0.72202	75.19234	43.93660	0.07279	511.73340	1987.13745							
-0.30189	-0.15600	0.96886	0.0	1.00000	0.00000	0.00000							
1.26493	0.93379	0.93357	0.9380	0.9359	1.0000	1.0000	1.0000	1.0000	1.0000	1.0000	1.0000	639.28857	20140
12.88327	586.95097	603.66260	1.11605	5.89093	0.0	33.73703							
392.00379	719.77734	0.64764	5050.35156	32.99904	557.13867	2679.00342							
197.67407	635.20361	0.57155	589.68286	18.13144	547.61108	2521.89479							
0.74018	0.79824	57.97983	43.93660	0.07369	514.05151	2020.87012							
-0.22164	-0.11605	1.000354	0.0	1.00000	0.00000	0.00000							
1.26607	0.9419	0.93309	0.9420	0.9400	1.0000	1.0000	1.0000	1.0000	1.0000	1.0000	1.0000	644.93286	20140
13.72128	570.77002	579.42700	1.04508	2.49746	0.0	32.62685							
365.39366	695.72002	0.61412	5013.75000	32.23443	556.86084	2676.58447							
262.07014	636.17261	0.57033	628.03979	24.39367	541.49536	2587.30713							
0.17483	0.93573	24.89597	43.93660	0.07512	517.83569	2075.19092							
-0.08401	-0.74508	1.07169	0.0	0.99999	0.00001	0.00000							
1.26493	0.9449	0.9430	0.9450	0.9431	1.0000	1.0000	1.0000	1.0000	1.0000	1.0000	1.0000	655.47388	20140
14.51550	563.33179	569.12622	1.02551	1.42936	0.0	31.42398							
344.18111	645.13645	0.59507	4995.99828	31.16374	556.72559	2674.45117							
320.20923	635.02271	0.58426	664.30233	29.36354	555.40137	2657.22681							
0.14380	0.71953	14.12372	43.93660	0.07588	519.93726	2104.94019							
-0.04734	-0.72551	1.09214	0.0	0.99999	0.00001	0.00000							
1.26392	0.9440	0.9430	0.9450	0.9431	1.0000	1.0000	1.0000	1.0000	1.0000	1.0000	1.0000	648.56079	20140
15.09070	554.52466	557.92065	1.01134	0.73909	0.0	29.22441							
310.22876	638.37085	0.56972	4960.61719	29.07600	556.45508	2670.16382							
421.66235	699.33962	0.62413	731.89111	37.08105	563.23462	2785.90820							
0.11084	0.70986	5.24125	43.93660	0.07686	522.56567	2142.64551							
-0.02105	-0.71134	1.10744	0.0	1.00000	0.00000	0.00000							
1.26189	0.9449	0.9430	0.9450	0.9431	1.0000	1.0000	1.0000	1.0000	1.0000	1.0000	1.0000	631.21167	20140
17.67496	550.62139	552.65308	1.00549	0.49531	0.0	27.01817							
292.67383	619.94131	0.55216	4960.89453	26.22447	556.45557	2670.16211							
528.33091	754.55445	0.68108	809.00464	43.71104	573.10464	2940.85620							
0.09014	0.70415	7.63251	43.93660	0.07757	524.50562	2170.62207							
-0.31020	-0.70548	1.11389	0.0	0.99999	0.00001	0.00000							
1.26189	0.9449	0.9430	0.9450	0.9431	1.0000	1.0000	1.0000	1.0000	1.0000	1.0000	1.0000	616.46045	20140
18.37500	459.61816	461.25464	1.00596	0.54992	0.0	35.63737							
320.50906	566.95084	0.49850	6054.70703	35.56100	564.77832	2583.89678							
511.53933	588.78687	0.60583	841.04539	47.93495	577.50171	2793.74048							
0.08447	0.70065	0.64856	43.93660	0.07576	538.06250	2190.62578							
-0.31125	-0.70594	1.11336	0.0	0.99999	0.00001	0.00000							
1.22112	0.6699	0.6604	0.6700	0.6605	1.0000	1.0000	1.0000	1.0000	1.0000	1.0000	1.0000	563.50038	20140

19.10442	548.28467	550.01270	1.00560	0.32971	0.0	25.34305
259.67725	508.23193	4960.98047	4960.98047	25.27338	556.45557	2670.16919
614.75537	874.38672	0.73399	874.43262	48.19144	582.26074	3129.95483
0.07946	-0.00278	1.43112	43.93660	0.07801	525.69141	2187.85742
-0.01345	-0.00560	1.11376	0.0	0.99999	0.00000	0.00000
1.24189	0.9449	1.76193	0.9450	0.99772	1.0000	1.00000
	0.9430		0.9432			20140
21.13042	555.63042	556.02407	1.01266	0.41631	0.0	22.89807
234.70667	604.76035	0.53757	4959.44922	22.85220	556.44434	2668.02319
732.45850	920.14111	0.81845	967.14528	52.75247	596.44873	3403.14819
0.06695	-0.01151	0.26801	43.93660	0.07809	526.07080	2191.78514
-0.02373	-0.01266	1.10590	0.0	0.99999	0.00001	0.00000
1.26083	0.9419	1.26091	0.9420	0.99499	1.0000	1.00000
	0.9399		0.9401			20140
22.14732	563.51147	564.56641	1.02013	0.54912	0.0	22.02341
227.94144	629.94521	0.54145	5049.28906	21.98619	557.12036	2668.02637
785.76880	967.55762	0.86045	1013.71045	54.30313	504.10596	3543.76459
0.06122	-0.02069	1.61494	43.93660	0.07785	526.29468	2185.73779
-0.01781	-0.02013	1.09790	0.0	0.99999	0.00001	0.00000
1.26089	0.9259	1.26091	0.9260	0.99702	1.0000	1.00000
	0.9234		0.9235			20140
23.10759	576.82129	577.61255	1.03979	0.95732	0.0	21.65074
228.97090	621.34033	0.55226	5290.96484	21.62383	558.96704	2668.01758
828.69189	1010.13184	0.89783	1057.64284	55.12280	611.66455	3652.10205
0.05240	-0.03793	6.72982	43.93660	0.07716	526.86377	2168.72583
-0.07527	-0.03979	1.07714	0.0	0.99999	0.00001	0.00000
1.26089	0.8849	1.26091	0.8850	0.99414	1.0000	1.00000
	0.8810		0.8811			20140
23.56905	585.94165	586.53599	1.05882	1.39267	0.0	21.90050
235.55296	632.04763	0.56134	5551.52344	21.88940	562.94971	2668.02588
843.18604	1027.12573	0.91210	1078.73901	55.17677	615.40234	3692.07910
0.04505	-0.05212	12.74344	43.93660	0.07652	527.22949	2154.33839
-0.11205	-0.05882	1.05778	0.0	0.99999	0.00001	0.00000
1.26089	0.8449	1.26092	0.8450	0.97654	1.0000	1.00000
	0.8397		0.8398			20140
24.01569	599.00769	599.32666	1.09111	2.14848	0.0	22.22101
244.70480	667.35840	0.57446	5876.75000	22.21016	563.42480	2668.01978
854.52271	1043.74365	0.92620	1099.22754	54.95575	612.10669	3712.92775
0.03390	-0.07317	23.96452	43.93660	0.07565	528.57886	2133.33203
-0.17568	-0.07111	1.02647	0.0	0.99999	0.00001	0.00000
1.26088	0.7999	1.26091	0.8000	0.96390	1.0000	1.00000
	0.7932		0.7933			20140

557.64917	2666.71440	1.25993	0.9108	0.9078	1.25996	0.9109	0.9070	526.32520	5117.69531	9.35620	20150
390.33862	5245.70000	321.26709	5058.45313		0.0	0.99000		13.00000	45.90509	0.20070	
* STATOR OPT4											
* NISRF											
* MASS AVERAGE TOTAL PRESSURE											
DELTA-T COOLING = 0.0											
TOTAL DELTA-T = 0.0											
NASA FAN ENGINE SPLITTER STUDY											
LUMP = 0											
Bypass Duct Stator Inlet Station											
Blading Station 4											
12.78700	619.69531	624.31104	0.99993		1.02500	0.0		32.53735			
395.35791	733.76704	0.66640	5052.67148		32.34486	557.15601		2676.57642			
189.59839	652.46582	0.58840	594.95430		16.89311	547.14917		2511.89746			
0.12228	0.74860	-23.35367	45.90509		0.07279	511.73950		1987.21118			
0.00012	0.30007	1.12008	0.0		1.03000	0.00001		0.00000			
1.26497	0.9337	1.26497	0.9380	0.9350	1.03000	1.00000	1.00000	1.00000	1.00000	739.01787	20150
13.21668	609.01392	612.49756	1.00298		1.04022	0.0		32.10576			
382.11914	721.19992	0.64973	5050.34375		31.95882	557.13867		2678.99345			
222.82446	651.76978	0.58660	604.94360		19.99121	549.12695		2546.42676			
0.10711	0.73121	-15.42428	45.99272		0.07360	513.79443		2017.33179			
-0.00537	-0.30298	1.11668	0.0		0.02990	0.00001		0.00000			
1.26605	0.9410	1.26611	0.9420	0.9400	0.99825	1.00000	1.00000	1.00000	1.00000	719.77734	20150
14.02493	592.76055	595.05103	1.01337		1.24937	0.0		31.12366			
357.48730	694.17773	0.62296	5013.73047		30.99504	556.86094		2676.57886			
284.45093	659.54370	0.59188	641.93823		25.54909	552.96289		2611.59415			
0.10964	0.73119	-5.87165	46.15494		0.07474	516.78491		2060.49027			
-0.07445	-0.31337	1.10523	0.0		1.00000	0.00001		0.00000			
1.26492	0.9449	1.26496	0.9450	0.9431	0.99291	1.00000	1.00000	1.00000	1.00000	685.02002	20150
14.79710	578.31519	580.73193	1.00998		0.99049	0.0		30.27719			
337.63135	671.74731	0.60144	4995.26884		30.17325	556.72559		2674.44214			
239.65039	672.76440	0.60235	677.28174		30.32190	556.83911		2676.34717			
0.09152	0.02456	-5.10427	46.30992		0.07562	510.19840		2094.48315			
-0.01836	-0.30998	1.10893	0.0		0.99999	0.00002		0.00000			
1.26391	0.9449	1.26395	0.9450	0.9431	0.99503	1.00000	1.00000	1.00000	1.00000	665.10645	20150
16.24489	552.17378	561.20776	1.00078		0.53020	0.0		28.62460			
305.29224	639.37207	0.57019	4960.65625		28.54591	556.45509		2670.15527			
438.43921	712.16797	0.63561	743.73145		37.99344	564.68655		2811.14990			
0.08105	0.71356	-5.71450	46.60126		0.07694	522.51245		2141.87964			
-0.00145	-0.30078	1.11912	0.0		1.00000	0.00002		0.00000			
1.26189	0.9449	1.26192	0.9450	0.9431	0.99864	1.00000	1.00000	1.00000	1.00000	639.37095	20150
17.92946	548.83618	550.59302	0.99414		0.24338	0.0		26.75462			
276.69189	616.20703	0.54873	4960.93357		26.68109	556.45557		2670.14917			
543.96143	773.98094	0.68922	820.65332		44.65285	574.68604		2989.31245			
0.08008	0.00261	-7.70485	46.93854		0.07771	524.49915		2176.03174			
0.01094	0.00587	1.12661	0.0		0.99999	0.00003		0.00000			
1.26188	0.9449	1.26192	0.9450	0.9431	1.00249	0.00000	0.00000	1.00000	1.00000	619.94131	20150
19.63219	457.29356	458.66528	0.99143		0.22360	0.0		35.39804			
324.96240	562.11597	0.49421	6056.75781		35.31760	564.77832		2583.89014			
527.85571	609.29931	0.61482	852.91812		49.01149	579.15920		2821.92334			
0.07735	0.70394	0.78030	47.07956		0.07612	538.50906		2196.74829			
0.01568	0.30837	1.12946	0.0		0.99999	0.00001		0.00000			
1.22112	0.6699	1.22115	0.6700	0.6605	1.00290	0.9995	0.9995	1.00000	1.00000	566.86084	20150

19.36664	542.72998	544.26880	0.98899	0.06904	0.0	25.26689	20150
256.16382	601.53833	0.53491	4961.03125	25.20433	556.45557	2670.15771	
630.27100	832.74894	0.74051	886.43481	49.18781	594.01636	3163.16016	
0.077536	0.70532	-7.96799	47.22696	0.07826	526.36499	2197.68457	
0.02038	0.01101	1.13246	0.0	0.99998	0.00002	0.00000	
1.26189	0.9449	1.26192	0.9450	1.00449	0.9997	1.00000	608.23193
21.43771	533.53906	535.85645	0.96575	-0.49900	0.0	23.44170	
231.34624	593.56284	0.51816	4959.48828	23.35120	556.44434	2668.00830	
749.88647	921.46797	0.81823	981.23071	54.45099	598.72495	3448.88794	
0.09331	-0.70266	-10.83584	47.64262	0.07886	528.11621	2221.76392	
0.06295	0.73425	1.15972	0.0	0.79997	0.00003	0.00001	
1.26087	0.9419	1.26090	0.9420	1.01368	0.9999	0.99999	604.36035
22.50113	529.34302	532.40430	0.94892	-0.86467	0.0	22.96933	
224.35851	577.74658	0.51230	5048.31641	22.85086	557.12035	2668.01880	
805.54590	965.58716	0.85621	1079.90454	56.53831	606.83352	3600.62012	
0.10771	-0.70301	-13.40935	47.85605	0.07899	529.36401	2230.69946	
0.09323	0.05108	1.18029	0.0	0.99999	0.00002	0.00000	
1.26088	0.9259	1.26091	0.9260	1.02057	0.9999	0.99999	608.84521
23.53130	520.26782	524.30811	0.91816	-1.58829	0.0	23.37309	
224.85004	570.49779	0.50466	5291.01172	23.21211	558.96704	2668.00732	
852.20430	1000.57715	0.88513	1077.05640	58.39861	615.10083	3731.73096	
0.12487	3.00281	-16.09563	48.06279	0.07902	531.90503	2242.26636	
0.14730	0.38184	1.21984	0.0	0.99999	0.00002	0.00000	
1.26087	0.8849	1.26090	0.8850	1.03391	1.0000	1.00000	621.34033
24.03986	511.46143	516.05640	0.87449	-2.22780	0.0	24.29982	
230.93188	565.37036	0.49899	5551.56641	24.10820	560.94971	2668.02002	
869.40210	1011.02637	0.89231	1100.33398	59.30756	619.40786	3774.96313	
0.13435	0.70989	-18.13858	48.16446	0.07895	534.37231	2250.81372	
0.18781	0.10552	1.25213	0.0	1.00000	0.00001	0.00000	
1.26089	0.8449	1.26092	0.8450	1.04478	1.0000	1.00000	632.06763
24.54999	498.39331	503.66895	0.86144	-3.21019	0.0	25.65503	
239.37894	557.65991	0.49072	5876.74609	25.42035	563.42480	2668.01563	
884.30820	1017.68188	0.89552	1123.69335	60.33563	523.61965	3808.76709	
0.14549	0.70099	-22.01118	48.26729	0.07891	537.56885	2263.13306	
0.24276	0.13856	1.30015	0.0	0.99999	0.00001	0.00000	
1.26089	0.7999	1.26091	0.8000	1.06084	1.0000	1.00000	647.35840

*STATOR IDP?		*NISP		*MASS AVERAGE TOTAL PRESSURE		DELTA-T CUMING =		TOTAL DELTA-T =		Blading Station 5	
557.66260	2639.52124	1.24741	0.8711	0.3670	1.24744	0.9712	0.8671	535.4653	9.35939	0.32407	20160
390.33760	5745.70000	374.49634	5058.30453	0.0	0.0	0.98000	0.0	13.00000	0.20790	1.00000	
12.95000	563.44849	0.76249	0.0	0.0	32.34486	0.0	0.0	0.0	1.54863	1.00000	
0.0	0.49897	0.0	0.0	0.0	0.0	557.15601	2620.36816	0.0	1.31151	0.66648	
592.73755	917.90933	0.72423	502.73755	46.45110	0.37907	530.75684	2210.81377	0.66648	0.0	1.52135	20160
0.02875	0.03050	-23.37193	48.26720	0.0	0.89171	0.09154	0.02100	0.0	738.76704	0.0	
0.32407	0.50326	1.82811	0.0	0.8498	1.11242	0.8339	0.9313	0.97900	0.0	0.0	
1.23836	0.8531	1.23840	0.8533	0.8498	0.0	0.0	0.0	0.0	0.31164	1.00000	
13.38602	565.35791	0.78313	0.0	0.0	31.25082	0.0	0.0	0.0	1.47096	1.00000	
0.0	0.50076	0.0	0.0	0.0	0.0	557.13867	2638.80859	0.0	1.27693	0.64981	
612.60459	833.49115	0.73842	612.60459	47.30999	0.0	530.56030	2223.52759	0.64981	0.0	0.0	
0.03745	0.02760	-19.03760	43.35703	0.0	0.0	0.0	0.0	0.0	1.44565	721.91992	20160
0.31164	0.47984	1.77773	0.0	0.8779	1.10222	0.8656	0.8637	0.01500	0.0	0.0	
1.24707	0.8815	1.24711	0.8816	0.8779	0.0	0.0	0.0	0.0	0.29555	1.00000	
14.18866	556.49023	0.90165	0.0	0.0	30.09606	0.0	0.0	0.0	1.38391	1.00000	
0.0	0.49265	0.0	0.0	0.0	0.0	556.96084	2647.13647	0.0	1.24742	0.62303	
649.43237	952.24487	0.75713	649.43237	49.40712	0.0	531.10996	2242.56323	0.62303	0.0	0.0	
0.04289	0.01753	-17.30806	48.52483	0.0	0.07915	0.04779	0.01100	0.0	694.17773	0.0	20160
0.29555	0.45634	1.73107	0.0	0.8973	0.93895	0.8945	0.8931	0.99900	0.0	0.0	
1.25101	0.9004	1.25105	0.9005	0.8973	1.08837	0.8945	0.8931	0.99900	0.0	0.0	
14.95687	547.35475	0.81482	0.0	0.0	30.17325	0.0	0.0	0.0	0.27743	1.00000	
0.0	0.49624	0.0	0.0	0.0	0.0	556.72559	2647.69751	0.0	1.27276	0.60149	
684.50424	875.50781	0.77544	684.50424	51.35557	0.0	505.67163	3355.86279	0.60149	0.0	0.0	
0.04788	0.01218	-14.72885	48.68451	0.0	0.07949	0.04611	0.01000	0.0	671.74731	0.0	20160
0.27743	0.43514	1.69808	0.0	0.9013	0.94236	0.8905	0.8792	0.99000	0.0	0.0	
1.25127	0.9043	1.25131	0.9044	0.9013	1.07692	0.8905	0.8792	0.99000	0.0	0.0	
16.40988	532.35840	0.83539	0.0	0.0	29.54591	0.0	0.0	0.0	0.24657	1.00000	
0.0	0.47175	0.0	0.0	0.0	0.0	556.45509	2646.12378	0.0	1.21227	1.00000	
751.10359	921.40967	0.81444	751.10359	54.60359	0.0	503.33154	3513.57300	0.0	1.19704	0.57024	
0.05649	0.0701	-11.51095	49.99556	0.0	0.07894	0.04549	0.00900	0.0	0.0	0.0	
0.24657	0.40236	1.66569	0.0	0.9053	0.94519	0.8967	0.8661	0.99100	0.0	0.0	
1.25053	0.9082	1.25056	0.9083	0.9053	1.26391	0.8967	0.8661	0.99100	0.0	0.0	
18.10905	520.77661	0.84705	0.0	0.0	26.68109	0.0	0.0	0.0	0.22575	1.00000	
0.0	0.46901	0.0	0.0	0.0	0.0	556.45557	2646.11769	0.0	1.18057	0.54877	
828.87378	979.52563	0.86497	828.87378	57.83060	0.0	513.53369	3724.47559	0.0	0.0	0.0	
0.06736	0.07095	-10.69084	49.33933	0.0	0.09033	0.04863	0.00900	0.0	616.20703	0.0	20160
0.22575	0.37635	1.60973	0.0	0.9053	0.94274	0.8968	0.8657	0.99100	0.0	0.0	
1.25053	0.9091	1.25056	0.9082	0.9053	1.05126	0.8968	0.8657	0.99100	0.0	0.0	
18.80687	459.50675	0.81934	0.0	0.0	35.31740	0.0	0.0	0.0	0.26376	1.00000	
0.0	0.40174	0.0	0.0	0.0	0.0	564.77832	2560.99331	0.0	1.48667	1.22049	
860.91372	976.27930	0.85157	860.91372	61.85156	0.0	547.14390	3680.71753	0.0	0.49424	0.0	
0.06796	0.07083	-2.19269	49.48491	0.0	0.07850	0.05791	0.00890	0.0	562.11597	0.0	20160
0.26376	0.46836	1.71650	0.0	0.9396	0.92673	0.8996	0.8945	0.99110	0.0	0.0	
1.21025	0.6399	1.21028	0.6400	0.6302	1.06790	0.8996	0.8945	0.99110	0.0	0.0	



557.65796	2639.54565	1.24742	0.8713	0.9672	1.24745	0.8714	0.9673	537.89307	0.0	9.35833
300.36719	5245.70000	324.51480	5058.41737	0.0	0.0	0.98000	0.0	13.00000	51.33839	0.20181
*STATOR	NPT4	DELTA-T COLLINS = 0.0 TOTAL DELTA-T = 0.0								
*NISP	LUMP= 1									
*MASS AVERAGE TOTAL PROPSUPE	NASA FAN ENGINE SPLITTER STUDY									
12.95000	502.24585	502.27344	0.89143	0.0	0.0	0.0	0.0	2620.36035	0.0	20170
0.0	502.27344	0.44255	0.0	0.0	557.15601	0.0	0.0	0.0	0.0	0.0
502.73755	776.92749	0.68455	592.73755	49.72273	586.35449	3134.10352	0.0	0.0	0.0	0.0
-0.01052	-0.00501	-14.83423	51.33839	0.28004	536.17920	2290.72339	0.0	0.0	0.0	0.0
0.19551	0.10857	1.25641	0.0	0.99999	0.00002	0.00000	0.0	0.00000	0.0	0.0
1.23835	1.84886	1.23840	0.8487	1.03624	1.00000	0.99999	1.00000	1.00000	1.00000	563.44849
13.41822	514.61914	514.61914	0.91375	0.0	0.0	0.0	0.0	0.0	0.0	20170
0.0	514.61914	0.45388	0.0	0.0	557.11867	2638.80249	0.0	0.0	0.0	0.0
614.16346	801.27124	0.70670	614.16346	50.03092	589.48608	3196.93213	0.0	0.0	0.0	0.0
-0.00093	-0.10273	-12.40509	51.43288	0.08025	535.11792	2291.14233	0.0	0.0	0.0	0.0
0.16282	0.08975	1.23043	0.0	0.99999	0.00001	0.00000	0.0	0.00000	0.0	0.0
1.24707	0.8815	1.24711	0.8816	1.03041	1.00000	0.99999	1.00000	1.00000	1.00000	565.35791
14.26170	518.57056	518.52354	0.93195	0.0	0.0	0.0	0.0	0.0	0.0	20170
0.0	518.57056	0.45767	0.0	0.0	556.96084	2647.12109	0.0	0.0	0.0	0.0
652.86743	833.79028	0.73580	652.86743	51.53717	592.28174	3285.85522	0.0	0.0	0.0	0.0
0.01431	0.00104	-8.48444	51.60350	0.08041	534.49585	2293.02954	0.0	0.0	0.0	0.0
0.12474	0.08805	1.20177	0.0	0.99999	0.00004	0.00001	0.0	0.00001	0.0	0.0
1.25107	0.9004	1.25104	0.9005	1.02250	1.00000	0.99999	1.00000	1.00000	1.00000	556.49023
15.06107	516.59717	516.75122	0.94409	0.0	0.0	0.0	0.0	0.0	0.0	20170
0.0	516.75122	0.45601	0.0	0.0	556.72559	2647.63945	0.0	0.0	0.0	0.0
689.36401	941.50199	0.76027	689.36401	53.14453	596.21606	3366.62939	0.0	0.0	0.0	0.0
0.02443	0.00307	-6.76544	51.76442	0.08051	534.52173	2295.86230	0.0	0.0	0.0	0.0
0.10319	0.05591	1.18633	0.0	0.99999	0.00002	0.00000	0.0	0.00000	0.0	0.0
1.25127	0.9043	1.25131	0.9044	1.01795	1.00000	0.99999	1.00000	1.00000	1.00000	547.35425
16.55354	509.34364	510.34644	0.95623	0.0	0.0	0.0	0.0	0.0	0.0	20170
0.0	510.34644	0.45024	0.0	0.0	556.45508	2646.11084	0.0	0.0	0.0	0.0
757.67603	913.52417	0.80594	757.67603	56.03703	604.15527	3530.41040	0.0	0.0	0.0	0.0
0.03773	0.00519	-5.18739	52.06558	0.08070	534.79810	2302.57080	0.0	0.0	0.0	0.0
0.08139	0.04377	1.17127	0.0	0.99998	0.00003	0.00000	0.0	0.00000	0.0	0.0
1.25052	0.9081	1.25055	0.9082	1.01340	1.00000	0.99999	1.00000	1.00000	1.00000	533.70774
18.28223	503.22266	503.76221	0.96514	0.0	0.0	0.0	0.0	0.0	0.0	20170
0.0	503.76221	0.44420	0.0	0.0	556.45557	2646.10986	0.0	0.0	0.0	0.0
846.80005	976.73462	0.86176	846.80005	58.95157	614.62964	3749.87524	0.0	0.0	0.0	0.0
0.04633	0.00576	-3.38793	52.41444	0.08091	535.35400	2310.95630	0.0	0.0	0.0	0.0
0.06521	0.03486	1.16045	0.0	0.99999	0.00002	0.00000	0.0	0.00000	0.0	0.0
1.25052	0.9081	1.25056	0.9082	1.01022	1.00000	0.99999	1.00000	1.00000	1.00000	521.95679
18.59283	439.26147	439.84033	0.95500	0.0	0.0	0.0	0.0	0.0	0.0	20170
0.0	439.84033	0.38312	0.0	0.0	554.77832	2560.88062	0.0	0.0	0.0	0.0
860.32520	974.26172	0.84862	860.32520	63.16252	627.54541	3705.97388	0.0	0.0	0.0	0.0
0.05136	0.00700	-7.26288	52.55786	0.07906	548.69556	2314.34033	0.0	0.0	0.0	0.0
0.08479	0.04500	1.17278	0.0	0.99997	0.00005	0.00000	0.0	0.00000	0.0	0.0
1.21025	0.6399	1.21027	0.6400	1.00097	1.00000	0.99999	1.00000	1.00000	1.00000	460.56616

19.73936	496.7664C	497.55884	0.96192	0.0	0.0	556.45557	2646.38721	0.0	
0.0	497.55884	0.43852	0.0	0.0	0.0	624.26294	3960.66162	0.0	
903.49812	1031.43970	0.90906	903.49512	61.15816	0.08112	535.87061	2319.01514	1.0000	517.25732
0.05659	0.70888	-3.70825	52.70853	0.08112	0.99998	0.00002	0.00000	1.0000	20170
0.07121	0.03808	1.16434	0.0	0.99998	1.01094	0.9999	1.00000	1.0000	
1.25066	0.9086	1.25069	0.9087	0.9057	0.0	0.0	0.0	1.0000	
21.90883	480.64331	481.56982	0.94961	0.0	0.0	556.44434	2644.25464	0.0	
0.0	481.56982	0.42392	0.0	0.0	0.0	639.95630	4318.24609	0.0	
1002.79419	1112.43213	0.97927	1002.79419	64.34834	0.08155	537.16138	2336.92407	1.0000	507.12378
0.06213	0.01447	-4.10386	53.14636	0.08155	0.99999	0.00002	0.00000	1.0000	20170
0.09393	0.05039	1.17943	0.0	0.99999	1.01382	0.9999	1.00000	1.0000	
1.24965	0.9055	1.24968	0.9056	0.9026	0.0	0.0	0.0	1.0000	
23.03484	470.36011	471.31445	0.94127	0.0	0.0	557.12036	2644.25562	0.0	
0.0	471.31445	0.41433	0.0	0.0	0.0	649.41797	4527.45703	0.0	
1056.33276	1154.98257	1.01524	1054.33276	65.91405	0.08177	538.65039	2349.67871	1.0000	500.75000
0.06374	0.02071	-3.88045	53.37361	0.08177	0.99996	0.00005	0.00001	1.0000	20170
0.10930	0.05878	1.18995	0.0	0.99996	1.01563	0.9999	1.00000	1.0000	
1.24965	0.8902	1.24968	0.8903	0.8867	0.0	0.0	0.0	1.0000	
26.13331	456.63892	457.59985	0.92395	0.0	0.0	558.96704	2644.25269	0.0	
0.0	457.59985	0.40119	0.0	0.0	0.0	660.24756	4743.30469	0.0	
1104.61230	1195.64429	1.04826	1104.61230	67.49756	0.08192	541.55713	2366.78271	1.0000	495.26685
0.06491	0.03162	-4.84103	53.59529	0.08192	0.99997	0.00003	0.00000	1.0000	20170
0.14054	0.07605	1.21219	0.0	0.99997	1.01955	0.9999	1.00000	1.0000	
1.24965	0.8507	1.24968	0.8508	0.8460	0.0	0.0	0.0	1.0000	
24.67976	443.46558	444.42944	0.90688	0.0	0.0	560.94971	2638.65894	0.0	
0.0	444.42944	0.39859	0.0	0.0	0.0	666.84766	4841.44141	0.0	
1120.62329	1213.00479	1.06137	1120.62329	68.52373	0.08195	544.52832	2377.79614	1.0000	490.06396
0.06597	0.04033	-6.16991	53.70557	0.08195	0.99997	0.00004	0.00000	1.0000	20170
0.17097	0.09312	1.23500	0.0	0.99997	1.02315	0.9999	1.00000	1.0000	
1.24700	0.8046	1.24704	0.8047	0.7984	0.0	0.0	0.0	1.0000	
25.23999	416.67578	417.63980	0.87574	0.0	0.0	563.42480	2619.97876	0.0	
0.0	417.63989	0.36370	0.0	0.0	0.0	674.16040	4918.83984	0.0	
1155.26563	1228.43848	1.06970	1155.26563	70.12450	0.08165	548.92432	2391.23096	1.0000	476.90210
0.06907	0.05348	-8.18967	53.81970	0.08165	0.99995	0.00004	0.00000	1.0000	20170
0.22545	0.12426	1.27892	0.0	0.99995	1.02864	0.9999	1.00000	1.0000	
1.23817	0.7372	1.23821	0.7373	0.7292	0.0	0.0	0.0	1.0000	



*NISR#		*MASS AVERAGE TOTAL PRESSURE		*DELTA-T COOLING =		*TOTAL DELTA-T =			
557.65820	2639.55811	1.24743	0.8713	0.9672	0.8714	0.8673	538.54956	0.0	9.35834
390.34937	5245.70000	324.49854	5058.41797	0.0	0.98000	13.00000	57.63759	0.0	0.0
*STATCR OPT4		NASA FAN ENGINE SPLITTER STUDY		LOOP# =					
12.95000	465.03447	465.04077	0.92587	0.0	0.0	2620.34570	0.0	0.0	20180
0.0	465.74077	0.40861	0.0	0.0	557.15601	2620.34570	0.0	0.0	0.0
592.73755	753.39282	0.66198	592.73755	51.88350	586.15449	3134.08594	0.0	0.0	0.0
0.00526	0.70000	-1.44661	57.63759	0.08120	539.17456	2335.85352	0.0	0.0	0.0
0.13691	0.07413	1.20967	0.0	0.99997	0.00004	0.00001	0.0	0.0	0.0
1.23935	7.84846	1.23839	0.8537	0.8487	1.01970	0.99999	1.0000	1.0000	502.27344
13.44751	478.76099	478.77441	0.93035	0.0	0.0	2638.79590	0.0	0.0	20180
0.0	478.77441	0.42111	0.0	0.0	557.13867	2638.79590	0.0	0.0	0.0
615.50928	779.79272	0.68587	615.50928	52.12238	588.62305	3199.52368	0.0	0.0	0.0
0.00753	0.70000	-2.46888	57.63759	0.08137	538.07910	2335.85229	0.0	0.0	0.0
0.12861	0.76965	1.20945	0.0	0.99994	0.00002	0.00000	0.0	0.0	0.0
1.24707	0.8915	1.24711	0.8916	0.9778	1.01951	0.99999	1.00000	1.0000	514.61914
14.33751	434.53037	484.66040	0.93451	0.0	0.0	2647.11450	0.0	0.0	20180
0.0	484.56040	0.42658	0.0	0.0	556.86084	2647.11450	0.0	0.0	0.0
656.24536	915.91470	0.71805	656.24536	53.55278	597.64917	3293.00146	0.0	0.0	0.0
0.01117	0.70000	-4.19658	57.63759	0.08148	537.32959	2335.88428	0.0	0.0	0.0
0.12104	0.76549	1.19844	0.0	0.99999	0.00002	0.00000	0.0	0.0	0.0
1.25100	7.9003	1.25104	0.9005	0.9973	1.01869	0.99999	1.00000	1.0000	518.62354
15.16039	485.11548	485.17310	0.99889	0.0	0.0	2647.67651	0.0	0.0	20180
0.0	485.17310	0.42710	0.0	0.0	556.72559	2647.67651	0.0	0.0	0.0
694.32178	847.03931	0.74565	694.32179	55.05918	596.78589	3377.90747	0.0	0.0	0.0
0.01542	-0.70000	-4.66109	57.63759	0.08150	537.15308	2335.68042	0.0	0.0	0.0
0.11319	7.76111	1.19290	0.0	0.99996	0.00004	0.00000	0.0	0.0	0.0
1.25126	7.9243	1.25130	0.9044	0.9013	1.01734	0.99999	1.00000	1.0000	516.75122
16.71014	483.95986	483.99072	7.76436	0.0	0.0	2646.10547	0.0	0.0	20180
0.0	483.99072	0.42613	0.0	0.0	556.45508	2646.10547	0.0	0.0	0.0
764.84399	905.11499	0.79691	764.84399	57.67444	605.06128	3549.00928	0.0	0.0	0.0
0.02328	-0.70000	-4.43726	57.63759	0.08153	536.97778	2335.59717	0.0	0.0	0.0
0.09615	7.03164	1.18099	0.0	0.99998	0.00002	0.00000	0.0	0.0	0.0
1.25052	7.9081	1.25055	0.9087	0.9053	1.01435	0.99999	1.00000	1.0000	510.34644
18.47171	433.57767	493.84399	0.96046	0.0	0.0	2646.10400	0.0	0.0	20180
0.0	483.34399	0.42599	0.0	0.0	556.45557	2646.10400	0.0	0.0	0.0
845.47290	974.13013	0.85766	845.47290	60.21940	615.84059	3775.85913	0.0	0.0	0.0
0.03127	0.70000	-3.93549	57.63759	0.08153	536.98999	2335.77686	0.0	0.0	0.0
0.07447	0.73954	1.16611	0.0	0.99999	0.00002	0.00000	0.0	0.0	0.0
1.25052	7.9391	1.25055	0.9087	0.9053	1.01074	0.99999	1.00000	1.0000	503.76221
19.19327	419.44556	419.68140	0.93417	0.0	0.0	2560.87646	0.0	0.0	20180
0.0	419.58140	0.36508	0.0	0.0	544.77832	2560.87646	0.0	0.0	0.0
878.49756	973.57668	0.84693	878.49756	64.46490	628.87573	3731.62158	0.0	0.0	0.0
0.03355	7.70000	-2.71823	57.63759	0.07959	550.13623	2335.69287	0.0	0.0	0.0
0.08663	0.74583	1.17380	0.0	0.99999	0.00002	0.00000	0.0	0.0	0.0
1.21024	0.6399	1.21027	0.6400	0.6301	1.00923	0.99999	1.00000	1.0000	439.84033



APPENDIX III  
DYNAMIC ANALYSIS METHODS

Blade Vibration Analysis

The method used to analyze the compressor and turbine blades is a transfer matrix technique. This method has proven to be extremely useful and easily adaptable to digital computer computation. It can be used to compute the coupling between two orthogonal bending and torsional modes of vibration. The coupling arises from the pretwist and noncolinearity of the elastic and centroidal axes.

The dynamic system assumed for the blade has two related but not colinear spanwise axes. These axes are the centroidal axis, which is assumed to be straight and colinear with a radial axis, and the elastic axis which, in general, is neither straight nor colinear with the centroidal axis. The elastic axis is a line along which the principle elastic bending and torsional properties are assumed to act.

For the analysis the blade is broken into segments of length (l) with two principle axes of inertia. The axis of minimum area moment of inertia is designated by using the Greek symbol eta ( $\eta$ ). The other principle axis is designated the zeta ( $\zeta$ ) axis. These two axes form a coordinate system which will be called the gamma( $\gamma$ ) system. This system makes an angle  $\gamma$  with the selected Y-Z coordinate system of the blade.

The unknown quantities at the end of any section to be determined are the shears ( $V_Y, V_Z$ ), bending moments ( $M_Z, M_Y$ ), slopes ( $\theta, \psi$ ), and deflections ( $W, V$ ). In addition, the torque (T) and angular deflection ( $\theta$ ) about the X-axis are also computed. These quantities at the right or left of any section will be called the state vector at that point. The state vector of a point in the X, Y, Z, coordinate system will be labeled  $Z_i$ .

The state vector in the gamma system ( $Z^{\gamma}_i$ ) at point i can be related to the state vector in the X, Y, Z coordinate system ( $Z_i$ ) by a transformation of coordinates

$$Z^{\gamma}_i = G^{\gamma}_i \cdot Z_i \tag{10}$$

Superscript  $\gamma$  indicates Gamma system. The transformation equation, assuming no torsional coupling, is shown below in matrix form.

$\Phi$	$Y$	1									$\Phi$
T		1									T
v			$\cos\gamma_i$					$-\sin\gamma_i$			v
$\theta$				$\cos\gamma_i$				$-\sin\gamma_i$			$\theta$
$M_z$					$\cos\gamma_i$				$-\sin\gamma_i$		$M_z$
$-V_y$	=					$\cos\gamma_i$				$-\sin\gamma_i$	$-V_y$
$-w$			$\sin\gamma_i$				$\cos\gamma_i$				$-w$
$\psi$				$\sin\gamma_i$				$\cos\gamma_i$			$\psi$
$M_y$					$\sin\gamma_i$				$\cos\gamma_i$		$M_y$
$V_z$						$\sin\gamma_i$				$\cos\gamma_i$	$V_z$

Also the state vector at the right of point i in the Gamma system ( $Z_i$ ) can be related to the state vector at the left of i in the Gamma system as

$$Z^Y R_i = F_i^Y \cdot Z^Y i \quad (11)$$

where  $F_i$  is a field transfer matrix.

$\Phi$	R	$\Phi$	L	1	$\frac{1}{GK}$							$\Phi$	L
T		T			1							T	
V		V				1	1	$\frac{1^2}{2EI_\zeta}$	$\frac{1^3}{6EI_\zeta}$			V	
$\theta$		$\theta$					1	$\frac{1}{EI_\zeta}$	$\frac{1^2}{2EI_\zeta}$			$\theta$	
$M_z$		$M_z$						1	1			$M_z$	
$-V_y$	= $F_i^Y$	$-V_y$	=						1			$-V_y$	
$-w$		$-w$								1	1	$\frac{1^2}{2EI_\eta}$	$\frac{1^3}{6EI_\eta}$
$\psi$		$\psi$								1	$\frac{1}{EI_\eta}$	$\frac{1^2}{2EI_\eta}$	
$M_y$		$M_y$									1	1	
$V_z$		$V_z$	$i$									1	$i$

Field Transfer Matrix

By using the transformation Eq (10) for the left side

$$Z_i^L = G_i^Y \cdot Z_i^L \quad (12)$$

and by substitution into Eq (11), the following is obtained

$$Z^{YR} = F_i^Y \cdot G_i^Y \cdot Z_i^L \quad (13)$$

also for the right side of section i

$$Z_i^{YR} = G_i^Y \cdot Z_i^R \quad (14)$$

or

$$Z_i^R = G_i^{Y-1} \cdot Z_i^{YR} \quad (15)$$

$$G_i^{Y-1} = \text{the inverse of } G_i^Y$$

therefore, by substituting Eq (13) into Eq (15), the following is obtained

$$Z_i^R = G_i^{Y-1} \cdot F_i^Y \cdot G_i^Y \cdot Z_i^L \quad (16)$$

or

$$Z_i^R = F_i^Y Z_i^L \quad (17)$$

This relates the state vector at the right of section i to the state vector on the left in the X, Y, Z coordinate system. Also since

$$Z_i^R = Z_{i+1}^L \quad (18)$$

and as for Eq (16) but for section i + 1

$$Z_{i+1}^R = G_{i+1}^{Y-1} \cdot F_{i+1}^Y \cdot G_{i+1}^Y \cdot Z_{i+1}^L \quad (19)$$

or

$$Z_{i+1}^R = F_{i+1}^Y Z_{i+1}^L \quad (20)$$

By substituting the expression for  $Z_i^R = Z_{i+1}^L$ , the following is obtained

$$Z_{i+1}^R = \left| G_{i+1}^{Y-1} \ F_{i+1}^Y \ G_{i+1}^Y \right| \cdot \left| G_i^{Y-1} \ G_i^Y \ G_i^Y \right| Z_i^L \text{ etc.}$$

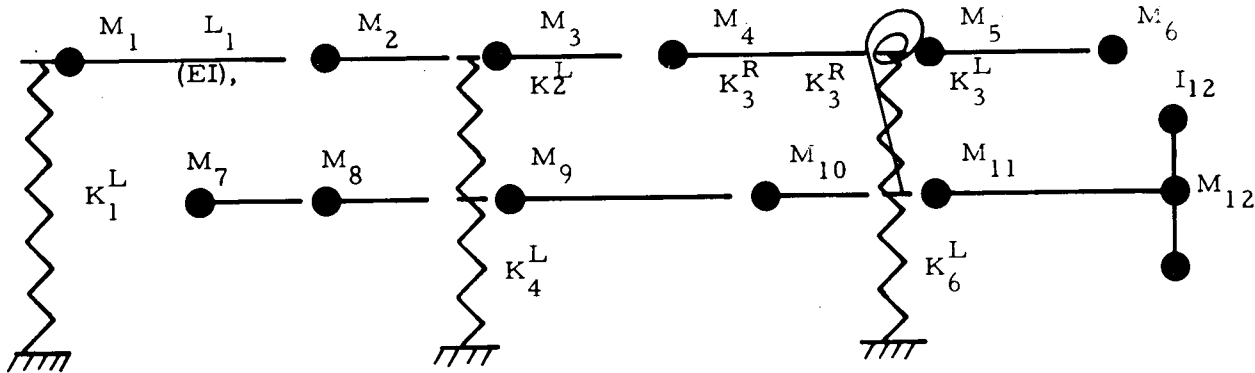
As shown, the state vector at the right end of a system can be related by a product of the above transformation matrices, field transfer matrices, and a mass point matrix for each individual section. The boundary

conditions that exist at the extreme ends of the system can then be inserted upon obtaining the system transfer matrix. With this, a reduced frequency determinant can be determined at a number of discrete frequencies and the frequencies, at which the determinant becomes zero, signify the eigenvalues or natural frequencies.

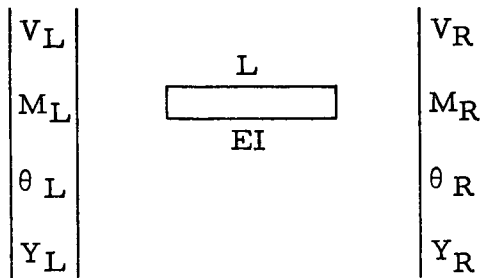
### Rotor Analysis In Critical Speed

The methods employed to analyze the rotor systems use a matrix technique similar to that described for the blades. The method selected depends upon the system being analyzed. One method can include the effects of damping and unbalance if these quantities are known. Another method which is employed extensively is based on the classical influence coefficient method. The procedure used to calculate the influence coefficients is again a transfer matrix method. This method will be described here to illustrate the general procedure.

The system to be analyzed is reduced to an equivalent mass elastic system. A typical two beam level system is shown in the following sketch:



The system is made up of sections of length  $L$  and constant stiffness  $EI$ . The matrix equation for a shaft section relating the shear, moment, slope, and deflection at the right end in terms of these quantities on the left is as follows:



$$\begin{bmatrix} V \\ M \\ \theta \\ Y \\ 1 \end{bmatrix}_R = \begin{bmatrix} 1 & 0 & 0 & 0 & 0 \\ L & 1 & 0 & 0 & 0 \\ \frac{L^2}{2EI} & \frac{L}{EI} & 1 & 0 & 0 \\ \frac{L^3}{6EI} & \frac{L^2}{2EI} & L & 1 & 0 \\ 0 & 0 & 0 & 0 & 0 \end{bmatrix} \cdot \begin{bmatrix} V \\ M \\ \theta \\ Y \\ 1 \end{bmatrix}_L$$

To compute the influence coefficients, a unit load has to be placed at each mass point individually in the system. The transfer matrix representing a unit load would be:

$$\begin{bmatrix} V \\ M \\ \theta \\ Y \\ 1 \end{bmatrix}_R = \begin{bmatrix} 1 & 0 & 0 & 0 & -1 \\ 0 & 1 & 0 & 0 & 0 \\ 0 & 0 & 1 & 0 & 0 \\ 0 & 0 & 0 & 1 & 0 \\ 0 & 0 & 0 & 0 & 1 \end{bmatrix} \cdot \begin{bmatrix} V \\ M \\ \theta \\ Y \\ 1 \end{bmatrix}_L$$

This matrix simply states that a change in the shear across a load is unity. It is similar for a unit moment.

$$\begin{bmatrix} V \\ M \\ \theta \\ Y \\ 1 \end{bmatrix}_R = \begin{bmatrix} 1 & 0 & 0 & 0 & 0 \\ 0 & 1 & 0 & 0 & -1 \\ 0 & 0 & 1 & 0 & 0 \\ 0 & 0 & 0 & 1 & 0 \\ 0 & 0 & 0 & 0 & 1 \end{bmatrix} \cdot \begin{bmatrix} V \\ M \\ \theta \\ Y \\ 1 \end{bmatrix}_L$$

The matrix relation for a support point anywhere in the system would depend on the number of beam levels in the system. For a two level system this relation is:

$$\begin{bmatrix} V^1 \\ M^1 \\ \theta^1 \\ Y^1 \\ 1 \\ V^2 \\ M^2 \\ \theta^2 \\ Y^2 \\ 1 \end{bmatrix}_R = \begin{bmatrix} 1 & 0 & 0 & -(S_2) & 0 & 0 & 0 & 0 & K_2 & 0 \\ 0 & 1 & S_2^T & 0 & 0 & 0 & 0 & -K_2^T & 0 & 0 \\ 0 & 0 & 1 & 0 & 0 & 0 & 0 & 0 & 0 & 0 \\ 0 & 0 & 0 & 1 & 0 & 0 & 0 & 0 & 0 & 0 \\ 0 & 0 & 0 & 0 & 1 & 0 & 0 & 0 & 0 & 0 \\ 0 & 0 & 0 & K_2 & 0 & 1 & 0 & 0 & -(S_3) & 0 \\ 0 & 0 & -K_2^T & 0 & 0 & 0 & 1 & S_3^T & 0 & 0 \\ 0 & 0 & 0 & 0 & 0 & 0 & 0 & 1 & 0 & 0 \\ 0 & 0 & 0 & 0 & 0 & 0 & 0 & 0 & 1 & 0 \\ 0 & 0 & 0 & 0 & 0 & 0 & 0 & 0 & 0 & 1 \end{bmatrix} \begin{bmatrix} V^1 \\ M^1 \\ \theta^1 \\ Y^1 \\ 1 \\ V^2 \\ M^2 \\ \theta^2 \\ Y^2 \\ 1 \end{bmatrix}_L$$

The superscripts stand for level 1 and 2.

Here:

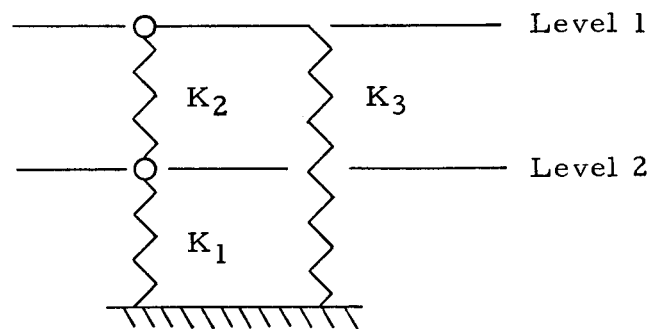
$$S_2 = K_2 + K_3$$

$$S_3 = K_2 + K_1$$

$$S_2^T = K_2^T + K_3^T$$

$$S_3^T = K_2^T + K_1^T$$

#### Spring Location Number System



Where:

$K$  = Lateral Stiffness (lb/in.)

$K^T$  = Rotational Stiffness (in.-lb/rad)

It can be observed that by placing section matrices together, the quantities, shear, etc., on the right of one section is the same as those same quantities on the left of the next section. Therefore, a matrix representing the entire beam can be produced by multiplying through these matrices and representing loads, moments and supports by their



respective matrices at the proper section. Using the product matrix and boundary conditions, the shear, moment, slope, and deflection at the left end can be determined. Using these values and stepping back through the individual matrices, these quantities are determined at all selected sections. The deflection and slope at the mass points selected are singled out and placed in matrix form.

The method used to solve for the frequencies and mode shapes is the matrix iteration method. For a linear system with N degrees of freedom, the equations of motion may be expressed in terms of influence coefficients with the loads, the inertia loads ( $m_i \omega^2 y_i$ ) at each mass.

$$\begin{aligned}
 y_1 &= \alpha_{11}(m_1 \omega^2 y_1) + \alpha_{12}(m_2 \omega^2 y_2) + \alpha_{13}(m_3 \omega^2 y_3) + \dots \\
 y_2 &= \alpha_{21}(m_1 \omega^2 y_1) + \alpha_{22}(m_2 \omega^2 y_2) + \alpha_{23}(m_3 \omega^2 y_3) + \dots \\
 y_3 &= \alpha_{31}(m_1 \omega^2 y_1) + \alpha_{32}(m_2 \omega^2 y_2) + \alpha_{33}(m_3 \omega^2 y_3) + \dots
 \end{aligned} \tag{21}$$

A convenient way to write these equations is by means of the matrix notation.

$$\begin{bmatrix} y_1 \\ y_2 \\ y_3 \\ \cdot \\ \cdot \\ \cdot \\ \cdot \\ y_n \end{bmatrix} = \omega^2 \begin{bmatrix} \alpha_{11} & \alpha_{12} & \alpha_{13} & \dots \\ \alpha_{21} & \alpha_{22} & \alpha_{23} & \dots \\ \alpha_{31} & \alpha_{32} & \alpha_{33} & \dots \\ \cdot & \cdot & \cdot & \dots \\ \cdot & \cdot & \cdot & \dots \\ \cdot & \cdot & \cdot & \dots \\ \cdot & \cdot & \cdot & \dots \\ \cdot & \cdot & \cdot & \dots \end{bmatrix} \begin{bmatrix} m_1 & 0 & 0 & 0 \\ 0 & m_2 & 0 & 0 \\ 0 & 0 & m_3 & 0 \\ \cdot & \cdot & \cdot & \cdot \\ \cdot & \cdot & \cdot & \cdot \\ \cdot & \cdot & \cdot & \cdot \\ \cdot & \cdot & \cdot & \cdot \\ \cdot & \cdot & \cdot & \cdot \end{bmatrix} \begin{bmatrix} y_1 \\ y_2 \\ y_3 \\ \cdot \\ \cdot \\ \cdot \\ \cdot \\ y_n \end{bmatrix} \tag{22}$$

The iteration procedure is started by assuming a set of deflections  $y_1, y_2, y_3, \dots$  for the right column of the matrix equation. After multiplying, the resulting column is normalized; i. e., reducing one of the amplitudes to unity by dividing each term of the column by the particular amplitude. The procedure is now repeated by using the normalized column as the new set of deflections. The amplitude will then stabilize, and the fundamental frequency can be found from the matrix equation. Since the iteration procedure converges to the lowest mode, certain manipulations are required to obtain the higher modes. Upon performing these manipulations, all desired modes can be obtained.

APPENDIX IV  
LIST OF SYMBOLS

A	area - $\text{ft}^2, \text{in.}^2$
BR	bypass ratio - $W_{aS}/W_{aP}$
C	blade chord - ft or in.
$C_p$	specific heat at constant pressure - $\text{Btu/lb} - ^\circ\text{F}$
$C_v$	specific heat at constant volume - $\text{Btu/lb} - ^\circ\text{F}$ , or nozzle velocity coefficient
D	diameter - ft, or blade diffusion factor
$F_g$	gross thrust - lb
$F_n$	net (total) thrust - lb
$F_{t, y}$	tensile yield stress - $\text{lb/in.}^2$
$F_{t, u}$	tensile ultimate stress - $\text{lb/in.}^2$
f	blade or sound frequency - cps
g	gravitational constant - $32.17 \text{ ft/sec}^2$
h	specific enthalpy - $\text{Btu/lb}$
i	blade incidence - deg
J	mechanical equivalent of heat - $778 \text{ ft-lb/Btu}$
k	$C_p/C_v$
$k_h$	stress concentration factor in hoop stress
$k_t$	stress concentration factor in tension
M	Mach number
N	rotative speed - rpm

P	pressure - lb/in. <sup>2</sup> or lb/ft <sup>2</sup>
PNL	perceived noise level
PNdB	perceived noise in decibels
q	dynamic pressure - $1/2 \rho V^2$
S	blade pitch - ft or in.
SM	surge margin = $\left[ \left( \frac{P_{rs}}{P_{ro}} \times \frac{W_{ao}}{W_{as}} \right) \right]^{-1} \times 100$
SPL	sideline perceived level or sound pressure level
T	temperature, °R or °F
TSFC	thrust specific fuel consumption - lb/hr-lb
U	wheel speed - ft/sec
V	absolute velocity vector - ft/sec
W	flow - lb/sec, or relative velocity - ft/sec
$W_{aP}$	primary or core flow - lb/sec
$W_{as}$	secondary or bypass flow - lb/sec
$W_c$	cooling air - lb/sec
$W_L$	leakage air overboard - lb/sec
$\alpha$	absolute flow angle measured from axis - deg
$\beta$	relative flow angle measured from axis - deg
$\gamma$	setting angle - deg
$\delta$	blade deviation - deg, or referred pressure - P/14.69

$\eta$	efficiency
$\theta$	camber angle - deg, or referred temperature - $T/518.7$
$\theta_{cr}$	$= \frac{\left(\frac{2k}{k+1}\right) T_t}{\left(\frac{2k}{k+1}\right) (518.7)}$
$\lambda$	blade flutter coefficient = $\frac{W}{2 \pi f C}$
$\nu$	relative thickness - pct
$\rho$	mass density - slugs/ft <sup>3</sup>
$\sigma$	blade solidity - C/S, or stress
$\sigma_h$	hoop stress - lb/in. <sup>2</sup>
$\sigma_r$	radial stress component - lb/in. <sup>2</sup>
$\sigma_t$	tangential stress component - lb/in. <sup>2</sup>
$\phi$	flow coefficient - nondimensional ( $V_z/U$ )
$\psi$	pressure coefficient - nondimensional ( $\Delta h/U^2/2gJ$ )
$\psi_a$	Zweifel load coefficient
$w$	pressure loss coefficient - $\Delta Pt/q_1$ , or radians/sec

### Subscripts

a	adiabatic
am	ambient
B	burner
f	flight
h	hub

M	mechanical
o	operating
p	polytropic
r	radial component
s	surge
T	turbine
t	total or tip
W	relative
Z	axial component
$\theta$	tangential component
1	inlet
2	exit

## REFERENCES

1. Fujjii, Shoichi, "Some Studies of Front Fans With and Without Snubbers," ASME Paper 72-GT-4, 1972.
2. Smith, M. J. T., and House, M. E., "Internally Generated Noise From Gas Turbine Engines, Measurement and Prediction," Journal of Engineering for Power, pp. 177-190, April 1967.
3. Kobrynski, M., "General Methods for Calculating the Sound Pressure Field Emitted by Stationary or Moving Jets," O.N.E.R., May 1969.

## BIBLIOGRAPHY

Lycoming ALF-502A Turbofan Engine, Volume II, Technical Description, No. 4510-8, August 1970.